CHARACTERIZATION OF THE MECHANISM OF ACTION OF SPIN-FILTERS FOR ANIMAL CELL PERFUSION CULTURES

THÈSE N^{O} 3488 (2006)

PRÉSENTÉE LE 9 JUIN 2006

À LA FACULTÉ SCIENCES DE BASE

Laboratoire de génie chimique et biologique

SECTION DE CHIMIE ET GÉNIE CHIMIQUE

ÉCOLE POLYTECHNIQUE FÉDÉRALE DE LAUSANNE

POUR L'OBTENTION DU GRADE DE DOCTEUR ÈS SCIENCES

PAR

Florentina VALLEZ-CHETREANU

ingénieure chimiste diplômée EPF

de nationalité suisse et originaire de Lancy (GE)

acceptée sur proposition du jury:

Prof. P. Vogel, président du jury

Dr I.W. Marison, Prof. U. von Stockar directeurs de thèse

Dr A. Kadouri, rapporteur

Prof. R. Spier, rapporteur

Prof. F. Wurm, rapporteur

ÉCOLE POLYTECHNIQUE
FÉDÉRALE DE LAUSANNE

Lausanne, EPFL

2006

Préface

Ce manuscrit concrétise cinq belles années de ma vie, passées au sein du LGCB. Par ces quelques lignes, j'aimerais remercier toutes les personnes qui ont contribué de près ou de loin à la réalisation de cette thèse.

Tout d'abord, je tiens à remercier le Prof. Ian Marison, qui est à l'origine de ce travail de recherche et sans qui il n'aurait pas pu se faire. Je le remercie pour la confiance qu'il m'a témoignée, sa disponibilité et son éternel enthousiasme, ainsi que pour ses innombrables idées. J'aimerais ensuite remercier le Prof. Urs von Stockar pour m'avoir accueillie au sein de son groupe et m'avoir donné l'opportunité de réaliser ce travail de doctorat, avec grande liberté. Merci pour son implication au sein de ce projet ainsi que pour les nombreuses discussions scientifiques et non-scientifiques que nous avons eues.

Je tiens également à remercier le partenaire industriel impliqué dans ce projet, à savoir «le team Serono»: Dr A. Kadouri, Dr P.-A. Ruffieux, Dr F. Meuwly, ainsi que Dr D. Voisard, pour leur intérêt et leurs investissements dans ce projet, ainsi que pour avoir apporté un peu de réalisme dans un monde académique, qui parfois peut être loin des contraintes industrielles.

Un grand merci à Patrick pour ses nombreux conseils techniques, son aide précieuse et les «opérations à cœur ouvert» sur le bioréacteur. Merci à mes stagiaires pour leur contribution aux résultats de ce projet. J'ai une pensée toute particulière pour mon diplômant, L. Guilherme Ferreira, qui nous a quittés beaucoup trop tôt.

Je remercie les anciens membres du LGCB, en particulier Christoph, Raph, David et Chris, à qui je dois mon initiation au monde biotech. Merci pour l'excellente ambiance qu'ils ont créé dès le début de cette thèse, ainsi que pour leur rigueur dans le travail, dont je me suis inspirée. Le «girls team»: Adona, Anne et Manu pour leur soutien, leurs encouragements, leur présence et leur amitié, qui m'a énormément apporté. Merci

également aux membres du LGCB les moins anciens. A Agnès pour sa bonne humeur inépuisable, Thierry pour les nombreuses discussions sur ces bloody cellules animales et tout spécialement merci à Carmen et Jonas, pour leurs encouragements, les nombreuses discussions, qui dépassaient souvent le cadre de la thèse, ainsi que leur soutien lors de la longue rédaction de cette thèse. Un merci tout particulier à Anne, qui a débuté cette aventure avec moi, avec qui j'ai vécu des magnifiques moments. Merci pour sa complicité, son énergie, son soutien, nos nombreuses discussions et les «pétages de plombs» sur un air de Claude François.

Enfin, je profite de cette occasion pour remercier mes amis et ma famille pour leur présence, leur soutien et leur affection tout au long de ces années. Merci à mes parents de m'avoir permis d'accomplir mes études d'ingénieur, ainsi que pour leurs encouragements et réconfort. Un merci tout particulier à David, pour son affection et son soutien quotidien. Merci d'avoir toujours répondu présent aux moments où j'en avais besoin et pour sa patience à la réalisation de cette thèse.

Fl. Vallez

Florentina Vallez–Chetreanu

Table of contents

Summary

The growing demand for high levels of recombinant proteins of medical and pharmaceutical interest stimulates the development of cell bioprocess technology. Spin–filter technology is employed in order to reach high levels of such compounds. The aim of this thesis was to characterize the mechanisms of cell retention, as well as filter fouling during animal cell spin–filter perfusion cultures. A good understanding of these mechanisms would allow a good optimization of spin–filter parameters and culture conditions in order to achieve high cell density cultures at large scale operation and for long–time and thus increase proteins productivity.

The first part of the thesis was focused on the study of particle retention as a function of four main parameters: filter pore size, filter rotation speed, perfusion rate and particle concentration, during perfusion simulations of agarose beads of 13 μm in diameter. Bead retention by filters with pore sizes of 13 and 14.5 μm, larger than the mean particle diameter was found to be dependent mainly on the filter rotation velocity and filter pore size. Filter retention followed a saturation dynamics with an initial direct correlation with respect to filter rotation rate. A plateau was reached above a filter tangential velocity of 0.45 m/s and 0.87 m/s for filters with pore size of 13 and 14.5 μm respectively. The lower the filter velocity was, the greater the influence of perfusion rate on bead retention, whereas the retention was slightly improved when the particle concentration was increased. The presence of a draft tube around open spin–filters was observed to lower the retention, with the effect being greater for non–porous than for porous draft tubes.

In the second part of this work, a prediction of radial particle migration near the surface of rotating filter was developed. The lift force was demonstrated to be important in the spin–filter system since it contributes to particle removal from the filter surface. Competition between centrifugal sedimentation, lift forces, Stokes drag and perfusion forces were found to be responsible for determining particle motion relative to the filter. At certain filter rotation rates, centrifugation and lift forces are sufficiently high as to balance perfusion flow and result in the movement of particles away from the filter, a situation that experimentally was found to correspond to maximum particle retention. The model also revealed that filter acceleration is the key parameter to be conserved from small to large

scale in order to achieve similar retention rates. This hypothesis has been confirmed experimentally.

Then spin–filter cell retention was modeled using response surface methodology. A second–order polynomial model was used to predict the effects of the filter pore size, cell concentration, perfusion capacity and filter acceleration on cell retention. The retention rates obtained experimentally during two different spin–filter perfusion cultures of CHO *SSF3* agreed with those predicted by the model, indicating the applicability of the model to animal cell perfusion culture.

In the last part of this work the study of filter fouling during long–term perfusion simulations with CHO animal cells was investigated. It was demonstrated that at low filter acceleration, below 6.2 m/s^2, a high perfusion rate of 25 cm/h induced rapid filter pore, whereas increasing the filter acceleration to 25 m/s^2 increased filter longevity eight times, for filters with a pore size of 8.5 μm. Increasing the filter pore size to 14.5 μm improved filter longevity by 84% and revealed less viable and dead cell deposits on filter surface. Ultrasonic technology was used to reduce filter fouling. Filter vibration, induced by a piezo actuator, improved filter longevity by 113% during real CHO perfusion culture.

This work allowed a better understanding of the mechanism of action of spin–filters. The cell retention model developed in this study permits to choose the optimal acceleration at which the filter, of a certain pore size has to be operated in order to achieve similar retention rates for small scale as well as for large–scale processes. The ultrasonic technology through the use of piezoactuators was demonstrated to be a powerful technique for the on–line reduction of filter–fouling, during animal cell perfusion cultures.

Keywords: Perfusion culture, CHO animal cell, separation, spin–filter, retention, fouling, response surface methodology, filter vibration, piezoelectric.

Résumé

La demande croissante en quantités élevées de protéines recombinantes, d'intérêt médical et pharmaceutique, produites par des cellules animales, stimule le développement de la technologie des bio–procédés cellulaires. Une des technologies qui permet d'atteindre des niveaux élevés de production de tels composés est le filtre tournant. Le but de cette thèse a été de caractériser les mécanismes de rétention cellulaire et de colmatage des filtres lors de cultures de cellules animales, en utilisant le filtre tournant pour le recyclage continu des cellules. Une bonne compréhension de ces mécanismes permettrait une meilleure optimisation des paramètres opérationnels du filtre tournant, pour la réalisation de cultures à haute densité cellulaire à grande échelle et à longue durée, afin d'atteindre une haute productivité de protéines.

La première partie de cette thèse se concentre sur l'étude de la rétention de particules en fonction de quatre paramètres principaux: la taille des pores du filtre, la vitesse de rotation du filtre, le taux de perfusion et la concentration de particules, lors de simulations de recyclage de billes d'agarose de 13 μm de diamètre. La rétention des billes par des filtres avec des tailles de pore de 13 et 14.5 μm, plus grandes que le diamètre moyen des particules, s'est avérée dépendre principalement de la taille des pores ainsi que de la vitesse de rotation du filtre. Le profil de la rétention en fonction de la vitesse de rotation du filtre suit comme une dynamique de saturation. Un plateau est atteint au–dessus d'une vitesse tangentielle de filtre de 0.45 m/s et de 0.87 m/s pour des filtres avec une taille de pores de respectivement 13 et 14.5 μm. Plus la vitesse de rotation de filtre est basse et plus l'influence du taux de perfusion sur la rétention des billes est élevée, alors que celle–ci a été légèrement améliorée lorsque la concentration de particules a été augmentée. Il a été observé que la présence d'un tube, faisant office de chicane et placé autour du filtre tournant d'une taille de pores supérieure au diamètre des particules diminue la rétention de celles–ci. L'effet est plus grand pour des tubes non–poreux que pour des tubes poreux.

Dans la deuxième partie de ce travail un modèle, qui prédit la migration radiale de particules près de la surface du filtre tournant, a été développé. La force d'ascenseur ou « lift force » a été démontrée être importante dans le mécanisme de rétention des filtres

tournants, car elle contribue au déplacement de particules de la surface filtrante. La compétition entre la force centrifuge, la force d'ascenseur, la force de traînée ainsi que celle de perfusion s'est avérée responsable de la détermination du mouvement des particules par rapport au filtre. À des vitesses de rotation du filtre suffisamment élevées, la centrifugation et la force d'ascenseur sont suffisamment importantes pour contrebalancer l'effet de la perfusion, ceci ayant pour résultat l'éloignement des particules de la surface du filtre. Dans ces conditions, une rétention maximale des particules par le filtre a été observée expérimentalement. Le modèle a également indiqué que l'accélération du filtre est le paramètre principal à conserver de petite à grande échelle, afin d'obtenir des taux de rétention similaires, une hypothèse qui a été confirmée aussi expérimentalement.

Afin de pouvoir définir les paramètres optimaux du filtre tournant, à n'importe quelle échelle, la rétention de particules a été modélisée en utilisant la méthodologie des surfaces de réponse. Un polynôme de second ordre décrit les effets de la taille des pores du filtre, de la concentration en particules/cellules, de la capacité de perfusion et de l'accélération du filtre, sur la rétention. Les rétentions obtenues expérimentalement lors de deux différentes cultures de cellules CHO avec recyclage de cellules à l'aide du filtre tournant ont corrélé avec ceux prévus par le modèle, indiquant l'applicabilité du modèle à la rétention de cellules animales.

Dans la dernière partie de ce travail, le colmatage du filtre tournant a été étudié lors de simulations de cultures continues de longue durée avec recyclage de cellules animales CHO. Il a été démontré qu'à basse accélération du filtre (6.2 m/s^2), un taux élevé de perfusion (25 cm/h) induit une obstruction rapide des pores, alors qu'une augmentation de l'accélération du filtre (25 m/s^2) augmente de huit fois la longévité du filtre, pour des filtres avec une taille petite des pores (8.5 μm). L'augmentation de la taille des pores (14.5 μm) a amélioré la longévité du filtre de 84% et a révélé un dépôt moindre de cellules viables et mortes sur la surface du filtre. La technologie ultrasonique a été utilisée afin de réduire l'encrassement des filtres tournants. La vibration du filtre, induite par un piézoélectrique a permis à améliorer la longévité du filtre de 113% pendant une culture continue avec recyclage de cellules CHO.

Ce travail a permis une meilleure compréhension du mécanisme d'action des filtres tournants. La modélisation de la rétention des cellules par le filtre tournant permet de définir l'accélération optimale à laquelle le filtre, d'une certaine taille de pore, doit être utilisée de manière à obtenir des taux similaires de rétention lors de son fonctionnement à petite et grande échelle. Le système piézoélectrique s'est avéré à l'utilisation être une technique puissante pour la réduction en ligne de l'encrassement des filtres, lors de cultures de cellules animales.

Mots–clés: Culture cellulaire, mode perfusion, cellule animale CHO, séparation, filtre tournant, rétention, colmatage, méthodologie des surfaces de réponse, vibration du filtre, piézoélectrique.

1

Separation devices for suspended animal cells in continuous cultures

1.1 Introduction

Biotechnology is occupying an increasingly important place in our current life. From the production of ethanol and fermented foods during antiquity, to the application of recombinant technology to produce proteins of medical and pharmaceutical interest, biotechnology has advanced dramatically and the need for bioprocess technology has become important for the viable economic production of such compounds.

Prior to the development of recombinant technology, proteins were directly extracted from tissues, such as insulin from pig and cow pancreas, factor VIII for the treatment of hemophilia, and immunoglobulins from fractionated blood or erythropoietin from urine. All of these products are presently produced commercially in bioreactors using microorganisms (yeast, bacteria, fungi) or higher eucaryotic cells (animal or plant).

1.1.1 The expression system

Starting from a gene sequence or cDNA, which codes for a protein of interest, the gene sequence is inserted into a commercially available expression vector. This expression vector is then transferred to host cell lines, provided by prokaryotic organisms such as bacteria or eukaryotic organisms, such as yeasts, mammalian cells or insect cells. The purpose of such a transfection is to generate an individual cell containing the gene sequence of interest or cDNA permanently integrated into the chromosome of the host cell, which will express the protein of interest during its growth. Bioprocess engineering tools then permit cultivation of the recombinant cells in a defined, confined environment and allow the efficient production of such protein.

Bacterial processes are in general less expensive, due to their rapid growth rate on relatively simple substrates and higher productivity compared with eukaryotic cells. However, recombinant proteins often accumulate as bacterial inclusion bodies that make the separation and purification steps more time consuming and more expensive due to folding and re–folding of the protein. In addition, many proteins of therapeutic and diagnostic interest have chains of sugar attached to asparagine (N–glycosidic bond) and serine or threonine (O–glycosidic bond) moieties resulting in the post–translational modification termed glycosylation. It constitutes one of the most important post–translational protein modifications and may have numerous effects on structure, function and targeting of particular proteins (Helenius and Aebi, 2001). Bacteria are generally unable to glycosylate proteins to any appreciable extent (Jenkins and Curling 1994).

Yeasts and insect cells glycosylate proteins differently to animal cells. Glycan structures not present in humans are potentially antigenic and different glycoforms may show differences in biological behavior (Nahrgang, 2002). For these reasons, mammalian cells, are commonly required for the correct post–translational processing (including human–like glycosylation) and production of large and complex biopharmaceutical proteins for use as prophylactics, therapeutic or diagnostic products.

In Table 1.1 are represented the therapeutic biological products approved by the Food and Drug Administration from 1998 to 2004 (www.fda.gov/cber). A total of 31 products have been approved and 24 of them are produced in mammalian cells. This demonstrates the increasing use of mammalian cells as expression systems. The remaining listed biological products are produced in bacteria or yeast, in italic in Table 1.1.

Table 1.1: Therapeutic biological products approved by the FDA from 1998 to 2004

Product	Description	Product type	Cell type	Approval	Company
Avastin™/ Bevacizumab	Metastatic colorectal cancer	mAb	CHO	2/26/2004	Genentech, Inc.
Erbitux™/ Cetuximab	Colorectal cancer	mAb	Murine myeloma	2/12/2004	ImClone Systems, Inc.
Raptiva™/ Efalizumab	Plaque psoriasis	mAb	CHO	10/27/2003	Genentech, Inc.
Advate/ Antihemophilic Factor	Hemophilia A	glycoprotein	CHO	7/25/2003	Baxter Healthcare Corp.
Bexxar®/ Tositumomab	CD20 positive, follicular, non-Hodgkin's lymphoma	mAb	Mammalian cell	6/27/2003	Corixa Corp.
Xolair®/ Omalizumab	Persistent asthma	mAb	CHO	6/20/2003	Genentech, Inc.
Aldurazyme®/ Laronidase	Mucopolysaccharidosis I	glycoprotein	CHO	4/30/2003	Biomarin Pharmaceutical Inc.
Fabrazyme®/ Agalsidase beta	Fabry disease	glycoprotein	CHO	4/24/2003	Genzyme Corp.
Amevive®/ Alefacept	Chronic plaque psoriasis	glycosylated fusion protein	CHO	1/30/2003	Biogen, Inc.,
Humira™/ Adalimumab	Rheumatoid arthritis	mAb	Mammalian cell	12/31/2002	Abbott Laboratories
PEGASYS® / Peginterferon alfa-2a	*Hepatitis C*	*PEG-ylated interferon alfa-2a*	*E. coli*	*10/16/2002*	*Hoffman-La Roche, Inc.*
Elitek™/ Rasburicase	*Acute leukemia and non-Hodgkin's lymphoma*	*recombinant urate-oxidase enzyme*	*S. cerevisiae*	*7/12/2002*	*Sanofi-Synthelabo, Inc.*
Rebif®/ Interferon beta-1a	Multiple sclerosis	glycoprotein	CHO	3/7/2002	Serono, Inc.
Zevalin™/ Ibritumomab Tiuxetan	B-cell non-Hodgkin's lymphoma	mAb - chelator	CHO	2/19/2002	IDEC Pharmaceuticals
Neulasta™/ Pegfilgrastim	*Febrile neutropenia*	*protein and a 20 kD glycol molec.*	*E. coli*	*1/31/2002*	*Amgen, Inc.*
Xigris™/ Drotrecogin alfa	Severe sepsis	glycoprotein	Recombinant cell	11/21/2001	Eli Lilly & Co
Kineret™/ Anakinra	*Rheumatoid arthritis*	*nonglycosylated protein*	*E. coli*	*11/14/2001*	*Amgen, Inc.*
Aranesp™/ Darbepoetin alfa	Anemia associated with renal failure	glycoprotein	CHO	9/17/2001	Amgen, Inc.
Campath®/ Alemtuzumab	B-cell chronic lymphocytic leukemia	mAb	CHO	5/7/2001	Millennium and ILEX Partners, LP
PEG-Intron™/ Peginterferon alfa-2b	*Hepatitis C*	*PEG-ylated interferon alfa-2b*	*E. coli*	*1/19/2001*	*Schering Corporation*
MYOBLOC™/ Botulinum Toxin Type B	*Cervical dystonia*	*neurotoxin*	*C. botulinum type B*	*12/8/2000*	*Elan Pharmaceuticals*
Kogenate® FS/ Antihemophilic Factor	Hemophilia A	glycoprotein	BHK	6/26/2000	Bayer Corp.
TNKase™/ Tenecteplase	Acute myocardial infarction	glycoprotein	CHO	6/2/2000	Genentech, Inc.
* ReFacto® / Antihemophilic Factor	Hemophilia A	glycoprotein	CHO	3/6/2000	Genetics Institute, Inc.
NovoSeven® / Coagulation Factor VIIa	Hemophilia A or B with inhibitors to Factor VIII or Factor IX	glycoprotein	BHK	3/25/99	Novo Nordisk A/S
Ontak™/ Denileukin diftitox	*Cutaneous T-cell lymphoma*	*recombinant cytotoxic protein*	*E. coli*	*2/5/1999*	*Seragen, Inc.*
Enbrel™/ Etanercept	Rheumatoid arthritis	dimeric fusion protein	CHO	11/2/1998	Immunex Corp.
Herceptin®/ Trastuzumab	Metastatic breast cancer	mAb	CHO	9/25/1998	Genentech, Inc.
* Remicade™/ Infliximab	Crohn's disease	mAb	Recombinant cell	8/24/1998	Centocor, Inc.
Synagis™/ Palivizumab	Prophylaxis	mAb	NSO (murine myeloma)	6/19/1998	MedImmune, Inc.
Simulect®/ Basiliximab	Acute kidney transplant rejection	mAb	Mouse myeloma cell	5/12/1998	Novartis Pharmaceutical Corp.

* continuous perfusion mode

1.1.2 Mammalian cell expression: suspended or attached cells?

Different technologies are employed in order to accomplish the culture of animal cells (de la Broise et al., 1991; Mercille et al., 1994). There are systems which maintain the cells freely suspended in the culture medium, free or fixed on microcarriers (Reiter et al., 1990) and systems where cells are maintained apart from the circulating medium using either a cell exclusion barrier, such as hollow–fiber modules (Tanase et al., 1997), vesicles, beads or capsules where cells are entrapped (Gugerli et al., 2003).

Suspended cell culture systems, provide an homogeneous mixed system, enabling an accurate monitoring and control of the culture parameters, nutrients, metabolites and products and permit better protein quality while facilitating product purification (Werner et al., 1992). In addition, suspension culture has a defined duration, is generally stable, robust, and reproducible and facilitates rapid scale–up. For these reasons, suspended cell culture is generally the most efficient system for cell culture at large–scale operation and is the most used in industrial applications.

1.1.3 Culture modes

Suspension culture systems can be operated in different modes: batch, fed–batch and continuous with and without cell retention. The difference between these modes is the way in which nutrients are supplied and medium is removed from the bioreactor. The four different culture modes are represented in Figure 1.1.

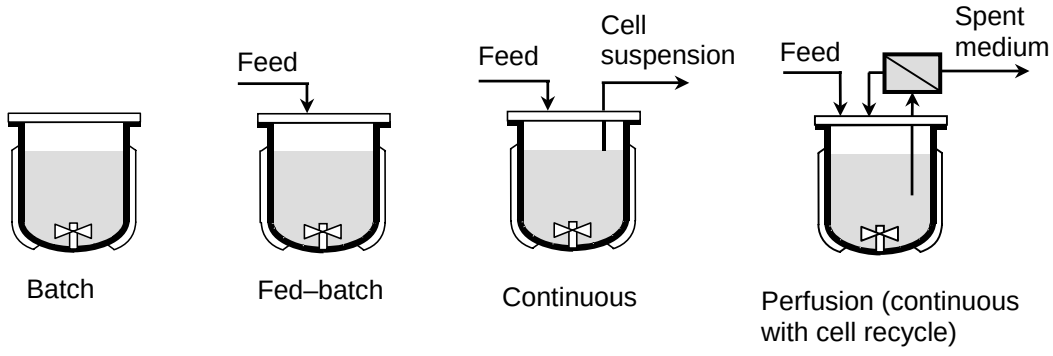

Figure 1.1: Different cultivation modes for suspended cells

Batch culture refers to a partially closed system in which medium is loaded into the reactor and is not altered by further additional or removal. It is the culture mode the most commonly used, however cells are exposed to a constantly changing environment that limits the full expression of growth. Average total cell concentrations between $1–2 \cdot 10^6$ cell/ml are generally achieved with rapid viability declining due to substrate depletion or accumulation of toxic products (Dorresteijn et al., 1996; Eyer et al., 1995; Schneider et al., 1997). As a result of the lower cell densities and high proportion of unproductive time (down–time) between batches, comprising the charge and discharge of the reactor vessel, the volumetric productivity ($mg \cdot L^{-1} \cdot h^{-1}$) of such cultures is generally limited. The low cell density, the cell growth inhibition by high substrate levels, as well as osmotic stresses on the cells may partly be overcome by the use of fed–batch cultures. In such systems, a certain amount of fresh medium is continuously added without the removal of culture fluid. The nutritional environment can be maintained approximately constant during the course of the growth and the production of by–products that are generally related to the presence of high concentrations of substrate (present in batch mode) can also be avoided. Thus compared to batch systems, higher cell concentrations ($5–7 \cdot 10^6$ cell/ml) and operating time (Figure 1.2) are achieved thereby improving the volumetric productivity.

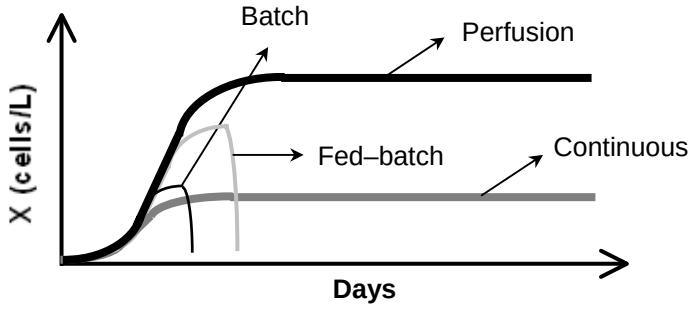

Figure 1.2: Evolution of animal cell concentration as a function of time for different culture modes.

Continuous cultures allow the continuous feeding of nutrients and the same volume removal of culture medium, thereby enabling steady–state conditions. Due to low cell growth of animal cells, the cell concentration stabilizes at lower levels than those obtained in batch mode, however higher operation time than in batch and fed–batch modes can be achieved (Figure 1.2). Immobilization of the cells or the implementation of a cell retention system allows, for a continuous operation, higher cell densities ($1–2 \cdot 10^7$ cell/ml) (Banik and Heath, 1995; Griffiths, 1992; Jäger, 1996) and thus higher volumetric productivities than those obtained in batch and fed–batch systems (Reuveny et al., 1986; Trampler et

al., 1994). It has been reported that volumetric productivity in perfusion systems are up to 10–fold greater than in batch/fed–batch processes (Heine et al., 1999) and thus the required reactor volume for a given production rate can be reduced. As for fed–batch systems, inhibition of cell growth by high substrate concentrations is avoided by limiting its quantity to the amounts that are required only for cell growth and/or maintenance, however, perfusion culture also offers the added advantages of rapid removal of products (thereby avoiding degradation) and toxic by–products, better product quality due to stable conditions within the bioreactor, as well as reduction of capital costs due to higher operation time and reduced reactor working volume (Prior et al., 1989). This culture mode remains thus the most suitable technique for production of high concentrations of recombinant proteins for a long period of time, although product recovery and purification stages are more laborious due to product titers smaller than in fed–batch systems.

1.2 Cell retention systems

Several different separation devices have been used for retaining cells in the bioreactor during perfusion cultures. These devices are positioned inside and outside the bioreactor. Although internal devices permit very simple and safe operation, external devices offer a greater flexibility for scale–up and maintenance. However, external systems require the use of pumps that could damage the cells through mechanical shear stress and long residence time in the external separation loop.

Many methods of separation have been investigated according to the physical and chemical properties of animal cells: size, mass, charge, hydrophobicity and density, however size and density remain the properties the most explored. In industrial animal cell culture, the most investigated separation processes based on these properties use filters, hollow fiber modules, plate–and–frame modules (Avgerinos et al., 1990; Büntemeyer et al., 1994; Vogel and Kroner, 1999) for separations based on size and settling devices, centrifuges, hydrocyclones and acoustic filters (Ryll et al., 2000; Searles et al., 1994; Tokashiki et al., 1990; van Erp et al., 1991; Vastola, 2000) for separations based on density. The main requirements for separation devices during perfusion of animal cells are high cell retention efficiency, being harmless to cells, stable over long term operation, cleanable and sterilizable and, from an industrial point of view, it has to be able to allow high perfusion flow rates at large scale operation, which is the main limitation for new cell

separation devices development. Based on the literature, this review discusses the advantages and the limitations of each animal cell separation technique available to date, for implementation at large-scale (perfusion flows above 400 L/day that would represent a perfusion rate of 2 day^{-1} for a 200 L working volume bioreactor), for long–time operation (over 30 days) and at high cell densities (above 10^7 cell/ml).

1.2.1 Separation by size

The separation of cells from culture medium using filtration systems, were the earliest devices used. The principle is simple, involving separating cells by sieving. The main problem associated with this separation method is the fouling of the filter, which limits stability, perfusion rates and reduces long–term cell cultivation. Internal and external filtration systems are available. The most developed systems are internal or external rotating sieves, such as spin–filters, hollow fiber modules, vortex flow filters and external plate–and–frame modules.

1.2.1.1 Spin–filter devices

Spin–filters are cylindrical wire cages with a porous wall, which are placed internally or externally to the bioreactor (Figure 1.3). The cells are cultured by continuous addition of fresh nutrient medium to the outside of the spin–filter and continuous removal of the spent medium from within the spin–filter. The maximum cell density that can be reached in such a process (without considering physiological limitations of the cell itself) depends upon the capacity of the spin–filter device to minimize cell loss at a specific perfusion rate and on the longevity of the culture.

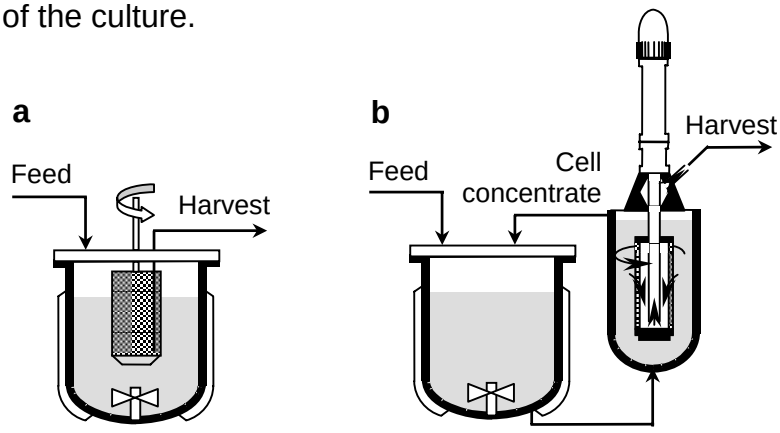

Figure 1.3: Schematic representation of **a**: internal and **b**: external spin–filter devices.

The longevity of the culture is mostly related to filter fouling with time due to cell, DNA, proteins and/ or cell debris accumulation on the filter mesh and represents the main problem of such a system. In order to reduce this phenomenon, rotating filters have been developed. These systems use fast rotating cylinder filters mounted either on the stirrer shaft or driven independently by a rotor. Additionally, using synthetic neutrally charged materials instead of micro–porous positively charged stainless steel filters, which can interact with the negatively charged cells and/or DNA have also been shown to reduce filter fouling (Esclade et al., 1991).

The prerequisites for large–scale operation at long–term of spin–filter devices are a minimum filter fouling and optimum cell retention at high specific perfusion rates. Cell retention is influenced by several parameters, the most important being the material of construction of the filter, filter porosity, rotational speed of the filter, perfusion rate and cell concentration within the reactor. A number of investigators have studied the influence of filter pore size on the retention of cells. Animal cells have an average diameter of about 10–15 μm, consequently filter pore sizes less than 10 μm retain cells completely although, as a result, have a greater tendency to clog. High–density cultures of $1–2 \cdot 10^7$ cells/ml could be achieved in 30 days using spin–filters with pore sizes of about 10 μm (Van Wezel et al., 1985). Pore sizes greater than the average cell diameter are also used, maintaining good retention rates and avoiding fouling (Iding et al., 2000; Jan et al., 1992; Siegel et al., 1991). It is generally recommended that a mesh pore size equivalent to 1.5 times that of the cell diameter should be used, although pore sizes greater than 50 μm have been used for cell lines that have a tendency to form aggregates (Varecka and Scheirer, 1987).

By increasing the rotational velocity of the filter, the cells are swept off the screen surface by an increase in tangential velocity thus increasing the perfusion capacity of the system (Yabannavar et al., 1994). An increase in perfusion capacity induces an increase in perfusion rate, and thus an increase in cell density. However, increasing the cell density increases particle–screen interactions, which induce fouling of the filter (Deo et al., 1996; Yabannavar et al., 1992). As a result, optimization is needed for long–term cultures operation at high cell densities.

The most relevant published result with respect to high perfusion flow and long–term operation appears to be the internal spin-filter successfully applied in continuous perfusion culture at 500 L scale, at a perfusion rate of 500 L/day, with a cell density exceeding $1 \cdot 10^7$ cell/ml and for a period of 30 days (Deo et al., 1996).

Placing the spin–filter module outside the reactor has the advantage of easier scale–up and the added advantage of easy replacement of the unit thus preventing a premature termination of the culture (Woodside et al., 1998). External spin–filters have been developed for bioreactors up to 50 L (B. Braun Biotech, Melsungen, Germany) . The filter is operated in a glass cylinder with stainless steel top and bottom plates and is connected to the bioreactor by an external loop (Figure 1.3b). An adjustable stirrer is used for rotating the filter. The filter mesh is made of stainless steel with a pore size of 10 μm. The annular gap between the filter and the filter housing is minimal, in order to have a maximum filtration area per unit volume and to reach high surface Taylor vortices. Perfusion rates up to 100 L/day can be obtained, however higher harvest rates have not been reported since the commercial module can only be used with bioreactors up to 50 liters. External spin–filter for equipping reactors of 500 L to 1000 L, allowing high perfusion rates of about 350 L/day have also been developed (Bioengineering AG, Wald, Switzerland), however few information has been provided on the utilization of such devices for continuous animal cell separation at large–scale.

External spin–filters have many advantages compared to internal spin–filter devices. Clogging is minimal, due to formation of vortices at the surface of the filter, thus longer perfusion cultures can be achieved. The filter can be exchanged during operation of the reactor, thus reducing operational costs, and the system is versatile because it can be connected to different bioreactor sizes. However external filtration modules present some disadvantages, including retention of dead cells within the reactor and high residence time of cells outside the reactor under sub–optimal conditions. But the major problem is the need for pumps to provide high circulation rates of cells through the separation unit, which exposes animal cells to high shear stresses and limits the utilization of such devices at large–scale operation. The highest perfusion rate reported, using such separation device corresponds to 100 L/day that permitted to achieve a high cell density of $1.9 \cdot 10^7$ cell/ml for 58 days (Fraune et al., 1997).

1.2.1.2 Cross–flow filtration

Cross–flow filtration is an external separation process. It consists in generating flows tangential to the filter surface, in order to reduce filter fouling due to cell deposition and concentration of proteins, DNA and cell debris, in filter pores. The flow rate has to be optimized in order to avoid the disruption of cells due to generated shear rates. There are

two principle systems employed for tangential flow filtration: hollow fiber modules and plate–and–frame modules.

1.2.1.2.1 Hollow fiber modules

The separation module consists in hollow fiber tubular membranes in an arrangement of static or cross flow elements (Figure 1.4). Certain configurations of the separation system may be incorporated within the bioreactor, such as hollow fiber modules (Blasey and Jäger, 1991) or polymer fibers coiled as loose spirals within the bioreactor (Banik and Heath, 1994), however the majority of the units are employed as external modules.

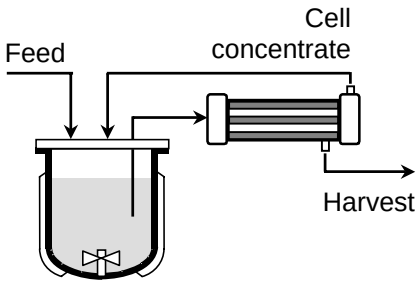

Figure 1.4: Schematic representation of an external hollow fiber module

The culture medium passes through the membrane fibers and cell–free supernatant passes through the pores of the membrane, while the concentrated cells are returned to the reactor and the permeate containing the harvested product is collected. Many polymeric membranes are used, such as polypropylene, PTFE or polysulfone membranes (Büntemeyer et al., 1994). The pores of the membrane range from 0.1 to 10 μm so that it retains both viable and non–viable cells, as well as cell debris. In spite of retention is maximal that facilitates the downstream processing of the process, filter fouling remains the principal problem. In order to diminish fouling of the membrane and increase its lifetime, the feed can be pulsed into the membrane (Smith et al., 1991) or the nutrients and/or oxygen can be introduced by back flushing into the membrane (Blasey and Jäger, 1991; Lehmann et al., 1988). Using back–flushing of the harvest line with fresh medium through the membrane of an internal hollow fiber module enabled viable cell densities of $1 \cdot 10^7$ cell/ml at 23 L scale to be reached during 16 days of operation (Büntemeyer et al., 1987). It was concluded that, in order to guarantee a stable culture for long operation

times, the filtration rate should not exceed more than one liter of culture broth per meter membrane and per day.

Fouling may also be reduced by increasing the shear rate at the surface of the filter, thereby increasing the perfusion flow in such a way that the trans–membrane pressure is not too high and cell deformation into the pores is avoided (Maiorella et al., 1991). However, in this case flow is limited by the shear sensitivity of the cell line. Cell damage was observed to occur above shear rates of 1200 s^{-1} for a hybridoma cell line (Zhang et al., 1993), while others observed no cell damage for shear rates up to 3000 s^{-1} for a range of animal cell lines (NS–1 myeloma, human hybridoma and murine hybridoma) using hollow fiber modules as well as flat and plate systems for cell separation (Maiorella et al., 1991).

Such hollow fiber systems work well for small–scale cultures, however large–scale cultures with high perfusion rates are not feasible over long term operation. The largest external hollow fiber culture reported was obtained in a 10 L–scale bioreactor, where only $3.6 \cdot 10^6$ cell/ml were achieved over a short period of 10.5 days of operation (Smith et al., 1991). In this case, the pore size was small and clogging appeared early in the culture. The inhomogeneous type of high–density cell culture, due to fiber structure, leads rapidly to clogging of the membrane. The separation of viable and non–viable cells is not possible and shear sensitive cells are subjected to high pumping rates that damage the cells and limit the cell density at high perfusion rates.

1.2.1.2.2 Plate and frame modules

To protect cells from shearing effects, low linear speeds applied at the membrane surface were necessary and separation modules achieved by cross–flow filtration were developed (de la Broise et al., 1991; de la Broise et al., 1992; Velez, 1989), as represented in Figure 1.5.

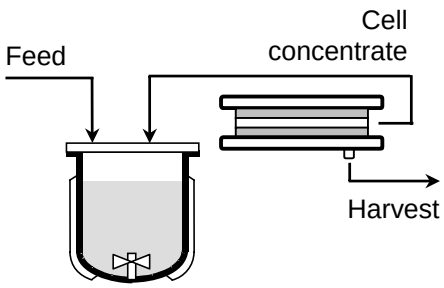

Figure 1.5: Schematic representation of an external plate–and–frame module.

The simplest module consists of synthetic (nylon, PVDF) membranes sandwiched between channel plates and filtrate plates (Kawahara et al., 1994; Velez, 1989). The culture broth pumped through the channel plate passes over the surface of the membrane causing a pressure increase that forces cell free liquid through the membrane. The flow of liquid over the surface helps to clear the membrane and retards clogging of the filter pores.

More complicated modules consist of an external plate and frame cross–flow filtration module with three stainless steel plates supporting two membranes (Mercille et al., 1994). The upper and lower plates support the membranes and collect the permeate. The middle plate contains open zigzag paths along its length, which channel the cell suspension horizontally and tangentially between the two membranes, such that a high pressure is not applied directly to the membrane surface. In order to minimize cell accumulation, a compressible geotextile material was developed, which reduces secondary flow and obliges the flow of medium to go through the channels (Mercille et al., 1994). Increasing the membrane surface area and washing the membrane once a day (medium flushed into the device at a flow–rate about eighty times greater than that of the cell suspension, by closing the permeation line) was found to reduce the clogging of the membrane (Kawahara et al., 1994). Under such conditions, high–density cell cultivation was achieved over approximately one month using a 1 L reactor volume, however the clogging of the membrane could not be completely eliminated and, after about 20 days, the perfusion rate decreased because of membrane fouling.

This perfusion system may be run continuously for several months by replacing the membrane if fouling occurs, since the filter unit is located outside the reactor and is scalable by stacking filter units. However, it only permits low perfusion rates for small–scale cultures. Indeed, the largest plate–and–frame perfusion culture reported was realized at 3.6–L scale and at a perfusion rate of 3.6 L/day (de la Broise et al., 1991). Additionally, cross–flow filtration induces high–pressure drops generated by high shear flows that create inhomogeneous filtration conditions over the filtration surface and make the system neither very stable nor robust. Furthermore pumping the cells at high velocity induces mechanical stress on the cells. The rapid fouling of the filter remains the main limitation, as well as the long residence time of cells inside the device. These residence times are significantly longer than for hollow fiber filtration systems.

1.2.1.3 Dynamic filtration

Dynamic filtration is based on high shear generation at the filter surface. This shear force is formed by the motion of a rotor in the separation chamber (Figure 1.6). The rotor may have a number of different configurations, including a concentric cylinder (Kroner and Nissinen, 1988; Rebsamen et al., 1987), a conically shaped disc (Vogel et al., 2002; Vogel and Kroner, 1999) and a disk–type rotor (Castilho and Anspach, 2003).

The separation mechanism is based on size separation by filtration, while fouling is prevented by the motion of the rotor, generating a Taylor–Couette flow in the annular gap between the rotor and the filter surface (Wereley and Lueptow, 1999). This Taylor–Couette flow creates vortices, which clean the surface of the filter, thereby preventing concentration polarization and reducing filter fouling. Thus the shear rate induced by the motion of the rotor is not coupled to the perfusion flow.

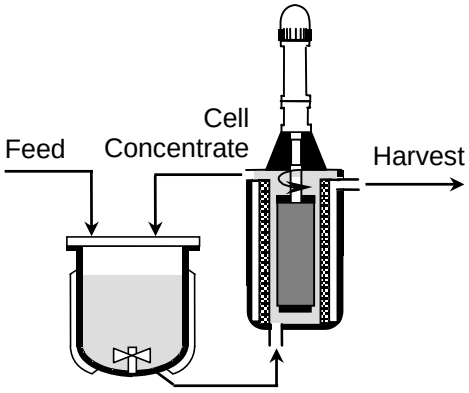

Figure 1.6: Schematic representation of a vortex–flow filter.

Taylor numbers up to 700 were found to have no effect on the viability of human breast carcinoma cells. However, cell loss was observed within the reactor, caused by cells remaining within the filtration unit (Rebsamen et al., 1987). The longevity of filtration membranes was found to be considerably greater using a vortex–flow filtration module than a static plate–and–frame cross–flow filtration module (Mercille et al., 1994). The use of vortex–flow filtration in conjunction with DNaseI allowed maintenance of perfusion cultures for more than 1 month without membrane fouling or antibody retention.

Three–fold higher flux rates were obtained employing a conically shaped disc than with a conventional cylinder motor, however the main disadvantage of such a configuration was the low membrane surface available which limits the perfusion capacity at larger scale (Vogel and Kroner, 1999).

The decoupling of shear generation and perfusion flow through the filter enables low pressure operation without the problems of filter pressure drop along the membrane, as found in the case of cross–flow filtration systems, however there is no real advantage compared to external spin–filter systems and scale–up remains difficult. In spite of high cell concentration of $4.6 \cdot 10^7$ cell/ml achieved, maximum perfusion flows of only 7 L/day were reported during hybridoma cell culture at 1.6–L scale (Mercille et al., 2000).

1.2.2 Separation by density

Many separation techniques based on the difference in density between cells and the medium have been developed for cell removal. In each technique, the force acting on the cell is different, however the basic separation principle remains the same. Centrifugation uses centrifugal forces to settle particles within the liquid, in settling devices separation is due to gravity forces, while in acoustic devices, a standing wave drives the cells towards the nodes of a resonance electric field.

1.2.2.1 Centrifugation

Separation of cells by continuous centrifugation is a process that is applicable to large–scale cultures. Although the principle is very simple, centrifuges are rather complex devices (Figure 1.7).

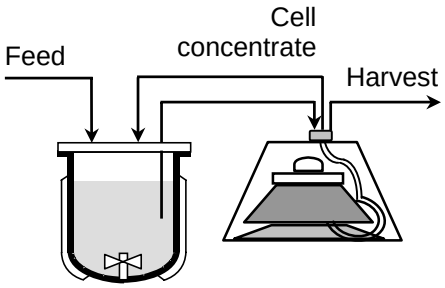

Figure 1.7: Schematic representation of an external centrifuge.

The centrifuge is required to separate cells from culture medium without damage to the cells while allowing the cells to return to the culture tank under sterile conditions, without losing proliferation capability, the latter being the main limitation of such a technique. Two centrifuges are available on the market for continuous large–scale

perfusion cultures: the Centritech centrifuge (Kendro Laboratory Products, Geneva, Switzerland) and the Westfalia centrifuge (Westfalia Separator AG, Oelde, Germany).

1.2.2.1.1 The Centritech centrifuge

Kendro has two continuous centrifuges available for cell separation, with different capacities. The Centritech Lab centrifuge is a small–scale system with operating flow rates from 12 to 240 L/day, while the Centritech Cell centrifuge is suitable for pilot–to–production scale operation since it can handle flow rates up to 2800 L/day. The Centritech Lab centrifuge has been extensively tested, unfortunately there is little published information concerning the successful scale–up of the Centritech Cell device (Johnson et al., 1996).

The Centritech centrifuge was developed in such a way that the shear stress is minimal. Cell separation takes place in a pre–sterilized insert, the configuration of which is like an inverted question mark and permits one end of the tube to be rotated while the other end is fixed (Figure 1.7). The cell suspension is fed into an inlet at the top of one end of a pre–sterilized insert and the cells are drawn to the bottom of the rotor by the centrifugal force. Concentrated cell suspensions are drawn back into the reactor from an outlet at the bottom of the insert, while the clarified supernatant exits from an outlet at the top of the other end. The system can be operated in either continuous or intermittent modes, which result in different separation and discharge times. The separation efficiency for non–viable cells is smaller than for viable cells. As a result, the accumulation of dead cells and cell debris is reduced compared to other separation modules. High perfusion rates are achieved in an intermittent function mode and for longer time periods, since clogging does not occur. However, the insert has an operational lifetime of approximately 20 million revolutions (corresponding to 12 days of continuous operation at 1200 rpm) and therefore has to be replaced during culture operation.

Mammalian cells, such as hybridoma and CHO cells, have been reported to withstand the centrifugal forces involved, with centrifugal accelerations of 200 g having no effect on cell viability or productivity (Chatzisavido et al., 1994; Tokashiki et al., 1990). The Centritech centrifuge efficiently separates viable from dead cells over a certain range of rotational speeds (Johnson et al., 1996). It seems that the cell content of the centrifuge supernatant and concentrate is not only determined by centrifugation parameters (times of separation and of discharge, feed rate, rotor speed, etc.) but also by the total amount of

cells (viable and dead) fed to the separation chamber (Johnson et al., 1996). The latter authors compared the Centritech Lab centrifuge and a filtration module for cell separation and observed similar growth rates although, MAb concentrations were 35% lower using the centrifuge. However, utilization of the centrifuge in an intermittent fashion decreased the daily cell residence time outside the reactor, the daily pelleted–cell residence time in the centrifuge, and the frequency of cell passage to the centrifuge. This led to higher numbers of viable cells in the bioreactor and an accompanying increase in MAb concentration, to levels comparable with the performance of filter–based perfusion systems with the same cell line. It has been hypothesized that having cells periodically packed at the bottom of the centrifuge insert is deleterious to the culture by exposing the pelleted cells to prolonged nutrient limitations.

The system has the advantage of separating cells from the medium broth at high rates and with high retention efficiency. However, operating the centrifugal system at high perfusion rates has certain disadvantages. High bowl speeds result in high operating costs for noise protection and power consumption (Axelsson, 2000). Adverse conditions common to high centrifugation flow rates are cell shearing that causes mammalian cells to brake–up inside the centrifuge and may reduce yield and purity of the product. Thus centrifugation rate has to be optimized in order to get high retention efficiency and avoid shear–induced disruption of cells.

1.2.2.1.2 The Westfalia centrifuge

In this system, the cells are separated from the supernatant by means of a disc stack. During simulations of large–scale perfusion culture of CHO cells, it was shown that cells were not damaged by high centrifugal forces up to 500g (Björling et al., 1995). By contrast to the Centritech centrifuge, a cooling system is available, which removes the frictional heat, which might otherwise precipitate or denature the protein product.

The parameters that have to be optimized in such separation device are: the separation capacity, the rotor speed and the feed and/or the supernatant flow rates. The separation capacity is dependent on the rotor speed. If the supernatant flow rate exceeds the maximum flow rate with a fixed rotor, cells would appear in the supernatant and induce cell accumulation in the rotor, which will clog with time and thus reduce the separation efficiency and long–term operation.

A viable cell density of about $1 \cdot 10^7$ cell/ml was obtained during intermittent centrifugal separation of HeLa cells with a 21 L bioreactor operating at a perfusion rate of up to 43 L/h (Jäger, 1992a). After 12 days of operation, the rotor was opened and no sediment or clogging was detected, as a result of the continuous circulation velocity being maintained higher than the sedimentation velocity generated by the centrifugal force. However, during the performance of a longer perfusion culture with the same cell line, signs of clogging after 27 days of operation at maximal perfusion flow of 13.5 L/h were observed (Jäger, 1992b). During continuous separation of hybridoma cells by centrifugation, a cell density of 10^7 cell/ml was obtained during 37 days with stable productivity with a 10 L bioreactor operating at a perfusion rate of up to 20 L/day (Tokashiki et al., 1990). However under identical culture conditions, it was found that the viable cell density and protein productivity obtained using this system were equivalent to those obtained by intermittent centrifugation and by gravitational settlement cell separation.

The advantage of the Westfalia centrifuge over the Centritech Lab centrifuge is the existence of a cooling system and a shorter residence time of cells in the device. However, the disc–stacks are more exposed to clogging during long–term cultures due to the complex channel structure compared with the simple bowl structure. Both centrifuges permit continuous cell separation with high separation efficiencies, however cells sensitive to centrifugal fields and/or static pressures cannot be separated by such systems. However, centrifugal forces could be reduced by expanding the separation area and/or by using a smaller rotor, although this would be accompanied by a loss in separation efficiency. The Westfalia centrifuge permits higher perfusion flows than the Centritech centrifuge, which would favor its use for large–scale culture operations. Indeed, a 100–L scale perfusion culture at 1000 L/day during 16 days of operation has been reported, although the achieved cell density of $3 \cdot 10^6$ cell/ml was low (Björling et al., 1995). The influence of residence time of cells out of the reactor has also to be considered. Too long residence times could change the physiology of cells due to nutrient and oxygen limitations and thus change the product quality. The aggregation of cells in the centrifuge is a disadvantage, creating diffusion problems and rotor clogging that limits cultures operation. Although the system requires higher investment costs than other separation systems, because of the complexity of the device, it allows high perfusion rate operations and appears to be one of the most relevant devices for animal cell separation at large–scale operation.

1.2.2.2 Gravitational settling devices

In gravitational settling devices, the cells are separated from the culture in the settling zone by gravity, while some of the insoluble components originating from dead cells are removed from the culture, together with the supernatant, through the top of the settling zone (Figure 1.8). The driving force of gravitational settling is the density difference between animal cells and the culture media that corresponds to approx. 50 kg/m^3. Mammalian cells settle at a low rate of 1 to 3 cm/h in a gravitational field, resulting in a low cell separation capacity (Tokashiki and Takamatsu, 1993).

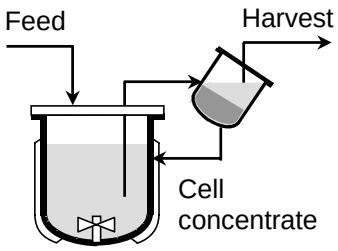

Figure 1.8: Schematic representation of an external inclined settler.

Most of the devices are used externally (Hülscher et al., 1992; Searles et al., 1994), however internal devices to the bioreactor have also been developed (Arai et al., 1993; Knaack et al., 1994; Sato et al., 1985; Shintani et al., 1991). Two different settler configurations are mainly employed: vertical settlers and inclined settlers. The advantage of using inclined settlers is the enhancement of settling velocity by taking advantage of the Boycott effect (Acrivos and Herbolzheimer, 1979), with the main disadvantage being cell accumulation on the lower part of the settling plate. In order to reduce cell attachment and to enhance return of cells back to the reactor, a vibrating external three–port inclined settler was developed (Searles et al., 1994). Although low perfusion rates were employed, high cell density culture of $1 \cdot 10^7$ cell/ml could be obtained with an inclined settler device that selectively retained viable cells and removed non–viable cells (Batt et al., 1990). Working at higher perfusion rates necessitates increasing the settler dimensions, either by increasing the area of a single plate, or by utilizing multiple settling plates. Indeed, the overflow rate at which hybridoma cells were first washed–out was observed to be lower with a short settler than with a much larger one (Batt et al., 1990). Using a multi–lamella inclined settler that contains mirror–polished stainless steel plates, in order to increase the settling surface permitted to reach a viable cell density of $5 \cdot 10^6$ cell/ml at maximum perfusion rate of 2.4 day^{-1} (50 L/day) (Thompson and Wilson, 1994). Comparable cell

concentrations ($4 \cdot 10^6$ cell/ml) at higher perfusion rates of 4 day^{-1} have been obtained using a lamellar clarifier in a by–pass stream, where free flow convection through the settler was achieved by cooling the cell suspension before it enters the settler (Stevens et al., 1994). A perfusion system for animal cell cultures, involving two–step sequential sedimentation, comprising a vertical settling tank and a horizontal flat settler, was also studied (Wen et al., 2000). Using a small volumetric ratio of settling device to culture volume, the system showed high separation efficiency, with a cell density of $1.3 \cdot 10^7$ cell/ml obtained after 16 days using a 1.5 L bioreactor at a maximum dilution rate of 2 day^{-1}.

Gravitational settling devices are simple and convenient to operate and have no physical barriers such as membranes, which can clog. Sensitive cells can be efficiently separated because of very low shear forces. Extended cultures can be achieved since dead–cell and debris are removed from the culture with the culture supernatant without problems of clogging for simple settler configurations. Multiple plate designs however, share two common problems. First, a single pump removes the overflow from many plates, causing flow distribution problems that decrease the separation efficiency of such a device. The second is the increase of uncontrollable residence time of the cells in the settler. Indeed, once the cells have settled and are sliding off the top of the channels, they adhere on the plate surface, enhancing the fouling of the device or are retained in the up–flow through the lower channels. As a result, viable cells are not returned rapidly to the reactor and are exposed to non–optimal growth conditions.

The low gravitational settling of cells in vertical configurations is not efficient enough to permit fast perfusion rates needed in order to maintain high cell densities, at large–scale operation. Increasing the perfusion rate decreases the separation efficiency of such devices, unless the settler surface is increased to high extents that involve higher ratios of separation volume per working volume of the bioreactor than those involved in other separation devices. Using an internal vertical configuration settler, high cell density of $1.2 \cdot 10^6$ cell/ml could be achieved with a maximal perfusion flow of 100 L/day, during 30 days (Arai et al., 1993). Although inclined settlers improve cell–settling velocity, they are limited in time operation because of cells and debris adhesion at the wall that foul the inclined surface. The maximal perfusion rate reported using an external inclined settler was 50 L/day, during the culture of hybridoma cells for 24 days, within a 21 L bioreactor (Thompson et al., 1994). However, combined with another separation system, settling devices could be effective modules as a first–stage cell separation system during continuous cell culture.

1.2.2.3 Acoustic devices

The acoustic aggregation sedimenter exploits, as with the centrifugal separator, the inertial properties of cells instead of using physical barriers to perform the separation and relies on cell aggregation in a standing acoustic field followed by enhanced sedimentation, as the separation principle (Bierau et al., 1998; Gaida et al., 1996; Kilburn et al., 1989; Ryll et al., 2000). Such a separation device is shown schematically in Figure 1.9.

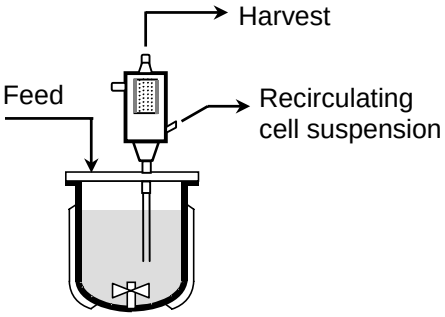

Figure 1.9: Schematic representation of an ultrasonic filter.

This system uses high frequency resonant ultrasonic waves to separate cells instead of a physical mesh or membrane. Cell separation takes place within a defined volume of the resonance chamber, which is sterilizable in situ. Basically, the resonator is composed of two opposed parallel glass surfaces, of which at least one surface is piezoelectrically activated and acts as an ultrasonic source. As a result, at specifically selected frequencies, an acoustic standing field is established within the cell suspension between the glass walls. The acoustic energy mesh acts as a virtual filter capable of capturing cells within the antinodes of the field and thus, retaining cells from the fluid. The trapped cells form aggregates which settle out of the acoustic field by periodically shutting off the resonator, and return back to the bioreactor through the continuous re–circulation of cell suspension, followed by cells re–suspension by stirring. The clarified medium exits from the reactor via a harvest pump. The retention efficiency depends mainly on the frequency of the resonator, the perfusion flow, as well as the power input and the frequency of the on/off cycles.

Ultrasonic treatments at high power levels (up to 5 W) were reported to have no negative effects on either cell viability or cell productivity (Bierau et al., 1998; Trampler et al., 1994). Power inputs of up to 80 W were applied to a human hybridoma cell line and neither decrease in cell viability nor degradation of filter performance, within a 50–ml

resonator chamber, was observed (Gröschl et al., 1998). No effect on cell viability was observed until power levels of 260 W/L (Pui et al., 1995). The main disadvantage of using acoustic power is the associated rise in temperature. The medium temperature increases within the resonator chamber at a rate of 1.3 °C per minute during acoustic treatment at 180 W/L (Pui et al., 1995). However, by cooling the outside surfaces of the transducers with a cross flow of ambient air, free convection could be minimized and resonance power and stability increased (Trampler et al., 1994).

Using such a device, high viable cell densities ($2.2 \cdot 10^7$ cell/ml) and high cell retention (90 to 96%) were obtained after 700 hours of hybridoma cell culture at a final dilution rate of 3 day^{-1} (Trampler et al., 1994). It has been observed that increasing the flow rate, the cell separation efficiency decreases due to the increased upward fluid drag on cell aggregates (Zhang et al., 1998). For separation efficiency of over 90%, the maximum perfusion rate was determined to be about 8 L/day during Sf9 insect cell cultures (Zhang et al., 1998), and 12 L/day during hybridoma cell culture (Trampler et al., 1994). The acoustic device retained viable cells with an efficiency of about 3% higher than non–viable cells, due to size and compressibility differences between viable and non–viable cells (Trampler et al., 1994). However, this was not sufficient to prevent the accumulation of dead–cell debris. The separation performance was found to be inversely proportional to cell concentration and perfusion rate, as a consequence of cell accumulation in the resonator chamber at high cell densities (Ryll et al., 2000). By comparing a 10 ml ultrasonic chamber device with a spin–filter device under similar constraints, similar maximum cell densities have been achieved (Bierau et al., 1998). The ultrasonic filter was operated at perfusion rates between 0.7 and 2 day^{-1} at high cell retention (about 99%) and no dependence between the separation efficiency and flow rate was observed. Visible cell aggregates within the reactor were formed after the cell density reached $1 \cdot 10^6$ cell/ml, which may be caused by the ultrasonic field during the aggregation phase of the cells, which after returning to the reactor, do not disperse completely. Alternatively this aggregation may result from dead cell material, including DNA.

The most common acoustic device is the BioSep commercialized by AppliSens (Schiedam, Holland). Three BioSep systems have been developed for application at different scales. For separation efficiency above 95%, the perfusion capacities are 10 L/day, 50 L/day and 200 L/day for 10 L, 50 L and 250 L Biosep respectively. For animal cell culture, the 10 and 50 L Biosep have mainly been tested. This separation module has no moving parts, is easily cleaned and sterilized in situ. Cells sensitive to shear forces

may be easily separated. The retention level of the device is very high, involving high separation efficiency. However, at long–term operation, a local temperature gradient is created inside the resonator chamber, which could damage cells and/or the product and which disturbs the acoustic field, thereby decreasing its performance (Doblhoff–Dier et al., 1994). Another limitation is the change of separation efficiency with an increase of perfusion rate. Thus any change in perfusion rate requires high supervision in order to modify the separation parameters of the acoustic device.

At present, the ultrasonic device is used for small–scale perfusion culture, with acoustic devices for large–scale cultures yet to be successfully tested. A 200 L BioSep device was evaluated during CHO perfusion cultures (Gorenflo et al., 2002). This separator is divided into four parallel temperature–controlled compartments within a single separator. The maximum separation performance (96%) was obtained at 200 L/day by setting the separator to 35.1°C and the power to 90 W. Higher flows decreased the separation efficiency to 57% at a perfusion rate of 400 L/day. However, these results were carried out during short culture simulations and no actual perfusion cultures were undertaken over long–term operation at large–scale. The maximum perfusion rate that can be achieved for long–term continuous cell culture corresponds to 50 L/day. The most relevant published culture with respect to high perfusion flow and long–term operation achieved $8.7 \cdot 10^6$ cell/ml at 28.5 L/day during 42 days of operation (Gröschl et al., 1998).

1.3 Discussion and general conclusions

In the previous sections the different separation techniques for animal cell separation and recycle during continuous cultures were discussed. Many reviews have been published until now on these separation techniques (Castilho and Medronho, 2002; Voisard et al., 2003; Woodside et al., 1998).

All of the separation systems present advantages and disadvantages and the difficulty is to decide on which basis they can be compared. In the previous section, they have been compared according to perfusion flow performance and culture longevity during high cell density cultures. The best cultures of each separation technique, in terms of scale–up (reactor size/ perfusion capacity), viable cell density reached and operation time have been summarized in Table 1.2.

Table 1.2: Comparison of animal cell separation techniques

	Working volume (l)	Perfusion flow (l/day)	Culture time (days)	Viable cell density ($1{\cdot}10^6$ cell/ml)	Cell line	Fouling	Type	Reference
Internal spin-filter	500	500 - 600	30	11	Hybridoma	?	Stainless steel 15 µm	Deo et al., 1996
Centrifuge	100	1000	16	3	CHO	Yes, rotor clogged	Disc-stack centrifuge	Björling et al., 1995
External spin-filter [a]	60	100	58	12	Hybridoma	?	Stainless steel 10 µm	Fraune et al., 1997
Internal settler	50	100	30	12	Mouse/ human hybridoma	No	Inner and outer cylinders	Arai et al., 1993
External settler [b]	21	50	24	5	Mouse/ mouse hybridoma	?	Conical inclined lamellar settler	Thompson et al., 1994
External hollow fiber module	10	15	10.5	2.1 - 3.6	Hybridoma	Yes	Cellulose ester, 0.2 µm	Smith et al., 1991
Ultrasonic filter	5.25	28.5	42	8.7	Human hybridoma	Yes	50-ml resonator chamber	Gröschl et al., 1998
Plate & frame module [c]	3.6	3.6	46	4.0 - 6.0	Hybridoma	Yes	Nucleopore, 2 µm	de la Broise et al., 1991
Internal hollow fiber module	2	1.6	41	7	Rat/ mouse hybridoma	Yes	Polypropylene, 0.3 µm	Büntemeyer et al., 1994
Vortex flow filtration	1.6	2.5/ 6.8	28/ 21	14.9/ 45.7	Mouse/ mouse hybridoma	?	Polysulfone, 0.8 µm	Mercille et al., 2000

[a] viability at the end: 63%, [b] viability at the end: 47%, [c] viability at the end: 30% and membrane changed during process

The technique with the least potential appears to be the internal hollow fiber and the plate–and–frame filtration modules. In spite of long–term operation greater than 40 days, and maximum cell density attained of 4–7·10^6 cell/ml, published cultures have been achieved only at small–scale operation. Cross–flow filtration suffers from relatively low perfusion capacity due to the use of limited perfusion flows, in order to avoid high shear forces and loss in cell viability. In the same way, despite the use of a continuous cleaning strategy, internal hollow fiber modules have not yet been operated at high operation scale. Vortex–flow filtration cultures have been carried out at small–scale operation, reaching quite high cell densities up to 4.5·10^7 cell/ml for more than 20 days. Despite the reduction of fouling at small scale, due to Taylor vortex formation, the maximum perfusion rate achieved of 7 L/day is relatively low and limits its operation at large scale.

External hollow fiber modules were reported to operate at maximal perfusion rates of 15 L/day within a 10 L bioreactor. The maximal cell density is quite low (3.6·10^6 cell/ml) and rapid filter fouling permitted operation of the culture for only 10 days. Ultrasonic filtration devices have been operated for more than 42 days at 5.3 L scale and perfusion rates of 28.5 L/day. The cell density reached almost 1·10^7 cell/ml. However, the highest cell concentration is reached very slowly and system parameters have to be defined before each culture performance, which reduces the versatility of the system. Moreover, system parameters change during operation requiring higher culture control than usual. Heat evacuation during the process remains a major problem for large–scale operation and results in reduced separation efficiency. External settlers show a higher scale–up potential, with reports of cultures carried out at 21 L scale. In spite of high perfusion flows employed of 50 L/day, the cell density reached is quite low (5·10^6 cell/ml) because of low cell sedimentation velocities and reduced capacity to yield cell–free harvest.

Results of cultures using internal settlers and external spin–filter devices have been published for mid–scale operation up 50 and 60 L respectively. Similar perfusion rates of 100 L/day have been achieved. Although these perfusion rates are lower than those required for large–scale operation (above 400 L/day), high viable cell densities of 1.2·10^7 cell/ml were obtained for both systems during 30 days and respectively 58 days of operation. However, the internal settler needs special reactor configurations that make the system inflexible and, being internal, it suffers from limited space that leads to low separation capacity at larger scale. External spin–filters have the advantage not being limited by the choice of surface per working volume ratio, however increasing scale induces much higher perfusion rates within the module, thus increasing the shear rate

which may be harmful for the cells. Additionally, the need for pumps to provide high circulation rates of cells through the separation unit exposes also the animal cells to high shear stresses and limits the utilization of such device for large–scale animal cell perfusion cultures.

The techniques with the highest potential for large–scale cell separation with respect to perfusion capacity appear to be centrifuges and internal spin–filters. The published data show scale–up until 100 L and 500 L for perfusion culture using disc–stack centrifuges and internal spin–filters respectively. The centrifuges show high scale–up potential, allowing high perfusion flows of 1000 L/day, however the viable cell density reached is very low (approximately $3 \cdot 10^6$ cell/ml). At high perfusion rates, the system does not permit particle–free harvest, which explains the low viable cell density reached. Moreover, rotor clogging limited culture operation at 16 days, which is not sufficient for long–term cultures, which require over 30 days of operation. Cell aggregation within the separation device could also be harmful for the cells and the quality of the protein of interest. Additionally, the working parameters of the device have to be defined before the operation, thereby making the system difficult to use. Unlike to centrifuges, spin-filter cell separation systems permit to reach high cell densities ($1.1 \cdot 10^7$ cell/ml) and for long–time (30 days of operation). They allow also high perfusion flows of 600 L/day, despite filter pore size of 15 μm, which is greater than the average cell diameter. Decreasing the filter pore size permits higher filtration capacities at high cell retentions, however the major drawback of this separation technique is fouling of the filter. Such devices can be mounted internally in any bioreactor without any previous manipulations. However, a second limitation is the reduced filtration surface per reactor volume at higher scale–up.

Despite the advantage of fast replacement during operation of external separation modules, considerable drawbacks of these external devices compared to devices located inside the reactor have to be considered. First, is the residence time of the cells outside the controlled environment of the bioreactor and second the necessity of pumping cell–containing suspension that could damage the cells. For these reasons, and based on Table 1.2, it appears that internal spin–filters are the most suitable techniques for continuous cell separation at large–scale, in order to reach high cell density cultures and for long–time. It has been extensively used in industrial processes. However, although largely studied, it remains a very poorly understood technique with respect to cell retention and filter fouling mechanisms. Detailed literature survey should permit to identify why these mechanisms are poorly understood, and also identify the requirements for detailed

experimentation in order to define the operating culture conditions, as well as filter characteristics and parameters to be applied for successful operation of spin–filters at large–scale and long–time.

References

Acrivos, A. and E. Herbolzheimer, 1979. Enhanced sedimentation in settling tank with inclined walls. Journal of Fluid Mechanics. 92(3): p. 435-457.

Arai, T., Yokoyama, S., Tokashiki, M., 1993. 50 L scale perfusion culture of hybridoma cells by gravitational settling for cell separation. In: Kaminogawa S, Ametani A, Hachimura S, editors. Animal Cell Technology: Basic and Applied Aspects. Dordrecht, The Netherlands: Kluwer Academic Publishers. p 341–346.

Avgerinos, G.C., Drapeau, D., Socolow, J.S., Mao, J.–I., Hsiao, K., Broeze, R.J., 1990. Spin filter perfusion system for high density cell culture: production of recombinant urinary type plasminogen activator in CHO cells. Bio–Technol. 8:54–58.

Axelsson, H., 2000. Recent trends in disc bowl centrifuge development. Filtration & Separation. p 20–23.

Banik, G.G., Heath, C.A., 1994. An investigation of cell density effects on hybridoma metabolism in a homogeneous perfusion reactor. Bioprocess Eng. 11:229–237.

Banik, G.G., Heath, C.A., 1995. Hybridoma growth and antibody production as a function of cell density and specific growth rate in perfusion culture. Biotechnol. Bioeng. 48:289–300.

Batt, B.C., Davis, R.H., Kompala, D.S., 1990. Inclined sedimentation for selective retention of viable hybridomas in a continuous suspension bioreactor. Biotechnol. Progr. 6:458–464.

Bierau, H., Perani, A., Al–Rubeai, M., Emery, A.N., 1998. A comparison of intensive cell culture bioreactors operating with Hybridomas modified for inhibited apoptotic response. J. Biotechnol. 62:195–207.

Björling, T., Dudel, U., Fenge, C., 1995. Evaluation of a cell separator in large scale perfusion culture. In: al. ECBe, editor. Animal Cell Technology: Developments towards the 21st century: Kluwer Academic Publishers. p 671–675.

Blasey, H.D., Jäger, V., 1991. Strategies to increase the efficiency of membrane aerated and perfused animal cell bioreactors by an improved medium perfusion. In: Sasaki

R, Ikura K, editors. Animal Cell Culture and Production of Biologicals: Kluwer Academic Publishers. p 61–73.

Büntemeyer, H., Bödeker, B.G.D., Lehmann, J., 1987. Membrane–stirrer–reactor for bubble free aeration and perfusion. In: Spier RE, Griffiths J.B., editors. Modern approaches to animal cell technology. p 411–419.

Büntemeyer, H., Bohme, C., Lehmann, J., 1994. Evaluation of membranes for use in online cell–separation during mammalian–cell perfusion processes. Cytotechnology 15(1–3):243–251.

Castilho, L.R., Anspach, F.B., 2003. CFD–aided design of a dynamic filter for mammalian cell separation. Biotechnol. Bioeng. 83(5):514–524.

Castilho, L.R., Medronho, R.A., 2002. Cell retention devices for suspended–cell perfusion cultures. In: Scheper T, editor. Advances in Biochemical Engineering/ Biotechnology. Berlin Heidelberg: Springer–Verlag. p 129–169.

Chatzisavido, N., Björling, T., Fenge, C., Boork, S., Lindner–Olsson, L., Apelman, S., 1994. A continuous cell centrifuge for lab scale perfusion processes of mammalian cells. In: al. TKe, editor. Animal Cell Technology: Basic & Applied Aspects: Kluwer Academic Publishers. p 463–468.

de la Broise, D., Noiseux, M., Lemieux, R., Massie, B., 1991. Long–term perfusion culture of hybridoma: A "grow or die" cell cycle system. Biotechnol. Bioeng. 38:781–787.

de la Broise, D., Noiseux, M., Massie, B., Lemieux, R., 1992. Hybridoma perfusion systems: A comparison study. Biotechnol. Bioeng. 40:25–32.

Deo, Y.M., Mahadevan, M.D., Fuchs, R., 1996. Practical considerations in operation and scale–up of spin–filter based bioreactors for monoclonal antibody production. Biotechnol. Progr. 12:57–64.

Doblhoff–Dier, O., Gaida, T., Katinger, H., Burger, W., Gröschl, M., Benes E., 1994. A novel ultrasonic resonance field device for the retention of animal cells. Biotechnol. Progr. 10:428–432.

Dorresteijn, R.C., Numan, K.H., de Gooijer, C.D., Tramper, J., Beuvery, E.C., 1996. On–line estimation of the biomass activity during animal–cell cultivations. Biotechnol. Bioeng. 50:206–214.

Esclade, L.R.J., Carrel, S., Péringer, P., 1991. Influence of the screen material on the fouling of the spin filters. Biotechnol. Bioeng. 38:159–168.

Eyer, K., Oeggerli, A., Heinzle, E., 1995. On–line gas analysis in animal cell cultivation: II. Methods for oxygen uptake rate estimation and its application to controlled feeding of glutamine. Biotechnol. Bioeng. 45:54–62.

Fraune, E., Meichsner, S., Kamal, M.N., 1997. A new spinfilter design. In: al. MJTCe, editor. Animal cell technology: Kluwer Academic Publishers. p 283–287.

Gaida, T., Doblhoff–Dier, O., Strutzenberger, K., Katinger, H., Burger, W., Gröschl, M., Handl, B., Benes, E., 1996. Selective retention of viable cells in ultrasonic resonance field devices. Biotechnol. Progr. 12:73–76.

Gascoyne, P.R.C., Wang, X.–B., Huang, Y., Becker, F.F., 1997. Dielectrophoretic separation of cancer cells from blood. IEEE T Ind. Appl. 33(3):670–678.

Gorenflo, V.M., Smith, L., Dedinsky, B., Persson, B., Piret, J.M., 2002. Scale–up and optimization of an acoustic filter for 200 L/day perfusion of a CHO cell culture. Biotechnol. Bioeng. 80(4):438–444.

Griffiths, J.B., 1992. Animal cell culture processes – batch or continuous? J. Biotechnol. 22:21–30.

Gröschl, M., Burger, W., Handl, B., 1998. Ultrasonic separation of suspended particles – Part III: Application in Biotechnology. Acustica 84:815–822.

Gugerli, R., 2003. Polyelectrolyte–complex and covalent–complex microcapsules for encapsulation of mammalian cells: potential and limitations [N° 2720]. Lausanne: Swiss Federal Institute of Technology. 388 p.

Heine, H., Biselli, M., Wandrey, C., 1999. High cell density cultivation of hybridoma cells: spin filter vs immobilized culture. In: A. Bernard et al., editor. Animal cell technology: Products from cells, cells as products: Kluwer Academic Publishers. p 83–85.

Helenius, A., Aebi, M., 2001. Intracellular functions of N–linked glycans. Science 291:2364–2369.

Hubble, J., 1997. Affinity cell separation: problems and prospects. Trends Biotechnol. 15(7):249–255.

Hülscher, M., Scheibler, U., Onken, U., 1992. Selective Recycle of viable animal cells by coupling of airlift reactor and cell settler. Biotechnol. Bioeng. 39:442–446.

Iding, K., Lütkemeyer, D., Fraune, E., Gerlach, K., Lehmann, J., 2000. Influence of alterations in culture condition and changes in perfusion parameters on the retention performance of a 20 μm spinfilter during a perfusion cultivation of a recombinant CHO cell line in pilot scale. Cytotechnology 34:141–150.

Jacobsen, C.N., Fremming, C., Jakobsen, M., 1997. Immunomagnetic separation of Listeria monocytogenes for flow cytometric determination of viable cells in liquid. J. Immunol. Methods 31:75–81.

Jäger, V., 1992a. High density perfusion culture of animal cells using a novel continuous flow centrifuge. In: Murakami H, editor. Animal Cell Technology: Basic & Applied Aspects: Kluwer Academic Publishers. p 209–216.

Jäger, V., 1992b. The use of continuous flow centrifuge for long–term perfusion culture of animal cells. In: Kreysa G, Driesel AJ, editors. DECHEMA Biotechnology Conference 5 – Microbial principles in bioprocesses: cell culture technology, downstream processing recovery. Frankfurt, Germany. p 265–268.

Jäger, V., 1996. Perfusion bioreactors for the production of recombinant proteins in insect cells. Cytotechnology 20:191–198.

Jan, D.C.–H., Emery, A.N., Al–Rubeai, M., 1992. Optimization of spin–filter performance in the intensive culture of suspended cells. In: Spier RE, Griffiths JB, MacDonald C, editors. Animal cell technology: developments, processes and products. Oxford: Butterworth–Heinemann. p 448–451.

Jenkins N, Curling EMA. 1994. Glycosylation of recombinant proteins: Problems and prospects. Enzyme Microb. Tech. 16:354–364.

Johnson, M., Lanthier, S., Massie, B., Lefebvre, G., Kamen, A.A., 1996. Use of the Centritech Lab centrifuge for perfusion culture of hybridoma cells in protein–free medium. Biotechnol. Progr. 12:855–864.

Kawahara, H., Mitsuda, S., Kumazawa, E., Takeshita, Y., 1994. High–density culture of FM–3A cells using a bioreactor with an external tangential–flow filtration device. Cytotechnology 14:61–66.

Kilburn, D.G., Clarke, D.J., Coakley, W.T., Bardsley, D.W., 1989. Enhanced sedimentation of mammalian cells following acoustic aggregation. Biotechnol. Bioeng. 34:559–562.

Knaack, C., André, G., Chavarie, C., 1994. Conical bioreactor with internal lamella settler for perfusion culture of suspension cells. In: Spier RE, Griffiths JB, Berthold W, editors. Animal Cell Technology: Products of today, prospects for tomorrow. Oxford: Butterworth–Heinemann. p 230–233.

Kroner, K.H., Nissinen, V., 1988. Dynamic filtration of microbial suspensions using an axially rotating filter. J. Membrane Sci. 36:85–100.

Lehmann, J., Vorlop, J., Büntemeyer, H., 1988. Bubble–free reactors and their development for continuous culture with cell recycle. Animal Cell Biotechnology 3:221–237.

Maiorella, B., Dorin, G., Carion, A., Harano, D., 1991. Cross–flow microfiltration of animal cells. Biotechnol. Bioeng. 37(2):121–126.

Mercille, S., Johnson, M., Lanthier, S., Kamen, A.A., Massie, B., 2000. Understanding factors that limit the productivity of suspension–based perfusion cultures operated at high medium renewal rates. Biotechnol. Bioeng. 67(4):435–450.

Mercille, S., Johnson, M., Lemieux, R., Massie, B., 1994. Filtration–based perfusion of hybridoma cultures in protein–free medium: Reduction of membrane fouling by medium supplementation with DNase I. Biotechnol. Bioeng. 43:833–846.

Nahrgang, S., 2002. Influence of cell–line and process conditions on the glycosylation of recombinant proteins. Lausanne:Ecole Polytechnique Federale de Lausanne.150 p.

Prior, C.P., Doyle, K.R., Duffy, S.A., Hope, J.A., Moellering, B.J., Prior, G.M., Scott, R.W., Tolbert, W.R., 1989. The recovery of purified biopharmaceuticals from perfusion cell culture bioreactors. J. Parent. Sci. Techn. 43:15–23.

Pui, P.W.S., Trampler, F., Sonderhoff, S.A., Gröschl, M., Kilburn, D.G., Piret, J.M., 1995. Batch and semicontinuous aggregation and sedimentation of hybridoma cells by acoustic resonance fields. Biotechnol. Progr. 11:146–152.

Rebsamen, E., Goldinger, W., Scheirer, W., Merten, O.–W., Palfi, G.E., 1987. Use of a dynamic filtration method for separation of animal cells. Dev. Biol. Stand. 66:273–277.

Reuveny, S., Velez, D., Miller, L., Macmillan, J.D. 1986. Comparison of cell propagation methods for their effect on monoclonal antibody yield in fermentors. J. Immunol. Methods 86:61–69.

Reiter, M., Hohenwarter, O., Gaida, T., Zach, T., Schmatz, C., Blüml, C., Weigang, F., Nilsson, K., Katinger, H., 1990. The use of macroporous gelatin carriers for the cultivation of mammalian cells in fluidised bed reactors. Cytotechnology 3:271–277.

Ryll, T., Dutina, G., Reyes, A., Gunson, J., Krummen, L., 2000. Performance of small–scale CHO perfusion cultures using an acoustic cell filtration device for cell retention: Characterization of separation efficiency and impact of perfusion on product quality. Biotechnol. Bioeng. 69(4):440–449.

Sato, S., Kawamura, K., Hanai, N., Fujiyoshi, N., 1985. Production of interferon and monoclonal antibody using a novel type of perfusion vessel. In: al. HMe, editor.

Growth and differentiation of cell in defined environment. Heidelberg: Springer–Verlag. p 123–126.

Schneider, M., El Alaoui, M., von Stockar, U., Marison, I., 1997. Batch cultures of a hybridoma cell line performed with in situ ammonia removal. Enzyme Microb. Tech. 20:268–276.

Searles, J.A., Todd, P., Kompala, D.S., 1994. Viable cell recycle with an inclined settler in the perfusion culture of suspended recombinant chinese hamster ovary cells. Biotechnol. Progr. 10:198–206.

Shintani, Y., Kohno, Y., Sawada, H., Kitano, K., 1991. Comparison of culture methods for human–human hybridomas secreting anti–HBsAg human monoclonal antibodies. Cytotechnology 6:197–208.

Siegel, U., Fenge, C., Fraune, E., 1991. Spin filter for continuous perfusion of suspension cells. In: Murakami H, Shirahata S, Tachibana H, editors. Animal Cell Technology: Basic and Applied Aspects. Fukuoka, Japan: Kluwer Academic Publishers. p 434–436.

Smith, C.G., Guillaume, J.–M., Greenfield, P.F., Randerson, DH., 1991. Experience in scale–up of homogeneous perfusion culture for hybridomas. Bioprocess Eng. 6:213–219.

Stevens, J., Eickel, S., Onken, U., 1994. Lammelar clarifier – A new device for animal cell retention in perfusion culture systems. In: Spier RE, editor. Animal Cell Technology. Oxford: Butterworth–Heinemann. p 234–239.

Stryer, L., 1999. Biochemistry. New York: W. H. Freeman & Co. 1064 p.

Tanase, T., Ikeda, Y., Iwama, K., Hashimoto, A., Kataoka, T., Tokushima, Y., Kobayashi, T., 1997. Comparison of micro–filtration hollow fiber bioreactors for mammalian cell culture. J. Ferment. Bioeng. 83(5):499–501.

Thompson, K.J., Wilson, J.S., 1994. A compact gravitational settling device for cell retention. In: Spier RE, editor. Animal Cell Technology. Oxford: Butterworth–Heinemann. p 227–229.

Tokashiki, M., Arai, T., Hamamoto, K., Ishimaru, K., 1990. High density culture of hybridoma cells using a perfusion culture vessel with an external centrifuge. Cytotechnology 3:239–244.

Tokashiki, M., Takamatsu, H., 1993. Perfusion culture apparatus for suspended mammalian cells. Cytotechnology 13:149–159.

Trampler, F., Sonderhoff, S.A., Pui, P.W.S., Kilburn, D.G., Piret, J.M., 1994. Acoustic cell filter for high density perfusion culture of hybridoma cells. Bio–Technol. 12(3):281–284.

van Erp, R., Adorf, M., van Sommeren, A.P.G., Schönherr, O.T., Gribnau, T.C.J., 1991. Monitoring of the production of monoclonal antibodies by hybridomas. Part I: Long–term cultivation in hollow fibre bioreactors using serum–free medium. J. Biotechnol. 20:235–248.

Van Wezel, A.L., Van der Velden–de–Groot, C.A.M., de Haan, J.J., van den Heuval, N., Schasfoort, R., 1985. Large scale animal cell cultivation for production of cellular biologicals. Dev. Biol. Stand. 60:229–236.

Varecka, R., Scheirer, W., 1987. Use of a rotating wire cage for retention of animal cells in a perfusion fermentor. Dev. Biol. Stand. 66:269–272.

Vastola, M., 2000. Centrifuges: How they operate and how to select one. Filtration & Separation 37(4):16–19.

Velez, D., 1989. Use of tangential flow filtration in perfusion propagation of hybridoma cells for production of monoclonal antibodies. Biotechnol. Bioeng. 33:938–940.

Vogel, J.H., Anspach, F.B., Kroner, K.H., Piret, J.M., Haynes, C.A., 2002. Controlled shear affinity filtration (CSAF): a new technology for integration of cell separation and protein isolation from mammalian cell cultures. Biotechnol. Bioeng. 78:805–813.

Vogel, J.H., Kroner, K.H., 1999. Controlled shear filtration: A novel technique for animal cell separation. Biotechnol. Bioeng. 63(6):663–674.

Voisard, D., Meuwly, F., Ruffieux, P.–A., Baer, G., Kadouri, A., 2003. Potential of cell retention techniques for large–scale high–density perfusion culture of suspended mammalian cells. Biotechnol. Bioeng. 82(7):751–765.

Wen, Z.–Y., Teng, X.–W., Chen, F., 2000. A novel perfusion system for animal cell cultures by two step sequential sedimentation. J. Biotechnol. 79:1–11.

Werner, R.G., Walz, F., Noé, W., Konrad, A., 1992. Safety and economic aspects of continuous mammalian cell culture. J. Biotechnol. 22:51–68.

Woodside, S.M., Bowen, B.D., Piret, J.M., 1998. Mammalian cell retention devices for stirred perfusion bioreactors. Cytotechnology 28:163–175.

Yabannavar, V.M., Singh, V., Connelly, N.V., 1992. Mammalian cell retention in a spinfilter perfusion bioreactor. Biotechnol. Bioeng. 40:925–933.

Yabannavar, V.M., Singh, V., Connelly, N.V., 1994. Scaleup of spinfilter perfusion bioreactor for mammalian cell retention. Biotechnol. Bioeng. 43(2):159–164.

Yang, J., Huang, Y., Wang, X.J., Wang, X.B., Becker, F.F., Gascoyne, P.R.C., 1999. Dielectric properties of human leukocyte subpopulations determined by electrorotation as a cell separation criterion. Biophys. J. 76(6):3307–3314.

Zahler, S., Kowalski, C., Brosig, A., Kupatt, C., Becker, B.F., Gerlach, E., 1997. The function of neutrophils isolated by a magnetic antibody cell separation technique is not altered in comparison to a density gradient centrifugation method. J. Immunol. Methods 200:173–179.

Zhang, J., Collins, A., Chen, M., Knyazev, I., Gentz, R., 1998. High–density perfusion culture of insect cells with a BioSep Ultrasonic Filter. Biotechnol. Bioeng. 59(3):351–359.

Zhang, S., Handacorrigan, A., Spier R.E., 1993. A comparison of oxygenation methods for high–density perfusion cultures of animal cells. Biotechnol. Bioeng. 41:685–692.

2

Spin–filter as a separation device for animal cell perfusion cultures

Abstract

The growing demand for bio–engineered proteins in mammalian cells has stimulated the development of new cell culture techniques. The achievement of high cell densities, and thus high volumetric productivities, can be obtained using fed–batch or perfusion cultures. Perfusion culture may be preferred when the product may be subject to degradation and when the continuously dynamic culture conditions of batches may affect product quality. From an industrial point of view, external centrifuges and internal spin–filters show a high potential regarding perfusion capacity and culture longevity. Because of possible cell damage through pumping and a high residence time of cells outside the reactor, external devices are normally avoided. Thus, internal spin–filter devices would appear to be the most suitable technique for continuous cell separation at large–scale. This review will focus on spin–filter technology from its early development to the present day.

Keywords: animal cell, suspended cell, aggregate–forming cell, anchorage–dependent cell, spin–filter, cell retention, filter fouling.

2.1 Introduction

Progress in gene manipulation technology has made possible the production of physiologically active proteins such as monoclonal antibodies, recombinant therapeutic proteins and vaccines. Due to their complex structure, mammalian cells have been investigated and are commonly employed as hosts for the production of such proteins, particularly when the activity of the proteins is dependent on post–translational modifications. Many modes of mammalian cell cultivation exist including batch, fed–batch, continuous and perfusion cultures.

The high demand for conventional products, such as vaccines, necessitates a production volume of tens of thousands of liters per year. Therapeutic proteins, such as antibodies or tPA have an annual demand of about 10–20 kg per year, which would represent an annual reactor harvest of about 10^5 liters considering a protein concentration in the range of 100 mg/L (Hu and Peshwa 1991). Such relatively high culture volumes have stimulated the development of separation devices for continuous perfusion cultures, which enable higher cell concentrations (Figure 1.2) and higher volumetric productivities, R_p ($mg \cdot L^{-1} \cdot day^{-1}$) (Equations 2.1 and 2.2).

$$R_p\left(\text{continuous, perfusion}\right) = c_p \cdot D \cdot \frac{t_{prod}}{t_{run} + t_{dead}} = q_p \cdot X \cdot \frac{t_{prod}}{t_{run} + t_{dead}} \qquad \text{Eq.2.1}$$

where c_p (mg/L) is the product concentration per working volume, D (day^{-1}) is the dilution rate, q_p is the specific productivity ($mg \cdot cell^{-1} \cdot day^{-1}$), X ($cell \cdot L^{-1}$) the cell concentration, t_{prod} (day) is the duration of the production phase, t_{run} (day) is the duration of the bioreactor run and t_{dead} (day) the duration of the dead time between different runs.

$$R_p\left(\text{batch, fed}-\text{batch}\right) = c_p \cdot \frac{1}{t_{run} + t_{dead}} = q_p \cdot \int_0^{t_{run}} X\,dt \cdot \frac{1}{t_{run} + t_{dead}} \qquad \text{Eq.2.2}$$

where c_p (mg/L) is the product concentration per working volume, q_p is the specific productivity ($mg \cdot cell^{-1} \cdot day^{-1}$), t_{run} (day) is the duration of the bioreactor run and t_{dead} (day) the duration of the dead time between different runs.

The difference of volumetric productivities of different systems (batch/fed–batch and continuous/perfusion) depends mainly on the cell concentration achieved during the run and on the production, run and dead times of the processes. The animal cell concentration levels that can be reached in perfusion mode ($1–2 \cdot 10^7$ cell/ml) are higher

than in continuous (0.8–2·10^6 cell/ml), batch (1–2·10^6 cell/ml) or fed–batch (5–7·10^6 cell/ml) systems (Figure 1.2). Considering that dead times are similar for all systems and that the production time of perfusion/continuous systems is much longer than that of batch and fed–batch systems, it appears that the volumetric productivity of perfusion systems is higher than that of continuous, fed–batch and batch systems. Indeed, averaged protein productivity with a perfusion system of 660 mg·L^{-1}·day^{-1} was obtained compared to 15 and 27 mg·L^{-1}·day^{-1} for batch and fed–batch operation respectively (Reuveny et al. 1986). Comparison of batch and perfusion cultures employing an internal microfiltration device (at low perfusion rates) or an internal spin–filter (at high perfusion rates) concluded that the optimum solution for the production of the protein of interest, using human leukemia cells, is a high dilution rate perfusion process with cell retention (Stiens et al. 2000). Thus comparison of batch and/or fed–batch systems to perfusion systems shows that the latter in general achieve the highest volumetric productivity at smaller scale and for longer operation times (Favre and Thaler 1992; Griffiths 1992). Furthermore, it shows significant reduction in capital investment on bioreactors and building space (Kong et al. 1998) and considerable time savings (Werner et al. 2002). Additionally, perfusion culture is preferred to batch/fed–batch culture when products are susceptible to degradation e.g. by protease attack, or are affected by high culture residence times and/or by changes in culture conditions (Curling et al. 1990; Jenkins et al. 1994; Li et al. 1991), however the longevity of the culture depends on the robustness of the separation system and may represent a major limitation.

Many animal cell separation devices have been developed until now, according to the physical and chemical properties of the cells: size, mass, charge, hydrophobicity and density, with size and density the properties the most explored. In industrial animal cell culture processes, the most investigated separation processes based on these properties use spin–filters, hollow fiber modules, plate–and–frame modules (Avgerinos et al. 1990; Büntemeyer et al. 1994; Vogel and Kroner 1999) with respect to size separation and settling devices, centrifuges, hydrocyclones and acoustic filters (Ryll et al. 2000; Searles et al. 1994; Tokashiki et al. 1990) with respect to density separation. The majority of cell retention devices separate cells on the basis of size or density. Many reviews have been made until now on these separation techniques (Castilho and Medronho 2002; de la Broise et al. 1992; Voisard et al. 2003; Woodside et al. 1998). All of the separation systems present advantages and disadvantages and the difficulty is to decide on which basis they can be compared. The best published results, in terms of scale–up potential

(high perfusion capacity), high viable cell density achieved and high operation time of the animal cell separation device, external centrifuges and internal spin–filter devices present the biggest potential (Table 1.2).

Despite the advantage of fast replacement during operation of external separation modules, considerable drawbacks of external devices compared to devices located within the reactor have to be considered. First, is the residence time of the cells outside the controlled environment of the bioreactor and second the necessity of pumping cell–containing suspensions that could damage the cells. For these reasons, the use of internal separation devices is considered preferable and internal spin–filter device gained increasing recognition as one of the most efficient methods for the production of high value biologicals (Emery et al. 1995).

This review summarizes the published studies on the utilization of spin–filters as a cell separation device, since their development in 1969 (Himmelfarb et al. 1969), for lab–scale as well as for large–scale perfusion processes. The prerequisites for efficient operation at large–scale and for long–time of spin–filter devices are high cell retention at high specific perfusion rates and minimum filter fouling. As a result, this review will highlight the influence of each parameter related to culture characteristics and variables, as well as filter characteristics, on cell retention and filter fouling.

2.2 Spin–filters for suspended cell separation

A typical internal spin–filter device consists of a cylindrical wire cage with a porous wall, mounted either on the stirrer shaft or driven by an independent motor (Figure 2.1). Spent medium (permeate) is withdrawn from within the filter while fresh medium is added to the culture either at the same rate or at higher rate in order to allow a low bleed rate. Spin–filters devices allow the continuous separation of different types of cells including suspended cells, anchorage–dependent or immobilized cells and aggregate–forming cells.

The first reports of spin–filters as a cell separation technique described the successful perfusion of suspended mammalian cells (Himmelfarb et al. 1969). The stainless steel mesh was covered by a polymeric membrane filter with a porosity of 3 μm and rotated at 300 rpm, and attained a high viable cell density of about $6.5 \cdot 10^7$ cell/ml, within 10 days of operation. These first results showed the potential of such a device to allow the growth of animal cells to very high levels.

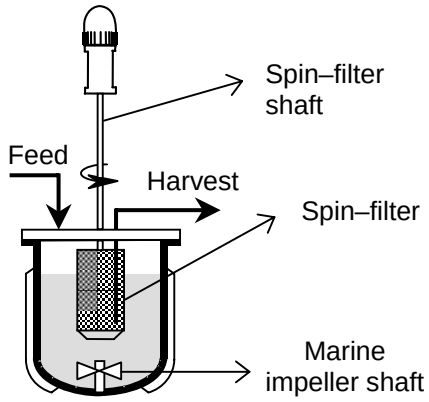

Figure 2.1: Schematic representation of an internal spin–filter device.

Further studies on spin–filters for use in perfusion culture systems are summarized in Table 2.1. These studies have been established in order to understand the mechanism of cell separation and to adapt the best filter configuration and operational conditions to the scale required by the process. The optimum conditions enable high retention rates and reduced fouling to be achieved, resulting in long duration perfusion cultures and high cell densities and thus productivities. Retention (R) is defined as:

$$R = \left(1 - \frac{c_{in,filter}}{c_{out,filter}}\right) \cdot 100\%$$

where $c_{in,filter}$ and $c_{out,filter}$ are the concentrations of particles inside and outside the spin–filter respectively. Thus 100% retention means that there are no cells within the spin–filter unit.

The parameters that influence the mechanism of cell retention and filter fouling could be divided into three categories: parameters relating to spin–filter design characteristics, such as screen material, filter design, filter surface and pore size, parameters relating to culture characteristics, such as cell concentration within the reactor, and parameters relating to operational culture variables, such as perfusion flow rate and filter rotation. The screen material influences mainly filter fouling, whereas filter pore size influence cell retention. Indeed, the use of a filter pore size larger than the mean cell diameter will allow the passage of cells through the filter. The perfusion rate as well as filter rotation influence both cell retention and filter fouling. Filter fouling implies also the reduction of filter pore size that will influence cell retention. High cell retention rates permit to achieve high cell densities that can be stabilized at certain levels by applying a bleed rate to the system. The cell density within the reactor influences the fouling of the filter that

influences the lifespan of the perfusion culture. Thus the achievement of high cell density cultures and for long time is related to the mechanisms of cell retention and filter fouling that are dependent on the above parameters. Although comparison of the published results (particularly with respect to filter fouling) is difficult because of the diversity and difference of the filter operational parameters and characteristics, as well as culture characteristics, the studies reported for each parameter will be discussed in the next section, in terms of cell retention and filter fouling.

2.2.1 Spin–filter design characteristics

The parameters related to spin–filter design characteristics are screen material, filter design, filter surface and pore size.

2.2.1.1 Filter material

The first efforts to characterize the particles responsible for filter fouling during spin–filter operation with animal cell cultures, indicated that viable and dead cells, debris, proteins and mainly DNA, as well as a combination of these factors, are involved (Esclade et al. 1991; Maiorella et al. 1991; Mercille et al. 1994). Two different families of filter material have generally been used for spin–filter construction, namely metallic and synthetic polymers. The metallic screens are made of stainless steel and have a positive surface charge density and are the most commonly used and quoted in the literature. They are available in a wide range of pore openings, from 5 to 300 μm. Synthetic screens are more neutral and are constructed from polymers such as ethylene–tetrafluoroethylene (ETFE), polyamide or polytetrafluoroethylene (PTFE) materials (Avgerinos et al. 1990; Esclade et al. 1991). Since cells, proteins and DNA are usually negatively charged, adherence to synthetic screens is weaker than to a metallic one, which would be expected to be an advantage with respect to fouling. However, the hydrophobic characteristics of proteins (Stryer 1999) also play an important role in protein adhesion to filter surfaces and thus filter fouling. In order to reduce protein adsorption to filter surfaces, it is generally preferable to use hydrophilic surfaces. The hydrophobic character of synthetic filters may therefore be modified by surface coating with polymers or hydrated chains (Fane et al. 1985; Kim et al. 1988; Lee et al. 1990).

Table 2.1: Published perfusion cultures using internal spin-filter for suspended mammalian cell separation

Cell line	Culture volume (l)	Spin-filter characteristics					Rotation dependent on the stirrer shaft?	Max. perfusion rate (vvd)	Max. viable cell density (10^6 cell/ml)	Culture time (days)	Viability at the culture end (%)	Fouling	Reference
		Material	Pore size (µm)	Diameter (cm)	Height (cm)	Rotation (rpm)							
Leukemia	1	Polymeric	3			300	Yes	1.7	65	10		?	Himmelfarb, 1969
Rat tumor	4	Porcelain	1	3.81	15.2	200 - 300	Yes		31	3	>90	Yes	Tolbert, 1981
Rat tumor	40	Porcelain	1	6.35	24.1	200 - 300	Yes		14	<6	>90	Yes	Tolbert, 1981
Hybridoma			10				Yes		13	21	67	Yes	van Wezel, 1985
Hybridoma	0.8	Stainless steel	5			200	Yes	1.5	22	7	73	Yes	Reuveny, 1986
Hybridoma	0.8	Stainless steel	10			200	Yes	2	54/ 19*	22	40	Yes	Velez, 1987
Hybridoma	1.5	Stainless steel	10	3.7	8	30	Yes	2	1.4	7	30	Yes	Esclade, 1991
Hybridoma	1.5	Polyamide 66	11	4	5.4	30	Yes	2	1.4	7	20	No	Esclade, 1991
CHO	2	Stainless steel	40	5	10	100 - 200	Yes	1.3	15	100	>90	No [a]	Fenge, 1991
Hybridoma	2	Stainless steel	10	5.8	12.8	90 - 300	Yes	1.4	13	36	30 - 50	Yes	Siegel, 1991
Hybridoma	2	Stainless steel	20	5.8	12.8	100 - 300	Yes	1.1	10	29		Yes	Siegel, 1991
Hybridoma	2	Stainless steel	40	5.8	12.8	100 - 300	Yes	0.93	3.5	17		Yes	Siegel, 1991
Hybridoma	12	Stainless steel	25	7	21.3	50	Yes	1	4.5	14	84	No	Yabannavar, 1992
Hybridoma	1	Stainless steel		4	5		Yes	4	13	21		No	Jan, 1992
Hybridoma	1	Stainless steel	40	4	5		Yes	2.5	11/5.4*	22	60	?	Al-Rubeai, 1992
Hybridoma		Stainless steel	20			200	Yes	1	15	28	>80	No	Fenge, 1993
Hybridoma	175	Stainless steel	25	22	32	28	No	0.5	2.8	8	64	No	Yabannavar, 1994
Hybridoma	1	Stainless steel				500	Yes	3	15	17.5	80	Yes	Emery, 1995
Myeloma	7	Stainless steel	15	6	18.4		No	1	11	30		No	Deo, 1996
Myeloma	500	Stainless steel	15				No	1	9	15		No	Deo, 1996
Hybridoma	500	Stainless steel	15				No	1.2	11	30		No	Deo, 1996
Hybridoma	1.2	Stainless steel	75				Yes	2	15	37		?	Heine, 1999
CHO	100	Stainless steel	20	20	42.5	100 - 150	Yes	1	5	14	90	?	Iding, 2000
Leukemia	2	Stainless steel	20				Yes	1.9	10	9	>90	No	Stiens, 2000
CHO	1					120		1.5	16.5	29	86	Yes	Werner, 2002

*Maximal/ final viable cell concentration [a] Aggregats of 100-200 cells formed

An early study on filter fouling using filters with a defined filter surface, porosity, agitation, cell concentration and perfusion flow were carried out with both a stainless steel screen with 10 μm pore size and a polyamide 66 screen with 11 μm pore size for mouse–mouse hybridoma perfusion culture simulations (Esclade et al. 1991). Despite the fact that viability began to fall on day 4, reaching 20% on day 6, for both filter materials, complete fouling of the metallic screen, as defined by the absence of permeate flow, was observed after 7 days, whereas no fouling of the polyamide membrane was detected over the same period. Analysis of the filter deposits after fouling revealed that protein and DNA adhesion is more important on the metallic screen than on the polyamide one. Additionally, it seems that proteins are not directly responsible for filter fouling, but facilitate it by inducing adhesion of cell and/or cellular debris to the filter screen.

A report of studies on synthetic membrane fouling compared a chemically modified permanent hydrophilic PTFE membrane and a hydrophilized polypropylene (PP) membrane (Büntemeyer et al. 1994). Although this study was performed using a hollow fiber module where the mechanisms of retention and fouling are quite different compared to spin–filter devices, the tendency to fouling is the same in both systems. This study, clearly showed that protein permeability was better with the PP membrane than a PTFE membrane, however fouling was much slower using the PTFE membrane, which favors long–term cultures.

Homemade porcelain filters, with a pore size of about 1 μm has been used to separate rat tumor cells (Tolbert et al. 1981). Despite attaining a high cell density of about $3 \cdot 10^6$ cell/ml, fouling occurred after 3 days, showing not only on inadequate choice of pore size, but also that this kind of filter material is not suitable for prolonged applications.
The addition of deoxyribonuclease I (DNAse I) to the culture medium prevented the formation of aggregates and significantly reduced fouling of polycarbonate and hydrophilized polysulfone membranes during cross–flow and vortex flow filtration cultures (Mercille et al. 1994).

Despite the advantages of using synthetic filters, the majority of the literature relating to perfusion cultures has used spin–filters made from stainless steel (Table 2.1). The reasons for this are due to the availability of a large range of pore sizes of metallic filters compared to synthetic ones combined with a longer life, robustness, resistance to deformation, ease of handling and resistance to cleaning and sterilization, through thermal or chemical means, compared with polymer membranes. Furthermore, from these reports, it appears that keeping the culture viability at high level through a good control of culture

parameters contribute to the reduced fouling of spin–filters and thus to longer culture duration.

2.2.1.2 Filter/support design

It is well known that filter pore size influences the passage of cells across a filter (Jan et al. 1992; Siegel et al. 1991) however, for stainless steel filters different weaving patterns and orientations exist which may exhibit similar pore sizes (Figure 2.2). As an example, two cylindrical stainless steel spin–filters, each having an average pore size of 25 μm but different weaving orientation, yielded very different retention profiles, at a relatively low rotational speed of 0.21 m/s (Jan et al. 1992). One filter achieved retention rates above 95% for perfusion flows between 1.6 and 4.8 cm/h, while the second only achieved retention rates of between 50 and 80% over the same perfusion flow range. Such results underline the importance of filter weaving orientation on retention profile.

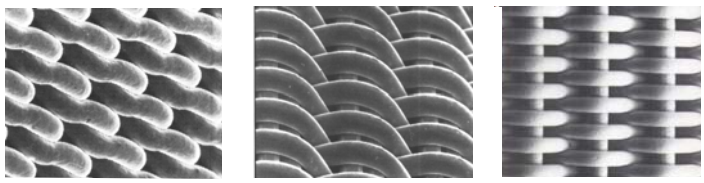

Figure 2.2: Stainless steel filters with different weaving orientations, having similar pore sizes of 15 μm.

One simple approach to attempt to reduce fouling involves placing a draft tube around the spin–filter in order to increase turbulence at the membrane surface. Although many authors have tried such an approach, a significant reduction in fouling has yet to be demonstrated (Iding et al. 2000; Yabannavar et al. 1992). Investigations on the influence of spin–filter design on cell retention indicate that the optimum design for achieving high cell retention with reduced fouling involves a conical lower mesh support combined with an axial upward fluid flow created by the presence of a draft tube (Siegel et al. 1991). Such a filter configuration avoids cell damage during rotation, by reducing shear forces, compared with more angular designs and induces constant washing of the filter surface through the turbulences created by the presence of the draft tube.

2.2.1.3 Filter pore size

Mammalian cells have a mean diameter of between 12 and 20 μm depending on cell line and culture conditions. Using membranes with pore sizes smaller than the mean cell diameter clearly would result in cell retention during perfusion operation approaching 100%. Thus the early spin–filters generally employed pore sizes (1–10 μm) smaller than the cell diameter. However, very small filter pores are actually less favorable than larger ones due to the higher levels of fouling by viable or dead cells, cell debris, proteins and/or DNA. An example is the reported mammalian cell suspension system using a porcelain spin–filter having 1 μm pore size (Tolbert et al. 1981). The small pore openings resulted in a high cell retention approaching 100% and resulted in the culture attaining a cell density of $3.1 \cdot 10^7$ cell/ml. In spite of a large filtration area of about 180 cm^2 (45 cm^2/L of culture volume) the filter became completely fouled within 3 days of operation. Polymeric spin–filters with the slightly larger pore size of 3 μm also resulted in relatively high viable cell densities of $6.5 \cdot 10^7$ cell/ml however, the culture lasted only 10 days in spite of employing a high filter rotation (Himmelfarb et al. 1969).

When the pore size of a stainless steel filter was increased to 5 μm, a viable cell density of $2.2 \cdot 10^7$ hybridoma cell/ml was obtained with fouling occurring after 7 days of cultivation (Reuveny et al. 1986). By increasing the filter pore size to 10 μm under the same conditions (culture volume and filter rotation), a maximum viable cell density of $5.4 \cdot 10^7$ cell/ml was attained while increasing the culture duration from 15 days to 22 days of operation, before fouling occurred (Velez et al. 1987).

By increasing the rotation velocity of the filter, larger filter pore sizes could be used (>15 μm). Under these conditions, retention, although not as high as with smaller pore sizes, was sufficiently high as to retain a majority of the viable cells within the reactor, thereby attaining a high cell density, while enabling a considerable increase in culture longevity and resulting productivity. Thus a stainless–steel spin–filter with a pore size of 15 μm was employed for the perfusion of myeloma cells in a 7 L bioreactor, reaching a viable cell density of about $1.1 \cdot 10^7$ cell/ml with no fouling observed after 30 days of operation (Deo et al. 1996). On the basis of this culture, a successful scale–up was achieved to a scale of 500 L, which retained the same high cell density and fouling–free operation over more than 30 days. Hybridoma cells have been cultured in 2 L spin–filter perfusion bioreactors having a similar configuration using stainless steel filters having pore sizes of 10, 20 and 40 μm and it was concluded that high retention rates, and thus high

cell densities, could only be obtained during long–term cultivation of suspended cells for pore sizes in the range of the cell size (Siegel et al. 1991). Indeed, using the 10 μm spin–filter resulted in a maximum density of $1.3 \cdot 10^7$ cell/ml with fouling after 36 days. Increasing the pore size to 20 μm resulted in a similar cell density ($1 \cdot 10^7$ cell/ml) and filter fouling after 29 days. Finally, employing the 40 μm pore size spin–filter, resulted in the cell density decreasing to $3.5 \cdot 10^6$ cell/ml and the operation time decreasing to 17 days. Consequently it seems that increasing the pore size from 1 to 15 μm results in improved culture performance with an increase in operation time of the culture, while increasing the filter pore size above 20 μm results in cells entering the spin–filter and causes a higher rate of filter fouling and consequent reduction in culture duration.

There are reports in which a 20 μm stainless steel spin–filter has achieved a maximum viable cell density of $1.5 \cdot 10^7$ CHO cell/ml during 28 days without filter fouling (Fenge et al. 1993). In the same study, a larger stainless steel spin–filter of 40 μm pore size, yielded a similar high density of about $1.5 \cdot 10^7$ cell/ml over 100 days without filter clogging (Fenge et al. 1991a). The reason for this apparent high retention for high porosity filters is due to the cells forming aggregates of 100–200 cells. Even more surprising were results obtained for hybridoma perfusion cultures using a 75 μm stainless steel spin–filter in which, despite a low retention (<50%) during the first 14 days of the culture, the cell concentration reached $1.5 \cdot 10^7$ cell/ml for over 37 days (Heine et al. 1999). Interestingly, although an initial fouling of the membrane was observed after 17 days, which resulted in an increase of retention rate, no further fouling or clogging of the spin–filter was observed for the following 20 days of operation.

Again it was observed that the high performance of the filter was due to the formation of large aggregates of cells. Thus, for aggregate–forming cells retention can be high even for large pore size filters, the latter showing much lower retention rates for homogeneous suspension cultures, which increase during the culture as the result of filter fouling.

2.2.1.4 Filter surface

The effective surface area of a spin–filter is a parameter of paramount importance with respect to perfusion flow rate. However, since the surface area is linked to a volume of bioreactor in which few or no cells are present (within the spin–filter), increasing the

size/volume of the filter effectively decreases the working volume of the bioreactor. Thus a compromise must be established between having as high a filtration surface as possible while maintaining the largest culture volume. The perfusion capacity clearly increases with increasing ratio between spin–filter surface to culture volume, and it has been postulated that during scale–up, a large filter aspect ratio of height to diameter should be chosen, since it was found that the perfusion capacity is proportional to the filter height and to the cube of the filter diameter (Deo et al. 1996).

2.2.2 Operational culture characteristics

Operational culture variables, such as perfusion rate and filter rotation influence cell retention as well as filter fouling. Filter rotational speed can be varied freely providing that the filter motor is independent from the reactor stirrer shaft, however the perfusion capacity of the spin–filter should be as high as possible in order to permit reaching high cell density cultures.

2.2.2.1 Filter rotational speed

Rotation of the filter is a parameter that may be varied over a wide range, providing that the filter motor is independent from the reactor stirrer shaft, and cell damage is avoided. Varying the filter rotation speed has a major impact on filter fouling as well as influencing cell retention for filter pores greater than the mean cell diameter. Many authors measured retention of mammalian cells during cultures or simulated cultures using cells or beads with a mean diameter similar to that of animal cells and obtained a broad range of results, which are difficult to compare due to the difference of various parameters (perfusion rate, cell/particle concentration) used. An attempt has been made here, where possible, to express the retention as a function of spin–filter rotation, which represents the filter tangential speed in m/s, whereas the perfusion flow normalized to the filtration surface is expressed in cm/h.

Using three different stainless steel wire cages with 10, 20 and 40 μm pore sizes, in perfusion simulation experiments using latex beads (11.9 ± 1.9 μm), it has been shown that particle retention depends on the rotation velocity of the filter (Siegel et al. 1991). Indeed, all three filters attained a maximum retention value at the same optimal spin–filter

rotation rate. Despite slight differences in retention rate for the filter pore sizes tested, the optimal rotational speed was about 0.61 m/s in all three cases. During 2–L scale perfusion culture simulations using agarose beads (13 ± 2 μm) at a perfusion flow of 0.4 cm/h, it was shown that retention, using a 20 μm pore size spin–filter, could be increased by the application of a spin–filter rotation velocity in the range from 0.15 to 0.43 m/s and decreased rapidly at velocities above 0.43 m/s (Iding et al. 2000). However, similar experiments at 100–L pilot scale, with a perfusion flow of 1.56 cm/h, showed a very different retention profile. Cell retention decreased from a rotational velocity of 0.37 m/s until a filter velocity of 0.73 m/s (Iding et al. 2000).

For tumor cell perfusion cultures the use of large stainless steel spin–filter pores of 53 μm resulted in a small decrease of the retention rate with increasing filter speed (Varecka and Scheirer 1987). On the other hand for mouse hybridoma cell perfusion simulations using two stainless steel spin–filters of 25 and 40 μm pore size and a perfusion flow from 1.6 to 6.3 cm/h, retention was actually observed to improve with increasing filter rotation speed for all pore sizes tested (Jan et al. 1992). In this case retention reached a plateau above a rotation speed corresponding to about 0.63 m/s. Despite the fact that many authors observed an effect of filter rotation rate on cell/particle retention, others observed no influence, even when using filters with pore sizes much larger than the mean cell diameter (Yabannavar et al. 1992).

For filter pores slightly larger than the mean diameter of cells (15–20 μm), some authors reach a plateau when increasing the filter rotation speed, while others obtain an optimum. On the other hand, for filters with pore sizes much larger than the mean cell diameter (> 25 μm), an increase in particle retention with increasing filter rotation is sometimes found, although certain researchers observe a decrease while for others the rate of rotation appears to have almost no effect on cell retention. Thus there is no clear–cut correlation between the retention profile reported by many authors as a function of rotation speed of the filter. However, despite the fact that retention was identified as being dependent on filter rotation speed, the majority of the published spin–filter perfusion cultures were done with the filter attached to the stirrer shaft (Table 2.1). Ideally, the filter rotation speed should be independent of the agitation speed in order to achieve the optimal filter rotation at which cell retention is maximal.

Studies on filter fouling using 10 μm stainless steel sieves during perfusion simulations using $2 \cdot 10^5$ cell/ml of suspended hybridoma cells at high perfusion flow rates

(>180 cm/h), showed that the rotation speed had little effect on filtration duration, until a critical filter rotation value of 0.6 m/s was attained due to a dynamic equilibrium being established between surface colonization and cell removal due to filter rotation (Favre 1993; Favre and Thaler 1992). However, such high perfusion rates are not easily employed, even at large scale. Fouling of 15 μm pore size stainless steel spin–filters, in a study similar to that of Favre and Thaler (1992) was shown to be primarily caused by interactions between the spin–filter screen and the cells and that such interactions are governed principally by the perfusion flow and the centrifugal force (Deo et al. 1996). In order to measure this phenomenon, hybridoma cell perfusion simulations were performed with cell densities between 0.8–1·10^7 cell/ml at rotation speeds in the range from 0.26 to 0.68 m/s and perfusion flows from 6 cm/h to 72 cm/h at 10 L scale (Deo et al. 1996). It was concluded that initial filter fouling is a rapid process, in that there is a sharp limit for the perfusion rate at any given rotational filter velocity. However, once again the perfusion flows employed are not very realistic, with 72 cm/h representing a perfusion rate of 6 vvd for working volumes of approximately 900 L, a value which is extremely large for animal cell perfusion cultures. By studying the influence of the rotational velocity on the tendency of a 25 μm pore size stainless steel spin–filter to fouling, during an actual perfusion culture of NS–1 cells, it was concluded that high filter rotation rates reduce the incidence of clogging but that they are of little use because of the associated high fluid exchange across the filter, which leads to high cell leakage (Yabannavar et al. 1992).

In conclusion, despite certain reports to the contrary, it generally appears that fouling is dependent on the rotation speed of the filter. For small filter pore sizes (<15 μm), the minimum filter rotation required to prevent the primarily fouling mechanism (the minimal interaction between the cells and the filter screen) is dependent on the perfusion flow employed during the culture. For high perfusion flows, and during cell perfusion simulations, the value of this minimum filter rotation was found to be 0.6 m/s, however this value has not been demonstrated for actual cell perfusion rates. For larger pore size filters, the mechanism of fouling has not been clearly described and the high rotation of the filter necessary to reduce fouling is considered unrealistic due to cell leakage.

2.2.2.2 Perfusion rate

Cell retention of a 40 μm stainless steel spin–filter was determined during the stationary phase of batch growth of a recombinant CHO cell culture and it was observed

that retention was only slightly affected by perfusion flow rates from 0.7 up to 16 cm/h (perfusion flow normalized to the filtration surface) (Fenge et al. 1991a). Even higher fluxes of 21 cm/h did not appear to influence cell retention. However, since aggregate formation occurred in this culture, it seems likely that the lack of effect of perfusion flow rate is probably due to the large particle size and, therefore, constant retention efficiency. The combination of perfusion rate, expressed in cm/h, and filter rotation, expressed in m/s, leads to different retention profiles. Employing low perfusion rates from 1.6 to 6.4 cm/h, it was observed that the retention rate of large pore size filters of 25 to 40 μm is independent of the perfusion rate at high filter rotation speeds (above 0.63 m/s) but declines with increasing perfusion rate at rotation speeds below 0.63 m/s during suspended hybridoma cell perfusion simulations (Jan et al. 1992). Further reports observed that the increase in perfusion rate did not change significantly the cell density inside a 25 μm spin–filter at a filter rotation of 0.4 m/s, until the perfusion rate reached the high level of 4.3 cm/h, after which a slight increase in retention was observed (Yabannavar et al. 1992). Retention by small filter pore sizes is not influenced by the perfusion flow rates, however, the mechanism is different for pore sizes larger than the cell diameter and seems to be dependent on a combination of rotational speed of the filter and the perfusion flow rate.

However, the clogging of screens has been shown to be associated with high perfusion rates (Deo et al. 1996; Yabannavar et al. 1992). In order to study fouling of a 10 μm stainless steel mesh filter, very high perfusion flows from 27 to 345 cm/h were employed during perfusion simulation with $2 \cdot 10^5$ hybridoma cell/ml (Favre 1993). The results indicate that flows higher than 86 cm/h led to very rapid fouling of the sieve because of high cell–filter sieve interactions. However, these high perfusion rates are not very realistic, since they do not occur even at large scale. Indeed, a perfusion rate of 6 vvd at 300 L working volume scale corresponds to a maximum perfusion flow of 25 cm/h. The perfusion flow rate may influence fouling, however there have been no studies to date which have quantified fouling as a function of perfusion flow rate and any comparison of published results is difficult due to the wide range of geometries, conditions and unspecified parameters.

2.2.3 Culture characteristics – cell concentration

Few studies have been reported concerning the influence of cell concentration on cell retention and filter fouling. Of these studies, retention was found to be independent of the cell density change in the range from 2–4.5·10^6 cell/ml (Yabannavar et al. 1992). Increasing the cell concentration from 0.2–1.5·10^6 cell/ml, during perfusion simulations with hybridoma cells, resulted in an increase in fouling at a high perfusion flow of 54 cm/h (Favre 1993). Increasing the cell concentration by a factor of more than 2, from 4.9·10^6–1.1·10^7 cell/ml, was reported to lead to a 2–fold decrease in the perfusion flux capacity, which indicates an increase in particle–screen interactions and thus an increase in the tendency of filter to fouling (Deo et al. 1996).

Cell concentration appears to have relatively little effect on cell retention, whereas filter fouling tends to increase with cell concentration. Additionally, high culture viability was proven to be important in order to increase filter performance with respect to filter fouling (Fenge et al. 1991b). Indeed, cell debris and DNA released during low viability cultures tend to increase the attachment of cells on the filter surface (Esclade et al. 1991).

2.3 Spin–filters for anchorage–dependent and aggregate–forming cell separations

Table 2.2 shows data for published perfusion cultures using internal spin–filters involving anchorage–dependent and aggregate–forming animal cell perfusion cultures. From a general point of view, the use of aggregated cells or cells grown on microcarriers permits the use of large filter openings, much larger than the mean cell diameter, which as a result decreases the tendency of filter fouling (Zhang et al. 1998). In one study, the performance of a stainless steel spin–filter was compared for three different modes of culture and cell types: suspended hybridoma cells, anchorage dependent CHO cells and adapted aggregate–forming rCHO cells (Fenge et al. 1993). Aggregate–forming cells, as well as cells grown on microcarriers, had a total diameter (140–240 μm) much larger than that of suspended cells. Despite the use of larger pore sizes (40 and 75 μm), filter rotation remained important in the prevention of filter fouling. Indeed, Hu et al. (Hu et al. 2000) used a stationary stainless steel filter and observed filter fouling after 21 days, which is relatively short compared to other cultures performed with rotating filters (Table 2.2).

Table 2.2: Published perfusion cultures using internal spin-filter for aggregates forming and anchorage dependent mammalian cell separation

Cell line	Product	Culture volume (l)	Spin-filter characteristics				Rotation dependent on the stirrer?	Perfusion rate (vvd)	Max. viable cell density (10^6 cell/ml)	Culture time (days)	Fouling	Microcarrier Bead Aggregats	Reference
			Material	Pore size (µm)	Diameter (cm)/ Surface (cm^2)	Rotation (rpm)							
Hybridoma	mAb			75			Yes				Yes	microcarrier	van Wezel, 1985
CHO	rscu-PA	10	ETFE	120	7.6/ 477	150	Yes	4	74/ 30*	31	No	[2]Cytodex 2	Avgerinos, 1990
CHO	mAB	2	Stainless steel	75	5.8/ 178.5	50	Yes	1	7	42	?	microcarrier	Fenge, 1993
CHO	scu-PA	2.5		200		100	Yes	1.5	16	32	?	[2]Cytodex 3	Jo, 1998
CHO	scu-PA	2.5		200		100	Yes	6	51	25	?	[1]Cultispher G	Jo, 1998
CHO	hSTC	2	Stainless steel	75			Yes	2.4	8	25	?	[1]Cytodex 1	Zhang, 1998
CHO	M-CIF	2	Stainless steel	75		50	Yes	2	6.2	17.5	Partially	[1]Cytodex 1	Kong, 1998
CHO	M-CIF	8	Stainless steel	75		45	Yes	2	3	35	?	[1]Cytodex 1	Kong, 1998
CHO	u-PA	20	Stainless steel	20		0	-	1	13	21	Yes	[1]Cytopore	Hu, 2000
Human tumor		11	Stainless steel	53	- / 420	80 - 120	Yes	2.9	10	60	No	Aggregats	Varecka, 1987
CHO	mAB	2	Stainless steel	40	5.8/ 167.5	100 - 200	Yes	1	20/ 3*	100	No	Aggregats	Fenge, 1993

* Maximal/ final viable cell concentration [1] microcarrier [2] bead

The use of synthetic membranes was also tested for anchorage–dependent CHO cell culture (Avgerinos et al. 1990). Thus a 120 μm ETFE synthetic spin–filter membrane was used to attach cells on 115–195 μm Cytodex 2 microcarrier beads. However cell morphology changed during the culture and cells formed clumped aggregates of 200 to 600 microns in size. The spin–filter retained both the attached cells and the aggregate–forming cells. The hydrophobic nature of the ETFE membrane apparently minimized the attachment of cells, since during the first 31 days of culture the filter showed no sign of fouling.

The use of aggregated cells or cells grown on microcarriers also allows much larger perfusion flows to be applied while maintaining the retention at a high levels (>95%).However, formation of large aggregates generally results in a loss of viability (Avgerinos et al. 1990; Van Wezel et al. 1985) and a decline in protein production (Jo et al. 1998) due to limited oxygen transfer and nutrient depletion within the core of the aggregate/ bead and renders the monitoring and control of the culture difficult. Additionally, the adaptation of the aggregate–forming cells during the culture as well as the cell seeding on the microcarriers or into the beads necessitates additional energy, costs and special experimental technique. Microcarriers are not easy to use as a re–utilizable substrate (Griffiths et al. 1987) and beads are generally not re–utilizable at all.

2.4 Scale–up strategies for spin–filter devices

Many authors attempted to understand the phenomena involved in particle/cell retention of open filters (filter pore size larger than the mean cell diameter) as well as the fouling mechanisms of filters. However, in spite of these efforts, the mechanisms remain unclear. The lack of understanding of these mechanisms and the unpredictability of the retention rate under different operating conditions, leads to difficulties in design and operation of spin–filter separators particularly at large–scale. Few empirical scale–up strategies have been developed to date. A first analogy was reported and considers the similarities between spin–filters and cross–flow filtration (Yabannavar et al. 1992). In cross–flow filtration, the flow containing cells is passed tangentially to the filtration membrane, which corresponds to the tangential velocity created by the spinning of the spin–filter, while the fluid permeation through the cross–flow membrane corresponds to

the perfusion flow through the spin–filter membrane. Based on studies of particle motion in laminar annulus flow with a porous wall (Belfort 1988), a method was developed to scale–up the spin–filter device during culture operation while avoiding clogging (Yabannavar et al. 1994). Expressing the screen speed (N_{screen} (s^{-1})) to be proportional to the reactor volume (V (l)) to the power of (–1/6), as represented in equation 2.3, a 175 L–working volume spin–filter culture was scaled–up on the basis of an optimized 12 L–working volume spin–filter culture.

$$N_{screen} \propto V^{-1/6} \qquad \text{Eq.2.3}$$

The model was validated by obtaining, the same fluid exchange across the screen for the spin–filters at the two scales.

Another empirical scale–up model was developed that describes the effects of operation conditions and spin–filter configuration on the perfusion capacity of the spin–filter (Deo et al. 1996). These effects have been identified during recycle perfusion studies. In this case, the perfusion rate (expressed in reactor volume per day) is proportional to the ratio of the spin–filter surface per reactor volume (A/V), proportional to the square of the rotational velocity and inversely proportional to the cell concentration, as expressed in equation 2.4.

$$\frac{RV}{day} \propto \frac{A}{V} \cdot \frac{v^2}{c} = \frac{\pi^3 H \cdot D^3 \cdot \omega^2}{V \cdot c} \qquad \text{Eq.2.4}$$

where A (m^2) is the filter surface, V (l) the working reactor volume, v (m/s) the filter tangential speed, c (cell/l) the cell concentration, H (m) the filter height, D (m) the filter diameter and ω (s^{-1}) the filter angular velocity. For scale–up purposes, from equation 2.4, it seems that it is preferable to increase the spin–filter area by increasing the filter diameter. Application of the above model, resulted in a successful scale–up from a 7 L optimized lab–scale perfusion process to a 500 L scale, in terms of culture longevity (>30 days) and high cell density (>10^7 cell/ml) (Deo et al. 1996).

Further theoretical considerations of cell retention phenomenon, as well as detailed experimentation are required in order to understand cell retention and filter fouling phenomena. Based on this understanding, culture operating conditions and filter characteristics could be defined in order to achieve high retention rates with reduced filter fouling similar at small and large–scale operation.

2.5 Conclusions

The lack of understanding of the mechanisms involved in cell retention and fouling of internal spin–filter perfusion devices arises from the fact that many parameters are involved during cell perfusion cultures. These parameters may be classified in several categories: one category of parameters are those that can be changed independently of the culture and which are related to filter characteristics, such as the material and the design of the filter, the pore size and the surface of the filter. A second category of parameters that depends on culture characteristics, such as cell concentration during the culture and a third category relating to the culture operational characteristics that includes perfusion rate and filter rotational speed.

During the development of suspended animal cell perfusion cultures, spin–filter porosity used during the early years was smaller (less than 10 μm) than the mean cell diameter. Later, an increase in filter pore size (10–15 μm) resulted in reduced fouling. However, the utilization of much larger filter pore sizes (over 20 μm) resulted in increased cell passage through the filter thereby limiting the achievement of high cell concentration and increasing filter fouling.

As far as the rotational speed of the filter is concerned, fouling tends to decrease with increasing rotation rate due to higher turbulence at the filter surface. However, it is possible that the fouling mechanism may be different for “closed” filters (filters in which pore sizes are smaller than the mean cell diameter) than for “open” ones (filters in which pore sizes are larger than the mean cell diameter). Consequently, fouling seems to be influenced by the passage of cells through the filter, although it is difficult to compare published results. By increasing the filter rotation velocity of open filters, the retention profile was found to increase and reach a plateau, or at least an optimal value of around 0.6 m/s. The influence of perfusion flow on the fouling of open filters was revealed as being important, while its influence on retention is less evident. Some authors observed a slight influence, whereas others observed no influence of the perfusion rate at high rotation speeds above 0.63 m/s and a decline of retention at rotation speeds below 0.63 m/s. Consequently it seems that cell retention is dependent on a combination of rotation velocity of the filter and perfusion rate.

The diversity and inter–dependence of all the different parameters make any comparison between the published studies difficult and showed contradictory tendency of

certain parameters with respect to retention and fouling. Whereas many reports describe studies on cell retention by spin–filters, fouling remains difficult to characterize. As a result little information has been provided concerning the operation time of the filters, since in most of cases, the cultures were of short duration and stopped before fouling occurred.

2.6 Aims and outline of the thesis

Continuous processes with cell separation enable to obtain the highest volumetric productivity levels during animal cell culture, however they require robust and reliable separation devices. Internal spin–filters have been identified as the most suitable technique for continuous cell separation at large–scale. The previous review permitted to establish a state of the art of spin–filter technology and to identify the most important parameters involved in the mechanisms of filter fouling and cell retention of filters in which pore size is larger than the mean cell diameter. It also permitted to underline the lack of understanding of the mechanisms involved in such mechanisms that makes the device difficult to operate and to scale–up. This is due mainly to the interdependence between parameters involved in such mechanisms and the lack of detailed systematic studies on cell retention and filter fouling. For these reasons, this thesis aims at the characterization of the mechanism of action of internal spin–filters for animal cell perfusion cultures in order to render the device easy to operate and to scale–up, i.e. allow high cell densities to be maintained for long–time. The aims were defined through four questions:

- What are the parameters that influence cell retention the most?
- How to vary the rotation speed of the filter when the scale is increased?
- What are the characteristics of the filter, as well as the culture parameters that have to be applied in order to get similar retention rates at small scale and large scale? And what limits the scale–up of the filter?
- What are the parameters that influence filter fouling the most? How to reduce this phenomenon during continuous culture?

The diversity and inter–dependence of all the different parameters involved in retention mechanism make comparison between the published studies difficult, and showed contradictory tendency of certain parameters with respect to retention. In order to

study the influence of different parameters on cell retention by spin–filters, in the absence of fouling effects, detailed systematic studies with inert polymer beads, the diameter of which is in the same range as animal cells size have been investigated during perfusion simulations (chapter 3). The main parameters studied were: the filter pore size, filter rotation velocity, perfusion rate and particle concentration. The influence of placing a draft tube around the spin–filter on bead retention was also studied.

The forces acting on cells near the filter surface govern cell transport towards the filter and thus the cell retention mechanism as well as the tendency of the filter to fouling. A study of the fluid mechanics around the spin–filter is thus important in order to understand this phenomenon. Lateral migration of particles across the filter membrane, related to filter fouling has been extensively studied for cross–flow systems and less so for spin–filter devices. In the present study, lateral particle migration, developed for Poiseuille flow in tubes or channels as well as for simple shear flow in slits, have been adjusted for rotating Couette flow systems such as spin–filter devices (chapter 4). The importance of lift phenomena in spin–filter particle retention have been demonstrated and the rotation parameter at which spin–filter has to be operated in order to reach maximum retention and reduced fouling, at small as well as at large scale have been characterized.

All of the reported scale–up strategies are based on carrying out large numbers of preliminary spin–filter cultures at small–scale and are, as a result, extremely time consuming. In the previous part, filter acceleration was identified to be the parameter that has to be conserved in order to keep similar particle lateral migration phenomena and thus similar retention profiles at small, as well as at large scale. Based on this result, response surface methodology was used to model retention as a function of four factors, namely filter rotation velocity, filter porosity (ratio of filter pore size to cell diameter), perfusion capacity (ratio of perfusion rate to filtration surface) and cell concentration, using a minimum of resources and quantitative data from an appropriate experimental design (chapter 5). The values for the four varied parameters relate to small scale, as well as large scale in such a way that it is no longer necessary to carry out prior small–scale cultures. Thus the model predicts, for any animal cell size, which varies from 12 to 15 μm from CHO cells to hybridoma cells respectively, the filter acceleration that has to be applied for a given filter pore size, in order to obtain the desired maximal retention at any culture scale (dictated by the perfusion rate used) and was validated during two actual spin–filter perfusion cultures carried out using CHO cells.

Filter fouling is an extremely important phenomenon, which is often reported to limit the duration, productivity and the use of spin–filters for animal cell perfusion cultures. Studies on filter fouling to date have been carried out over short–term operation, and mainly concern the primary fouling phenomena due to interactions between cells and the filter surface, and represent simulations at unrealistic perfusion rates. Since filter fouling is primary due to cell deposition on filter surfaces, which is governed by the hydrodynamic forces around the spin–filter, and then depends on cell colonization and growth on the filter surface, it clearly appears that it is a long–term phenomenon. No systematic characterization of filter fouling over long–term operation has been undertaken until now and, as a result, the main parameters that influence filter fouling remain unknown. For these reasons, the present study involves realistic spin–filter perfusion simulations carried out using CHO cells, in order to characterize filter fouling over long–term operation (chapter 6). Once it had been established which parameter influences filter fouling the most, a method was developed for reducing this phenomenon. This method consists in continuously vibrating the spin–filter through the use of a piezo–actuator placed on the filter support and that converts electrical energy into mechanical motion. The reduction of filter fouling was demonstrated during actual CHO cell perfusion cultures using such a vibrated spin–filter.

References

Arai T, Yokoyama S, Tokashiki M. 1993. 50 L scale perfusion culture of hybridoma cells by gravitational settling for cell separation. In: Kaminogawa S, Ametani A, Hachimura S, editors. Animal Cell Technology: Basic and Applied Aspects. Dordrecht, The Netherlands: Kluwer Academic Publishers. p 341–346.

Avgerinos GC, Drapeau D, Socolow JS, Mao J–I, Hsiao K, Broeze RJ. 1990. Spin filter perfusion system for high density cell culture: production of recombinant urinary type plasminogen activator in CHO cells. Bio–Technol. 8:54–58.

Belfort G. 1988. Membrane modules: comparison of different configurations using fluid mechanics. J. Membrane Sci. 35:245–270.

Björling T, Dudel U, Fenge C. 1995. Evaluation of a cell separator in large scale perfusion culture. In: al. ECBe, editor. Animal Cell Technology: Developments towards the 21st century: Kluwer Academic Publishers. p 671–675.

Büntemeyer H, Bödeker BGD, Lehmann J. 1987. Membrane–stirrer–reactor for bubble free aeration and perfusion. In: Spier RE, Griffiths JB, editors. Modern approaches to animal cell technology. p 411–419.

Büntemeyer H, Bohme C, Lehmann J. 1994. Evaluation of membranes for use in online cell–separation during mammalian–cell perfusion processes. Cytotechnology 15(1–3):243–251.

Castilho LR, Medronho RA. 2002. Cell retention devices for suspended–cell perfusion cultures. In: Scheper T, editor. Advances in Biochemical Engineering/ Biotechnology. Berlin Heidelberg: Springer–Verlag. p 129–169.

Curting EMA, Hayter PM, Baines AJ, Bull AT, Gull K, Strange PG, Jenkins N. 1990. Recombinant human interferon–g. Differences in glycosylation and proteolytic processing lead to heterogeneity in batch culture. Biochem J. 272:333–337.

de la Broise D, Noiseux M, Lemieux R, Massie B. 1991. Long–term perfusion culture of hybridoma: A "grow or die" cell cycle system. Biotechnol. Bioeng. 38:781–787.

de la Broise D, Noiseux M, Massie B, Lemieux R. 1992. Hybridoma perfusion systems: A comparison study. Biotechnol. Bioeng. 40:25–32.

Deo YM, Mahadevan MD, Fuchs R. 1996. Practical considerations in operation and scale–up of spin–filter based bioreactors for monoclonal antibody production. Biotechnol. Progr. 12:57–64.

Emery AN, Jan DC–H, Al–Rubeai M. 1995. Oxygenation of intensive cell–culture system. Appl. Microbiol. Biot. 43:1028–1033.

Esclade LRJ, Carrel S, Péringer P. 1991. Influence of the screen material on the fouling of the spin filters. Biotechnol. Bioeng. 38:159–168.

Fane AG, Fell CJD, Kim KJ. 1985. The effect of surfactant pretreatment on the ultrafiltration of proteins. Desalination 53:37–55.

Favre E. 1993. Constant Flow–Rate Filtration of Hybridoma Cells Suspensions. J. Chem. Technol. Biot. 58(2):107–112.

Favre E, Thaler T. 1992. An engineering analysis of a rotating sieves for hybridoma cell retention in stirred tank bioreactors. Cytotechnology 9:11–19.

Fenge C, Buzsaky F, Fraune E, Lindner–Olsson L. 1991a. Evaluation of a spin filter during perfusion culture of recombinant CHO cells. In: Murakami H, Shirahata S, Tachibana H, editors. Animal Cell Technology: Basic and Applied Aspects. Fukuoka, Japan: Kluwer Academic Publishers. p 429–433.

Fenge C, Fraune E, Freitag R, Scheper T, Schügerl K. 1991b. On–line monitoring of monoclonal antibody formation in high density perfusion culture using FIA. Cytotechnology 6:55–63.

Fenge C, Klein C, Heuer C, Siegel U, Fraune E. 1993. Agitation, aeration and perfusion modules for cell culture bioreactors. Cytotechnology 11:233–244.

Fraune E, Meichsner S, Kamal MN. 1997. A new spinfilter design. In: al. MJTCe, editor. Animal cell technology: Kluwer Academic Publishers. p 283–287.

Griffiths JB. 1992. Animal cell culture processes – batch or continuous? J. Biotechnol. 22:21–30.

Griffiths JB, Cameron DR, Looby D. 1987. A comparison of unit process systems for anchorage dependent cells. Dev. Biol. Stand. 66:331–338.

Gröschl M, Burger W, Handl B. 1998. Ultrasonic separation of suspended particles – Part III: Application in Biotechnology. Acustica 84:815–822.

Heine H, Biselli M, Wandrey C. 1999. High cell density cultivation of hybridoma cells: spin filter vs immobilized culture. In: A. Bernard et al., editor. Animal cell technology: Products from cells, cells as products: Kluwer Academic Publishers. p 83–85.

Himmelfarb P, Thayer PS, Martin HE. 1969. Spin filter culture: the propagation of mammalian cells in suspension. Science 164:555–557.

Hu W–S, Peshwa MV. 1991. Animal cell bioreactors – recent advances and challenges to scale–up. Can. J. Chem. Eng. 69:409–420.

Hu X, Xiao C, Huang Z, Guo Z, Zhang Z, Li Z. 2000. Pilot production of u–PA with porous microcarrier cell culture. Cytotechnology 33:13–19.

Iding K, Lütkemeyer D, Fraune E, Gerlach K, Lehmann J. 2000. Influence of alterations in culture condition and changes in perfusion parameters on the retention performance of a 20 μm spinfilter during a perfusion cultivation of a recombinant CHO cell line in pilot scale. Cytotechnology 34:141–150.

Jan DC–H, Emery AN, Al–Rubeai M. 1992. Optimization of spin–filter performance in the intensive culture of suspended cells. In: Spier RE, Griffiths JB, MacDonald C, editors.

Animal cell technology: developments, processes and products. Oxford: Butterworth–Heinemann. p 448–451.

Jenkins N, Castro P, Menon S, Ison A, Bull A. 1994. Effect of lipid supplements and the production and glycosylation of recombinant interferon–gamma expressed in CHO cells. Cytotechnology 15:209–215.

Jo EC, Yun JW, Jung KH, Chung SI, Kim JH. 1998. Performance Study of Perfusion Cultures for the Production of Single–Chain Urokinase–Type Plasminogen–Activator (Scu–Pa) in a 2.5 L Spin–Filter Bioreactor. Bioprocess Eng. 19(5):363–372.

Johnson M, Lanthier S, Massie B, Lefebvre G, Kamen AA. 1996. Use of the Centritech Lab centrifuge for perfusion culture of hybridoma cells in protein–free medium. Biotechnol. Progr. 12:855–864.

Kim KJ, Fane AG, Fell CJD. 1988. The performance of ultrafiltration membranes pretreated by polymers. Desalination 70:229–249.

Kong D, Gentz R, Zhang J. 1998. Long–term stable production of monocyte–colony inhibition factor (M–CIF) from CHO microcarrier perfusion cultures. Cytotechnology 26:131–138.

Lee JH, Kopeckova P, Kopecek J, Andrade JD. 1990. Surface properties of copolymers of alkyl methacrylates with methoxy (polyethylene oxide) methacrylates and their application as protein–resistant coatings. Biomaterials 11:455–464.

Li S–Y, Roder B, Wirth M. 1991. Fermentation of ATIII producing BHK cells in a double membrane perfusion bioreactor. In: Spier RE, Griffiths JB, Meignier B, editors. Production of biologicals from animal cells in culture: Butterworth–Heinemann. p 445–450.

Maiorella B, Dorin G, Carion A, Harano D. 1991. Cross–flow microfiltration of animal cells. Biotechnol. Bioeng. 37(2):121–126.

Mercille S, Johnson M, Lanthier S, Kamen AA, Massie B. 2000. Understanding factors that limit the productivity of suspension–based perfusion cultures operated at high medium renewal rates. Biotechnol. Bioeng. 67(4):435–450.

Mercille S, Johnson M, Lemieux R, Massie B. 1994. Filtration–based perfusion of hybridoma cultures in protein–free medium: Reduction of membrane fouling by medium supplementation with DNase I. Biotechnol. Bioeng. 43:833–846.

Pui PWS, Trampler F, Sonderhoff SA, Gröschl M, Kilburn DG, Piret JM. 1995. Batch and semicontinuous aggregation and sedimentation of hybridoma cells by acoustic resonance fields. Biotechnol. Progr. 11:146–152.

Reuveny S, Velez D, Miller L, Macmillan JD. 1986. Comparison of cell propagation methods for their effect on monoclonal antibody yield in fermentors. J. Immunol. Methods 86:61–69.

Ryll T, Dutina G, Reyes A, Gunson J, Krummen L. 2000. Performance of small–scale CHO perfusion cultures using an acoustic cell filtration device for cell retention: Characterization of separation efficiency and impact of perfusion on product quality. Biotechnol. Bioeng. 69(4):440–449.

Searles JA, Todd P, Kompala DS. 1994. Viable cell recycle with an inclined settler in the perfusion culture of suspended recombinant chinese hamster ovary cells. Biotechnol. Progr. 10:198–206.

Shintani Y, Kohno Y, Sawada H, Kitano K. 1991. Comparison of culture methods for human–human hybridomas secreting anti–HBsAg human monoclonal antibodies. Cytotechnology 6:197–208.

Siegel U, Fenge C, Fraune E. 1991. Spin filter for continuous perfusion of suspension cells. In: Murakami H, Shirahata S, Tachibana H, editors. Animal Cell Technology: Basic and Applied Aspects. Fukuoka, Japan: Kluwer Academic Publishers. p 434–436.

Smith CG, Guillaume J–M, Greenfield PF, Randerson DH. 1991. Experience in scale–up of homogeneous perfusion culture for hybridomas. Bioprocess Eng. 6:213–219.

Stiens LR, Büntemeyer H, Lütkemeyer D, Lehmann J, Bergmann A, Weglöhner W. 2000. Development of serum–free bioreactor production of recombinant human thyroid stimulating hormone receptor. Biotechnol. Progr. 16:703–709.

Stryer L. 1999. Biochemistry. New York: W. H. Freeman & Co. 1064 p.

Thompson KJ, Wilson JS. 1994. A compact gravitational settling device for cell retention. In: Spier RE, editor. Animal Cell Technology. Oxford: Butterworth–Heinemann. p 227–229.

Tokashiki M, Arai T, Hamamoto K, Ishimaru K. 1990. High density culture of hybridoma cells using a perfusion culture vessel with an external centrifuge. Cytotechnology 3:239–244.

Tokashiki M, Takamatsu H. 1993. Perfusion culture apparatus for suspended mammalian cells. Cytotechnology 13:149–159.

Tolbert WR, Feder J, Kimes RC. 1981. Large–scale rotating filter perfusion system for high–density growth of mammalian suspension cultures. In Vitro Cell Dev. B 17(10):885–890.

Trampler F, Sonderhoff SA, Pui PWS, Kilburn DG, Piret JM. 1994. Acoustic cell filter for high density perfusion culture of hybridoma cells. Bio–Technol. 12(3):281–284.

Van Wezel AL, Van der Velden–de–Groot CAM, de Haan JJ, van den Heuval N, Schasfoort R. 1985. Large scale animal cell cultivation for production of cellular biologicals. Dev. Biol. Stand. 60:229–236.

Varecka R, Scheirer W. 1987. Use of a rotating wire cage for retention of animal cells in a perfusion fermentor. Dev. Biol. Stand. 66:269–272.

Velez D, Reuveny S, Miller L, Macmillan JD. 1987. Effect of feeding rate on monoclonal antibody production in a modified perfusion–fed fermentor. J. Immunol. Methods 102:275–278.

Vogel JH, Kroner KH. 1999. Controlled shear filtration: A novel technique for animal cell separation. Biotechnol. Bioeng. 63(6):663–674.

Voisard D, Meuwly F, Ruffieux P–A, Baer G, Kadouri A. 2003. Potential of cell retention techniques for large–scale high–density perfusion culture of suspended mammalian cells. Biotechnol. Bioeng. 82(7):751–765.

Werner A, Lütkemeyer D, Poggendorf I, Lehmann J, Müthing J. 2002. Serum–free production of a chimeric E–selectin–IgG protein from 1 to 100 l scale: repeated batch cultivation versus continuous spin filter perfusion. Cytotechnology 38:47–56.

Woodside SM, Bowen BD, Piret JM. 1998. Mammalian cell retention devices for stirred perfusion bioreactors. Cytotechnology 28:163–175.

Yabannavar VM, Singh V, Connelly NV. 1992. Mammalian cell retention in a spinfilter perfusion bioreactor. Biotechnol. Bioeng. 40:925–933.

Yabannavar VM, Singh V, Connelly NV. 1994. Scaleup of spinfilter perfusion bioreactor for mammalian cell retention. Biotechnol. Bioeng. 43(2):159–164.

Zhang J, Collins A, Chen M, Knyazev I, Gentz R. 1998. High–density perfusion culture of insect cells with a BioSep Ultrasonic Filter. Biotechnol. Bioeng. 59(3):351–359.

3

Study of spin–filter particle retention for animal cell perfusion cultures

Abstract

Spin–filters are widely used in attempts to raise the concentration of animal cells in perfusion cultures, however the main limitation is reduced operational time, caused by filter fouling, although increasing the filter pore size may reduce this phenomenon. In order to study the mechanism of particle retention in the absence of fouling, the retention of agarose beads (13±2 μm diameter) by filters with pore sizes of 13 and 14.5 μm was shown to be mainly dependent on filter rotation speed and pore size and, to a lesser extent, on the perfusion rate and particle concentration. Filter retention followed saturation dynamics with an initial direct correlation with respect to filter rotation rate. A plateau was reached above a filter tangential velocity of 0.45 m/s and 0.87 m/s for filters with pore sizes of 13 and 14.5 μm respectively. A high perfusion rate of 13.5 cm/h resulted in reduced bead retention at low filter tangential speeds (<0.8 m/s), whereas it had little influence on bead retention at rotational velocities above 0.8 m/s using spin–filter with

pore size of 14.5 μm. Retention was improved with increasing particle concentration. CHO cell perfusion cultures were carried out using a spin–filter having a pore size diameter of 14.5 μm and despite cell retention of 0.8–0.85, a high cell density ($2 \cdot 10^7$ cell/ml) was achieved over a duration of 900 h. Positioning a draft tube around open spin–filters was observed to lower bead retention, with the effect being greater for non–porous than for porous draft tubes.

Keywords: High cell density culture, spin–filter, perfusion culture, animal cell culture, cell separation, cell retention

3.1 Introduction

Internal spin–filters are frequently used for suspended mammalian cell perfusion cultures mainly because of the relatively simple operation and low effect on cell viability, as a result cells not coming into contact with pumps. Such devices generally consist of a cylindrical wire support cage, on which a filter is mounted, that is rotated by a motor, either dependently or independently of the stirrer shaft. Fresh medium is fed continuously into the reactor containing cells, whereas medium is withdrawn from within the spin–filter (Figure 3.1). High cell concentrations ($>1 \cdot 10^7$ cell/ml) can be achieved (Fenge et al., 1991; Heine et al., 1999). The main disadvantage of spin–filter devices is usually associated with fouling of the filter surface (Esclade et al., 1991; Mercille et al., 1994), limiting operation of the cultures for long–time.

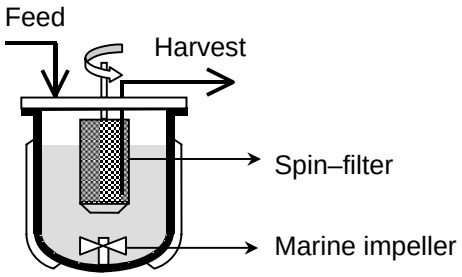

Figure 3.1: Schematic representation of an internal spin–filter device.

The earliest spin–filters used with cell cultures had pore sizes (3 μm) much smaller than the average animal cell diameter (12–15 μm) (Himmelfarb et al., 1969). As a result cell retention was maximal and a cell concentration of about $6.5 \cdot 10^7$ cell/ml was attained,

over a period of 10 days without any sign of filter fouling. However, many investigators have studied this system in order to operate over extended periods by minimizing filter fouling (Deo et al., 1996; Favre and Thaler, 1992). One way to do this involved increasing the filter pore size to values larger than the mean cell diameter. However, this increase induces cell leakage, thereby decreasing the cell concentration within the reactor. Further studies revealed that cell retention was dependent on many parameters, including filter pore size, filter rotation velocity, perfusion rate and cell concentration (Iding et al., 2000; Jan et al., 1992; Siegel et al., 1991).

The retention of open filters (filters in which the pore size is larger than the mean cell diameter) as a function of filter rotation velocity was found to have different tendencies. Thus, using pore sizes of 10, 20 and 40 μm, resulted in different optimum retention values of latex beads of 11.9±1.9 μm in diameter, despite similar retention profiles being obtained (Siegel et al., 1991). Indeed, bead retention increased with increasing filter rotation velocity until a maximum retention value of 0.71, 0.67 and 0.39 was reached at same filter tangential speed of 0.61 m/s for filter pore sizes of 10, 20 and 40 μm respectively. Above 0.61 m/s, retention decreased with increasing filter tangential speed (tip speed) for all tested filter pore sizes. However, using a 20 μm screen, it was found that the maximal retention of agarose beads (13±2 μm diameter) was at an optimal filter velocity of 0.43 m/s at 2–L scale (Iding et al., 2000). However, using the same filter porosity at large scale (100–L), resulted in a different retention profile, with low retention values, instead of the maximum previously obtained at small scale, when increasing filter tip speed (Iding et al., 2000). Elsewhere it has been observed also that retention increased as a function of filter rotation for pore sizes of 25 and 40 μm (Jan et al., 1992). However, in contrast to previous reports, an optimal retention was reached above 0.63 m/s. The retention studies of Yabannvar et al., using 25 μm pore size spin–filters, demonstrated that retention was not affected by the filter rotation speed, the latter only having an influence on filter clogging (Yabannavar et al., 1992). Thus particle retention was generally observed to decrease with increasing filter pore size, however the reported studies show the difficulty of making general conclusions on particle retention when varying filter velocity. Thus, increasing the filter rotation for a given filter pore size revealed different retention values as well as different retention profiles.

The influence of perfusion rate on cell retention has also been studied. In the present study the perfusion rate has been normalized with respect to the filtration surface

in order to compare the different published results. Thus the perfusion rate is expressed in cm/h, while the filter rotation speed is in m/s. Perfusion rates from 0.7 to 16 cm/h were found to have little effect on retention with large pore size (40 μm) spin–filters (Fenge et al., 1991). For filters with smaller pore sizes (25 μm), retention did not vary with perfusion rates from 1.6 to 6.4 cm/h at high filter speeds (> 0.63 m/s). However, retention was strongly dependent on perfusion flow at filter speeds below 0.63 m/s (Jan et al., 1992). With the same type of filter (25 μm) other reports conclude that retention was only affected slightly by perfusion rates above 4.3 cm/h for rotation speeds of 0.4 m/s (Yabannavar et al., 1992).

The influence of cell concentration on retention has received little attention compared with the effect on filter fouling. Thus it was observed that the retention rate remained constant when cell density increased from $2 \cdot 10^6$ to $4.5 \cdot 10^6$ cell/ml (Yabannavar et al., 1992).

The majority of reported studies on cell retention have been performed either during cell/bead simulations or during actual cell cultures. In all of these studies, the variation of multiple parameters at a time made it difficult to conclude which parameter has the greatest influence on cell retention. As a result, the literature is confusing with the retention tendency different from one author to another. For these reasons, in this paper, a detailed systematic study on cell/bead retention was carried out with particle retention measured as a function of four main parameters: filter pore size, filter rotational speed, perfusion rate and cell concentration, each of which was varied independently. The influence of placing a draft tube around an open spin–filter, in order to increase turbulence, on particle retention was also studied.

3.2 Materials and methods

3.2.1 Materials

Animal cell retention studies require sterile working conditions and large numbers of cells, the latter requiring considerable time and effort to produce. Furthermore, fouling of the filters can impede studies on the role of the principle parameters. In order to avoid these problems, Superose 6 beads (provided by Amersham Biosciences, Freiburg, Germany) were used in place of animal cells. The density of the polymer beads is 1.055

g/ml, which is in the range of that of animal cells, while the diameter specified by the supplier is about 13 ± 2 microns, which corresponds approximately to the mean diameter of animal cells. Particles were counted spectrophotometrically (Uvikon 930, Kontron Instruments, Switzerland) at a wavelength of 600 nm. A previous calibration was first necessary in order to convert absorbance to particles per milliliter. This was achieved microscopically using a hemocytometer.

The cell line used during the perfusion cell culture is a CHO *SSF3* cell line, producing human secretory component (hSC). The cell culture medium is a serum– and protein– free medium ChoMaster HP–1 (Cell Culture Technology, Zuerich, Switzerland), supplemented with 5 mM glutamine, 5 mM asparagine, 1 mM leucine, 1 mM glutamic acid and 1 mM serine. A minimal cell concentration was fixed at $2 \cdot 10^5$ cell/ml and cells were harvested upon reaching a maximal cell density of 1–$1.2 \cdot 10^6$ cell/ml. During passaging the cells were maintained at 37 °C, under a humidified air atmosphere containing 5% CO_2.

3.2.2 Experimental set–up

All bead retention studies were performed in an open glass vessel with an internal diameter of 12 cm and a working volume set to 1.6 L. No draft tube was placed around the filter unless specified otherwise. A magnetic agitator maintained the particles in suspension and baffles (1 cm in width) were placed inside the vessel, on the internal walls, in order to maintain the particles homogeneously in suspension. The open cylindrical stainless steel support was assembled with a solid ring at the top, a conical shaped bottom and four narrow vertical bars, in order to make the available open filtration area as large as possible.

The filter screen was made of 316L stainless steel (G. Bopp & Co. AG, Zuerich, Switzerland) with three different pore sizes of 8.5, 13 and 14.5 μm, which correspond to a porosity factor ε (ratio of filter pore size to the mean particle diameter) of 0.65, 1 and 1.12 respectively. The weave orientation of the mesh for filters which pore size corresponds to 8.5 and 13 μm is a twilled Dutch weave, while it is a Duplex weave for the filter which pore size corresponds to 14.5 μm. The external filter diameter was 4.28 cm and the wet/immersed height was 7 cm. Baffles of 1 cm width were placed within the spin–filter. The filter rotation is driven from the top by a motor and in the present study is expressed as the tangential filter velocity, expressed in m/s. The perfusion flow is removed from the

interior of the spin–filter using a peristaltic pump (Alitea, Bioengineering, Wald, Switzerland) and returned to the vessel, in order to keep the total volume and the particle concentration within the vessel constant (Figure 3.2).

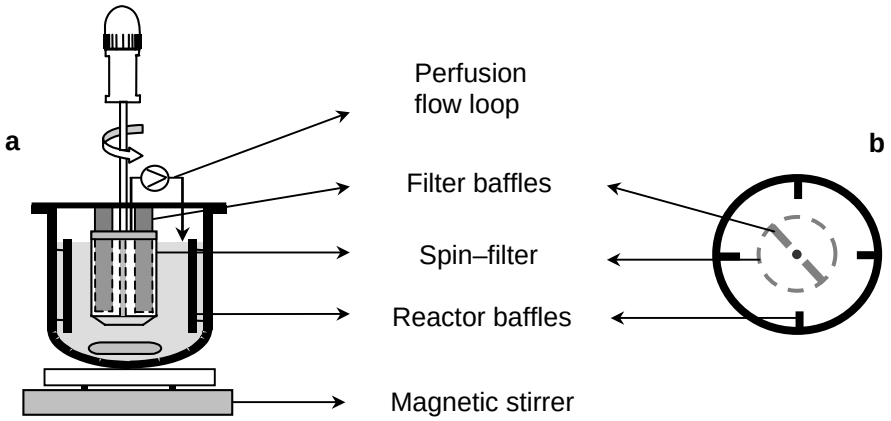

Figure 3.2: Bead perfusion simulation set–up. Section view (**a**) and top view (**b**).

The perfusion rate relates the ratio of the perfusion flow to the total immerged surface of the filter and is expressed in cm/h. Samples are taken directly from inside the spin–filter and from the vessel, in order to measure particle concentration and calculate the particle retention (R), defined as shown in Equation 3.1.

$$R = 1 - \frac{c_{in,filter}}{c_{out,filter}} \qquad \text{Equation 3.1}$$

where $c_{in,filter}$ and $c_{out,filter}$ are the concentrations of particles inside and outside the spin–filter respectively. A maximum retention value of 1 implies that there are no particles within the filter. This happens when the filter is completely closed (filters with pore sizes lower than the mean particle/cell diameter) and/or clogged. Retention values less than 1 occur when the filter is open (filters have a pore size greater than the particle/cell diameter) and particles pass through the filter.

Animal cell perfusion cultures of CHO *SSF3* were performed in a 2 L reactor (Bioengineering, Wald, Switzerland) with 1.65 L working volume. The reactor was operated at a temperature of 37°C, under gentle agitation using a marine impeller of 5 cm in diameter, at 150 rpm. Bubble–free aeration was achieved using 2 m of Teflon tubing (W. L. Gore & Associates GmbH, Putzbrunn, Germany). A regulation system injected a mixture of oxygen, nitrogen and carbon dioxide into the reactor via the Teflon tubing to

maintain the dissolved oxygen concentration at 80% air saturation and 5% CO_2 saturation during the culture. This system also allowed determination of the oxygen uptake rate on–line (Ducommun et al., 2000). For cell separation a stainless steel spin–filter was used with dimensions of 6.36 cm diameter and 8 cm height (4 cm immersion height). Baffles of 2 cm width were placed within the spin–filter. A filter pore size of 14.5 μm was used with the filter rotation rate set to 1.07 m/s. Medium was fed into the reactor using a peristaltic pump (Preciflow Lambda, Visperminen, Switzerland), while a second peristaltic pump (Preciflow Lambda, Visperminen, Switzerland) withdrew the perfusate from the bottom of the inside of the spin–filter.

3.2.3 Biomass and metabolite analysis

The cell concentration was determined by counting microscopically the cells with a Neubauer hemocytometer chamber of 0.1mm^3 volume. Viable and non–viable cells were distinguished using the Trypan blue extrusion method.

Glucose and lactate concentrations were quantified by HPLC (1100 system, Agilent, Palo Alto, California, United States) analysis using a Supelco H column (Supelco, Bellefonte, Pittsburgh, United States), H_2SO_4 0.02M as solvent and a refractive index detector (HP 1047 A, Hewlett Packard GmbH, Waldbronn, Germany). Glutamine concentration was quantified by HPLC (450–MT2, Kontron Instruments, Zurich, Switzerland) using an Aminex HPX–87C column (BIO–RAD, Hercules, California, United States), calcium nitrate 2 mM as solvent and a RI detector (ERC–7510, ERMA Optical Works Ltd, Tokyo, Japan).

The human secretory component (hSC) was quantified using a sandwich ELISA method that was developed by Stoll et al. (1997). This involved an anti–mouse IgA α–chain specific as coating, a biotinylated anti–mouse IgA α–chain specific, a streptavidin–horseradish peroxidase conjugate and orthophenylenediamine as a substrate. The assay was calibrated using a purified mouse IgA as standard.

3.2.4 Homogeneity inside the spin–filter

Previous studies of particle retention at fixed operational parameters showed large differences in retention values for repeated experiments (data not shown). The filter

rotation creates a centrifugal effect outside the filter but also creates fluid rotation within the spin–filter. The density of particles being higher than that of the fluid, these latter tend to sediment within the spin–filter. This phenomenon was observed to decrease the suspended particle concentration outside the filter (Figure 3.3), especially when a perfusion rate is applied, due to particle accumulation inside the spin–filter.

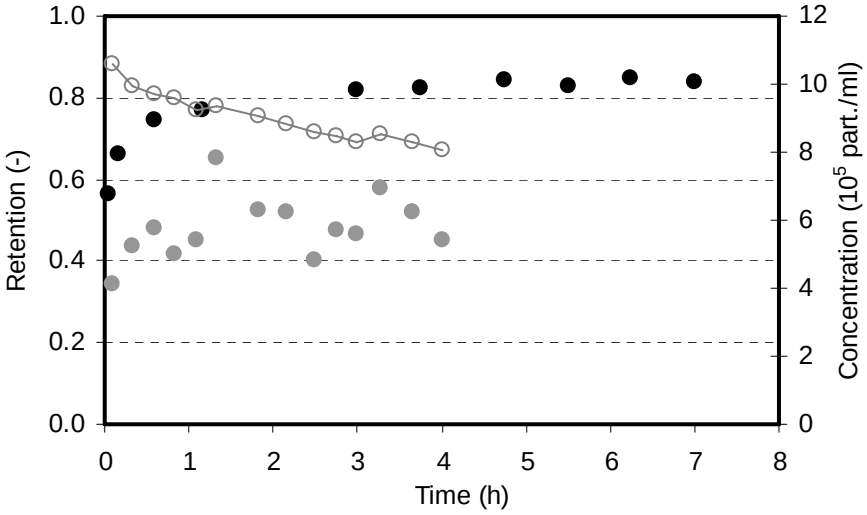

Figure 3.3: Open filter retention as a function of time, at 2.6 cm/h perfusion rate and 1.1 m/s rotational speed for different filter set–ups: ● spin–filter with baffles, ● spin–filter without baffles and –❍– particle concentration (10^5 part./ml) outside the spin–filter.

The irregularities in the retention rate (Figure 3.3) are also due to poor homogenization of the liquid inside the spin–filter, thus creating zones with particle depletion and zones with concentrated particles. Placing baffles (Figure 3.2a) completely immersed within the spin–filter resulted in homogenous particle distribution, through inhibition of particle/cell sedimentation and thus accumulation within the filter. As a result, reproducible retention rates could be obtained and spin–filters with baffles placed inside were used throughout this study.

3.2.5 Particle retention dynamics

The dynamics of the reaction are dependent on the parameters applied to the system. It has been observed that for open filters the lower the retention, the longer the time needed to reach equilibrium. Indeed, the time until steady state is dependent on the equilibrium of the forces applied to the system and identified as being mainly: the

perfusion drag force caused by the perfusion flow and the centrifugal force caused by the filter rotation (Deo et al., 1996; Favre and Thaler, 1992).

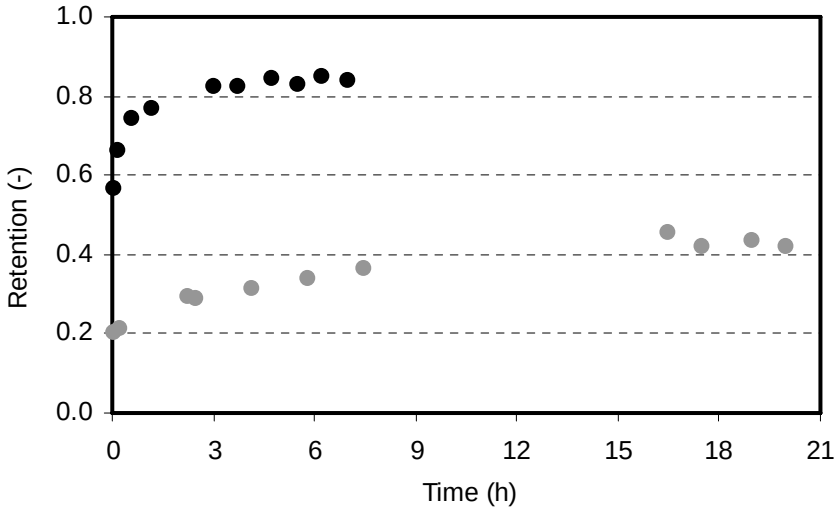

Figure 3.4: Filter retention as a function of time at a perfusion flow of 2.6 cm/h and for two rotational speeds: ● 1.1 m/s and ● 0.3 m/s. Filter pore size is 14.5 μm and filter contained baffles inside.

As represented in Figure 3.4, the time taken to reach equilibrium varies as a function of high or low rotation speed of the filter. At high rotation speeds (1.1 m/s), the equilibrium is reached quickly after 3 or 4 hours, whereas at lower rotational speeds (0.3 m/s), it takes at least 16 h for the system to reach equilibrium under these fixed conditions. Thus, in order to reach a stable steady state and obtain accurate retention values, it is necessary to let the system equilibrate, especially at low filter rotation speeds. The two different plateaux reached show a different retention value, which indicates that the retention is dependent on the filter rotational speed, as it will be shown in the next section.

3.3 Results and discussion

3.3.1 Retention study

Retention was demonstrated as being dependent on many parameters, such as the filter pore size and rotational speed and perfusion flow (Favre, 1993; Iding et al., 2000; Jan et al., 1992; Varecka and Scheirer, 1987), as well as a combination of parameters (Jan et al., 1992; Siegel et al., 1991). For these reasons, in order to study the influence of

all the parameters on retention, each parameter has been varied independently, while maintaining the others fixed. The four parameters studied are filter pore size, filter rotational speed, perfusion flow and particle concentration inside the vessel.

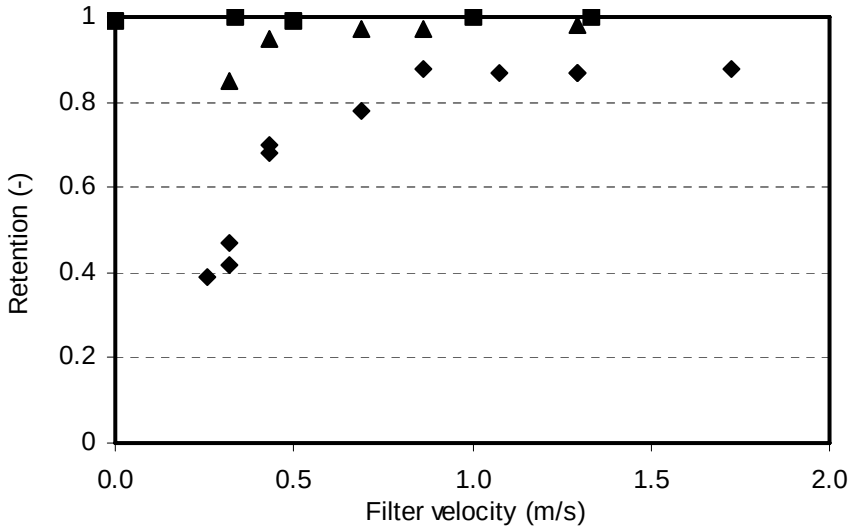

Figure 3.5: Particle retention as a function of rotational speed at a perfusion flow of 2.6 cm/h and particle concentration of $1 \cdot 10^6$ particle/ml, for different filter porosity factors: ■ $\varepsilon = 0.65$, ▲ $\varepsilon = 1$ and ◆ $\varepsilon = 1.12$. Filter contained baffles inside.

The bead retention profile was observed to be different for the three porosity factors chosen (Figure 3.5). Completely closed filters (filters which pore sizes are smaller than the average bead/cell diameter), as expected, show a maximal retention profile for any filter velocity tested. However increasing the porosity factor, which means increasing the filter pore size, results in a decreased retention. For a filter velocity of 0.3 m/s, 100% of the particles are retained within the vessel for a closed filter, which has a filter porosity of 0.65. On the other hand, 85% and 45% of particles are retained for an open filter having a porosity factor of 1 and 1.12 respectively. Although the filter having a porosity factor of 1 has pore sizes equal to the mean particle diameter, the retention is still below 1. This is due to the fact that the beads are not mono–disperse but follow a size distribution, which permits particles smaller than 13 μm to pass through the filter. By increasing the filter rotational velocity the retention also increases, even for open filters, in such a manner that at around 0.85 m/s, the retention reaches 0.85 for a filter having the largest porosity factor (1.12). Thus increasing the filter velocity also increases particle retention until a plateau is reached and for any filter porosity greater than 1, there is a minimal tangential filter

velocity that enables retention of a maximum of particles. Many researchers obtained one optimal filter velocity in order to get maximum cell retention, however retention profiles below and above this value seemed to not be similar (Iding et al., 2000; Jan et al., 1992; Siegel et al., 1991). Additionally one similar optimal filter rotation was found for different filter porosities. Indeed, for different filter porosities from 0.84 to 3.36, the optimum filter speed was found to be around 0.61–0.63 m/s (Siegel et al., 1991; Jan et al., 1992). In the present study, the minimal filter rotation speed at which the filter has to be rotated in order to reach maximal particle retention is dependent on the filter porosity. Indeed, employing a filter with a porosity factor of 1, the minimal filter rotation speed corresponds to 0.45 m/s, whereas for a filter porosity of 1.12, the value corresponds to 0.87 m/s. In real cell perfusion cultures, open filters should be operated at the maximum speed that the cells can support (no cell damage due to shearing forces); or for economic reasons, at least at the minimal filter velocity, where maximal retention is achieved, in order to minimize power consumption.

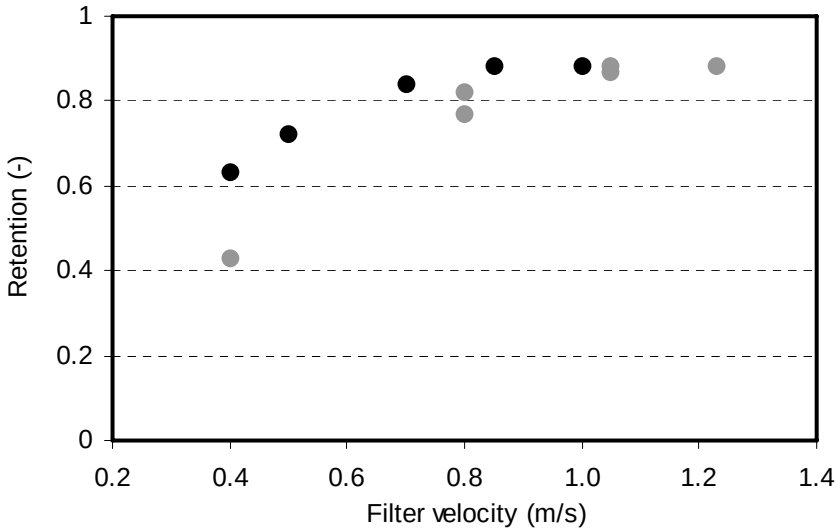

Figure 3.6: Particle retention as a function of rotational speed for filter porosity factor of 1.12 and particle concentration of $5.5 \cdot 10^6$ particle/ml, for two perfusion rates: ● 0.6 cm/h and ● 13.5 cm/h. Filter contained baffles inside.

The effect of perfusion flow on particle retention was also studied with a filter porosity factor of 1.12 (Figure 3.6). The influence of the perfusion rate was found to be dependent on the filter velocity range. At low filter rotations, below 0.7 m/s, increasing the perfusion rate decreases the particle retention. At intermediate filter velocities, ranging

from 0.7 to 1 m/s, by increasing the perfusion flow the retention decreases, albeit less than previously. However, at filter velocities above 1 m/s, a high perfusion rate of 13.5 cm/h seems to have no effect on particle retention and same retention rates (same plateau) are reached in the both cases. As a result, the minimal filter rotation speed at which retention is maximal is increased when the perfusion rate increases. Similar results have been described elsewhere (Jan et al., 1992). At this point, the centrifugal force seems to be large enough to compensate for the perfusion drag force. A perfusion rate of 13.5 cm/h corresponds to a perfusion flow of 3 vvd at 300 L scale, for a filter volume of 20% of the working reactor volume and for an immersed filter height of 50% of the reactor height. Retention has not been tested at higher perfusion rates since it was considered that 13.5 cm/h is a realistic working flow at large scale. However even at high filter rotations above 1 m/s, there must be perfusion flows higher than 13.5 cm/h, that the centrifugal force no longer compensate and particle retention would decrease.

The cell concentration during actual perfusion cell cultures increases from $2 \cdot 10^5$ to $1–1.5 \cdot 10^7$ cell/ml. Until now, the study of particle retention was undertaken only for a fixed particle concentration of $1 \cdot 10^6$ and $5.5 \cdot 10^6$ particle/ml. It is thus important to study the influence with particle concentrations smaller than $1 \cdot 10^6$ particle/ml. For such studies an open filter with a porosity factor of 1.12 was chosen. The filter velocity was set to 1.1 m/s, corresponding to the maximum particle retention (plateau), while the perfusion flow was set to 2.6 cm/h and the particle concentration was varied from $1.1 \cdot 10^5$ to $5.5 \cdot 10^6$ particle/ml. From the results (Figure 3.7) the influence of particle concentration appears to be less important for retention than the filter rotation velocity (Figure 3.6). Retention decreased with decreasing particle concentration. Thus at $5.5 \cdot 10^6$ particle/ml, retention was 0.87, at $1.05 \cdot 10^6$ particle/ml, retention reached 0.85, while for $1.1 \cdot 10^5$ particle/ml retention reached 0.72, corresponding to a decrease of 17%. The increase in particle retention with increasing particle concentration suggests that the balance of the permeation drag force and centrifugal force alone does not influence retention. Indeed, if this balance were to regulate the retention mechanism, for fixed filter porosity and rotational velocity and fixed perfusion rate, the higher the particle concentration is, the larger the number of particles that pass the filter and thus retention should be unchanged. However, in the present study, a different phenomenon is observed, therefore it appears that the particles act like a screen around the spin–filter, thereby improving particle retention. In spite of a lower particle retention of 14% at concentration of $1.1 \cdot 10^5$ particle/ml compared with that at a particle concentration of $1 \cdot 10^6$ particle/ml, retention is

sufficiently high that a high cell density should be reached during perfusion cultures, when inoculating with cells at concentration of $2 \cdot 10^5$ particle/ml. Indeed, during the batch phase and before the perfusion mode is started, cells go through the filter under the influence of the centrifugal effect, however the fraction of cells that pass the filter remains low.

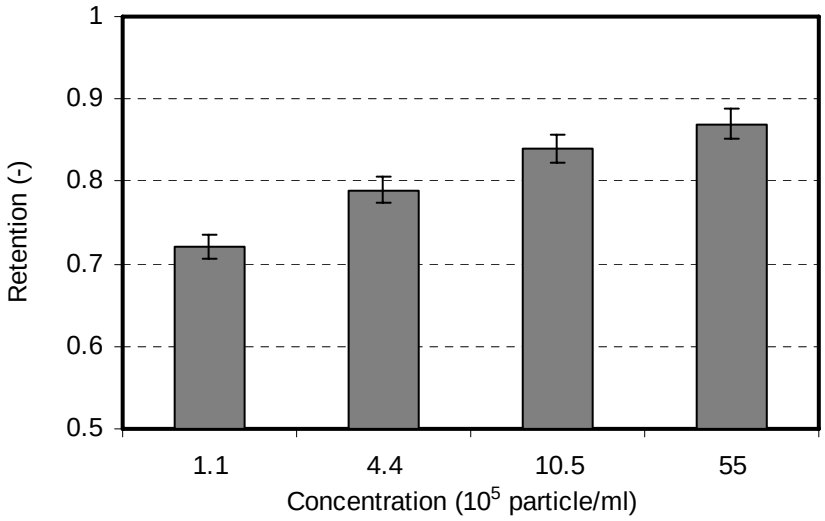

Figure 3.7: Particle retention as a function of particle concentration for filter porosity factor of 1.12, filter velocity of 1.1 m/s and perfusion rate of 2.6 cm/h. Filter contained baffles inside.

During actual perfusion cultures, the cell concentration is a parameter that is changing. Furthermore the low cell growth rate means that any disturbance of the retention mechanism due to cell increase is very slow. Thus in order to observe this influence on bead retention, a simulated perfusion culture with spin–filter porosity factor of 1.12 was performed (Figure 3.8). The bead concentration was increased from $1.5 \cdot 10^5$ to $1 \cdot 10^6$ particle/ml, more quickly than in an actual perfusion cell culture. At the beginning of the experiment, and thus at a low bead concentration of $1.5 \cdot 10^5$ particle/ml, the retention is low with a value of approximately 0.3. The system takes two hours to attain a steady state and thus for the retention to increase to a quasi–plateau at about 0.7, as previously observed in Figure 3.7. After this first steady state was attained, the particle concentration was increased step by step in order to reach $8 \cdot 10^5$ particle/ml and, as previously, the retention was observed to increase. Each time that the system is perturbed by changing the bead concentration, the retention does not change significantly and the time to reach steady state is shorter and is due mainly to the increase of particle concentration. The system was allowed to equilibrate for at least 12 hours before once again increasing the

concentration to $1 \cdot 10^6$ particle/ml. Only small differences in retention were observed when raising the particle concentration from $8 \cdot 10^5$ to $1 \cdot 10^6$ particle/ml, with the system equilibrating at 0.85 retention, as observed also previously in Figures 3.5 and 3.7. Thus during actual cell spin–filter perfusion, changes in retention would be expected for open filters during cell growth. However, once the first steady state had been reached, the retention would change slowly and increase with increasing cell density in a homogeneous way. Another important observation is the fact that after more than 25 hours, no filter fouling occurred, which would raise the retention to 1. The retention level was constant at 0.85, and indicates that the fouling mechanism is not simply the result of particle–sieve interactions. The values of particle retention achieved during different experiments, at a concentration of $1 \cdot 10^6$ particle/ml and 1.1 m/s (Figures 3.5, 3.7 and 3.8), are similar, thereby highlighting the reproducibility of the results.

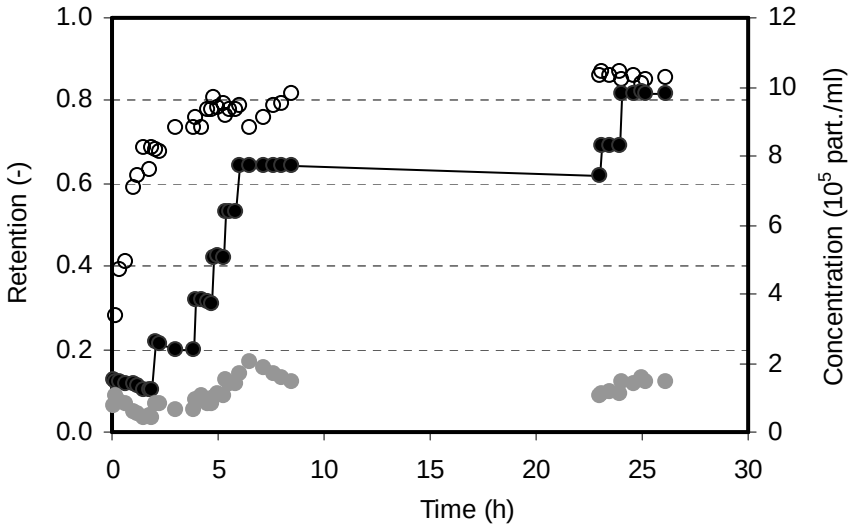

Figure 3.8: Bead perfusion simulation: filter rotation 1.1 m/s, perfusion flow 2.6 cm/h and ε = 1.12. ● Particle concentration outside the spin–filter, ● particle concentration inside the spin–filter and ❍ particle retention rate. Filter contained baffles inside.

The other parameter that is varied during actual cell perfusion cultures is the perfusion rate. As described before, this parameter has little influence on retention when high filter rotation speeds are applied however, as we have seen earlier, the system needs to reach a certain equilibrium state before the retention reaches its maximum value and thus changing the perfusion rate could also destabilize the system.

3.3.2 Animal cell perfusion culture

In order to validate bead retention profiles with inert particles to that with animal cell, a CHO cell perfusion culture was carried out using a large filter pore size of 14.5 μm that corresponds to ε of 1.21 and a filter velocity of 1.1 m/s (Figure 3.9).

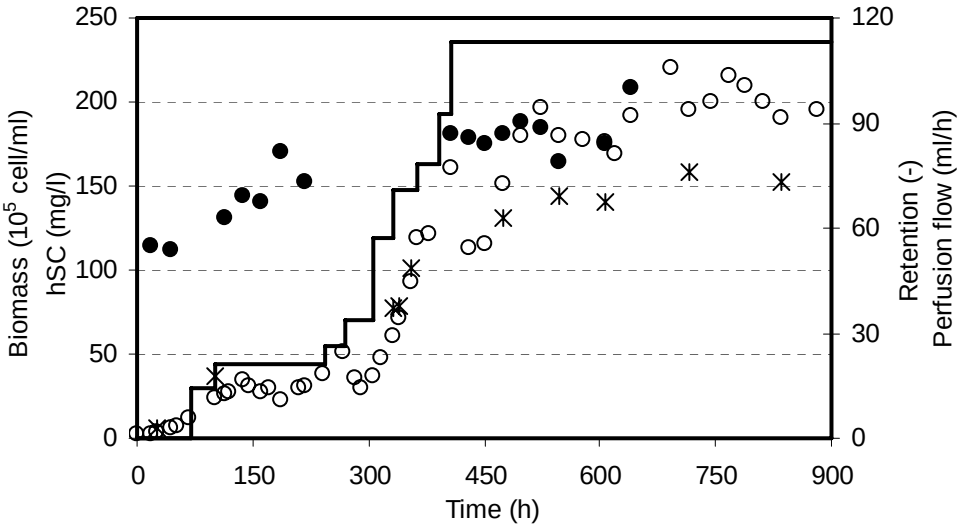

Figure 3.9: CHO perfusion culture for spin–filter porosity of 1.21. ❍ CHO viable cell concentration, ● Cell retention, **–** Perfusion flow and ∗ hSC concentration.

At the beginning of the culture, cell retention was low (0.6) because the system has not reached the steady state. Indeed, the changing sampling and perfusion rate influence the measurement of the retention mainly at low cell concentration, as previously described for particles. During this period, the dynamics of the retention phenomenon do not permit the cell density to increase because of cell leakage through the filter. Once the system has attained a certain equilibrium, cell retention reached 0.75–0.8 at $3.5 \cdot 10^6$ cell/ml. At 1.1 m/s and a bead concentration of $5.5 \cdot 10^6$ cell/ml, retention was equal to 0.85 at ε of 1.12 (Figure 3.7). Considering that cell concentration is lower than $5.5 \cdot 10^6$ cell/ml and that filter porosity is greater, this would induce a lower cell retention than previously observed with beads, and thus the retention value obtained during actual cell perfusion is in accordance with the one obtained during bead retention. Increasing the perfusion flow from 21 to 113 ml/h, corresponding to a perfusion rate of 1.4 cm/h, enabled a cell density of $1.8 \cdot 10^7$ cell/ml to be reached. The retention increased to a level of 0.87–0.90, as previously observed with beads at filter rotation of 1.1 m/s (extrapolating Figure 3.7). Cell concentration was stabilized at $1.8 \cdot 10^7$ cell/ml by increasing the rate of bleed and after 650

h the filter showed signs of fouling. Cell retention increased to a value of 1 and the cell concentration increased to $2 \cdot 10^7$ cell/ml. Because of filter fouling, at a filter rotation of 1.1 m/s and perfusion flow of 113 ml/h, the spin–filter emptied. In order to extend the culture, the filter rotation was lowered, firstly to 0.73 m/s and then to 0.37 m/s. In this way, cell concentration could be maintained at the high level of $2 \cdot 10^7$ cell/ml, with the hSC attaining high levels of 150 mg/l during 450 h with the culture operated during 900 h. The cell retention obtained during the actual animal cell cultures corresponds to bead retention during the same operational conditions (perfusion rate, particle concentration) and filter parameters (porosity and rotational velocity) and thus validates the studies carried out with polymer beads.

3.3.3 Vortex phenomena

The flow phenomena between two concentric cylinders, in movement or at rest, have been extensively studied (Bird et al., 1960; Schlichting, 1979). The rotation of the inner cylinder, with the outer cylinder being at rest, brings to the system a centrifugal instability resulting in Taylor–Couette flow. Mixing in Taylor–Couette flow systems has been extensively studied for rotating filtration devices (vortex flow filtration (VFF), rotating reverse osmosis, etc.) and catalytic reactors, mainly for mixing improvements and shear stress minimization (Kroner and Nissinen, 1988; Margaritis and Wilke, 1978). At sufficiently high rotation speeds, centrifugal forces overcome viscous forces and instabilities are created inducing pairs of counter–rotating toroidal (or Taylor) vortices that fill the space between the cylinders. The flow is characterized by the Taylor number (Ta), named also the rotational Reynolds number that is mainly expressed as described in Eq. 3.2, although other forms are possible (Kroner and Nissinen, 1988; Lieberherr, 1979; Recktenwald et al., 1993).

$$Ta = \frac{\omega \cdot r_i \cdot d}{\nu} \qquad \text{Equation 3.2}$$

where ω (s^{-1}) is the angular filter velocity, r_i (m) the radius of the inner cylinder, d (m) the gap between the cylinders and ν (m^2/s) the cinematic fluid viscosity. The critical Taylor number (Ta_{cr}) defines the passage from stable laminar circular Couette flow to Taylor vortex flow, where the flow becomes unstable. The transition from stable circular Couette flow to Taylor vortex flow has been investigated mainly as a function of the η factor, which

represents the ratio of the inner cylinder radius to the outer cylinder radius (Cognet, 1984; Lieberherr, 1979). At higher rotation speeds the Taylor vortex flow becomes unsteady and develops further different instabilities, as wavy vortex flow, modulated wavy vortex flow or turbulent Taylor vortex flow (Davey et al., 1968; Hwang and Yang, 2004).

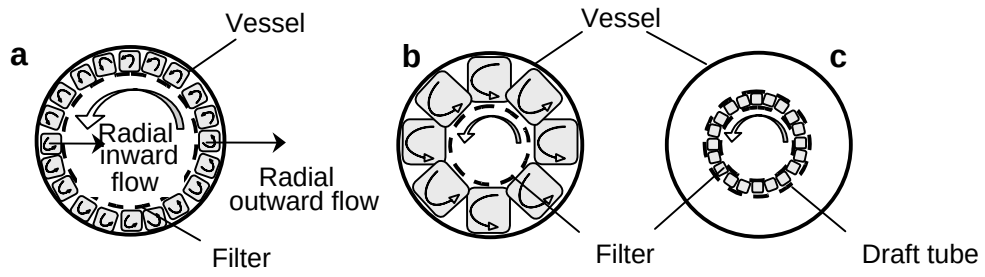

Figure 3.10: Taylor vortices representation (in gray in the Figure) in the gap between the rotating filter and the draft tube/vessel. **a**. VFF system (η>0.5), **b**. Spin–filter system (η<0.5) and **c**. Spin–filter with draft tube system (η>0.5).

In VFF systems, an inner porous cylinder is rotating inside a stationary nonporous outer cylinder (vessel) and the suspension enters the annular gap axially, while filtrate passes radially inward through the inner porous cylinder (Figure 3.10a). These flows were found to alter the stability of Taylor vortex flow and thus Ta_{cr} changes (Lieberherr, 1979; Min and Lueptow, 1994a; Recktenwald et al., 1993). The case of a single rotating inner porous cylinder is not easy to analyze since no stable analytical solution exists for the flow, however some authors have investigated the case of an inner porous rotating cylinder and a stationary outer porous cylinder (Johnson and Lueptow, 1997). In this case, while the axial velocity was found to have a stabilizing effect, further studies proved that inward radial flow (perfusion flow, in the present study) or strong radial outward flow also have a stabilizing effect, thereby increasing the Ta_{cr}. (Johnson and Lueptow, 1997; Min and Lueptow, 1994a; Min and Lueptow, 1994b). Indeed, the radial inward flow as well as a strong radial outflow was found to wash the incipient vortical motion out of the annulus through the porous inner and outer cylinder, respectively, stabilizing the flux. Simulating the motion of dilute, rigid, spherical particles in flows just above the transition to supercritical Taylor vortex flow, using computational particle tracking, Wereley and Lueptow (1999) observed that even when a radial inward flow is imposed, particles can remain trapped in retention zones that are away from the wall of the annulus, contributing to the anti–plugging character of rotating filter devices. However, at high enough radial

velocities, no particles will be trapped within the vortex retention zone and the limit cycle path will not occur because the drag related to radial flow will overwhelm the centrifugal force on the particles, and they will all end up at the inner cylinder.

The Taylor vortices created above Ta_{cr} decrease the plugging of the filter pores by washing particles away from the filter surface due to a high shear rate in the gap between the cylinders and the centrifugal effect on particles, which are more dense than the fluid. This is the reason why a draft tube is usually placed around the spin–filter during actual perfusion cultures, as represented in Figure 3.10c (Siegel et al., 1991; Yabannavar et al., 1994). The washing of closed filters (filters in which the pore size is smaller than mean particle/cell diameter) by the Taylor vortices has no influence on particle retention, however instabilities at the filter surface could influence the cell passage through the filter and thus retention of open filters (filters which pore size is greater than mean particle/cell diameter). For these reasons, in order to measure the influence of instabilities on bead retention of open filters, a study was carried out using a draft tube placed around the open spin–filter of porosity factor of 1.12 (Figure 3.11). The two draft tubes tested were stainless steel cylinders with a radius r_o of 2.5 cm and height h of 12 cm. One draft tube was porous and had a pore size of 30 μm and the other was non–porous. The resulting gap width ($d = r_o - r_f$) was 0.36 cm and the radii ratio η was 0.86, whereas the resulting gap width was 2.86 cm and radii ratio η was 0.43 when no draft tube was placed around the spin–filter (the gap width corresponds to the distance between the outer surface of the filter and the baffles of the vessel).

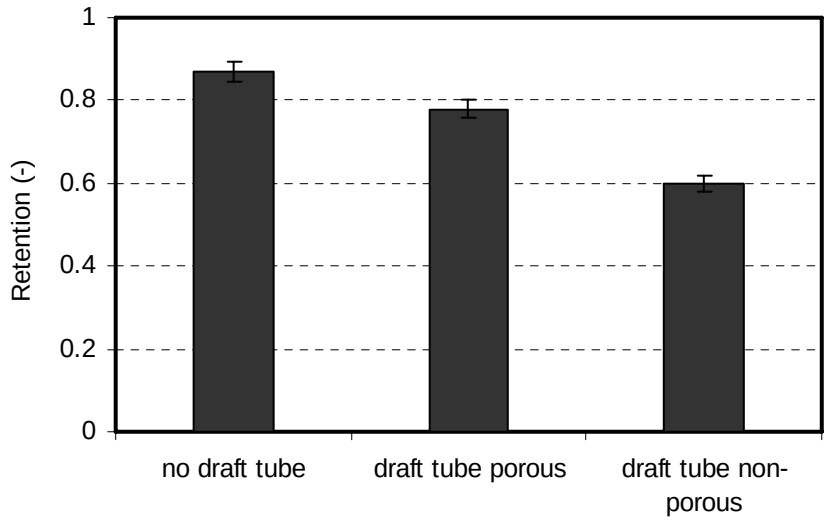

Figure 3.11: Influence of vortices on bead retention for an open spin–filter. Rotation was set to 1.1 m/s, perfusion rate to 2.6 cm/h and bead concentration to $1 \cdot 10^6$ particle/ml. ε equals to 1.12.

A comparison of bead retention using an open spin–filter without draft tube with that of an open spin–filter surrounded by a draft tube showed that the draft tube has a clear negative effect on bead retention (Figure 3.11). This effect was apparently more important when using a non–porous draft tube compared to a porous one. Indeed, retention reached a maximum of 0.86 in the absence of a draft tube around the filter, decreased by 9% to 0.78 for the porous draft tube and decreased further to 0.6 for a non–porous draft tube, a value representing a decrease of retention of 26%. The critical Taylor number, calculated according to Johnson and Lueptow (1997) for radial inward flow of 2.6 cm/h and η = 0.86, is around 116, whereas for η = 0.43, the Ta_{cr} approaches 68. The Taylor number calculated for our system at 1.1 m/s is around 42500 and 4000 for filter without and with draft tube respectively. Although the flow regime inside the annulus is supercritical for both filter configurations, different instabilities could be created that are dependent not only on the rotation speed of the internal filter but also on the gap width, which is different for both filter configurations (Figures 3.10b and c). Indeed, for small gap widths (high η factor) it was observed that the instabilities set in at small Ta numbers, whereas as the gap width is increased (low η factor <0.5), they set in at higher and higher Ta numbers (Atkhen et al., 2000; Fasel and Booz, 1984). Despite the presence of vortices in both configurations, the higher retention observed in the case where no draft tube is placed around the filter (low η), compared to the case where there is a draft tube around the filter (high η), could be explained by the fact that particles are more trapped by the vortices. Indeed, the influence of the vessel/draft wall is more important in the case where the gap width is narrow and thus instabilities are stronger even if the Taylor number is smaller, increasing the passage of particles through the filter and resulting in reduced bead retention. However, placing a porous draft tube around the spin–filter, instead of a non–porous one, induces less instability and tends to stabilize the flow more, thereby increasing the bead retention from 0.6 to 0.78. Similar effects have been described by Min and Lueptow (1994b), who stated that the incipient vortical motion that first appears near the rotating inner cylinder propagates then radially outward to the stationary cylinder. In the present study, the vortical motion is washed more through the porous cylinder than through the non–porous one, resulting in an increase of particle retention (Figure 3.11).

When placing a porous draft tube around the spin–filter at lower rotation speeds, the retention was observed to decrease much more than at higher speeds (Figure 3.12).

Indeed, for a particle concentration of $1 \cdot 10^6$ particle/ml without draft tube around the filter, the retention is around 0.7 and 0.8 at 0.45 m/s and 0.72 m/s respectively.

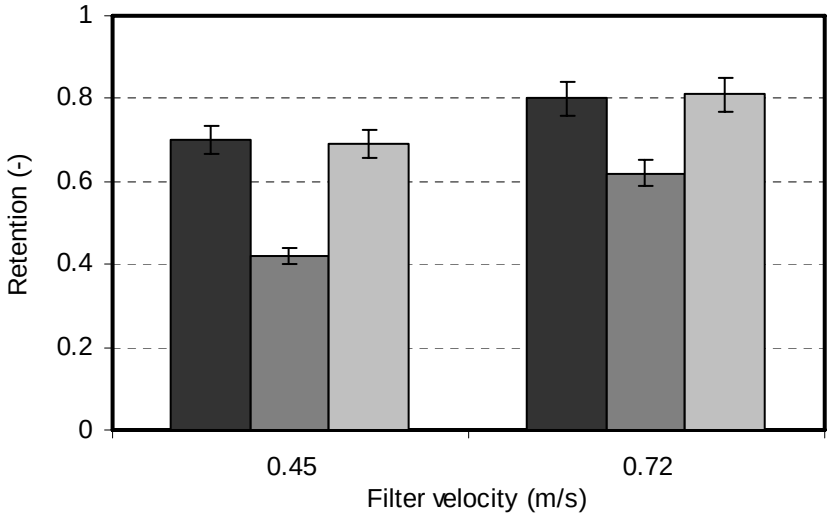

Figure 3.12: Influence of porous draft tube placed around the spin–filter on bead retention for an open spin–filter (ε = 1.12) at different filter rotations, at a perfusion rate of 2.6 cm/h. ■ $1 \cdot 10^6$ particle/ml, without draft tube, ■ $1 \cdot 10^6$ particle/ml, with draft tube, ■ $5.5 \cdot 10^6$ particle/ml, with draft tube.

Placing the porous draft tube around the spin–filter decreases the retention by 40% and 23% for 0.45 m/s and 0.72 m/s respectively. For a fixed geometry (fixed η factor), the improvement of bead retention at high rotation speeds may be explained by the fact that higher filter rotation will create different instability regimes and stronger vortices, as observed by Wereley and Lueptow (1998). The beads will be trapped differently inside the vortices and will not be able to reach the filter surface at sufficiently high rotation speeds, increasing thus particle retention. However, at higher particle concentrations, the vortices induced by the porous draft tube seem to influence the retention much less than at lower concentrations. Indeed, for a particle concentration of $1 \cdot 10^6$ particle/ml, a decrease of particle retention of 32% was observed when filter rotation was decreased from 0.72 to 0.45 m/s, whereas only a decrease of 15% was observed for particle concentration of $5.5 \cdot 10^6$ particle/ml. The influence of draft tube on particle retention is thus less important when the particle concentration and/or filter speed is increased.

3.4 Conclusions

The use of polymer beads, which have a diameter similar to that of animal cells, instead cells is a useful means to perform retention studies, since the problems of filter fouling, long–term sterility, cell density variation and low cell growth rate were avoided. Placing baffles within the spin–filter was crucial, since these latter permit good medium homogeneity and reduced bead/cell accumulation within the spin–filter, which would otherwise lead to cell leakage.

Particle retention was found to be mainly dependent on filter pore size and filter rotation velocity and to a lesser extent on the perfusion flow rate and cell concentration. Open filters have retention rates lower than 1, however operating the filters at high rotation speeds can maintain retention at high levels. It would be necessary to determine whether such speeds can be used in practice with animal cell perfusion cultures, since the related shear forces may result in poor cell viability. Retention was found to increase with increasing filter rotation velocity until it reaches a plateau. This plateau fixes the minimal filter rotation speed that has to be applied in order to achieve maximum particle retention and depends on the filter pore size. At a filter porosity of 1, the minimal filter rotation speed corresponds to 0.45 m/s, whereas at a filter porosity of 1.12, this value corresponds to 0.87 m/s. Retention was also found to be dependent on the perfusion flow rate but to a lesser extent. The influence of the perfusion rate is much more important at low perfusion flows and has no influence at high perfusion rates. However the minimal filter rotation speed at which retention is maximal is increased when the perfusion rate increases. The influence of cell concentration on particle retention is less important compared to the filter rotation rate, the retention rising with increase of the cell concentration.

The animal cell perfusion culture performed with a spin–filter of pore size of 14.5 μm demonstrated that retention values are similar to that obtained with beads. The influence of the parameters studied on bead retention has been validated to be alike to that on animal cells. The use of filter pore sizes larger than the mean animal cell diameter permitted reach a high cell density of $2 \cdot 10^7$ cell/ml during 900 h.

Many investigators found that placing a draft tube around the spin–filters reduces filter fouling, although the retention mechanism was not investigated. In this study, placing a draft tube around the filter was found to influence the particle retention of open filters. However, this influence was negative because of increased cell leakage due to the

formation of Taylor vortices in the gap between the filter and the draft tube. This influence becomes smaller with increasing cell concentration.

References

Atkhen, K., Fontaine, J., Wesfreid, J.E., 2000. Highly turbulent Couette–Taylor bubbly flow patterns. J. Fluid Mech. 422, 55–68.

Bird, R.B., Stewart, W.E, Lightffot, E.N., (1960) Transport phenomena. John Wiley&Sons, Inc., New York, 780 p.

Cognet, G., 1984. Les étapes vers la turbulence dans l'écoulement de Couette–Taylor entre cylindres coaxiaux. J. Mec. Theor. Appl., 7–44.

Davey, A., Di Prima, R.C., Stuart, J.T., 1968. On the instability of Taylor vortices. J. Fluid Mech. 31, 17–52.

Deo, Y.M., Mahadevan, M.D., Fuchs, R., 1996. Practical considerations in operation and scale–up of spin–filter based bioreactors for monoclonal antibody production. Biotechnol. Progr. 12, 57–64.

Ducommun, P., Ruffieux, P.–A., Furter, M.–P., Marison I., von Stockar U., 2000. A new method for on–line measurement of the volumetric oxygen uptake rate in membrane aerated animal cell cultures. J Biotechnol. 78(2), 139–147.

Esclade, L.R.J, Carrel, S., Péringer, P., 1991. Influence of the screen material on the fouling of the spin filters. Biotechnol. Bioeng. 38, 159–168.

Fasel, H., Booz, O., 1984. Numerical investigation of supercritical Taylor–vortex flow for a wide gap. J. Fluid Mech. 138, 21–52.

Favre, E., 1993. Constant Flow–Rate Filtration of Hybridoma Cells Suspensions. J. Chem. Technol. Biot. 58(2), 107–112.

Favre, E., Thaler, T., 1992. An engineering analysis of a rotating sieves for hybridoma cell retention in stirred tank bioreactors. Cytotechnology 9, 11–19.

Fenge, C., Buzsaky, F., Fraune, E., Lindner–Olsson, L., 1991. Evaluation of a spin filter during perfusion culture of recombinant CHO cells. In: Murakami H, Shirahata S, Tachibana H, editors. Animal Cell Technology: Basic and Applied Aspects. Fukuoka, Japan. Kluwer Academic Publishers, p 429–433.

Heine, H., Biselli, M., Wandrey, C., 1999. High cell density cultivation of hybridoma cells: spin filter vs immobilized culture. In: A. Bernard et al., editor. Animal cell technology: Products from cells, cells as products: Kluwer Academic Publishers. p 83–85.

Himmelfarb, P., Thayer, P.S., Martin, H.E., 1969. Spin filter culture: the propagation of mammalian cells in suspension. Science 164, 555–557.

Hwang, J.–Y., Yang, K.–S., 2004. Numerical study of Taylor–Couette flow with an axial flow. Computers & Fluids 33, 97–118.

Iding, K., Lütkemeyer, D., Fraune, E., Gerlach, K., Lehmann, J., 2000. Influence of alterations in culture condition and changes in perfusion parameters on the retention performance of a 20 μm spinfilter during a perfusion cultivation of a recombinant CHO cell line in pilot scale. Cytotechnology 34, 141–150.

Jan, D.C.–H., Emery, A.N., Al–Rubeai, M., 1992. Optimization of spin–filter performance in the intensive culture of suspended cells. In: Spier RE, Griffiths JB, MacDonald C, editors. Animal cell technology: developments, processes and products. Oxford: Butterworth–Heinemann. p 448–451.

Johnson, E.C., Lueptow, R.M., 1997. Hydrodynamic stability of flow between rotating porous cylinders with radial and axial flow. Phys. Fluids 9(12), 3687–3696.

Kroner, K.H., Nissinen, V., 1988. Dynamic filtration of microbial suspensions using an axially rotating filter. J. Membrane Sci. 36, 85–100.

Lieberherr, J., 1979. Hydrodynamics of the annular gap flow between permeable cylinder walls. Escher Wyss News 2, 24–30.

Margaritis, A., Wilke, C., 1978. The rotorfermentor. I. Description of the apparatus, power requirements, and mass transfer characteristics. Biotechnol. Bioeng. 20(5), 709–726.

Mercille, S., Johnson, M., Lemieux, R., Massie, B., 1994. Filtration–based perfusion of hybridoma cultures in protein–free medium: reduction of membrane fouling by medium supplementation with DNase I. Biotechnol. Bioeng. 43, 833–846.

Min, K., Lueptow, R.M., 1994a. Circular Couette flow with pressure–driven axial flow and a porous inner cylinder. Exp. Fluids 17, 190–197.

Min, K., Lueptow, R.M., 1994b. Hydrodynamic stability of viscous flow between rotating porous cylinders with radial flow. Phys. Fluids 6, 144.

Recktenwald, A., Lücke, M., Müller, H.W., 1993. Taylor vortex formation in axial through–flow: linear and weakly nonlinear analysis. Phys. Rev. E 48(6), 4444–4454.

Schlichting, H., 1979. Boundary–layer theory. Kestin J, translator. New York: McGraw–Hill. 817 p.

Siegel, U., Fenge, C., Fraune, E., 1991. Spin filter for continuous perfusion of suspension cells. In: Murakami H, Shirahata S, Tachibana H, editors. Animal Cell Technology: Basic and Applied Aspects. Fukuoka, Japan: Kluwer Academic Publishers. p 434–436.

Stoll, T.S., Chappaz, A., von Stockar, U., Marison, I., 1997. Effects of culture conditions on the production and quality of monoclonal IgA. Enzyme Microb. Technol. 21(3), 203–211.

Varecka, R., Scheirer, W., 1987. Use of a rotating wire cage for retention of animal cells in a perfusion fermentor. Dev. Biol. Stand. 66, 269–272.

Wereley, S.T., Lueptow, R.M., 1999. Inertial particle motion in a Taylor Couette rotating filter. Phys. Fluids 11(2), 325–333.

Yabannavar, V.M., Singh, V., Connelly, N.V., 1992. Mammalian cell retention in a spinfilter perfusion bioreactor. Biotechnol. Bioeng. 40, 925–933.

Yabannavar, V.M., Singh, V., Connelly, N.V., 1994. Scaleup of spinfilter perfusion bioreactor for mammalian cell retention. Biotechnol. Bioeng. 43(2), 159–164.

4

Lateral migration of particles in a spin–filter system

Abstract

Particle migration near a rotating spin–filter system determines mass transport through the filter and is involved in the particle retention mechanism, with filter pore sizes larger than the particle mean diameter, as well as filter fouling. In this study a prediction of radial particle migration near the surface of rotating filter is developed. The lift force is demonstrated to be important in the spin–filter system since it contributes to particle removal from the filter surface. Competition between centrifugal sedimentation, lift forces Stokes drag and perfusion forces is responsible for determining particle motion relative to the filter. At certain filter rotation rates, centrifugation and lift forces are sufficiently high as to balance perfusion flow and result in the movement of particles away from the filter, a situation that experimentally corresponds to maximum particle retention. The model also reveals that filter centrifugal acceleration is the key parameter to be conserved during spin–filter scale–up. This hypothesis has been confirmed experimentally.

4.1 Introduction

Pressure–driven membrane systems, such as cross–flow filters, have been widely reported for use in cell separation during perfusion cultures. High tangential flow rates (Poiseuille flow) across the surface of the membrane, inducing high shear rates are used to decrease filter fouling (Belfort, 1988; Green and Belfort, 1980; Maiorella et al., 1991; Schwille et al., 2002). The rotation of the spin–filter also generates a shear rate (Couette flow) on the filter surface and similarities with cross–flow systems could be established, as represented in Figure 4.1.

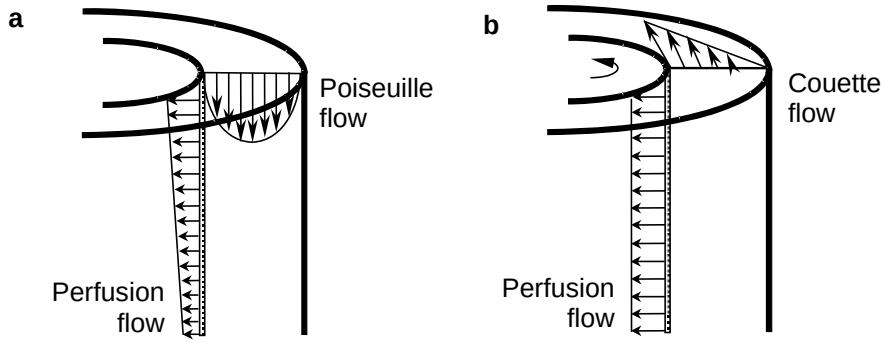

Figure 4.1: Comparison between cross–flow filtration (a) and spin–filter system (b).

Since mass transport to a filter surface is dependent on the fluid flow in the vicinity of the filter, an understanding of fluid mechanics in the annulus between the two concentric cylinders, namely the inner rotating one and the outer stationary one is necessary in order to study mass transport through the filter and thus explain particle retention as well as filter fouling in such devices. Filter fouling is also related to lateral migration of particles across the filter membrane, which has been extensively studied for cross–flow systems and less so far for spin–filter devices.

In the present study, lateral particle migration, developed for Poiseuille flow in tubes or channels as well as for simple shear flow in slits, will be adjusted for rotating Couette flow systems such as spin–filter devices. The importance of lift phenomena in spin–filter particle retention will be demonstrated and a strategy for spin–filter scale–up is proposed.

4.2 Material and methods

4.2.1 Materials

Animal cell retention studies require sterile working conditions and large numbers of cells, the latter requiring considerable time and effort to produce. Furthermore, fouling of the filters can impede studies on the role of the principle parameters. In order to avoid these problems, polymer beads (Superose 6, Amersham Biosciences, Freiburg, Germany) were used in place of animal cells. The density of the polymer beads is 1.055 g/ml, which is in the range of that of animal cells, while the diameter specified by the supplier is about 13 ± 2 microns, which corresponds approximately to the average diameter of viable animal cells (Searles et al., 1994). Particles were counted spectrophotometrically (Uvikon 930, Kontron Instruments, Switzerland) at a wavelength of 600 nm. A calibration was undertaken to relate particle concentration (particles/ml) with optical density. This was achieved microscopically using a hemocytometer.

4.2.2 Experimental set–up

Simulations of bead perfusion were performed using an open glass vessel, in which four baffles of 1 cm width were placed (Figure 4.2). The internal diameter was 12 cm and the total working volume was set to 1.6 L and beads were maintained in suspension using a magnetic stirrer under gentle agitation at 100 rpm. The turbidity of the bead suspensions was measured spectrophotometrically (Uvikon 930, Kontron Instruments, Switzerland) at 600 nm and related to a calibration curve of optical density to number of particle/ml. The bead concentration within the vessel was fixed at a value of $1 \cdot 10^6$ particle/ml.

The spin–filter used for the particle retention study was purpose–built. The open cylindrical stainless steel support was assembled with a solid ring at the top, a conical shaped bottom and four vertical bars, in order to make the available filtration area as large as possible. The filter screen was made of stainless steel (G. Bopp & Co. AG, Zurich, Switzerland) with an average pore size of 14.5 μm, a value larger than the mean bead diameter (13±2 μm). The open filter surface is approximately 5% of the total surface, as communicated by the supplier. Three different external filter radii of 2.14, 3.18 and 4.16 cm with a wet/immersed height of about 7 cm were used in this study. Immobile baffles of 1, 2 and 3 cm in width (for filter which radius was 2.14, 3.18 and 4.16 cm respectively)

were placed within the spin–filter in order to keep a homogeneous particle suspension. Filter rotation was independent of the central agitator shaft and was driven from the top, by a motor (Eurostar, IKA–Werke GMBH, Staufen, Germany). Filter velocities ranged from 50 to 450 rpm. Medium from within the spin–filter was removed at a perfusion rate of 3.7 vvd (perfusion flow over total working volume including volume of the spin–filter basket), using a calibrated peristaltic pump (Alitea, Bioengineering, Wald, Switzerland) and returned to the vessel in order to maintain the volume and bead concentration constant within the vessel (Figure 4.2).

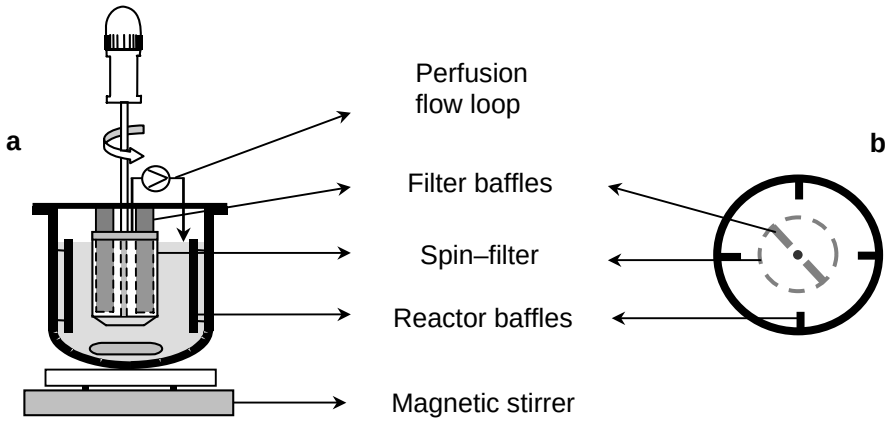

Figure 4.2: Bead perfusion simulation set–up. **a**: Section view and **b**: top view.

Once the perfusion rate had been attained, samples were collected with a pipette from the reactor vessel and directly inside the spin–filter. The system was considered to be in steady state when the concentration inside the spin–filter was stable. Retention was then calculated from $1–(c_{in,filter} / c_{out,filter})$, where $c_{in,filter}$ and $c_{out,filter}$ are the concentrations of particles inside and outside the spin–filter respectively.

4.2.3 Experimental methods

Experiments performed in the absence of perfusion indicated that a certain quantity of liquid from inside the filter is displaced to the outside during filter rotation, resulting in a difference in liquid level on either side of the filter. Thus when the centrifugal force is balanced by the hydrostatic force, the liquid level inside the filter stabilizes creating this difference (Δh) in liquid level, as represented in Figure 4.3.

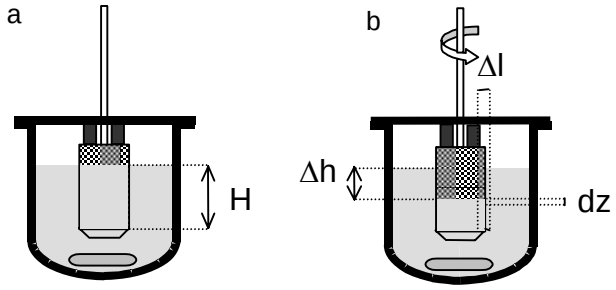

Figure 4.3: Effect of filter rotation on liquid level inside the spin–filter. Stationary (a) and rotating (b) spin–filter.

Quantification of Δh is important, since the total wet filter surface is altered, which in turn induces a change in the linear perfusion velocity (perfusion flow divided by the wet filter surface). In order to quantify Δh, two hypotheses have been formulated. One considers that the liquid inside and outside the filter (bulk) are very well mixed and are not rotating with the filter, and the second considers that Δh is not influenced by the perfusion flow and fluid goes freely from one side of the filter to the other.

Baffles are placed inside the spin–filter in order to avoid vortex flow formation. Thus the liquid in contact with the baffles is not subjected to the centrifugal force. There is only a small quantity of liquid (Δl) considered to rotate under the influence of the centrifugal force that comprises the liquid layer between the internal baffles and the internal surface of the filter, the liquid inside the filter pores and a small layer of liquid formed near the external surface of the rotating filter (Figure 4.3). In order for the liquid level to remain constant, the centrifugal force acting on the elemental volume $2\pi r_f \cdot \Delta l \cdot dz$ must be balanced by the hydrostatic force acting on the surface $2\pi r_f \cdot dz$ (equation 4.1). The value of Δl can be obtained by measuring Δh at different filter centrifugal accelerations (equation 4.2).

$$2\pi r_f \cdot \Delta l \cdot dz \cdot \rho_L \cdot \omega^2 r_f = \rho_L \cdot g \cdot \Delta h \cdot 2\pi r_f \cdot dz \qquad \text{Equation 4.1}$$

$$\Delta l \cdot \omega^2 r_f = g \cdot \Delta h \quad \rightarrow \quad \Delta h = \frac{\Delta l}{g} \cdot \omega_f^{\,2} r_f \qquad \text{Equation 4.2}$$

in which ρ_L (kg/m^3) is the fluid density, g (m/s^2) is the gravitational constant, ω_f (rpm/60$\cdot 2\pi$ s^{-1}) is the filter angular speed of rotation and r_f (m) the filter radius. Three different filter radii of 2.14, 3.18 and 4.16 cm have been used in order to measure Δh as a function of filter acceleration, with a set–up similar to that represented in Figure 4.3. The liquid inside the vessel was pure water and the height of liquid inside the filter was measured before

and during filter rotation (Figure 4.4). Equation 4.2 was found to explain the phenomenon observed, with Δh being linearly related to filter acceleration and independent of filter radius. In Figure 4.4, the slope corresponds to $\Delta l/g$ and Δl was determined to have a value of 0.315 cm. Thus for any filter radius, Δh can be calculated as a function of filter acceleration.

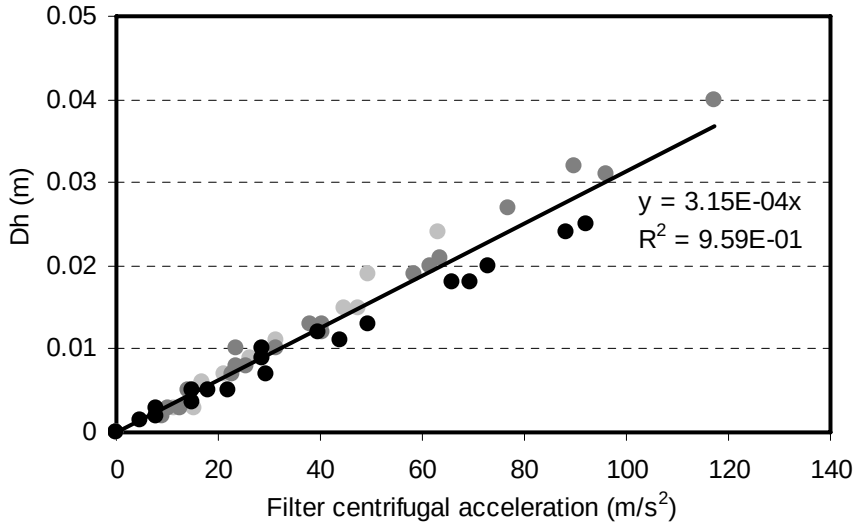

Figure 4.4: Δh as a function of filter acceleration for three different filter radii (r_f): ● 2.14 cm, ● 3.18 cm and ● 4.16 cm.

However, the influence of perfusion flow was not considered in the model described by equation 4.2, since it was assumed that the pore size of the filter was sufficiently large and permitted the fluid to freely traverse the filter in both directions.

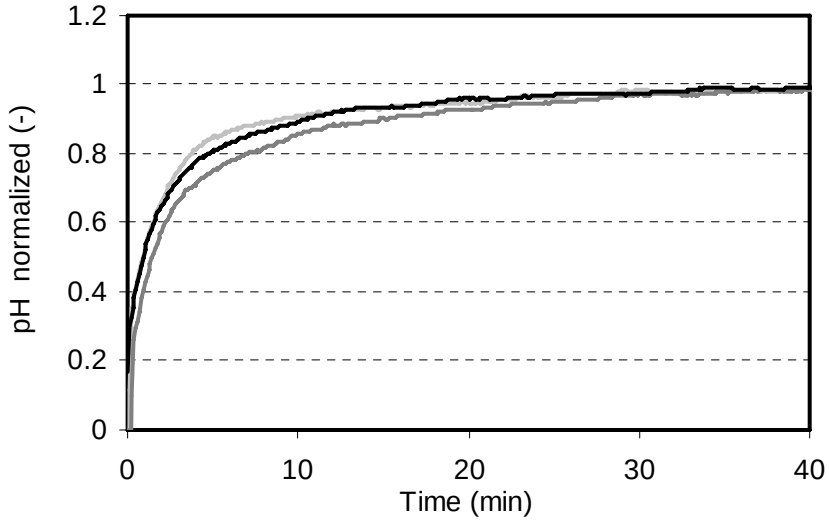

Figure 4.5: Normalized pH outside the filter versus time after a pulse of NaOH inside the filter for different perfusion flows: — 0 vvd, – – 3.7 vvd, **– –** 15 vvd.

In order to test this hypothesis, an experiment was performed in which a pulse of 0.5 ml NaOH 2M was added to the inside of the filter and the pH of the fluid surrounding the filter (water without particles) was measured for different perfusion flows (Figure 4.5). It can be observed that the pH profile is the same at low perfusion flows as well as at high perfusion flows. Even at high perfusion rates, no delay in the profile is observed and the fluid circulates from the inside to the outside of the filter, to equilibrate the pH within approximately 20 minutes. These results confirm the hypothesis that only a small quantity Δl of liquid surrounding the filter is subjected to centrifugal forces and fluid goes freely from one side of the filter to the other without influencing Δh.

4.3 Hydrodynamics around the spin–filter

The forces acting on cells near the filter surface govern cell displacement towards the filter and thus the retention mechanism as well as the tendency of the filter to fouling. A study of the hydrodynamics around the spin–filter is thus important in order to understand these phenomena. In the present study, a simple system will be considered comprised of a fluid and a single particle, since concentrated solutions would be difficult to model due to non–Newtonian viscous behaviour, especially near the filter surface, in the mass boundary layer.

The particle suspended in the fluid due to vessel agitation and situated near the filter surface lies in the fluid when the filter is at rest. When the filter rotates the fluid around the filter surface (in the Δl layer) is induced to flow in the direction of rotation. Due to the density difference between the particle and the fluid, the particle is subjected to a centrifugal force, which is radially outward for a particle more dense than the fluid, as expressed in equation 4.3.

$$F_c = \frac{4}{3}\pi \cdot R_p^3 \cdot (\rho_p - \rho_L) \cdot \omega_f^2 r_f \qquad \text{Equation 4.3}$$

in which R_p (m) is the particle radius, ρ_p and ρ_L (kg/m^3) are the particle and fluid densities respectively, ω_f (s^{-1}) is the filter angular speed of rotation and r_f (m) is the filter radius. When the particle is subjected to an acceleration force, it is balanced by the Stokes force (Bird et al., 1960) which for Re<0.1 can be expressed by equation 4.4.

$$F_S = 6\pi\mu_L \cdot R_p \cdot v_p$$ Equation 4.4

in which μ_L (kg/m·s) is the liquid viscosity and v_p (m/s) the terminal particle velocity. At steady state the forces are equal and the terminal velocity of the particle in the radial direction is expressed by equation 4.5.

$$v_p = \frac{2}{9} R_p^2 \cdot \frac{(\rho_p - \rho_L)}{\mu_L} \cdot \omega_f^2 r_f$$ Equation 4.5

If the particle is more dense than the fluid, the terminal particle velocity is directed in the direction opposite to the filter surface and the particle is discarded from the filter with a force proportional to the filter acceleration, represented by the term $\omega_f^2 r_f$. However, during spin–filter perfusion culture, a flow of liquid is withdrawn from the inside of the filter and the particle is subjected to another force directed towards the filter surface, which as a result carries the particle closer to the filter. If we consider that the filter volume is 20% of the reactor working volume, the perfusion velocity can be expressed by equation 4.6.

$$v_{pf} = \frac{\dot{V}}{\zeta \cdot S_f} = \frac{2.5 \cdot r_f \cdot D}{\zeta}$$ Equation 4.6

in which $\dot{V}$ (m^3/s) is the perfusion flow, ζ (%) is the percentage of the open surface of the filter (porosity), S_f (m^2) is the internal immersed filter surface and D (s^{-1}) is the dilution rate (perfusion flow divided by the working reactor volume). The total velocity of the particle can then be expressed by equation 4.7.

$$v_p = \frac{2}{9} R_p^2 \cdot \frac{(\rho_p - \rho_L)}{\mu_L} \cdot \omega_f^2 r_f - \frac{2.5 \cdot r_f \cdot D}{\zeta}$$ Equation 4.7

Particle trajectory towards the screen mainly depends on the filter acceleration and perfusion flow rates. When the terminal particle velocity is positive, the particle is rejected from the filter surface and there is no interaction between the particle and the screen. On the other hand a negative particle velocity will result in the particle moving toward the filter screen and the particle–screen interaction will increase. For filters with a pore size larger than the mean particle diameter, the particle is more likely to pass through, thereby decreasing particle retention. The particle velocity as a function of filter rotation, for three different perfusion rates is shown in Figure 4.6.

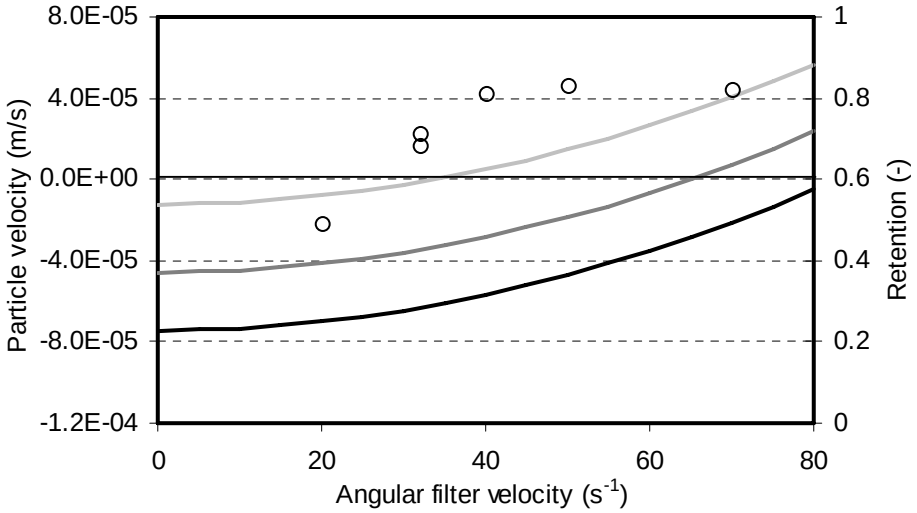

Figure 4.6: Particle velocity as a function of filter angular velocity at different perfusion rates: ⎓ 1 vvd, ⎓ 3.7 vvd and ⎓ 6 vvd. ❍ Particle retention at 3.7 vvd with filter radius of 2.14 cm and filter pore size of 14.5 μm, as a function of the angular velocity of the filter.

At a high perfusion flow of 6 vvd and filter rotation rates of 0 to 80 s^{-1} the particle velocity appears to be negative, which suggests that the centrifugal particle acceleration is not high enough to overcome the perfusion flow. However, at a lower perfusion flow of 1 vvd, the velocity becomes positive at an angular filter rotation greater than 35 s^{-1}. Under these conditions particle retention was measured with a filter pore size larger than the mean particle diameter and was found to be dependent on filter rotation speed. At a fixed perfusion rate of 3.7 day^{-1} (vvd), particle retention increased with increasing filter rotation from 14 to 40 s^{-1} until a plateau was reached above 40 s^{-1}. It was expected that, retention would correlate with the calculated direction of particle movement near the filter, however, from Figure 4.6 it seems that this phenomenon is not demonstrated. Particle retention measured experimentally gave higher rates than those predicted by the theory. Indeed, at 3.7 vvd the predicted particle velocity is negative over almost the whole range of filter rotations tested, which means that particles should be carried towards the filter. Theoretically from 40 to 60 s^{-1} particles would be expected to migrate toward the filter and would not allow the achievement of the high retention rates observed experimentally. Thus there is a difference between the prediction of radial migration compared with experimental determination, which may be attributed to the approximations used in the simulation or to the presence of a further unaccounted force, which modifies the particle trajectory away from the filter surface.

4.4 Lift phenomenon

Radial displacement of dilute suspensions of neutrally buoyant spheres in Poiseuille flow was first studied by Segré and Silberberg (1961). Concentration of spheres in certain regions of the tube was observed as a function of radial and longitudinal position in the tube. It was first postulated that a transverse force exists, directed inwards with respect to the tube axis, which arises from the combination of a rotary and a translatory particle motion relative to the undisturbed flow of the fluid and which is proportional to the square of the flow (Segré and Silberberg, 1961). When studying the behaviour of non–neutrally buoyant particles in vertical Poiseuille flow, Oliver (Oliver, 1962) observed a different phenomenon. The rotation of the spheres resulted in an outward movement away from the tube centre and, in the absence of rotation, the spheres drift towards the tube centre, away from the tube wall. Thus, when placed close to the wall, the spheres tended to move inwards, revealing a hydrodynamic repulsive force present between the particles and the wall, in a manner previously observed by Segré and Silberberg (1961). These phenomena were also reported by Repetti and Leonard (Repetti and Leonard, 1964), in terms of the factors producing the radial drift. These authors pointed out that circulation can arise with a translating sphere either by sphere rotation or by non–symmetrical streaming about the non–rotating sphere.

Rubinow and Keller first performed analytical studies on radial forces, also termed lift forces, acting on particles in an unbound uniform flow, for low Reynolds numbers (Rubinow and Keller, 1961). These authors found a lift force ($F_{l\Omega}$, $kg{\cdot}m{\cdot}s^{-2}$) acting on the particle due to the rotation of the particles in a uniform flow and that this force could be expressed by equation 4.8.

$$F_{l\Omega} = \pi R_p^{\,3} \rho_f \; \Omega \times U \qquad \text{Equation 4.8}$$

in which R_p (m) is the radius of the sphere, ρ_f (kg/m^3) is the fluid density, Ω (s^{-1}) is the rotation vector of the sphere and U (m/s) the fluid flow velocity. A schematic representation of such phenomena is described by Figure 4.7.

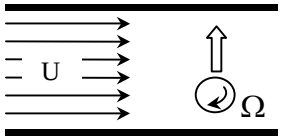

Figure 4.7: Lift force acting on a rotating spherical particle in a uniform flow

Further studies on lateral particle migration of a rotating sphere translating with velocity v through a uniform unbound simple shear flow were carried out by Saffman (Saffman, 1965), who found that the combination of fluid inertia and the presence of walls play an important role in lift force generation. An expression for the lift force induced by shear flow is expressed by equation 4.9 (Saffman, 1965; 1968).

$$F_l = K \cdot \mu R_p^{\,2} \, (G/\upsilon)^{0.5} \, V_s \qquad \text{Equation 4.9}$$

in which K is a constant with a value of 6.46, μ (kg/m/s) and υ (m^2/s) are the dynamic and the cinematic viscosities of the fluid respectively, R_p (m) is the radius of the sphere, V_s (m/s) is the particle slip velocity (particle velocity relative to the fluid velocity) and G (s^{-1}) is the rate of shear, where both Reynolds numbers based on particle slip velocity ($Re_V = V_s \cdot R_p/\upsilon$) and on particle shear ($Re_G = G \cdot R_p^2/\upsilon$) are assumed to be smaller than unity and $Re_V << Re_G^{0.5}$. This force due to the shear when the Reynolds number is small is larger by an order of magnitude to that due to particle rotation (Saffman, 1965).

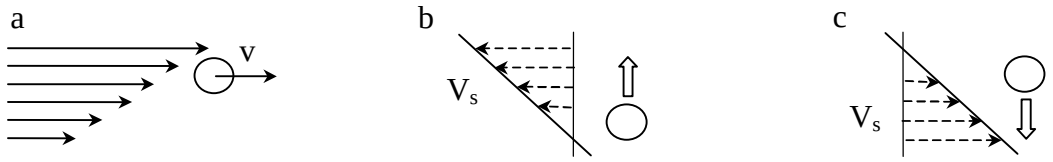

Figure 4.8: Lift force on a spherical particle in a uniform simple shear flow. a: Particle translating through a sheared fluid. b: Particle velocity relative to the fluid when the particle is lagging the fluid and c: when the particle is leading the fluid

The direction of the force is such that if the particle lags behind the undisturbed fluid, it would migrate in the direction of the larger undisturbed velocity, while if the particle leads the undisturbed flow, it would migrate in the direction of the smaller undisturbed velocity, as represented in Figure 4.8. An extension of Saffman's theory has been derived for an inertial lift force acting on a particle that translates in an unbound linear shear flow, with no restriction placed on the ratio $Re_G^{0.5}/Re_V$, Re_G and Re_V being smaller than unity (McLaughlin, 1991). It was shown that when Re_V becomes larger than $Re_G^{0.5}$, the magnitude of the inertial migration velocity rapidly decreases to very small values (Cherukat et al., 1999; McLaughlin, 1991).

However, in the studies of Rubinow and Keller (1961) and Saffman (1965) the effects of the boundary conditions of walls and shear rate across the channel have been omitted. The boundary conditions are important since they give rise to different lateral migration expressions. Theories related to lateral migration of particle have spawned a

number of experimental studies in Couette and Poiseuille flow systems, in slits as well as in tubes, which are generated by different boundary conditions and flow geometries (Altena and Belfort, 1984; Drew et al., 1991; McLaughlin, 1993).

Theoretical work on the lateral migration of solid particles suspended in bounded laminar vertical tube flows has been further investigated (Cox and Brenner, 1968) and a general form for lateral motion due to inertial effects of neutrally and non–neutrally buoyant spheres at low Reynolds number (Re<<1) has been derived. Such theory was mainly developed for cross–flow membrane filtration systems, where lift force has been invoked to supplement particle back–diffusion resulting in lower particle concentrations near the membrane than predicted by the theory. The general expression of lift velocity for neutrally and non–neutrally buoyant particles whether allowed to rotate or not, in dimensional form (Vasseur and Cox, 1976), is represented by equation 4.10.

$$v_l = Re_p \cdot \kappa^2 \cdot U_m \cdot f(\beta) \qquad \text{Equation 4.10}$$

where $Re_p = R_p \cdot U_m/\upsilon$ and $\kappa = R_p/l$ with R_p (m) the radius of the particle, υ the cinematic viscosity (m^2/s) of the fluid and l (m) the channel width or radius of the tube and U_m (m/s) the characteristic velocity of the undisturbed flow field. The function $f(\beta)$ is the result of a numerical integration and depends on the β factor, which represents the distance of the particle from the wall compared with the channel width. Different $f(\beta)$ profiles have been obtained by authors, depending on the particle location from the wall, presence of wall near the particle, particle inertia and buoyancy and system geometry, for Poiseuille flow systems (Cox and Hsu, 1977; Ho and Leal, 1974; Ishii and Hasimoto, 1980; Schonberg and Hinch, 1989) (Altena and Belfort, 1984; Weigand et al., 1985), as well as for Couette flow systems (Ho and Leal, 1974; Vasseur and Cox, 1976). This work enabled measurement of particle trajectories and determination of equilibrium positions and the proposed theory could describe particle trajectories, however there is as yet no general solution.

The lift force experienced by an immersed particle in a rotating fluid has been studied but still remains incomplete. Only a few studies have been successfully carried out in some limiting cases, such as for vortex flow systems, in which the gap between an inner rotating cylinder and an outer stationary cylinder is very small compared to the inner cylinder radius (Belfort et al., 1993; Schwille et al., 2002). However in such systems, the cause for reduced particle concentration near the filter surface was shown to be related to vortex phenomena induced by rotational shear rather than to lift phenomena. Indeed

particles were found to remain trapped in retention zones, away from the porous inner cylinder, contributing to the anti–plugging character of vortex filter devices (Wereley et al., 2002; Wereley and Lueptow, 1998). In spin–filter systems, the width of the gap between the two cylinders is large compared to the inner cylinder and the mechanism for vortex formation is different. Indeed, the size of vortices (flow instabilities) on rotating ultrafiltration modules was revealed to be reduced with increasing gap width (Vigo and Uliana, 1986). However, Halow and Wills also studied such vortex flow systems and related particle lateral migration to lift phenomena (Halow and Wills, 1970a; Halow and Wills, 1970b).

Since no suitable general expression can adequately describe the functioning of spin–filter devices, different approaches for the lift mechanism developed for Poiseuille flow and shear flow systems will be outlined in the next section and will be adapted to spin–filter Couette system.

4.4.1 Lift velocity simulations for spin–filter system

Theories relating to lateral migration of particles in shear flow systems similar to spin–filters were considered in the present study to be those of Saffman, Ho and Leal and Cox and Hsu (Saffman, 1965, 1968; Ho and Leal, 1974; Cox and Hsu, 1977). Saffman theory is applied to an unbound domain in which the inertia of the far field cannot be ignored and in which the lift force depends on the viscosity and slip velocity, as represented in equation 4.9. Ho and Leal theory is considered in bound domains and is valid when the sphere is not close to the wall. This lift force depends on inertia alone, without any dependence on viscosity that originates from the shear field acting on the sphere, rather than the presence of a wall–induced lag velocity. The Cox and Hsu theory on the other hand considers the presence of wall and found that velocity correction due to wall in the inertia region cannot be ignored. The constraint common to all such theories is low particle Reynolds number, additional constraints of each theory will be discussed.

4.4.1.1 Saffman lift force theory

Saffman viscous theory (Saffman, 1965) refers to the lateral migration of particles in an unbound shear flow. The inertial terms due to shear are large compared to the

inertial terms due to the velocity of the sphere relative to the fluid velocity and the condition $Re_V << Re_G^{0.5}$ is required as described previously (see equation 4.9). In order to calculate these Reynolds numbers in the present study, it is necessary to know the maximum shear rate of the flow, as well as the particle slip velocity (particle velocity relative to the undisturbed fluid). Navier–Stokes equation describing the motion of fluid between an inner rotating cylinder and an outer stationary cylinder was solved by Belfort et al., who formulated an azimuthal flow velocity within the gap between the cylinders, as expressed in equation 4.11 (Belfort et al., 1993).

$$v_\theta(r) = \frac{\omega_f r_f^2}{r_c^2 - r_f^2} \cdot \left(\frac{r_c^2}{r} - r\right) \qquad \text{Equation 4.11}$$

in which ω_f is the angular filter velocity (s^{-1}), r_f (m) radius of rotating cylinder (filter radius in the present study, 0.0214 m), r_c (m) radius of stationary cylinder (vessel radius in the present study, 0.06 m) and r (m) particle position within the gap. The shear rate (G) is obtained after derivation of azimuthal flow velocity upon r, considering the derivative of radial flow velocity upon θ as being equal to zero (Bird et al., 1960), and is expressed in equation 4.12.

$$G(r) = r\frac{\partial}{\partial r}\left(\frac{v_\theta(r)}{r}\right) \quad \rightarrow \quad G(r) = \frac{-2\,\omega_f\, r_f^2\, r_c^2}{r_c^2 - r_f^2} \cdot \frac{1}{r^2} \qquad \text{Equation 4.12}$$

The azimuthal flow velocity, as well as flow shear rate, as a function of the radial position in the gap between the rotating filter and the outer vessel, for different filter angular velocities is shown in Figure 4.9.

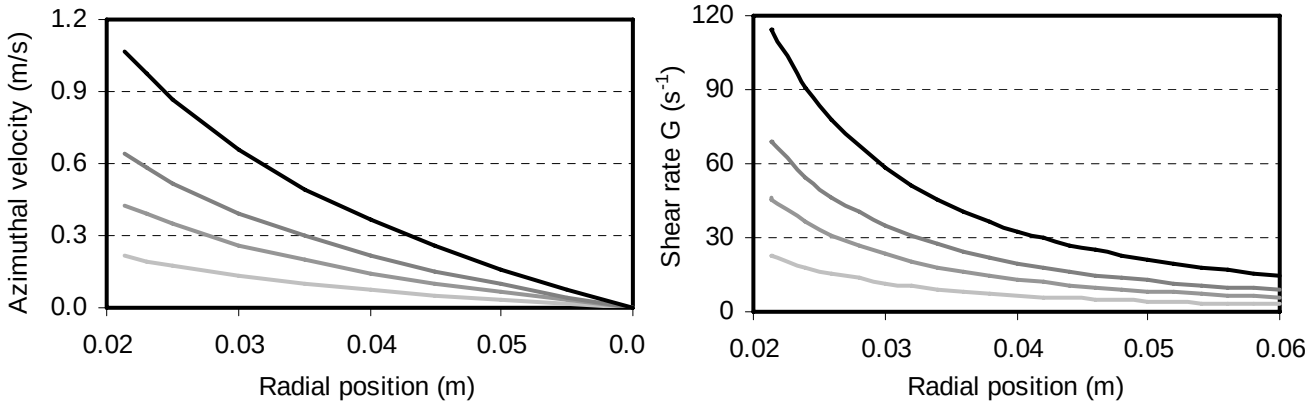

Figure 4.9: Azimuthal velocity and shear rate of flow in the gap width at different angular filter rotations (ω). – 10 s^{-1}, – 20 s^{-1}, – 30 s^{-1} and – 50 s^{-1}.

At the filter surface, the azimuthal flow velocity is maximal and drops to zero with increasing radial coordinates. The velocity distribution in the gap width is not simple shear, since there is a curvature in the velocity distribution. With increasing angular filter velocity, the azimuthal velocity increases and the profile becomes more curved. The shear rate has a similar tendency. The absolute value of the shear rate is maximal at the filter surface and decreases rapidly to minimal value with increasing radial coordinates and increases with increasing filter angular velocity.

Halow and Wills studied rotating Couette systems, where an inner cylinder is rotating inside a stationary cylinder, for gap widths which are small compared with the cylinder radius and for a small ratio of particle to gap width (annular thickness is 5 – 30 times the particle diameter) and developed an approximate expression for slip velocity applicable to neutrally buoyant particles (Halow and Wills, 1970a, 1970b). This expression changes sign at the midpoint of the annular gap between the cylinders (Halow and Wills, 1970b). This means that in the outer half of the gap (close to the stationary cylinder) particles lag the fluid and move into the faster stream of undisturbed shear flow, whereas in the inner part of the annular gap (near to the rotating cylinder) particles lead the fluid and move into the slower stream. This anti–symmetry of the slip velocity implies that Saffman lift rejects particles from the walls towards the centre of the channel and explains particle migration to an equilibrium position located approximately midway between the cylinder walls, as observed experimentally by other authors (Feng et al., 1994; Ho and Leal, 1974; Vasseur and Cox, 1976) for neutrally buoyant particles. For non–neutrally buoyant particles, when the density difference is large enough (as is the case in the present study, i.e. $\Delta\rho$ = 0.050 kg/m^3) the equilibrium position was observed to shift towards the centreline of the channel, during lateral migration simulations of particle in Couete flow (Feng et al., 1994). Using the expression for slip velocity developed by Hallow and Wills (1970a) and the expression for shear rate expressed in equation 4.12, Reynolds numbers relative to the slip velocity and shear rate have been calculated. Re_V (slip velocity ranging from $2.5 \cdot 10^{-4}$ to $3.5 \cdot 10^{-3}$ m/s for angular velocities ranging from 5 to 70 s^{-1}) and Re_G at a particle distance from the rotating filter equal to one particle diameter are smaller than unity and the condition $Re_V << Re_G^{0.5}$ is accomplished. Viscous Saffman lift forces represented in equation 4.9, can thus be expressed in the present study by replacing the shear rate with the expression obtained in equation 4.12. Considering that the lift force is a Stokes force, the lift velocity can be expressed by equation 4.13.

$$v_l = 0.485 \cdot R_p \left(\frac{\omega_f}{\upsilon} \right)^{0.5} \cdot \frac{r_f \cdot r_c}{\left(r_c^{\,2} - r_f^{\,2} \right)^2} \cdot \frac{V_s}{r}$$

Equation 4.13

The Saffman lift velocity depends linearly on the slip velocity and is inversely dependent on r, which means that the lift velocity is maximal in the vicinity of the filter (small r) and decreases with increasing distance from the filter surface. The slip velocity considered here is that of Halow and Wills (1970a) and is expressed within the rotating layer Δl that is involved in particle migration. Considering that Δl is relatively small compared to gap width, a simple shear flow approximation within this layer should be valid. Adding lift velocity to the total particle velocity expressed in equation 4.7, we obtain the general expression for particle displacement, as represented in equation 4.14.

$$v_p = \frac{2}{9} R_p^2 \cdot \frac{(\rho_p - \rho_L)}{\mu_L} \cdot \omega_f^2 r_f - \frac{2.5 \cdot r_f \cdot D}{\zeta} + v_l$$

Equation 4.14

The lift force is directed away from the filter surface in such a way that it contributes to the removal of particles from the filter surface.

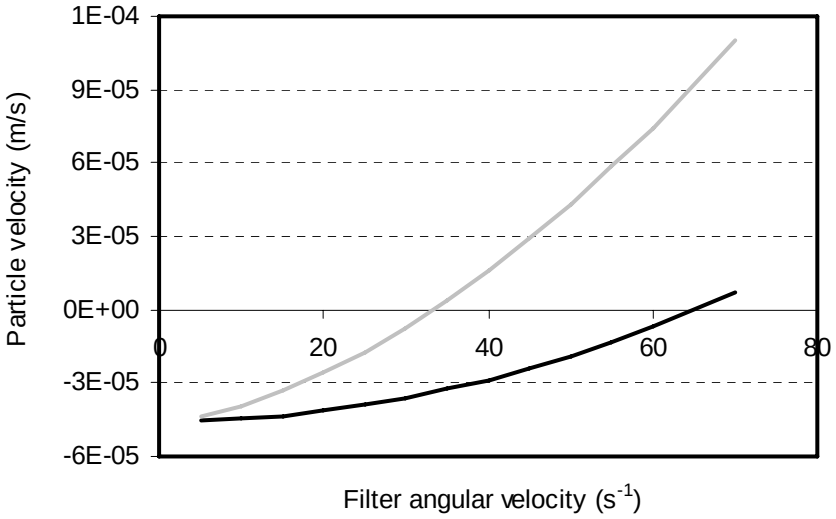

Figure 4.10: Particle velocity at a distance from the filter surface equal to one particle diameter and at a perfusion rate of 3.7 vvd, as a function of filter angular velocity. **––** Without lift effect and –– considering lift velocity upon Saffman (1965).

In Figure 4.10, negative particle velocity signifies that particles are directed toward the filter surface, whereas a positive particle velocity directs particles away from the filter surface. If the lift force is not considered, the particle migration velocity is negative up to a high filter rotation of 60 s^{-1} and particles tend to move toward the rotating filter. The

centrifugal buoyancy force is not strong enough to compensate for the perfusion force. The contribution of lift velocity is well demonstrated in Figure 4.10. At low filter rotations, it is not strong enough to balance the perfusion rate and the particle velocity is still negative, however above 33 s^{-1} it is dominant and total particle velocity becomes positive and particles are carried away from the filter surface.

4.4.1.2 Ho and Leal lift force theory

The Saffman theory applies to viscous flow at Reynolds numbers less than unity, which is the case in the present study. However the presence of walls was not considered. This is important in the present study, since inertial effects differ from those in an unbound flow and we are interested in particle migration near the wall represented by the filter surface. All the studies consider particles located at a distance from the closest wall that is large compared to its diameter ($R_p/\delta<<1$), where δ is the distance of the particle from the wall and $Re_p/\kappa^2<<1$. Drew (1988) approximated the lateral force on a spherical particle in a Poiseuille flow channel, accounting for the inertial force on the particle due to the presence of the wall (sphere is sufficiently near a solid wall) and observed that the resulting wall–induced lift force is smaller than the force in the same unbound shear flow. For this reason, Ho and Leal analysis (Ho and Leal, 1974) of neutrally buoyant particles in a simple shear flow bounded by two parallel plane walls was considered in the present study. The lift velocity expressed by Ho and Leal analysis is represented in equation 4.15.

$$v_l = Re_p \cdot \kappa^2 \cdot V_w \cdot \frac{4}{6\pi} G_1(s) \qquad \text{Equation 4.15}$$

in which $Re_p = R_p \cdot V_w/\upsilon$ and $\kappa = R_p/d$ with R_p (m) the radius of the particle, υ (m^2/s) the cinematic viscosity of the fluid, d (m) the channel width and V_w (m/s) the maximal characteristic fluid velocity at the wall. The function $G_1(s)$ was determined numerically and depends on parameter s, which represents the particle distance from the wall over the channel width. Since $G_1(s) = -G_1(1-s)$, the lateral force is positive for $0<s<0.5$ and negative for $0.5<s<1$, which means that a stable equilibrium position for a sphere in a simple shear flow between two plane walls is reached at the centre–line of the channel, as discussed previously.

In the present study neither the condition $Re_p<<\kappa$ nor $Re_p<<\kappa^2$ imposed by the inertial perturbation theory of Ho and Leal are met. However lateral migration of particles

was successfully predicted by this theory although experimental parameters chosen for experimentation did not fit the conditions of $Re_p << \kappa^2$ (Ho and Leal, 1974). Agreement between experiment and theory was also observed by Otis et al. (1986) especially since the condition $Re_p << \kappa$ was not met, for neutrally buoyant particle moving in Poiseuille flow in a slit. As a result the effect of lift velocity upon Ho and Leal has been calculated for a small s value (particle is one particle diameter from wall) and yields a function $G_1(s)$ equal to 6.296 within the Δl layer. Total particle velocity is compared with the one obtained upon Saffman lift theory and is represented in Figure 4.11.

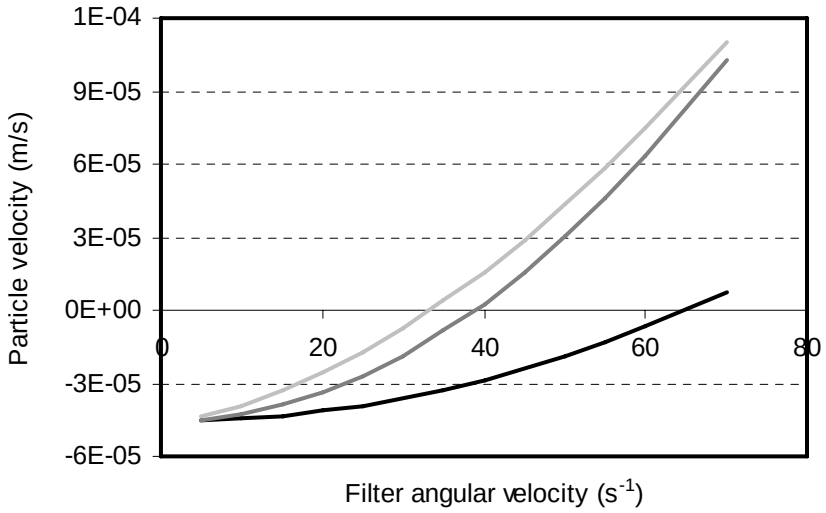

Figure 4.11: Particle velocity at a distance from the filter surface equal to one particle diameter and at a perfusion rate of 3.7 vvd, as a function of filter angular velocity. **––** Without lift effect, considering lift velocity upon — Saffman (1965) and –– Ho and Leal (1974).

A slight discrepancy is observed in the particle velocity profile when comparing Ho and Leal and Saffman lift theories. Saffman unbound theory depends mainly on the viscosity, whereas the Ho and Leal lift force arises from inertia alone in a bound system, without any dependence on viscosity. Particle displacement becomes positive above $39 s^{-1}$ in the present theory, which is slightly larger than in the previous one ($33\ s^{-1}$). Wall–induced effects appear to be important, as a result lowering slightly the lift force. Similar observations have been reported elsewhere (Drew, 1988). In a spin–filter system, the particles were considered to be located at one particle diameter from the wall. However, the present theory is not valid when a sphere is very close to the wall, as related also by Vasseur and Cox (1976) when comparing the results obtained by Ho and Leal (1974) with those of Cox and Hsu (1977) for lateral migration of particle near the wall.

4.4.1.3 Cox and Hsu lift force theory

The Saffman theory overestimates particle velocities near the wall/ filter surface. Lateral migration of non–neutrally buoyant particles, free to rotate, for which the condition $Re_p << \kappa^2$ has not to be met has been studied by Cox and Hsu (Cox and Hsu, 1977) in laminar Poiseuille flow bound by a single wall. The lift velocity derived from such theory is represented in equation 4.16.

$$v_l = \frac{3}{32}\frac{R_p V_s^{\,2}}{\upsilon} - \frac{1}{128}\frac{R_p V_s \cdot \omega_f r_f}{\upsilon}\cdot s\left(44-105\,s\right) + \frac{5}{228}\frac{R_p \cdot \omega_f^{\,2} r_f^{\,2}}{\upsilon}\cdot \kappa^2 s^2\left(1-s\right)\left(22-73\,s\right)$$

Equation 4.16

in which V_s (m/s) is the particle slip velocity, R_p (m) particle radius, υ (m/s^2) fluid viscosity, ω_f (s^{-1}) filter angular velocity, r_f (m) filter radius, κ (–) the ratio of particle radius over distance of particle from wall and s (–) the ratio of particle distance from wall over channel width, Figured also in Ho and Leal lift expression. The total particle velocity resulting from such theory at a distance equal to one particle diameter from filter surface and located in the Δl layer, corresponds well to the one obtained previously by Ho and Leal (1974), as shown in Figure 4.12. The theories seem to hold for filter rotations up to $40 s^{-1}$ and a slight discrepancy is observed at higher rotations, due mainly to the difference in slip velocity between neutrally and non–neutrally buoyant particles at high filter rotation speed. Non–neutral particles have larger slip velocities and it has been observed that the difference in velocity across the particle, caused by shear, is less important when the slip is large (Feng et al., 1994). Cherukat and McLaughlin (1994) studied particle translation in a linear shear flow near a wall and found similar results to those of Cox and Hsu, when $G \cdot R_p << V_w$, as is the case in the present study.

The effect of lift force is widely demonstrated in rotating Couette flow, as represented in Figure 4.12. When this effect is not considered, the lateral migration of particles at a perfusion rate of 3.7 vvd is negative at filter rotations from 5 to 65 s^{-1}. This means that particles move towards the filter surface thereby increasing the probability that particles pass the filter. As a result the high particle retentions observed in the present study, for filter rotation greater than 35 s^{-1}, could not be explained. However, when the lift phenomenon is considered, lateral migration of particles was predicted to become positive at filter rotations around 40 s^{-1}. Experimentally this value was found to correspond to maximal particle retention. The lift force contribution is to move particles away from filter surface and thus to decrease particle passage through the filter and thus increase particle

retention. The lift effect does not completely explain the particle retention phenomenon of a filter with a pore size larger than the mean particle diameter, since retention is not equal to zero when lateral particle velocity is negative. However the correlation between experimental maximal particle retention and theoretical positive lateral particle migration (migration away from filter surface) when considering lift phenomena was well demonstrated.

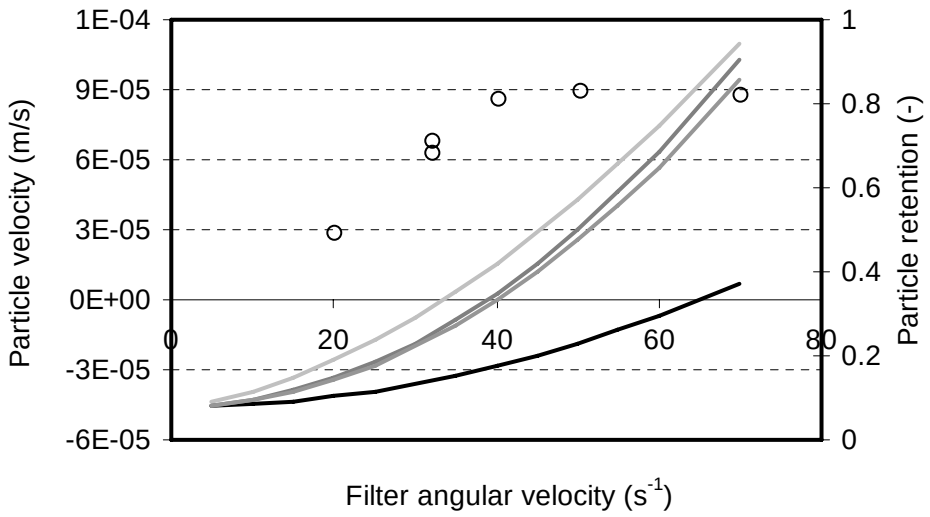

Figure 4.12: Particle velocity at a distance from the filter surface equal to one particle diameter and at a perfusion rate of 3.7 vvd, as a function of filter angular velocity. **––** Without lift effect, considering lift velocity upon –– Saffman (1965), –– Ho and Leal (1974), –– Cox and Hsu (1977). ❍ Particle retention at 3.7 vvd with filter pore size of 14.5 μm.

The general formula of lateral particle migration developed above is mainly dependent on filter angular speed. During scale–up of such a device, the filter radius changes and thus filter rotation has to be adjusted. Therefore it becomes important to identify which of the parameters filter angular speed, tip speed and acceleration, has to be conserved in order to keep valid the particle migration theory and thus particle retention at larger scale.

4.4.2 Spin–filter scale–up strategy

Filter rotation was demonstrated to be important in the phenomenon of lateral particle migration. At a fixed perfusion rate, an increase in rotational speed of the filter, increases the centrifugal force as well as the lift effect of particles near the filter and

contributes to particle flow away from the filter surface and thus to fewer particles passing through filter surface. During perfusion cultures the scale of the filter is increased for industrial purposes and filter rotation has to be adapted.

General particle lateral migration expressed in equation 4.14 is now considered by representing lift velocity with Cox and Hsu lift theory. At a fixed particle distance from the wall, lateral migration depends mainly on perfusion flow, filter angular speed and filter radius. At a fixed perfusion flow of 3.7 vvd and particle distance from wall corresponding to one particle diameter, the total particle lateral velocity can be expressed for different filter angular speeds (ω) and varying filter radius from small–scale to large scale (Figure 4.13). It can be observed at Figure 4.13 that at a low filter angular speed, the particle velocity is negative and particles are directed toward the filter surface, as observed previously. Increasing the filter angular speed results in a positive velocity, however the particle velocity profile is different at small and large scale. Thus at large scale, application of the same angular filter speed as at small scale creates higher centrifugal and lift forces that increase the total particle velocity. However, such high angular speeds cannot be employed at large scale and filter tangential speed (tip speed) is usually conserved during scale–up of internal spin–filter devices.

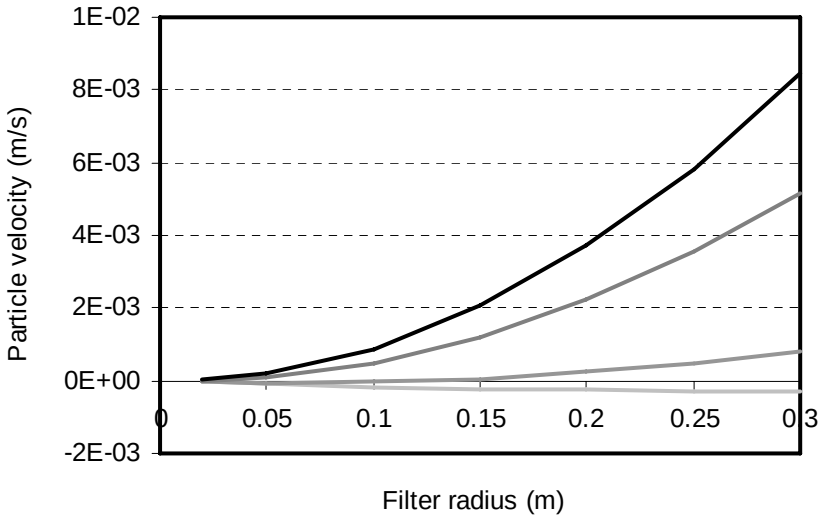

Figure 4.13: Particle velocity as a function of filter radius during the conservation of the filter angular velocity, at 3.7 vvd. — 10 s^{-1}, – – 20 s^{-1}, – – 40 s^{-1} and **– –** 50 s^{-1}.

The total lateral migration of particles with filter tip speed ($\omega_f r_f$) conservation from small to large scale is represented in Figure 4.14.

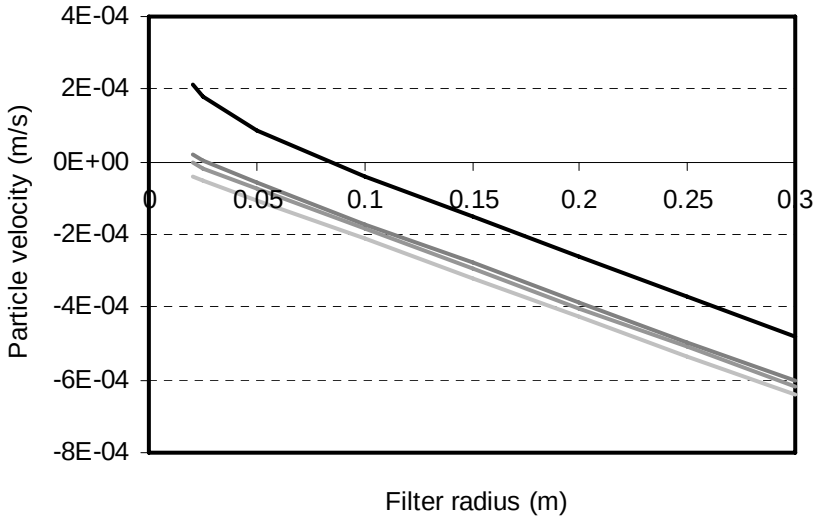

Figure 4.14: Particle velocity as a function of filter radius during the conservation of the filter tip speed, at 3.7 vvd. — 0.2 m/s, — 0.8 m/s, — 1.0 m/s and — 2.0 m/s.

It can be observed that at small scale, only high filter tip speeds greater than 0.8 m/s can give rise to a positive particle velocity. Increasing the scale means increasing the filter radius, such that particle velocity is almost always negative, even at high filter tip speeds. At large scale particle velocity differs from small scale and, compared to earlier profiles (see Figure 4.13) filter tip speed appears to be unrepresentative of the migration phenomena. Thus tip speed conservation does not seem to be a good approach to maintain a similar particle repulsion mechanism at the filter surface during scale–up.

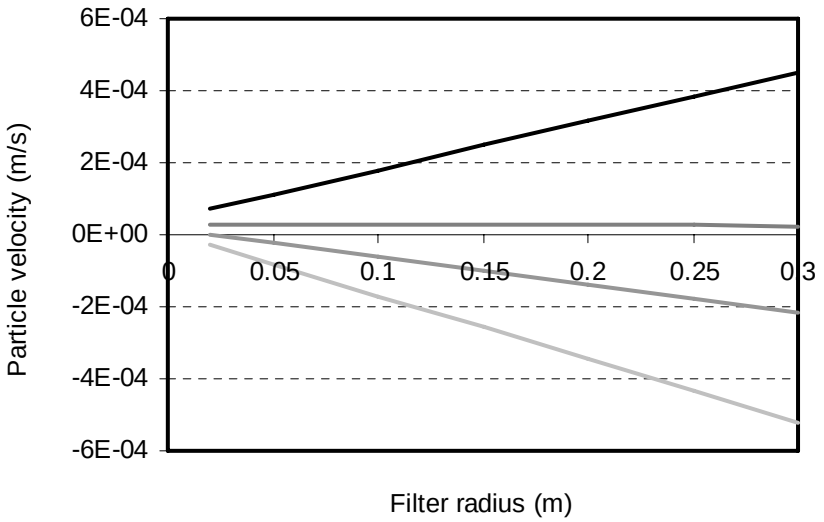

Figure 4.15: Particle velocity as a function of filter radius during the conservation of the filter acceleration, at 3.7 vvd. — 10 m/s^2, — 35 m/s^2, — 55 m/s^2 and — 90 m/s^2.

The optimum particle velocity profile would be expected to be flat for all filter radii. If the filter rotation is expressed in terms of filter acceleration ($\omega_f^2 r_f$), the particle profile obtained can be represented by Figure 4.15. At small scale and low filter acceleration, particle velocity is negative and particles are directed towards the filter surface. Increasing the filter acceleration, results in particle repulsion from the filter, as observed previously (Figures 4.13 and 4.14). However, at larger scale, the lateral velocity of particles is more flat (when comparing Figures 4.13, 4.14 and 4.15, attention must be paid to the difference between the scales) than observed previously and the particle attraction/repulsion mechanism is expected to be similar at both scales. Filter acceleration conservation during scale–up thus seems to be a better choice than tip speed in order to maintain a similar particle retention mechanism at small scale as well as at large scale.

The minimal angular speed at witch the filter has to rotate in order to reach a total particle lateral velocity close to zero and thus reach maximum particle retention, at one particle diameter from the filter surface, is represented in Figure 4.16 for different filter radii. It is observed that as filter radius increases, the filter angular speed can be reduced while maintaining the maximal particle retention. The perfusion flow seems to have a great influence on particle retention. Indeed a filter radius of 0.0214 m should have an optimal angular speed of 40 s^{-1} and 21 s^{-1} in order to reach positive lateral speeds, when the perfusion flow is set at 3.7 vvd and 1 vvd respectively.

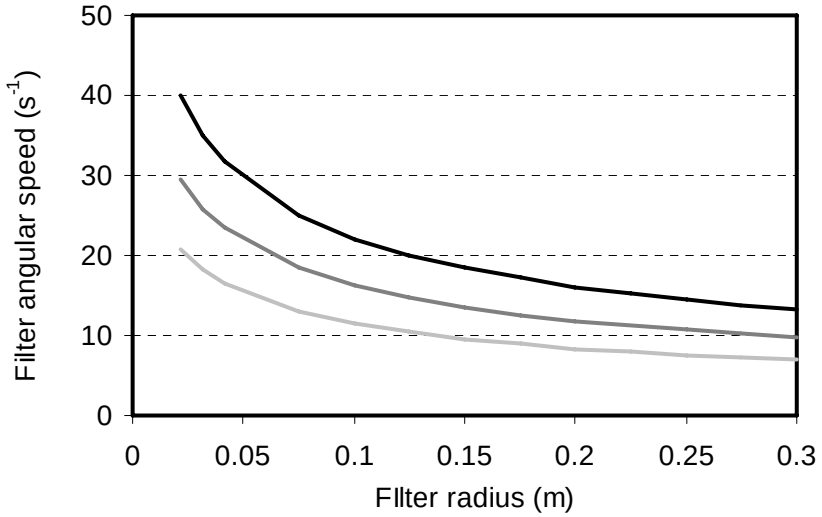

Figure 4.16: Scale–up strategy: minimal filter angular velocity as a function of filter radius at – – 1 vvd, – – 2 vvd and **– –** 3.7vvd. The particle diameter is 13 μm.

The prediction of the model is difficult to validate experimentally at the large scale, however retention of particle was measured at small scale, for different filter radii of 2.14, 3.18 and 4.16 cm, as a function of filter angular speed, filter tip speed and filter acceleration (Figures 4.17 and 4.18). It can be observed first that particle retention is low at low filter rotations and increases with increasing filter angular speed or tip speed, until it reaches a plateau of maximum particle retention. The minimum filter rotation at which the retention is maximal was demonstrated previously to correspond to positive total lateral migration of particles near the filter surface.

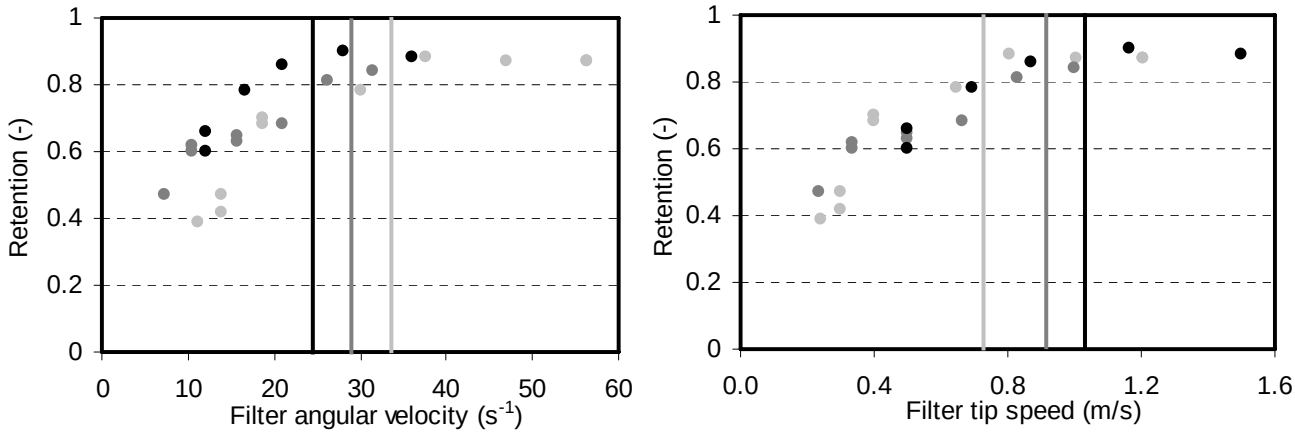

Figure 4.17: Particle retention with filter pore size of 14.5 μm, at 1 vvd as a function of **a**. filter angular velocity and **b**. filter tip speed for three different filter radii: ● 2.14 cm, ● 3.18 cm and ● 4.16 cm.

During angular as well as tip speed variation, the particle retention profile is different for all filter radii employed. The plateau of maximal retention is reached at different angular and tip speeds (represented in Figures by a line) for the three filter radii tested. The smallest filter radius has to be in rotation at a minimum angular speed of 33 s^{-1} and respectively minimum tip speed of 0.75 m/s, in order to reach maximum particle retention. Whereas the angular and tip speed of the largest filter has to be set at 25 s^{-1} and 1 m/s respectively. Experimentally, it was thus observed that at larger filter radius, the filter angular speed or filter tip speed has to be decreased or respectively increased in order to achieve maximum particle retention, as also predicted theoretically by the previous model (Figures 4.13 and 4.14). That means that during spin–filter scale–up, the conservation of the filter tip speed from small to large scale would result in different retention rates, much lower at large scale than at small scale.

Whereas during variation of filter acceleration, the particle retention profiles seem to be similar for all filter radii tested, and the plateau is reached at the same minimal filter

acceleration of 25 m/s^2 (Figure 4.18). These results, together with the previous simulations, clearly demonstrate that the filter rotation parameter that has to be conserved during spin–filter scale–up is the acceleration of the filter and not the filter angular or tip speeds.

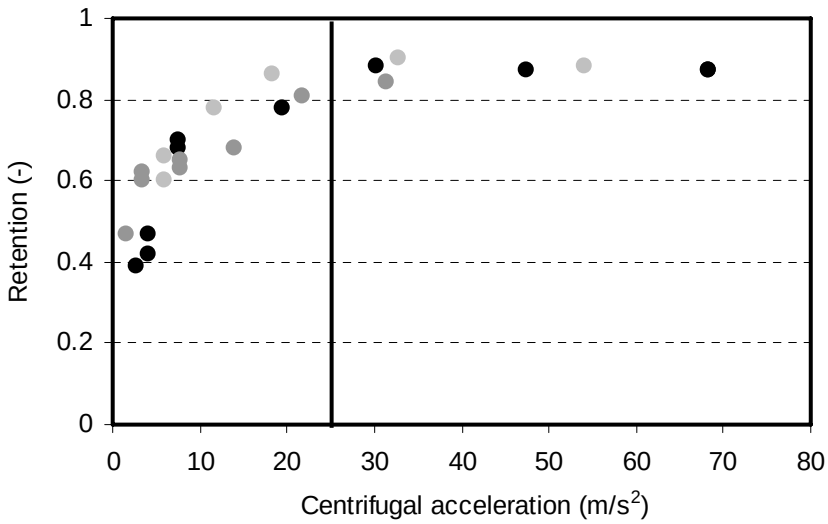

Figure 4.18: Particle retention with filter pore size of 14.5 μm, at 1 vvd as a function of filter acceleration for three different filter radii: ● 2.14 cm, ● 3.18 cm and ● 4.16 cm.

At high filter rotations particle retention was found to vary slightly when the perfusion flow is increased (chapter 3). Whereas at lower filter rotations particle decreases when perfusion flow is increased. The consequence of this phenomenon is the increase of minimal filter rotation at witch retention is maximal with the increase of the perfusion flow, as also observed experimentally during particle retention measurements at 1 and 3.7 vvd (Figures 4.12 and 4.17). This phenomenon was also observed during particle lateral velocity simulations. Indeed it was observed that the filter rotation at which the simulated particle migration is close to zero decreases when perfusion rate decreases (Figure 4.16). Although the simulations and the experimentation give rise to similarities between lateral particle migration and particle retention, as a function of filter rotation speed, the absolute values differ. At 3.7 vvd and 0.0214 filter radius, the predicted minimal filter rotation in order to have a lateral particle migration close to zero was 40 s^{-1} (Figures 4.12 and 4.16), which is quite similar with the experimental value situated between 35–40 s^{-1} (Figure 4.12). However at smaller perfusion flow of 1 vvd, the predicted value corresponded to 21 s^{-1} (Figure 4.16), whereas experimentally maximal retention was obtained above 33 s^{-1} (Figure 4.17). When the filter radius was increased from 0.0214 to 0.0416 m, similar minimal filter acceleration of 25 m/s^2 (Figure 4.18) was obtained experimentally for all filter

radii. The same phenomena happened during lateral particle migration simulations, however minimal filter acceleration corresponded to 10 m/s^2 (Figure 4.16). These discrepancies between the experiments and the simulations highlight the sensitivity of the model. The influence of perfusion flow on simulated particle lateral migration seems to have a smaller effect than experimentally observed.

The increase of the scale involves the decrease of the minimal filter angular speed, however the particle slip velocity increases and thus the condition $Re_V<<1$ required by Cox and Hsu (1977) theory is not valid any more. This latter condition was calculated to break down for filter radii greater than 7.5 cm, a value above which the predictions of particle lateral migration should not be valid any more. This condition breaks down mainly because larger scales imply larger gap widths between the filter and the vessel and involve higher particle lift velocities. Halow and Wills (1970a) expression for particle slip velocity used in the present study was developed for vortex–flow systems those gap widths are small compared with the cylinder radius, that is not the case for spin–filter systems and shows the approximate nature of the model.

The particle lateral migration model developed in the present study for spin–filter systems is limited to small scale. The influence of perfusion flow was revealed to be bigger during particle lateral migration simulations than experimentally. However the model together with experimentation demonstrated that the filter acceleration is the parameter that has to be conserved during filter scale–up in order to reach similar levels of retention at small as well as at large scale.

Although an adequate theory explaining lateral lift migration has been developed for dilute suspensions of particles, the theory needs to be extended to more concentrated suspensions, in which particle–particle interactions are not negligible, as is the case in the present study. Since the model is completely theoretical, particle image velocimetry techniques could be used in order to record particle trajectories and correlate the model with experimental data.

4.5 Conclusions

Studies of fluid dynamics around the spin–filter were carried out to understand particle retention of spin–filters, in which the pore size is larger than the mean cell diameter. Particle retention mechanism was related to particle migration across the filter

surface. Consideration of centrifugal buoyancy and perfusion forces only was demonstrated to be insufficient to explain the phenomena of particle retention entirely. And lift force invoked by the theory of cross–flow filtration systems was considered in the present study for spin–filter filtration systems.

In the present study, Cox and Hsu (1977) lift theory of non–neutrally buoyant particles in a simple shear flow bound by one wall was adapted for curved Couette flow. The particle slip velocity used was that of Halow and Wills (1970a). The lift force in a spin–filter system was revealed to contribute positively to particle migration by forcing particles away from the filter and thus enhancing particle retention. At a fixed perfusion rate, the increase of filter rotation increases particle retention until a plateau is reached. The maximum particle retention obtained experimentally was revealed to correspond exactly to a predicted positive particle lateral migration velocity, with the result that particles move away from the filter surface. When the filter rotation is not strong enough, lift and centrifugal forces cannot balance the perfusion force, particle retention decreases and a negative particle lateral migration (particles move toward the filter surface) was predicted.

The theoretical particle lateral migration model proposed is nevertheless sensitive to the perfusion rate. Experimentally, the minimal filter rotation at which retention is maximal increases with the increase of perfusion rate. Although the simulations of particle lateral migration showed the same phenomenon, the predicted minimal rotation at which particle lateral migration is close to zero differs from the experimental minimal value at which retention is maximal. At filter radius larger than 0.075 m, the model was revealed to break down because the condition $Re_V << 1$ required by the lift theory was not valid any more.

Although discrepancies were found between experimentation and simulations, the model permitted the identification of the importance of lift force in spin–filter systems and together with experimentation identified the filter acceleration to be the parameter that has to be conserved in order to keep similar particle lateral migration phenomena and thus similar particle retention profiles at small scale as well as at the large scale.

References

Altena, F.W., Belfort, G., 1984. Lateral migration of spherical particles in porous flow channels: application to membrane filtration. Chem. Eng. Sci. 39(2):343–355.

Belfort, G., 1988. Membrane modules: comparison of different configurations using fluid mechanics. J. Membrane Sci. 35:245–270.

Belfort, G., Pimbley, J.M., Greiner, A., Chung, K.Y., 1993. Diagnosis of Membrane Fouling Using a Rotating Annular Filter .1. Cell–Culture Media. J. Membrane Sci. 77(1):1–22.

Bird, R.B., Stewart, W.E., Lightffot, E.N., 1960. Transport phenomena: John Wiley & Sons. 780p.

Cherukat, P., McLaughlin, J.B., 1994. The inertial lift on a rigid sphere in a linear shear flow field near a flat wall. J. Fluid Mech. 263:1–18.

Cherukat, P., McLaughlin, J.B., Dandy, D.S., 1999. A computational study of the inertial lift on a sphere in a linear shear flow field. Int. J. Multiphase Flow 25:15–33.

Cox, R.G., Brenner, H., 1968. The lateral migration of solid particles in Poiseuille flow – I. Theory. Chem. Eng. Sci. 23:147–173.

Cox, R.G., Hsu, S.K., 1977. The lateral migration of solid particles in a laminar flow near a plane. Int. J. Multiphase Flow 3:201–222.

Drew, D.A., 1988. The lift force on a small sphere in the presence of the wall. Chem. Eng. Sci. 43(4):769–773.

Drew, D.A, Schonberg, J.A, Belfort, G., 1991. Lateral inertial migration of small sphere in fast laminar flow through a membrane duct. Chem. Eng. Sci. 46(12):3219–3224.

Feng, J., Hu, H.H., Joseph, D.D., 1994. Direct simulation of initial value problems for the motion of solid bodies in a Newtonian fluid. Part 2. Couette and Poiseuille flows. J. Fluid Mech. 277:271–301.

Green, G., Belfort, G., 1980. Fouling of ultrafiltration membranes: lateral migration and the particle trajectory model. Desalination 35:129–147.

Halow, J.S., Wills, G.B., 1970a. Experimental observations of sphere migration in Couette systems. Ind. Eng. Chem. Fundam. 9(4):603–607.

Halow, J.S., Wills, G.B., 1970b. Radial migration of spherical particles in Couette systems. AICHE J. 16(2):281–286.

Ho, B.P., Leal, L.G., 1974. Inertial migration of rigid spheres in two–dimensional unidirectional flows. J. Fluid Mech. 65(2):365–400.

Ishii, K., Hasimoto, H., 1980. Lateral migration of a spherical particle in flows in a circular tube. Journal of the Physical Society of Japan 48(6):2144–2155.

Maiorella, B., Dorin, G., Carion, A., Harano, D., 1991. Cross–flow microfiltration of animal cells. Biotechnol. Bioeng. 37(2):121–126.

McLaughlin, J.B., 1991. Inertial migration of a small sphere in linear shear flows. J. Fluid Mech. 224:261–274.

McLaughlin, J.B., 1993. The lift on a small sphere in wall–bounded linear shear flows. J. Fluid Mech. 246:249–265.

Oliver, D.R., 1962. Influence of particle rotation on radial migration in the Poiseuille flow of suspensions. Nature, 194:1269–1271.

Otis, J.R., Altena, F.W., Mahar, J.T., Belfort, G., 1986. Measurements of single spherical particle trajectories with lateral migration in a slit with one porous wall under laminar flow conditions. Exp. Fluids 4:1–10.

Repetti, R., Leonard, E.F., 1964. Segré–Silberberg annulus formation: a possible explanation. Nature. 203:1346–1348.

Rubinow, S.I., Keller, J.B., 1961. The transverse force on a spinning sphere moving in a viscous fluid. J. Fluid Mech. 11:447–459.

Saffman, P.G., 1965. The lift on a small sphere in a slow shear flow. J. Fluid Mech. 22(2):385–400.

Saffman, P.G., 1968. Corrigendum. J. Fluid Mech. 31:624.

Schonberg, J.A., Hinch, E.J., 1989. Inertial migration of a sphere in Poiseuille flow. J. Fluid Mech. 203:517–524.

Schwille, J.A., Mitra, D., Lueptow, R.M., 2002. Design parameters for rotating cylindrical filtration. J. Membrane Sci. 204(1–2):53–65.

Searles, J.A., Todd, P., Kompala, D.S., 1994. Viable cell recycle with an inclined settler in the perfusion culture of suspended recombinant chinese hamster ovary cells. Biotechnol. Progr. 10:198–206.

Segré, G., Silberberg, A., 1961. Radial particle displacements in Poiseuille flow of suspensions. Nature 189:209–210.

Vasseur, P., Cox, R.G., 1976. The lateral migration of a spherical particle in two–dimensional shear flows. J. Fluid Mech. 78(2):385–413.

Vigo, F., Uliana, C., 1986. Influence of the vorticity at the membrane–surface on the performances of the ultrafiltration rotating module. Separ. Sci. Technol. 21(4):367–381.

Weigand, R.J., Altena, F.W., Belfort, G., 1985. Lateral migration of spherical particles in laminar porous tube flows: application to membrane filtration. Physicochem. Hydrodyn. 6(4):393–413.

Wereley, S.T., Akonur, A., Lueptow, R.M., 2002. Particle–fluid velocities and fouling in rotating filtration of a suspension. J. Membrane Sci. 209:469–484.

Wereley, S.T., Lueptow, R.M., 1998. Inertial particle motion in a Taylor Couette rotating filter. Phys. Fluids 11(2):325–333.

5

The use of response surface methodology to model particle retention by spin–filters

Abstract

During spin–filter animal cell perfusion cultures, the use of filter pore sizes greater than the mean cell diameter increases filter operation time, however cell leakage from the reactor depends on several parameters. The impact of these parameters on particle retention by spin–filters was modeled for small–scale, as well as for large–scale systems, using experimental design methodology. A three level modified face–centered composite design was used to investigate the effects of filter porosity, particle concentration, perfusion capacity and filter acceleration, on the retention of polymer beads with a diameter in the range of the mean animal cell diameter. A series of 31 experiments enabled the second–order polynomial model to predict particle retention. An additional set of 10 data series checked the accuracy of the model predictions. By backward elimination the model equation could be reduced from 15 regression coefficients to 9 significant ones. The most relevant were revealed to be filter porosity and filter acceleration. The experimental results obtained during two perfusion cultures of CHO cells with different spin–filter pore sizes agreed with those predicted from the particle model, indicating the applicability of the model to animal cells during actual perfusion cultures. Optimized spin–filter acceleration

and pore size could thus be predicted as a function of the scale (perfusion rate) and culture parameters (cell size and concentration). Cell swelling, probably due to ammonia accumulation during glucose–limited growth, was revealed to have a positive effect on cell retention by the spin–filter due to an increase in the filter porosity factor.
Keywords: animal cell culture, CHO cells, high cell density, perfusion, cell separation, spin–filter, scale–up, cell retention, response surface methodology, cell swelling

5.1 Introduction

Spin–filters are the most commonly used separation devices for animal cell perfusion cultures. Many studies have been done in order to better understand the retention and fouling mechanisms behind this separation system. Several parameters have been identified as influencing cell retention: filter design (Jan et al., 1992; Siegel et al., 1991), filter pore size (Heine et al., 1999; Jan et al., 1992), filter velocity (Deo et al., 1996; Favre and Thaler, 1992; Iding et al., 2000; Siegel et al., 1991; Yabannavar et al., 1992), perfusion rate (Iding et al., 2000; Jan et al., 1992; Yabannavar et al., 1992) and cell concentration (Deo et al., 1996; Favre, 1993). The influence of all these parameters has been studied previously (see chapter 3), with retention found to be mainly dependent on filter velocity and filter pore size. An increase of filter pore size was found to induce a decrease in retention and, conversely, an increase in filter velocity induced an increase in cell retention until a constant level was reached. An increase of the cell concentration in the bioreactor increased the retention, but to lesser extent than filter pore size and filter velocity, while perfusion flow had a negative influence on retention, particularly at low filter velocities.

Filter fouling has been demonstrated to rise as the result of high perfusion rates and high cell concentrations, while an increase in filter rotational velocity and screen surface per reactor volume reduces filter fouling (Deo et al., 1996). The effects of the different parameters on cell retention (see chapter 3) and fouling, summarized in Table 5.1, show that only one parameter tends to increase filter fouling and at the same time reduces cell retention, namely the perfusion rate. This parameter is dependent on the cell concentration and cannot be varied independently. An increase of filter pore size was found to reduce filter fouling, but unfortunately at the same time reduced the cell retention, while an increase of cell concentration increased cell retention as well as filter fouling. The

only parameter that tends to reduce filter fouling and increase cell retention at the same time is the filter rotation velocity. From this summary it is apparent that an optimization of all parameters is necessary in order to achieve long–term, high cell concentration cultures, as a result of high cell retention and reduced filter fouling, at any operation scale.

		Filter fouling	Cell retention
Perfusion rate	↗	↗	↘
Filter pore size	↗	↘	↘
Cell concentration	↗	↗	↗
Filter rotation speed	↗	**↘**	**↗**

Table 5.1: Influence of raising operating parameters on filter fouling and cell retention.

Despite the widespread use of spin–filters and the plethora of retention studies, the mechanisms behind cell retention remains unclear. As a result the strategy for scale–up is difficult and remains the main limitation to industrial use, in addition to the problems associated with filter fouling. Indeed some authors tend to develop scale–up strategies by considering only filter fouling. The parameters taken into account in such studies are usually the filter dimensions (diameter and height), reactor volume and filter rotational velocity. Using the similarities between spin–filters and cross–flow micro–filtration and, based on the studies of particle motion in laminar annulus flow with a porous wall (Belfort et al., 1988), a method was proposed to predict scale–up of spin–filters during culture operation without filter clogging, by measuring fluid exchange across the screen (Yabannavar et al., 1992). This method expressed the screen speed (N_{screen}) as proportional to (reactor volume)$^{-0.166}$, and could be applied to a scale of 175 L–working volume on the basis of optimized 12 L–working volume experimentation (Yabannavar et al., 1994). Another empirical model described the effects of operating conditions and spin–filter configuration on perfusion capacity (Deo et al., 1996). In this case, the perfusion rate (reactor volume per day) was expressed as being proportional to the ratio of the spin–filter surface per reactor volume, to the square of the rotational velocity and inversely proportional to cell concentration. For scale–up purposes, the spin–filter area could be increased increasing its diameter. As a result the model was successfully used to scale–up a perfusion process from 7 to 500L–scale, while retaining an equivalent duration (>30 days) and high cell density (>10^7 cell/ml).

All of the reported scale–up strategies are based on carrying out large numbers of preliminary spin–filter cultures at small–scale and are, as a result, extremely time

consuming. In the present study, a strategy based on cell retention characterization and optimization is presented that avoids any preliminary cell cultures and is considered to be valid for many animal cells, at small–scale as well as at large scale. For this purpose, response surface methodology (RSM) was used to model retention as a function of four factors, namely filter rotation velocity, filter porosity (ratio of filter pore size to cell diameter), perfusion capacity (ratio of perfusion rate to filtration surface) and cell concentration, using a minimum of resources and quantitative data from an appropriate experimental design. A three–level modified face–centered composite design was used. The second–order polynomial model is based on retention measurements during perfusion simulations using polymer beads and would predict the optimal operation conditions and design of a spin–filter in order to obtain maximum cell retention with reduced filter fouling. The values for the four varied parameters relate to small scale, as well as large scale in such a way that it is no longer necessary to carry out prior small–scale cultures. In order to validate the model for real animal cell use, two CHO cells perfusion cultures have been successfully carried out using spin–filters with two different pore sizes.

5.2 Materials and methods

5.2.1 Materials

Superose 6 beads (Amersham Biosciences, Freiburg, Germany) with a mean bead diameter of 13±2 μm were used for perfusion simulations. The size of the beads was deliberately chosen to be similar to the mean diameter (12 μm) of the animal cells used in this study.

The cell line used throughout this work is a CHO *SSF3* (Novartis, Basel, Switzerland) cell line, producing human secretory component (hSC). The cell culture medium is a serum– and protein–free medium ChoMaster HP–1 (Cell Culture Technology, Zurich, Switzerland), supplemented with 5 mM glutamine, 5 mM asparagine, 1 mM leucine, 1 mM glutamic acid and 1 mM serine. A minimal cell concentration after inoculation of $2 \cdot 10^5$ cell/ml was defined and cells were harvested upon reaching a maximal cell density of $1 \cdot 10^6$ cell/ml. During passaging the cells were maintained at 37°C, under a humidified atmosphere containing 5% CO_2.

5.2.2 Experimental methods

Bead perfusion simulations were performed using a 12 cm diameter (d_v) glass vessel (Figure 5.1), in which four baffles of 1 cm width ($d_{b,v}$) and 15 cm height ($h_{b,v}$) were placed. The working volume was set to 1.6 L and beads were maintained in suspension using a magnetic stirrer under gentle agitation at 100 rpm. The turbidity of the bead suspensions was measured spectrophotometrically (Uvikon 930, Kontron Instruments, Switzerland) at 600 nm and related to a calibration curve of turbidity to number of particle/ml. The latter was determined microscopically using a Neubauer counting chamber. Three different spin–filter screens made of stainless steel (G. Bopp & Co. AG, Zurich, Switzerland) with nominal pore sizes of 13, 14.5 and 18 μm were used. The filter external diameter (d_f) was 6.36 cm and the total (h_f) and immersed height (h_i) were 8 and 4 cm respectively. Baffles of 2 cm width ($d_{b,f}$) were placed inside the spin–filter in order to maintain a homogeneous particle suspension. A top–drive motor (Eurostar, IKA–Werke GMBH, Staufen, Germany) rotated the filter at velocities ranging from 50 to 450 rpm. Medium from inside the spin–filter was removed at linear perfusion rates from 2 to 25 cm/h (ratio of perfusion flow to immersed filtration surface), using a calibrated peristaltic pump (Alitea, Bioengineering, Wald, Switzerland) and returned to the vessel in order to maintain the volume and bead concentration constant within the vessel (Figure 5.1).

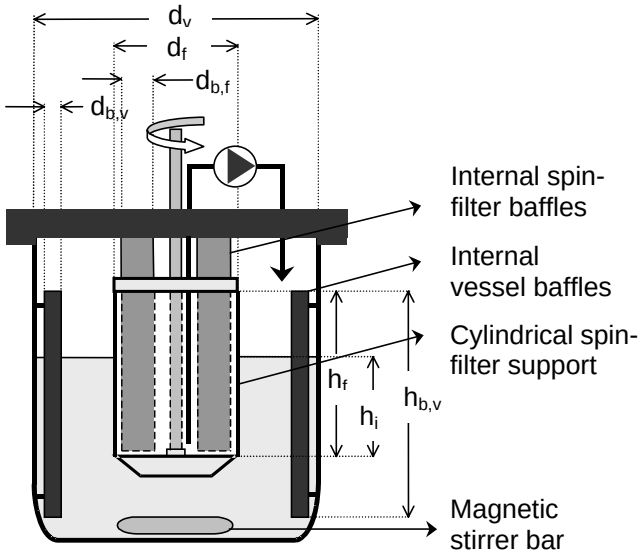

Figure 5.1: Experimental set–up during bead perfusion simulation. d_v: vessel internal diameter, d_f: spin–filter diameter, $d_{b,v}$: vessel baffle width, $d_{b,f}$: spin–filter baffle width, h_f: filter height, h_i: immersed filter height and $h_{b,v}$: vessel baffle height.

Once the desired perfusion rate was attained, samples were collected using a pipette from the vessel and from directly inside the spin–filter. The system was considered to be in steady state when the concentration inside the spin–filter was stable. The retention could then be calculated as 1– ($c_{in,filter}/c_{out,filter}$), where $c_{in,filter}$ and $c_{out,filter}$ are the concentrations of particles inside and outside the spin–filter respectively.

Animal cell perfusion cultures of CHO *SSF3* were performed in a 2 L reactor (Bioengineering, Wald, CH) and 1.65 L working volume. The reactor was operated at a temperature of 37°C, under gentle agitation using a marine impeller of 5 cm in diameter, at 150 rpm. Bubble–free aeration was achieved using 2 m of Teflon tubing (W. L. Gore & Associates GmbH, Putzbrunn, Germany). A regulation system injected a mixture of oxygen, nitrogen and carbon dioxide into the reactor via the Teflon tubing to maintain the dissolved oxygen and CO_2 concentrations at 80% air saturation and 5% respectively during the culture. This system also allowed determination of the oxygen uptake rate on–line (Ducommun, 2000). For cell separation a stainless steel spin–filter was used with dimensions of 6.36 cm diameter and 4 cm immersion height (same filter and baffle configurations as previously). Filter pore sizes of 8.5, 14.5 and 18 μm, with different weaving orientations were tested with the filter rotation rate set to 320 rpm. Medium was fed into the reactor using a peristaltic pump (Preciflow Lambda, Visperminen, Switzerland), while a second peristaltic pump withdrew the perfusate from the bottom of the inside the spin–filter.

Cell size distribution was measured with a Coulter Counter ZM (Beckman Coulter, Fullerton, California, United States) equipped with a 70μm orifice tube coupled to a Channelyzer 256. The instrument was set to 500 mA, an attenuation of 128 and a gain of 1. After instrument calibration using 9.6 μm latex beads (Beckman Coulter), the mean CHO cell diameter was found to be approximately 12 μm.

5.2.3 Biomass and metabolite analysis

Cell concentration was determined microscopically using a Neubauer hemocytometer chamber. Viable and non–viable cells were distinguished using the Trypan blue extrusion method.

Glucose and lactate concentrations were quantified by HPLC (1100 system, Agilent, Palo Alto, California, United States) using a Supelco H column (Supelco,

Bellefonte, Pittsburgh, United States), 0.02M H_2SO_4 as solvent and a refractive index detector (HP 1047 A, Hewlett Packard GmbH, Waldbronn, Germany). Glutamine concentration was quantified by HPLC (450–MT2, Kontron Instruments, Zürich, Switzerland) using an Aminex HPX–87C column (BIO–RAD, Hercules, California, United States), 2 mM calcium nitrate as solvent and a RI detector (ERC–7510, ERMA Optical Works Ltd, Tokyo, Japan).

5.2.4 Methodology and experimental design

Four parameters, previously reported as influencing particle retention the most have been chosen to compose the retention model, namely the particle concentration within the reactor, filter rotation velocity, filter pore size and perfusion flow rate. The filter rotation is a key parameter in cell retention, and may be expressed as filter angular velocity, filter tip–speed or filter acceleration. Preliminary studies demonstrated that only filter acceleration represents retention values equally well at both small–scale and large–scale (chapter 4). For these reasons, filter acceleration has been chosen in the present model to represent the filter rotation speed. The filter pore size was normalized with respect to particle diameter in order to predict the retention of a wide range of particle sizes; this term was named filter porosity. Finally, the perfusion flow was normalized with respect to the filtration surface in order to take into account the scale; this term was named perfusion capacity.

In the present study, only the particle concentration, the perfusion capacity and filter acceleration can be varied freely within the conditions imposed by the experimental design. The levels of these three factors take coded values of –1, 0 and 1 (Table 5.2). The porosity factor cannot be varied freely, since it has fixed values dependent on the filter pore sizes commercially available. The filter pore sizes tested could only take values of 13, 14.5 and 18 μm, which correspond to coded porosity values of –1, –0.385 and 1 (Table 5.2).

Variables	**Coded levels**			
	-1	**-0.385**	**0**	**1**
Filter porosity (-): x_1	1	1.12	-	1.39
Particle concentration (10^6 part./ml): x_2	1	-	5.5	10
Perfusion capacity (cm/h):x_3	2	-	13.5	25
Filter acceleration (m/s^2): x_4	5	-	20	35

Table 5.2: Independent variables and their corresponding levels.

A large experimental plan of 31 sets of experiments (Table 5.3) was built by combining all three levels of each parameter. Using the software NemrodW (developed by the LPRAI, Marseille, France) for experimental design, one matrix was selected according to the D–optimality criterion that minimizes the variance of the coefficients estimation (Goupy, 1999). The final matrix is composed of a combination of values that optimizes the response within the experimental domain to allow the design of a minimal number of experimental runs. This number corresponds to 31 experiments. Eight experiments represent 8 of the 16 tops of the 4–dimensional hypercube and are repeated, 6 others are situated in the middle of the 6 faces of the cube combined by the factors particle concentration, perfusion capacity and filter acceleration, while the filter porosity factor is fixed at –0.385, 3 points are situated in the center of the cube while the filter porosity is fixed at –1, –0.385 and 1, 2 points are repeated and finally 4 points are situated arbitrarily within the 4–dimensions hypercube. The matrix design resembles a face centered composite design. The 31 experiments have been undertaken randomly in such a way that the influence of any other parameter was eliminated. The domain was chosen in such a way that it could contain culture parameters at small scale as well as large scale. Indeed a perfusion capacity of 2 and 25 cm/h corresponds to 6 volumes per working volume per day (vvd) at 2–L and 300–L scale respectively, for a filter volume of 20% of the working reactor volume and for an immersed filter height of 50% of the reactor height. The particle concentration was varied between 10^6 and 10^7 particle/ml, which corresponds to the concentration range of typical animal cell perfusion cultures. The porosity coefficient was varied between 1 and 1.39, such that one filter has pore sizes equal to the particle diameter and two filters are open (the pore size is larger than the average particle diameter). Finally the filter acceleration was varied between 5 and 35 m/s^2.

The real parameters (U_i) have been modified to coded variables (x_i) as follows:

$$x_i = \frac{(U_i - U_i^0)}{\Delta U_i}$$

These new variables (x_i) are dimensionless and enable comparison of the effects of the different factors, which normally have different units. U_i^0 is the real value of an independent variable at the center point and is calculated from the formula: 0.5 (U_{max} + U_{min}), whereas ΔU_i is the step change and is calculated from: 0.5 (U_{max} – U_{min}).

	Uncoded variables (U_i)				Coded variables (x_i)				Y
N°	Filter porosity (-)	Particle concentration (10^6 part/ml)	Perfusion capacity (cm/h)	Filter acceleration (m/s^2)	Filter porosity	Particle concentration	Perfusion capacity	Filter acceleration	Retention (-)
1	1.12	1	13.5	20	-0.385	-1	0	0	0.68
2	1.12	5.5	25	20	-0.385	0	1	0	0.75
3	1.39	5.5	13.5	20	1	0	0	0	0.38
4	1.39	10	2	35	1	1	-1	1	0.7
5	1.39	1	25	35	1	-1	1	1	0.51
6	1.12	5.5	25	16	-0.385	0	1	-0.267	0.7
7	1.12	10	13.5	20	-0.385	1	0	0	0.86
8	1.39	1	25	5	1	-1	1	-1	0.11
9	1	10	2	35	-1	1	-1	1	0.99
10	1	10	25	5	-1	1	1	-1	0.98
11	1	1	25	5	-1	-1	1	-1	0.87
12	1.39	10	25	5	1	1	1	-1	0.2
13	1	10	25	35	-1	1	1	1	0.99
14	1	10	2	5	-1	1	-1	-1	0.99
15	1.39	3.4	9.8	16	1	-0.467	-0.322	-0.267	0.49
16	1	1	2	5	-1	-1	-1	-1	0.93
17	1.12	5.5	2	20	-0.385	0	-1	0	0.85
18	1	5.5	13.5	20	-1	0	0	0	0.99
19	1.12	9.6	9.8	16	-0.385	0.911	-0.322	-0.267	0.77
20	1.39	1	2	5	1	-1	-1	-1	0.27
21	1	3.4	9.79	16	-1	-0.467	-0.323	-0.267	0.98
22	1	1	2	35	-1	-1	-1	1	0.97
23	1.39	10	2	5	1	1	-1	-1	0.33
24	1	1	25	35	-1	-1	1	1	0.95
25	1.39	10	25	35	1	1	1	1	0.61
26	1.12	5.5	13.5	5	-0.385	0	0	-1	0.55
27	1.39	1	2	35	1	-1	-1	1	0.56
28	1.12	5.5	13.5	20	-0.385	0	0	0	0.81
29	1.12	5.5	13.5	20	-0.385	0	0	0	0.78
30	1.12	5.5	13.5	35	-0.385	0	0	1	0.87
31	1.12	5.5	13.5	35	-0.385	0	0	1	0.88
32	1.12	10	13.5	30	-0.385	1	0	0.667	0.89
33	1.12	1	13.5	30	-0.385	-1	0	0.667	0.78
34	1.12	1	1	7.8	-0.385	-1	-1.087	-0.813	0.59
35	1.12	1	1	21.8	-0.385	-1	-1.087	0.120	0.81
36	1.12	1	1	31.4	-0.385	-1	-1.087	0.760	0.86
37	1.12	5.5	0	5	-0.385	0	-1.174	-1	0.66
38	1.12	5.5	1.4	5	-0.385	0	-1.052	-1	0.66
39	1.12	5.5	3	5	-0.385	0	-0.913	-1	0.65
40	1.12	5.5	24.6	24	-0.385	0	0.968	0.267	0.81
41	1.12	5.5	25	30	-0.385	0	1	0.667	0.83

Table 5.3: Experimental plan and particle retention response.

The postulated model chosen to estimate the relationship between the set of controllable experimental factors (x_i) and particle retention results, was a second–degree polynomial expressed as follows:

$$Y = b_0 + \sum_{i=1}^{4} b_i x_i + \sum_{i=1}^{4} b_{ii} x_i^2 + \sum \sum_{i<j=2}^{4} b_{ij} x_i x_j + \varepsilon$$

where Y is the predicted response, ε is the random error, normally distributed and b_0, b_i, b_{ii} and b_{ij} are the mean value (in the center of the domain), main effect term coefficient, quadratic effect term coefficient and interaction effect between factors coefficient respectively. The model proposed for the response, by substituting the four variables, contains 15 coefficients. Additionally a set of 13 experiments has been performed in order to test the accuracy of the model predictions.

5.2.5 Statistical analysis

In the present investigation, the software NemrodW was used for regression analysis of the data obtained, the estimation of the coefficients of the regression equation, model validation, as well as response fitting as surface plots. Model coefficients were estimated using the least squares method. The fit of the regression model was checked by the coefficient of determination (R^2 and R^2_{adj}). The significance of each coefficient was determined using the Student *t*–test and *p*–value, while the statistical significance of the model was determined by the application of the Fischer–Snedecor *F*–test (Goupy, 1999).

5.3 Results and discussion

5.3.1 Experimentation

Response surface analysis uses multiple regression and correlation analysis tools in order to examine the influence of the four independent factors on retention. All 31 sets of experiments were carried out according to the experimental matrix and the retention measured during bead perfusion simulations as described in the materials and methods. The response (retention) of all experiments is shown in Table 5.3. Some of the 31 responses are figured below, in order to have an approximate representation of the response variation within the experimental domain.

In Figure 5.2 are represented the results obtained during the experiments with a porosity filter factor equal to 1.39. It can be seen that retention is low at low filter acceleration and increases as the filter acceleration increases. The perfusion capacity also influences retention and its influence is stronger at low filter acceleration. The particle

concentration also has an influence on open filter retention. By increasing the particle concentration, the retention increases.

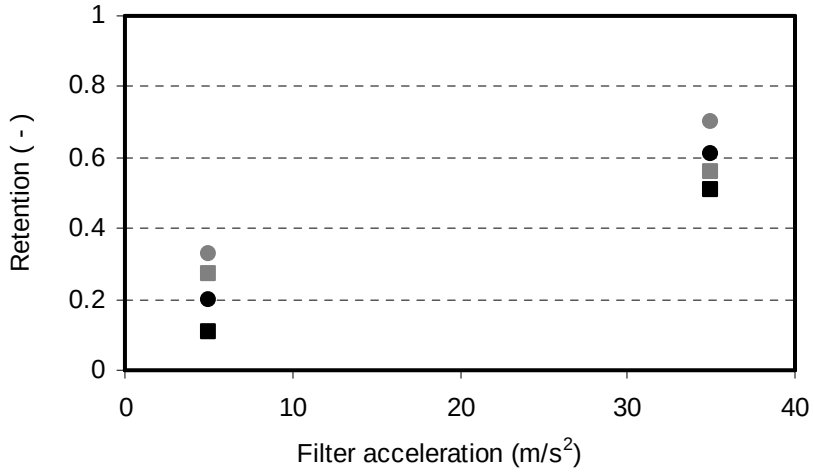

Figure 5.2: Retention versus filter acceleration for different particle concentrations and perfusion capacities, at ε = 1.39. ■ 1·10E^6 particle/ ml and 2 cm/h, ■ 1·10E^6 particle/ ml and 25 cm/h, ● 1·10E^7 particle/ ml and 2 cm/h, ● 1·10E^7 particle/ ml and 25 cm/h.

The same retention tendency is observed for a filter porosity of 1.12, as represented in Figure 5.3.

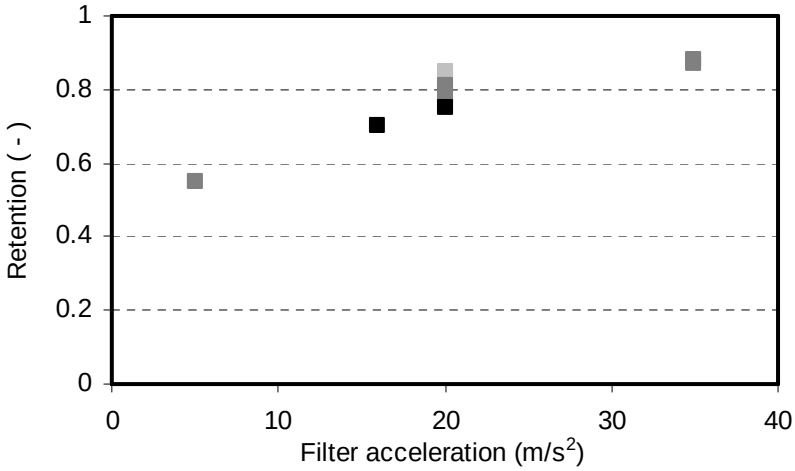

Figure 5.3: Retention versus filter acceleration for different perfusion capacities, at 5.5·10^6 particle/ ml and at ε = 1.12. ■ 2 cm/h, ■ 13.5 cm/h, and ■ 25 cm/h.

In Figure 5.3, we observe that retention increases with an increase of filter acceleration and tends to reach a plateau at filter accelerations above 30 m/s^2. The influence of perfusion capacity is less pronounced than for more open filter pore sizes.

Retention is better for ε =1.12 (Figure 5.3) than for ε =1.39 at identical conditions (Figure 5.2). The plateau reached is higher, since the pores are smaller and permit better particle retention. At higher filter pore sizes the particle retention may be improved by increasing the filter acceleration.

5.3.2 Model validation

Model quality checking is to identify if the model can describe reasonably well the response within the experimental plan. This is based mainly on analysis of variance, as well as analysis of residuals and statistical test validation.

In order to fit the quadratic polynomial model for particle retention the multiple regression coefficients were estimated (Table 5.4A) by employing the least squares technique (Myers and Montgomery, 1995). The R^2 and R^2_{adj} coefficients have been determined in order to test the precision of fit of the regression equation. A R^2 coefficient of 0.9759 was obtained that implies that there is about 98% reduction in the variability of the response obtained by using the model. A R^2_{adj} of 0.9548 was obtained, which is close to 1 and indicates that there is a high correlation between the observed and the predicted values and so the model explains more than 95% of the variability in new data.

	Value	Std. error	*t*-test	*p*-value	Value
$\mathbf{b_0}$	0.6693	0.0169	39.61	<0.0001	0.6721
$\mathbf{b_1}$	-0.2726	0.0111	-24.66	<0.0001	-0.2728
$\mathbf{b_2}$	0.0433	0.0104	4.16	0.0003	0.0417
$\mathbf{b_3}$	-0.033	0.0100	-3.32	0.0027	-0.0337
$\mathbf{b_4}$	0.1224	0.0104	11.75	<0.0001	0.1217
$\mathbf{b_{11}}$	0.0672	0.0227	2.96	0.0065	0.0647
$\mathbf{b_{22}}$	-0.0008	0.0197	-0.04	0.9680	0
$\mathbf{b_{33}}$	0.0045	0.0190	0.24	0.8149	0
$\mathbf{b_{44}}$	-0.0561	0.0219	-2.56	0.0166	-0.0529
$\mathbf{b_{12}}$	0.0048	0.0120	0.40	0.6913	0
$\mathbf{b_{13}}$	-0.0234	0.0120	-1.96	0.0613	-0.023
$\mathbf{b_{23}}$	0.0045	0.0117	0.39	0.7033	0
$\mathbf{b_{14}}$	0.0732	0.0120	6.08	<0.0001	0.0735
$\mathbf{b_{24}}$	-0.0048	0.0116	-0.41	0.6830	0
$\mathbf{b_{34}}$	0.0056	0.0113	0.49	0.6258	0

Table 5.4: Values and significance of regression coefficients (A) and coefficient values after model simplification (B).

The number of experiments being greater than the number of the model coefficients implies that the difference between the experimental and the calculated response gives rise to residuals. If the model is well represented, the difference between the experimental and the calculated value is only due to experimental error. During the experimental plan construction, two points have been repeated that give information on the experimental error. The null hypothesis is that the lack of fit (model adjustment variance) and the pure error (experimental variance) are identical and was tested by the application of an *F*–test from Fisher–Snedecor, representing the comparison of the two variances. Critical F_0–value at a significance level of 10% is equal to 9.42, which is lower than the *F*–value obtained of 13.55 and thus the null hypothesis is accepted with a risk of less than 10% (Table 5.5). Therefore, the quadratic model is adequate and there is a statistically insignificant lack of fit. The error of adjustment is accepted to be comparable to the error of the measured responses and the model was thus proven to be adequate for prediction of particle retention within the range of parameters employed.

	Sum of squares	Deg. of freedom	Mean square	***F* -value**
Residual	0.04792	16	0.00299	
Lack of fit	0.04742	14	0.00339	**13.55**
Pure error	0.00050	2	0.00025	

$R^2 = 0.9759$, $R^2_{adj} = 0.9548$

Table 5.5 Mean square of variations of adjustment and *F*–value for the 31 experiments

In addition to the experimental domain, 13 experiments have been performed prior to this study and the model validation has been investigated by considering all these experimental points. The functions of error of predictions were less than 1 for only 10 experiments, thereby indicating that the precision of the predicted responses is better than compared to the measured responses only for these 10 experiments that were considered for model validation. On the basis of the *F*–value of 10.65, the null hypothesis is accepted with a risk less than 10% (F_0–value at significant level of 10% is equal to 9.37). The retention of the 10 experiments is well represented by the model that shows insignificant lack of fit and validated the accuracy of the model predictions.

All of the 41 experimental points are taken in consideration for estimation of model coefficients. R^2_{adj} of 0.9535 indicates that the model explains more than 95% of the

variability in new data. Critical F_0–value at significance level of 10% is equal to 9.44, which is lower than the *F*–value of 10.47 (Table 5.6).

	Sum of squares	Deg. of freedom	Mean square	***F* -value**
Residual	0.06333	26	0.00244	
Lack of fit	0.06283	24	0.00262	**10.47**
Pure error	0.00050	2	0.00025	

$R^2 = 0.9698$, $R^2_{adj} = 0.9535$

Table 5.6: Mean square of variations of adjustment and *F*–value for the 41 experiments

The null hypothesis is thus accepted with a risk less than 10%. The *F*–value of 10.47 with 24 and 2 degrees of freedom corresponds exactly to a probability of 9.1% of making a mistake in rejecting the assumption that the adjustment variance is similar compared to the experimental variance, when it is in fact true. This probability obtained by considering all 41 experiments is greater than those obtained by considering the first 31 experiments (7.1%) and is mainly due to the increase of the degree of freedom. The variance of adjustment is only due to the experimental error and the postulated model is therefore accepted for particle retention prediction within the range of parameters employed.

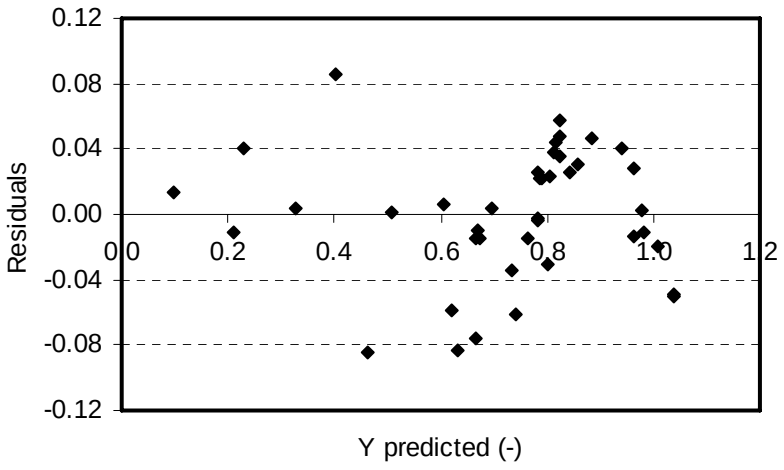

Figure 5.4: Analysis of residuals.

Since the residuals are only due to the experimental value, we can analyze their distribution as a function of the predicted response in order to check the model adequacy (Figure 5.4). The response seems to be randomly scattered and thus the variance of the

original observation is constant for all values of the response. The lack of dependency between the residuals and the predicted response implies that the second–degree polynomial model represents well the results of the experimental plan.

5.3.3 Model simplification

The significance of each coefficient was represented by the *p*–value from the Student *t*–test (Table 5.4A). The coefficients b_1 and b_4, related to filter porosity and filter acceleration terms respectively have the largest *t*–test value and thus the largest effect, followed by the interaction effect of filter porosity and filter acceleration (b_{14}). The linear terms of particle concentration (b_2) and perfusion capacity (b_3) follow, as well as the quadratic terms of porosity (b_{11}) and acceleration (b_{44}). The other terms are less significant with the corresponding *p*–values being greater. Advanced modeling was carried out for model reduction and elimination of terms that are not significant without altering the statistical hierarchy. A backward elimination method has been used, starting with the full model and removing one by one each coefficient, the significance of which was shown to be low with respect to the *p*–value. Six less significant coefficients have been removed from the model, in the order b_{22}, b_{33}, b_{23}, b_{12}, b_{24} and b_{34}. At each step, R^2, R^2_{adj} were calculated as statistical indicators and the regression coefficients have been re–estimated after model refinement (Table 5.4B) and the general expression of predicted retention is finally expressed as follows:

$$R = 0.6721 - 0.2728x_1 + 0.0417x_2 - 0.0337x_3 + 0.1217x_4 + 0.0647x_1^2 - 0.0529x_4^2 - 0.023x_1x_3 + 0.0735x_1x_4$$

The R^2 coefficient was estimated and corresponded to 0.9688, a value slightly lower than those obtained with the full model, which equaled to 0.9698. However the reduction in the variability of the response obtained by using the refined model is acceptable. On the basis of the *F*–value, the null hypothesis was accepted with a risk of 10.9% (Table 5.7), a value slightly higher than the 9.1% obtained for the full model. The quality of prediction of the refined model has decreased, but the risk is still low and the error of adjustment has been accepted to be comparable to the error of the measured responses and the simplified model was thus proven to be adequate for prediction of particle retention within the range of parameters employed.

	Sum of squares	Deg. of freedom	Mean square	***F* -value**
Residual	0.06532	32	0.00204	
Lack of fit	0.06482	30	0.00216	**8.64**
Pure error	0.00050	2	0.00025	

$R^2 = 0.9688$, $R^2_{adj} = 0.9610$

Table 5.7: Mean square of variations of adjustment and *F*–value for the modified model.

The form of the model response surface depends on the signs and magnitudes of the model coefficients and is illustrated in three dimensions, in Figure 5.5, where the response surface of particle retention is plotted versus the most influential parameters: filter porosity and filter acceleration. At fixed filter porosity and particle concentration, the model predicts the optimal filter acceleration that has to be applied at any operation scale (perfusion rate), in order to reach maximal particle retention.

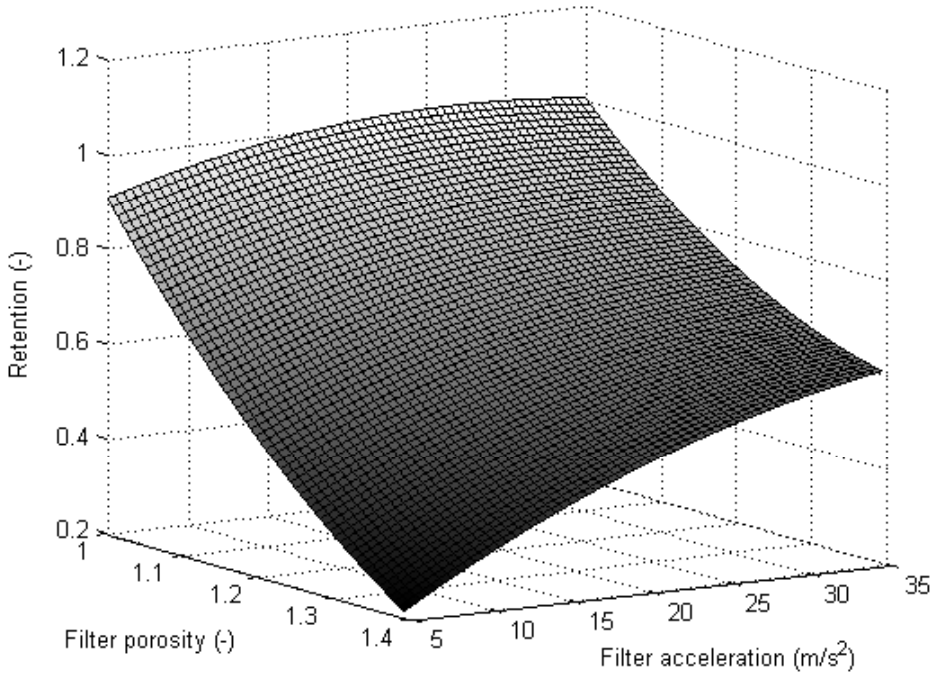

Figure 5.5: Retention surface response, at $5.5 \cdot 10^6$ part/ml and 13.5 cm/h.

5.3.4 Model verification

In order to validate the model to animal cells, two perfusion cultures were carried out using two different spin–filters, which have pore sizes (14.5 and 18 μm) greater than the mean cell diameter. The filter porosity ε of the first filter was equal to 1.21 and the second was equal to 1.5, relative to the mean cell diameter (12 μm). A filter acceleration of 35 m/s^2 was applied which, according to the model, corresponds to the maximum retention that could be obtained for this filter pore size. If the cell retention obtained for these perfusions is compared with particle retention predicted by the model, for actual changing operational conditions during the culture (cell concentration and perfusion flow), the results represented in Figures 5.6 and 5.7 are obtained.

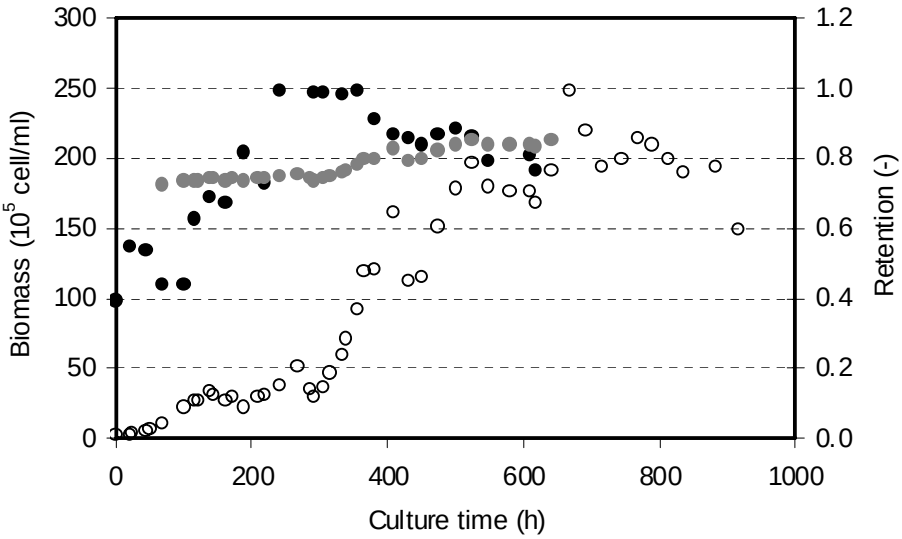

Figure 5.6: Retention model verification for filter porosity equal to 1.21. ● Predicted and ● measured retention, ❍ Viable CHO cell concentration (10^5 cell/ml).

Similar cell retention profiles were observed, in which there is a first phase during which the measured retention is low because the system had not reached steady state. Indeed, the changing sampling and perfusion rate influenced the measurement of the retention. This period corresponded to low cell density, with the difference between the measured and the predicted retention mainly due to non–steady state conditions, which lowered retention and prevented an increase of cell density due to cell leakage through the filter.

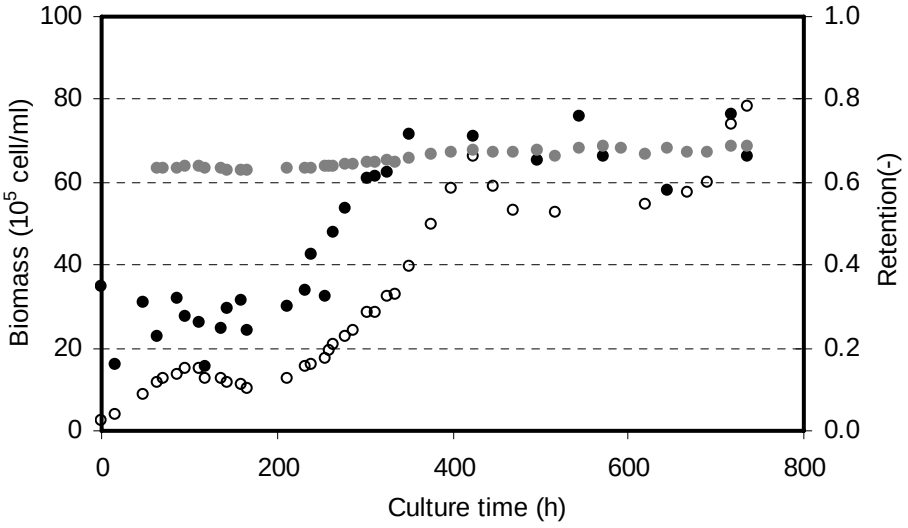

Figure 5.7: Retention model verification for filter porosity equal to 1.5. ● Predicted and ● measured retention, ❍ Viable CHO cell concentration (10^5 cell/ml).

Then a second phase followed, which corresponded to an increase of cell retention. The measured retention increased, even above the predicted level to reach 100% cell retention for the filter with a porosity equal to 1.21 (Figure 5.6) and 70% for a filter of porosity 1.5 (Figure 5.7). The high retention level of 100% was due to swelling of cells, observed microscopically. Substrate and principle metabolite concentrations for cultures performed with the filter having a porosity equal to 1.21, have been measured (Figures 5.8 and 5.9).

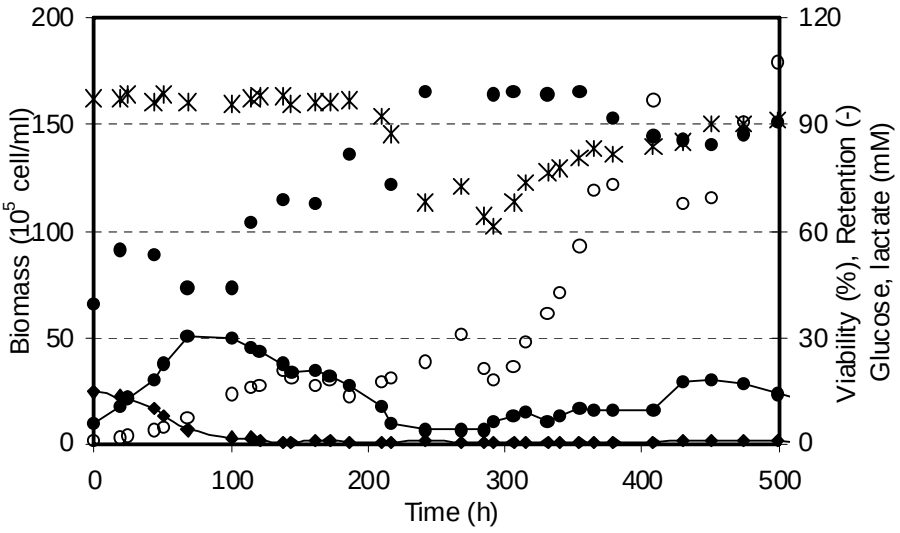

Figure 5.8: CHO *SSF3* perfusion culture for spin–filter porosity of 1.21. ❍ Biomass, ∗ Viability, ● Cell retention, –◆– Glucose and –●– Lactate.

High cell retention levels of 100% were revealed to correspond to a reduction in cell viability (Figure 5.8). Glucose concentration was almost zero for the entire culture, which indicated that the cell culture was glucose–limited. In the region where the viability started to drop, from 200 to 400 h, lactate concentration was very low (< 10 mM), having dropped from a maximum value of 30 mM at 80 h to stabilize at a value of 4 mM at 200 h during which time the viability dropped. Considering that almost all lactate produced takes place during glycolysis via pyruvate formation and that the initial glucose concentration in the feed medium was 16 mM, a maximum theoretical yield from glucose of 32 mM lactate could have been formed. However, such lactate concentrations are not achieved, which confirmed the hypothesis that the cell culture is glucose–limited.

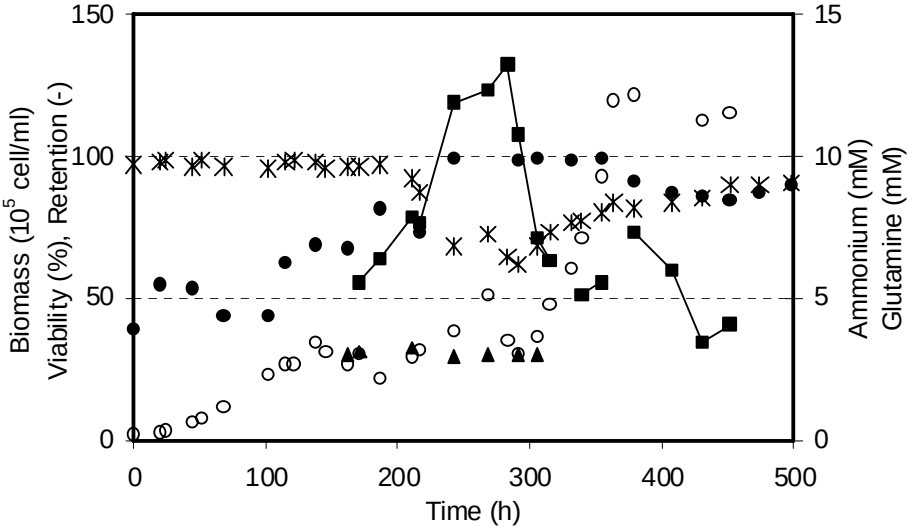

Figure 5.9: CHO *SSF3* perfusion culture for spin–filter porosity of 1.21. ❍ Biomass, ∗ Viability, ● Cell retention, ▲ Glutamine and –■– Ammonium.

From 200 to 400 h, the glutamine concentration was constant at a level of about 3 mM (Figure 5.9), which means that cell growth was not limited by glutamine. However, the concentration of ammonium released into the medium was variable. The decrease in viability appeared to correlate to an increase in ammonium concentration, which can be explained by a change in cell metabolism (with a higher rate of amino acids consumption) due to glucose–limitation. Viability started to drop when the ammonium level rose above 7 mM. Kurano et al. (1990) observed a reduction in cell growth during CHO cell culture for ammonium concentrations above 8 mM, a value which is similar to that found in the present study using CHO *SSF3* cells. These results suggest that toxic levels of ammonia were probably responsible for the decrease in cell viability, as well as swelling of the cells,

which resulted in cell retention values being higher than those predicted theoretically. In order to confirm this hypothesis, an additional culture was carried out under limited cell growth conditions and cell size as well as size distribution were determined (see section 5.4).

Finally a third phase occurred which corresponded to a quasi–steady state, during which the measured retention decreased as a result of the cell size decreasing due to attainment of non–limiting growth conditions. The measured retention become constant at a value which correlates well with that predicted by the model, namely 85% and 67% for a filter porosity of 1.21 and 1.5 respectively. During CHO cell perfusion cultures with a filter porosity of 1.21, the viable cell concentration reached $2 \cdot 10^7$ cell/ml, a value that is outside the experimental domain (from $1 \cdot 10^6$ to $1 \cdot 10^7$ cell/ml) where the model was validated. However, the measured and the predicted values for cell retention seem to correlate even outside this domain. The suitability of the predictive model was thus effectively verified by the retention data measured during actual CHO cell cultures.

5.4 Cell swelling related to ammonium toxicity

The porosity of the spin–filter, in particular filter pore size, mean cell diameter and cell size distribution were revealed to influence cell retention. Thus the size of dead animal cells is reported to be below 10 μm, while for viable animal cells is in the range from 10–20 μm (Searles et al., 1994). Consequently, non–viable cells should pass through open filters (filter pore size greater than mean cell diameter) more readily and are removed continuously during spin–filter perfusion cultures, thereby enabling maintenance of a high cell viability. Changes in cell size during cell cultures also influences cell retention. Animal cells are extremely sensitive to changes in their environment, which may induce changes in cell physiology, including cell size, and result in cell death. In general, cell death may follow two distinct patterns: apoptosis and necrosis. The prevalent mode of cell death is apoptosis and occurs spontaneously in late exponential phase of batch cultures, during nutrient deprivation, high levels of shear stress or oxygen limitation (Mercille and Massie, 1994a, 1994b; Vives et al., 2003). Necrosis is mainly induced by accumulation of toxic metabolites or oxidative stress of cells (Al–Rubeai, 1998; Carini et al., 1999). Apoptosis is an active intrinsically controlled mechanism and is morphologically characterized by a reduction in cellular volume (Chen et al., 2003; Pläsier et al., 1999), whereas necrosis is a

passive phenomenon and induces cell swelling (Carini et al., 1999). The change of cell size has different impacts on cell retention during spin–filter perfusion culture. A decrease in cell size due to apoptosis induces a decrease in filter retention, which allows the elimination of apoptotic cells. On the other hand an increase in cell size during cell growth or during necrosis improves cell retention. The change of cell morphology is thus important during spin–filter perfusion culture and the model response could be influenced and thus prediction of cell retention changed.

An animal cell culture was performed in perfusion mode using a spin–filter with a porosity of 0.71 in order to study the change of cell morphology during limited cell growth. A first steady state was reached for a perfusion rate of 110 ml/h (1.6 vvd) at a stable cell concentration of $1.7 \cdot 10^7$ cell/ml, from 500 to 720 h of culture time (Figure 5.10).

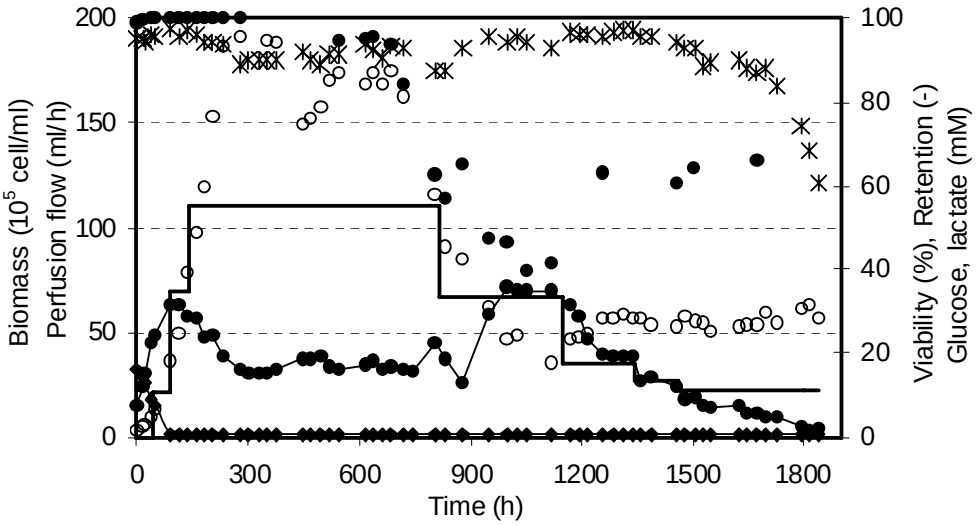

Figure 5.10: CHO *SSF3* perfusion culture for spin–filter porosity of 0.71. ❍ Biomass, ∗ Viability, ● Cell retention, **––** Perfusion flow, –◆– Glucose and –●– Lactate.

During this period the residual glucose concentration was less than 0.5 mM, which demonstrates that cells were glucose–limited, while a high lactate concentration of 18 mM was observed (Figure 5.11). The $Y_{lact/glucose}$ (the lactate yield with respect to glucose) was found to be 1.2–1.3 mol/mol (Figure 5.12), which is close to the value of 1.32 mol/mol found during glucose–limited continuous cultures of the same cell line and smaller than theoretical maximum value of 2 mol/mol, as a result of part of the glucose being converted to carbon dioxide and biomass (Ruffieux, 1998). The glutamine level throughout the culture remained above 3 mM (results not shown) and did not limit cell growth and high cell viability was maintained (higher than 95%).

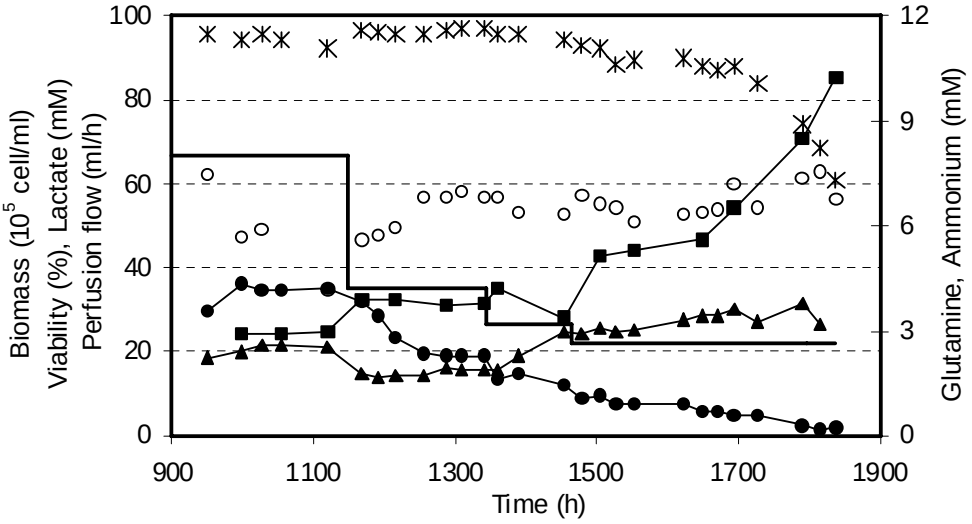

Figure 5.11: CHO *SSF3* perfusion culture for spin–filter porosity of 0.71. ❍ Biomass, ∗ Viability, **––** Perfusion flow, –▲– Glutamine, –●– Lactate and –■– Ammonium.

At 700 h, the spin–filter became mechanically damaged and cells were washed–out, resulting in a reduced total viable cell density. As a result the perfusion flow was decreased to 67 ml/h from 815 to 1150 h in order to recuperate the culture by avoiding cell wash–out. Despite this decease in flow rate the cell density continued to drop until finally stabilizing after 1000 h at a density of $4.7 \cdot 10^6$ cell/ml. It is generally accepted that the time necessary to reach a steady state for a continuous stirred bioreactor corresponds to 5τ (that is 5 times the reactor volume divided by the perfusion rate). From 1000 to 1150 h, the culture reached more than 5τ and was therefore considered to be in steady–state. Cell viability was stable at a high and constant level above 95%, in spite of the fact that residual glucose concentration was less than 0.15 mM. The data for residual substrate and metabolite concentrations (Figure 5.11) showed that the glutamine concentration remained above 2.5 mM and was not growth limiting, while the lactate concentration increased from 18 mM to a high stable level of 35 mM. These values indicate that the lactate yield ($Y_{lactate/glucose}$) increased to 2.4 mol/mol (Figure 5.12), a value which is 20% higher than the theoretical maximal yield. This suggests that amino acids other than glutamine were also metabolized to lactate. A low level of ammonia (3 mM) was observed that appeared not to inhibit cell growth. Cell growth seemed not to be nutrient–limited at a feed rate of 67 ml/h for a cell concentration of $4.7 \cdot 10^6$ cell/ml, as a result the perfusion rate was further decreased to 35 ml/h. Under these conditions a second steady state was reached at a cell concentration of $5.5 \cdot 10^6$ cell/ml from 1150 to 1340 h of culture time.

During this third steady state, viability remained above 95%. The lactate concentration decreased from 35 mM to 19 mM, which is the level reached during the first steady state (110 ml/h) and $Y_{lactate/glucose}$ attained a level of 1.2 mol/mol, as obtained previously. Glutamine was consumed, the concentration decreasing from 2.5 mM to 1.9 mM resulting in the ammonium concentration rising to 3.9 mM. The perfusion rate was further decreased to 27 ml/h during the period 1340 to 1460 h and was accompanied by a fall in lactate concentration and $Y_{lactate/glucose}$ to a value of less than 1.2 mol/mol, and the culture appeared to become glucose–limited. Perfusion flow was further decreased to 22 ml/h. As a result lactate concentration continued to decrease from 1460 h until it reached zero at 1840 h. This duration (380 h) corresponds exactly to 5τ and suggests that lactate was no longer produced from glucose and amino acids but was simply washed–out. This also suggests that cell metabolism changed and complete glucose oxidation could be achieved. However, during this time glutamine consumption also decreased and a high ammonium production was observed, suggesting that amino acids other than glutamine were consumed. A high ammonium concentration (10 mM) was reached, which is a value reported to be toxic to animal cells (Ozturk et al., 1992). The cells appeared to switch metabolism due to lack of glucose, while cell starvation was also observed as a result of the reduced viability (< 90%) from 1530 h of culture time (Figure 5.11).

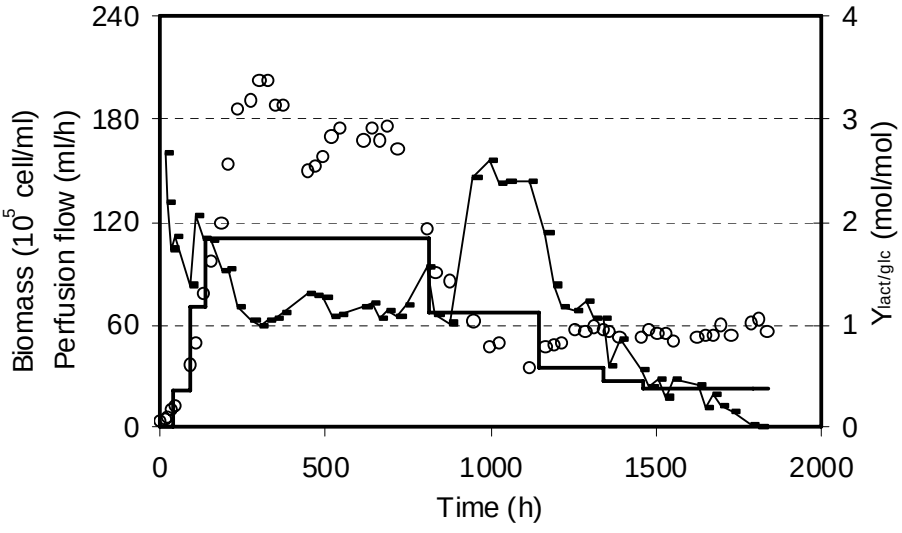

Figure 5.12: CHO *SSF3* perfusion culture for a spin–filter porosity of 0.71. ❍ Biomass, –– Perfusion flow and –––– $Y_{lactate/glucose}$ (mol/mol).

During this study, the CHO *SSF3* cell diameter and size distribution were measured (Figure 5.13). The distribution of cell size at 1000 h of culture time was compared to the

size distribution throughout the culture. At 1000 h the mean cell diameter was 12 μm, which corresponds to the mean cell size of a typical batch culture of CHO *SSF3* cells, during the exponential growth phase. Cell size distribution at 1310 h was found to be similar to that measured throughout the first 1000 hours of the culture (Figure 5.13A).

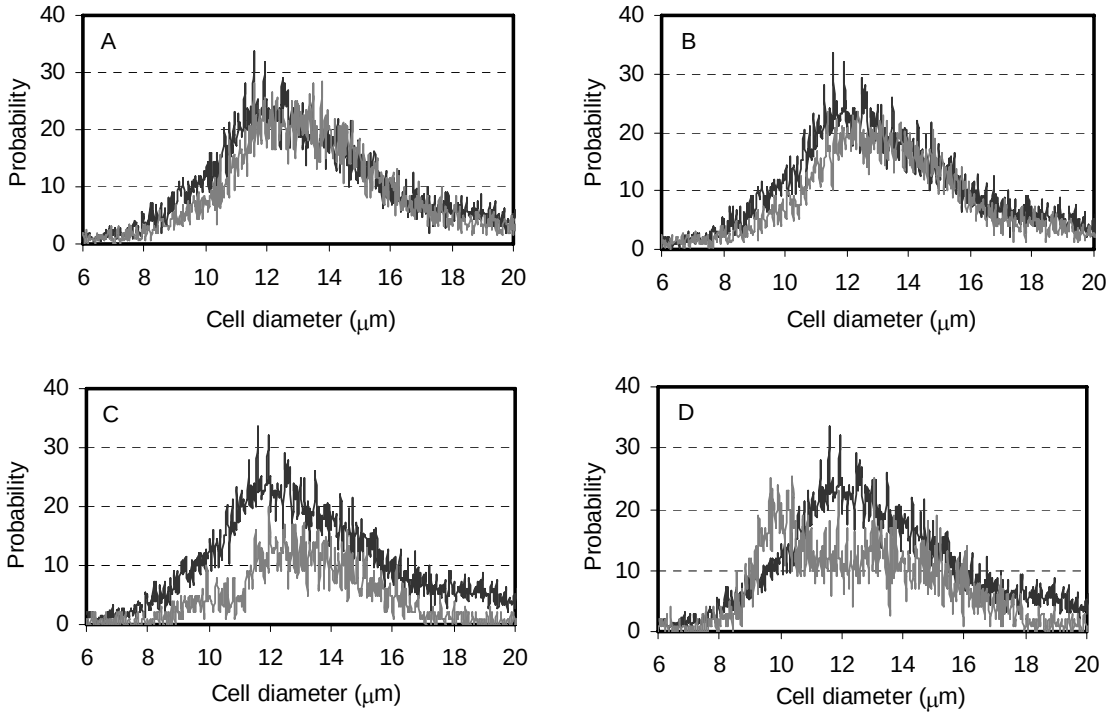

Figure 5.13: Cell diameter distribution during a CHO *SSF3* perfusion culture using a spin–filter porosity of 0.71 at different culture time: **––** 1000, ‒‒ **A**: 1310 h, **B**: 1480 h, **C**: 1730 h and **D**: 1840 h.

At 1480 h the diameter of the cells began to increase from a mean cell diameter of 12 μm to 12.5 μm. This state corresponds to the beginning of the last perfusion flow setting (22 ml/h), during which cell metabolism shifted and the ammonium concentration started to increase. After 1730 h of culture, growth became increasingly limited due to cell starvation and the ammonium concentration reaching 7 mM. This was accompanied by an increase in mean cell size from 12 to 14 μm. From 1840 h, the viability dropped to 60%, the ammonium concentration attained 10 mM and the cell diameter increased to an average of 15 μm. Non–viable cells, with a size range from 9 to 10 μm, were also commonly measured and their rate largely increased after 1730 h of culture (Figure 5.13). Glucose depletion during the culture resulted in a drop in viability, however this limitation also resulted in an altered metabolism with amino acid consumption, other than glutamine, playing an important role. This shift in metabolism is accompanied by an increase in ammonium concentration to high levels (>10 mM), and is in accordance with the

decreased ammonia yield from glutamine as a result of increased ammonia levels (Ozturk et al., 1992). Swelling of cells was observed after 1480 h and appears to be directly correlated with the increase of ammonia concentration to levels above 6 mM. The levels of ammonia, which exert a toxic effect on cell growth, are dependent on the cell line (Schneider et al., 1996). Kurano et al. (1990) observed a reduction in growth rate and maximum cell density for a CHO cell line at ammonium concentrations above 8 mM. During this culture, cell swelling due to ammonium accumulation above 6 mM was clearly demonstrated.

While the model developed to predict spin–filter operation is essentially valid an increase of cell size, due to cell necrosis is not a problem, since it actually improves cell retention and allows even higher cell concentrations to be attained. In addition, the decrease in cell size resulting from apoptosis means that cells are not retained, with the result that the retained cells have a high viability.

5.5 Conclusions

The application of response surface methodology enabled the formulation of a suitable model, from the experimental data, in order to predict the effects of four parameters: particle concentration, filter porosity, filter acceleration and perfusion capacity, on particle retention. The model is limited by boundary conditions and validity outside of the experimental domain is not guaranteed. The model is a second order polynomial and has been based on a modified central composite design of 41 sets of experiments. Since the model has shown the lack of fit to be insignificant, retention could be explained by the regression equation and the model was found to be suitable for prediction within the range of variables employed. From the *p*–values of Student *t*–tests, the coefficients of filter porosity and filter acceleration were revealed to be the most significant in the particle retention mechanism. The interaction of the latter was also significant, followed by the linear terms of particle concentration, perfusion capacity and the quadratic terms for filter porosity and filter acceleration.

The predictions provided by the model were confirmed by two CHO *SSF3* animal cell perfusion cultures carried out with two different spin–filter pore sizes. The two cell perfusions demonstrated that the model predicts very well the retention of cells as a function of the four parameters. Despite a filter pore size greater than the cell diameter

high retention, as related by the model prediction, has been achieved by applying a high filter acceleration. This allowed a high cell density of $2 \cdot 10^7$ cell/ml in 21 days, to be attained. Glucose–limited growth resulted in ammonia accumulation, which induces cell swelling that had a positive effect on cell retention by the spin–filter due to an increase in the filter porosity factor.

Since the model has also been established for perfusion capacities applied at large scale operation, it is relatively easy to determine, for any animal cell size, which mean diameter varies from 12 to 15 μm, the filter acceleration that has to be applied for a given filter pore size, in order to obtain the desired maximal retention at any culture scale, since it was considered that filter acceleration conservation is the key for retention conservation from small to large scale.

Acknowledgment: Financial support from Serono Pharma SA (Fenil–sur–Corsier, Switzerland) is gratefully acknowledged.

References

Al–Rubeai, M., 1998. Apoptosis and cell culture technology. Adv Biochem Eng/Biotechnol 59:225.

Belfort, G., 1988. Membrane modules: comparison of different configurations using fluid mechanics. J Membrane Sci 35:245–270.

Carini, R., Autelli, R., Bellomo, G., Albano, E., 1999. Alterations of cell volume regulation in the development of hepatocyte necrosis. Exp Cell Res 248:280–293.

Chen, C., Chen, K., Yang, S.–T., 2003. Effects of three–dimensional culturing on osteosarcoma cells grown in a fibrous matrix: analyses of cell morphology, cell cycle and apoptosis. Biotechnol Progr 19:1574–1582.

Deo, Y.M., Mahadevan, M.D., Fuchs, R., 1996. Practical considerations in operation and scale–up of spin–filter based bioreactors for monoclonal antibody production. Biotechnol Progr 12:57–64.

Ducommun, P., Ruffieux, P.–A., Furter, M.–P., Marison, I., von Stockar, U., 2000. A new method for on–line measurement of the volumetric oxygen uptake rate in membrane aerated animal cell cultures. J Biotechnol 78(2): 139–147.

Favre, E., 1993. Constant Flow–Rate Filtration of Hybridoma Cells Suspensions. J Chem Technol Biot 58(2):107–112.

Favre, E., Thaler, T., 1992. An engineering analysis of a rotating sieves for hybridoma cell retention in stirred tank bioreactors. Cytotechnology 9:11–19.

Goupy, J., 1999. Plans d'expériences pour surfaces de réponse. Paris: Dunod. 409 p.

Heine, H., Biselli, M., Wandrey, C., 1999. High cell density cultivation of hybridoma cells: spin filter vs immobilized culture. In: A. Bernard et al., editor. Animal cell technology: Products from cells, cells as products: Kluwer Academic Publishers. p 83–85.

Iding, K., Lütkemeyer, D., Fraune, E., Gerlach, K., Lehmann, J., 2000. Influence of alterations in culture condition and changes in perfusion parameters on the retention performance of a 20 μm spinfilter during a perfusion cultivation of a recombinant CHO cell line in pilot scale. Cytotechnology 34:141–150.

Jan, D.C.–H., Emery, A.N., Al–Rubeai, M., 1992. Optimization of spin–filter performance in the intensive culture of suspended cells. In: Spier RE, Griffiths JB, MacDonald C, editors. Animal cell technology: developments, processes and products. Oxford: Butterworth–Heinemann. p 448–451.

Kurano, N., Leist, C., Messi, F., Kurano, S., Fiechter, A., 1990. Growth behaviour of Chinese hamster ovary cells in a compact loop bioreactor. 2. Effects of medium components and waste products. J Biotechnol 15:113–128.

Mercille, S., Massie, B., 1994a. Induction of apoptosis in nutrient–deprieved cultures of hybridoma cells. Biotechnol Bioeng 44:1140–1154.

Mercille, S., Massie, B., 1994b. Induction of apoptosis in oxygen–deprived cultures of hybridoma cells. Cytotechnology 15:117–128.

Myers, R.H., 1999. Response surface methodology – current status and future directions. J Qual Technol 31:30–44.

Myers, R.H., Montgomery, D.C., 1995. Response surface methodology – Process and product optimization using designed experiments. New York: Wiley, J. and sons. 700 p.

Ozturk, S.S., Riley, M.R., Palsson, B.O., 1992. Effects of ammonia and lactate on hybridoma growth, metabolism and antibody production. Biotechnol Bioeng 39:418–431.

Pläsier, B., Lloyd, D.R., Paul, G.C., Thomas, C.R., Al–Rubeai, M., 1999. Automatic image analysis for quantification of apoptosis in animal cell culture by annexin–V affinity assay. J Immunol Methods 229:81–95.

Ruffieux, P.–A., 1998. Détermination des flux métaboliques pour des cellules animales lors de cultures continues. Thesis n° 1875: Ecole Polytechnique Fédérale de Lausanne, Switzerland. 224 p.

Schneider, M., Marison, I., von Stockar, U., 1996. The importance of ammonia in mammalian cell culture. J Biotechnol 46:161–185.

Searles, J.A., Todd, P., Kompala, D.S., 1994. Viable cell recycle with an inclined settler in the perfusion culture of suspended recombinant chinese hamster ovary cells. Biotechnol Progr 10:198–206.

Siegel, U., Fenge, C., Fraune, E., 1991. Spin filter for continuous perfusion of suspension cells. In: Murakami H, Shirahata S, Tachibana H, editors. Animal Cell Technology: Basic and Applied Aspects. Fukuoka, Japan: Kluwer Academic Publishers. p 434–436.

Vives, J., Juanola, S., Cairo, J.J., Godia, F., 2003. Metabolic engineering of apoptosis in cultured animal cells: implications for the biotechnology industry. Metab Eng 5:124–132.

Yabannavar, V.M., Singh, V., Connelly, N.V., 1992. Mammalian cell retention in a spinfilter perfusion bioreactor. Biotechnol Bioeng 40:925–933.

Yabannavar, V.M., Singh, V., Connelly, N.V., 1994. Scaleup of spinfilter perfusion bioreactor for mammalian cell retention. Biotechnol Bioeng 43(2):159–164.

6

A study on the fouling of spin–filters for animal cell perfusion cultures

Abstract

The main limitation in the use of spin–filters during perfusion cultures of animal cells was revealed to be filter fouling. This phenomenon involves both cell–sieve interactions as well as cell growth on the filter surface. The former effect has been analysed in the present study during long–term perfusion simulations with CHO animal cells. It was demonstrated that at low filter acceleration, below 6.2 m/s^2, a high perfusion rate of 25 cm/h induced rapid filter pore clogging within 3 days, whereas increasing the filter acceleration to 25 m/s^2 increased filter longevity from 3 to 25 days, for filters with a pore size of 8.5 μm. Increasing the filter pore size to 14.5 μm improved filter longevity by 84% and revealed less viable and dead cell deposits on filter surface. However, filter longevity was revealed to be not necessarily dependent on cell deposits on the filter surface, which was found to be governed by the hydrodynamic forces around the filter, created by filter acceleration

and perfusion rate, as well as being dependent on filter pore size. In the second part of this study, ultrasonic technology was used to reduce filter fouling. Filter vibration, induced by a piezo actuator, improved filter longevity by 113% during CHO cells perfusion culture.

6.1 Introduction

Filter fouling is an extremely important phenomenon, which is often reported to limit culture duration and productivity and thus the use of spin–filters for animal cell perfusion cultures. Many studies have been carried out in order to understand and characterize fouling, from which it was found that it is influenced by many factors, such as filter pore size, perfusion flow rate, cell concentration, cell culture viability and filter rotation rate (Esclade et al., 1991; Favre and Thaler, 1992; Iding et al., 2000; Jan et al., 1992; Siegel et al., 1991).

The first efforts made to characterize the materials responsible for filter fouling, indicated that viable and dead cells, cell debris, proteins and mainly DNA, as well as a combination of these factors, play an important role (Esclade et al., 1991; Maiorella et al., 1991; Mercille et al., 1994). Two different families of filter materials have generally been used for spin–filter perfusion cultures, namely metallic and synthetic filters (Büntemeyer et al., 1994; Esclade et al., 1991). Metallic screens are usually made of stainless steel and have a positive surface charge density, whereas, synthetic screens generally have more neutral surface properties and are made mostly from polymeric ethylene–tetrafluoroethylene, polyamide, polypropylene or polytetrafluoroethylene materials (Avgerinos et al., 1990; Büntemeyer et al., 1994; Esclade et al., 1991). Since cells, proteins and DNA frequently have a net negative charge, adherence to synthetic screens is weaker than to metallic ones. Analysis of the filter deposits on fouled spin–filters revealed that protein and DNA adhesion is more important on metallic screens compared to polyamide ones (Esclade et al., 1991). Although, it seems that proteins are not directly responsible for filter fouling, they facilitate it by inducing cell and/or cellular debris adhesion to the filter screen. The addition of deoxyribonuclease I (DNAse I) to the culture medium was found to prevent the formation of aggregates and significantly reduce fouling of polycarbonate and hydrophilized polysulfone membranes during cross–flow and vortex flow filtration cultures (Mercille et al., 1994). Despite the advantages of using synthetic filters over metallic ones, the majority of published work involving perfusion cultures use

stainless steel filters. The reasons for this include the longer filter life, robustness, ease of construction, rigidity, ease of cleaning and sterilizing in place using acids, bases, detergents and steam compared with polymeric membranes.

The use of filters with small pore size would be expected to induce more rapid filter fouling than filters having pore sizes larger than the mean cell diameter due to higher overall porosity of the available filtration surface, however, to our knowledge, there are few, if any published results of long–term perfusion cultures operated with different filter pore sizes and porosities.

In the presence of cells, screen fouling was found to be primarily caused by interactions between the spin–filter screen and the cells. Such interactions are principally governed by the perfusion flow and the centrifugal force induced by filter rotation. It is a rapid process found to occur at a sharply defined limit for the perfusion rate at any given rotational filter velocity (Deo et al., 1996). Filter speed was not found to affect filtration duration up to a critical filter rotation value of 0.6 m/s, which is due to a dynamic equilibrium between surface colonization and cell removal due to filter rotation (Favre, 1993; Favre and Thaler, 1992). However, from studies of the influence of filter velocity on the tendency of a 25 μm pore size stainless steel spin–filter (pore size much larger than mean cell diameter) to fouling during perfusion cultures of NS–1 cells, it has been concluded that high filter rotation rates reduce the incidence of clogging but that they are of little use because of the associated high fluid exchange across the filter, which leads to high cell leakage (Yabannavar et al., 1992).

Cell concentration was shown, in certain studies, to be directly related to filter fouling. Increasing the cell concentration from 0.2 to 1.5 $\cdot 10^6$ cell/ml, during simulation of perfusion cultures of hybridoma cells resulted in an increase in the tendency of filters to fouling at high perfusion flows of 54 cm/h (Favre, 1993). Increasing the cell concentration further, by a factor of more than 2, from 4.9 to 10.6 $\cdot 10^6$ cell/ml, was reported to lead to a 2–fold decrease in the perfusion flux capacity, which indicates an increase in particle–screen interactions and thus an increase in the tendency of the filters to fouling (Deo et al., 1996). Additionally, high culture viability was shown to be important in increasing filter performance with respect to filter fouling (Fenge et al., 1991). Indeed, cell debris and DNA released during loss of cell viability tends to increase the attachment of cells to the filter surface (Esclade et al., 1991).

Studies on filter fouling to date have been carried out over short–term operation, and mainly concern the primary fouling phenomena due to interactions between cells and

the filter surface, and represent simulations at unrealistic perfusion rates. Since filter fouling is primary due to cell deposition on filter surfaces, which is governed by the hydrodynamic forces around the spin–filter, and then depends on cell colonization/growth on the filter surface, it clearly appears that it is a long–term phenomenon. No systematic characterization of filter fouling over long–term operation has been undertaken until now and, as a result, the main parameters that influence filter fouling remain unknown. For these reasons, the present study involves realistic spin–filter perfusion simulations carried out using CHO cells, in order to characterize filter fouling over long–term operation. Two different stainless steel filter pore sizes have been used. The first had pore size of 8.5 μm, which is considerable smaller than the mean cell diameter of 12 μm, whereas the second had a pore size of 14.5 μm. These filters were tested at filter rotation accelerations of 1, 6.2 and 25 m/s^2 and at two different perfusion rates of 2 and 25 cm/h, during perfusion simulations using CHO cells, at a constant cell density of $1 \cdot 10^6$ cell/ml.

Once it had been established which parameter influences filter fouling the most, a method was developed for reducing this phenomenon. This method consists in continuously vibrating the spin–filter through the use of a piezo–actuator placed on the filter support and that converts electrical energy into mechanical motion.

6.2 Materials and methods

6.2.1 Cell line and medium

The cell line used in this study is a recombinant CHO *SSF3* (Novartis, Basel, Switzerland) cell line, producing human secretary component (hSC), a component of dimeric IgA. The cell culture medium is a serum– and protein– free medium ChoMaster HP–1 (Cell Culture Technology, Zurich, Switzerland), supplemented with 5 mM glutamine, 5 mM asparagine, 1 mM leucine, 1 mM glutamic acid and 1 mM serine. The cell concentration immediately after inoculation was fixed at $2 \cdot 10^5$ cell/ml and cells were harvested upon reaching a maximal cell density of $1 \cdot 10^6$ cell/ml. During passaging the cells were maintained at 37 °C, under a humidified air atmosphere containing 5% CO_2.

6.2.2 Perfusion simulations

CHO *SSF3* animal cell perfusion simulations were performed using Spinner flask (Bellco Biotechnology, United States), as represented in Figure 6.1.

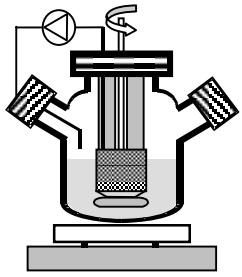

Figure 6.1: Experimental set–up during animal cell perfusion simulation.

The working volume was varied from 330 to 500 mL and cells were maintained in suspension by rotation of the spin–filter. The spin–filter support was purpose–built and made from PTFE. The open cylindrical support was assembled with a solid ring at the top, a conical shaped bottom and four vertical bars, in order to maximize the available filtration area. The spin–filter screen was made of stainless steel, and two different nominal pore sizes of 8.5 and 14.5 μm have been used (G. Bopp & Co. AG, Zurich, Switzerland). The filter external diameter was 50 mm and the wet height 15 mm. Baffles were placed inside the spin–filter in order to keep a homogenous particle suspension. A PTFE–coated magnetic stirrer was placed on the bottom of the filter support and set in motion at different agitation rates by placing the reactor on a magnetic stirrer. Spinner flasks were inoculated with 50% of the final working volume of fresh medium supplemented with 0.1% of Pluronic F–68 and 50 μg/ml of ampicillin and 50% of the volume of a cell suspension ($2 \cdot 10^6$ cell/ml), to give a cell concentration of $1 \cdot 10^6$ cell/ml. The Spinner flasks were then incubated at 28°C, under a humidified atmosphere containing 5% CO_2. Medium from inside the spin–filter was removed at two linear perfusion rates of 2 and 25 cm/h (ratio of perfusion flow to immersed filter surface) using a calibrated peristaltic pump (Alitea, Bioengineering, Wald, Switzerland) and returned to the flask in order to maintain the culture volume and cell concentration ($1 \cdot 10^6$ cell/ml) within the vessel, constant. Samples (1 ml) of cell suspension were collected daily from the Spinner vessel and from directly inside the spin–filter. Cell retention could then be calculated as $1–(c_{in,filter}/c_{out,filter})$, where $c_{in,filter}$ and $c_{out,filter}$ are cell concentrations inside and outside the spin–filter respectively. Glucose analysis was performed daily. When the glucose concentration dropped below

0.5 g/l, further glucose was added to the reactor to a concentration of 1 g/l. The whole cell suspension was replaced weekly with fresh cells in order to maintain cell viability above 95%. This process was repeated until fouling of the filter occurred, with the result that air started to circulate within the perfusion line.

6.2.3 Perfusion cultivation

Perfusion cultures of CHO *SSF3* cells were performed in a 2 L bioreactor (Bioengineering, Wald, CH) with a working volume of 1.65 L. The reactor was operated at a temperature of 37°C, under gentle agitation using a marine impeller of 5 cm in diameter, at 150 rpm. Bubble–free aeration was achieved by the use of 2 m of Teflon tubing (W. L. Gore & Associates GmbH, Putzbrunn, Germany). A controlled mass–flow meter system allowed the injection of a mixture of oxygen, nitrogen and carbon dioxide into the reactor via the Teflon tubing to maintain during the culture the dissolved oxygen concentration at 80% and CO_2 concentration at 5% saturation with respect to air. This system also allowed determination of the oxygen uptake rate on–line (Ducommun et al., 2000). The pH was maintained at a constant value of 7.2 by controlled addition of 0.1 M NaOH. For cell separation a stainless steel spin–filter was used with dimensions of 6.4 cm diameter and 2.5 cm immersion height. The spin–filter support was purpose–built and incorporated a piezoelectric vibration device to the base of the support as described in the next section. The filter pore size was 8.5 μm and the filter was motionless, unless otherwise specified. Medium was fed into the reactor using a peristaltic pump (Preciflow Lambda, Visperminen, Switzerland), while a second peristaltic pump (Preciflow Lambda, Visperminen, Switzerland) withdrew the perfusate from inside the spin–filter. Cell broth was removed continuously from the reactor at rates from 10 to 15% of the perfusion flow.

6.2.4 Piezoelectric filter set–up and working conditions

A Piezoelectric actuator type Pz27 (type soft PZT), used in this study was kindly supplied by Ferroperm Piezoceramics A/S (Kvistgaard, Denmark). It consists of a monolayer piezoelectric disk having a diameter 50 mm and 1 mm thick. A hole of 8 mm in diameter was laser cut in order to permit the passage of the axis. Each face of the

piezoactuator is covered with silver electrodes (screen printed and fired). The actuator is poled to provide the main displacement in radial mode (changing its diameter) when a difference of potential is applied. A 100V should create 0.85 μm change on its radius.

The PZT was glued on a thin disc support made of stainless steel, 64 mm in diameter and 0.2 mm thick using bi–component epoxy glue (Epsilon 2103, Abattech, La Chaux–de–Fond, Switzerland). Electrical contact (ground) between the support disk and the piezoactuator was ensured by four dots of electrically conductive epoxy silver glue (Epo–tek E4140, Polyscience AG–Cham, Switzerland). A cable was glued (using again silver epoxy glue) over the remained electrode (positive) to create a power line connecting the piezo actuator to a sliding electrical contact, placed over the reactor. This permits to test the setup in spin and ultrasonic mode. The positive electrode and connection was hence covered with a Polyurethane varnish (Urethan 71, Distrelec Schweiz AG, Switzerland) in order to avoid any short–circuit when immersed within the reactor, during perfusion cell culture. Finally a layer of silicon glue was added for the same purpose and also to avoid the contact between the culture and the chemical components as the varnish and epoxy glues.

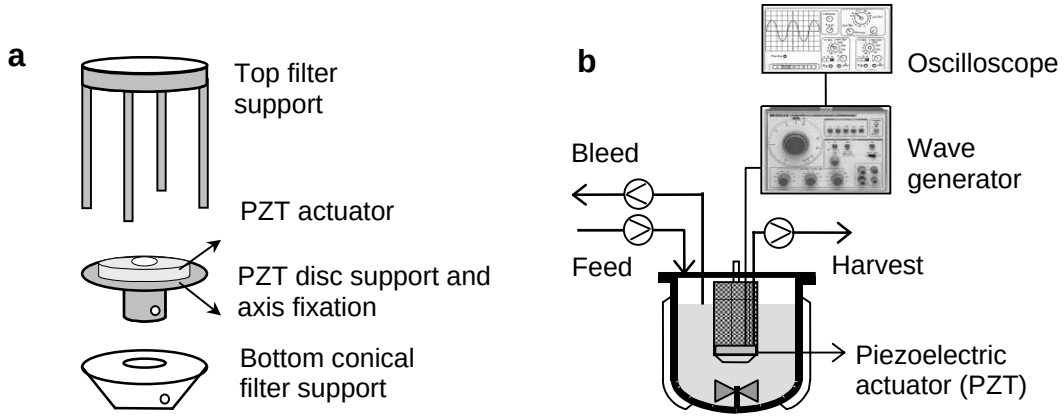

Figure 6.2: Piezoelectric filter set–up (**a**) and animal cell perfusion culture experimental set–up (**b**).

The disc with glued piezoactuator was then surrounded by a conical Teflon piece with dimensions of 64 mm in diameter and 15 mm in height and fixed on the filter axis (Figure 6.2 a). The filter support was glued on the top of the thin disc. It was assembled with a solid ring at the top and four thin vertical bars made in stainless steel.

During cell cultures, the piezoelectric actuator was connected to a sinusoidal wave generator (Dae Shin DOA–141, Rotronic, Switzerland) delivering a maximum potential of 10 V and which allowed frequency scanning. The signal was then amplified in order to

achieve amplitude of up to ±100 V (200 V_{pp}). The sinusoidal signal creates a radial expansion/contraction in the piezoactuator. As one of its faces (ground electrode) is firmly glued on the steel disk, part of the movement is constrained, crating a strain field that makes the piezoactuator and the plate to bend, crating an out of plane oscillatory movement (the vibrating filter). Changing the driving frequency, it is possible to amplify this oscillation, making the setup to work on one of its natural frequency. An oscilloscope (Tektronik TDS 2014, Servilec, Switzerland) was connected to the generator in order to accurately set the actuator working amplitude to 100V as well as frequency of the driving signal (Figure 6.2 b).

6.2.5 Biomass and metabolite analysis

Cell concentration was determined by counting the cells microscopically with a Neubauer hemocytometer. Viable and non–viable cells were distinguished using the Trypan blue extrusion method, whereas total cell counts were determined using the Crystal violet extrusion method.

Glucose concentrations were quantified by HPLC (1100 system, Agilent, Palo Alto, California, United States) analysis using a Supelco H column (Supelco, Bellefonte, Pittsburgh, United States), 0.02M H_2SO_4 as solvent and a refractive index detector (HP 1047A, Hewlett Packard GmbH, Waldbronn, Germany).

6.3 Results and discussion

6.3.1Filter fouling characterization

The main cause of fouling of spin–filters has been reported to be the result of cell–sieve interactions. This process is rapid and associated with defined limits for the perfusion rate at any rotational filter velocity. However, this limit exceeds largely the perfusion rates generally employed in perfusion cultures even at large–scale operation. The secondary cause of fouling appears to be the most important in perfusion cell cultures, and is a long process induced mainly by cell deposition by convection through the filter surface followed by cell adsorption to filter surface and cell growth. Many

parameters were identified as being responsible for such phenomena, including filter pore size, perfusion rate, filter velocity and cell concentration. The viability of the culture is also important since cell material, such as DNA, proteins and cell debris facilitate the attachment of cells to the filter surface.

In this study, fouling of spin–filters having pore sizes of 8.5 and 14.5 μm has been studied in the presence of CHO cells at fixed concentration of $1 \cdot 10^6$ cell/ml. The larger pore size of 14.5 μm does allow direct passage of cells through the filter, whereas the smaller pore size mesh does not. The fouling phenomenon could therefore be different, since the cells present within the filter of pore size greater than the mean cell diameter are subjected to the centrifugal force and may result in fouling of the filter from within. The filter velocity was varied from 0.2 to 0.8 m/s, corresponding to filter accelerations from 1 to 25 m/s^2, and for two different perfusion rates (2 and 25 cm/h) that correspond to the ratio of perfusion flow to wet filtration surface. These perfusion rates are realistic since they represent a perfusion rate of 6 vvd at both small–scale (filter radius, 3 cm) and large–scale (filter radius, 30 cm), where the spin–filter volume represents 20% of the working volume with an immersed filter height of 50% of the reactor height. These perfusion rates are dependent on the wet filter surface, which varies as a function of filter rotation rate. Indeed the greater the filter rotation, the smaller is height of liquid within the filter and thus the wet surface is reduced. In order to obtain the same perfusion rate for filters with different accelerations, the working volume was varied. For these reasons, the working volume of the culture, for spin–filter accelerations of 1 and 25 m/s^2, corresponded to 330 and 500 mL respectively, for a fixed wet filtration height of 1.5 cm. Subsequently the effect of each parameter was tested by sequential variation of the different parameters, with each experiment repeated in duplicate.

In order to quantify the deposition of viable and dead cells on the filter surface and to exclude the effect of cell growth, the CHO *SSF3* cells were cultured at 28°C, a temperature at which the cell growth rate approaches zero (Figure 6.3) and at which a viable cell concentration of $1 \cdot 10^6$ cell/ml could be maintained constant throughout the experiment. Fouling of the spin–filters resulted in cessation of permeate flux through the filter mesh with the result that the medium within the filter was completely removed and the wet filter height fall. When this occurred, the time taken for complete fouling was determined and the quantity of deposit on the filter determined by placing the filter in a solution containing 5 g/l of trypsin and 150 μg/ml of DNase in PBS 1%, for 1 h at 37°C under gentle agitation. The solution was then centrifuged and the pellet suspended in 2 ml

of cell medium in order to determine total cell counts. The surface protein coloration method (Ganesh et al., 2000) was then applied to the filter in order to verify, under UV light, that all biological material had been removed. The enzyme treatment of the filters was repeated until completely free of biological material.

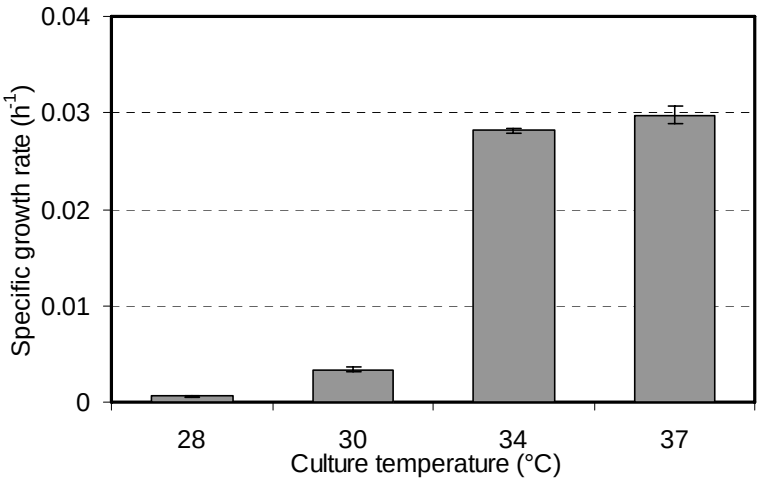

Figure 6.3: Specific growth rate of CHO *SSF3* cells at different culture temperatures.

6.3.1.1 Filter fouling (pore size 8.5 μm)

Cell perfusion simulations were initially carried out with spin–filters having a mean pore size of 8.5 μm at three different filter accelerations and for low and high perfusion rates (2 and 25 cm/h). The time taken until complete fouling of the filter corresponds to filter longevity. At a low perfusion rate of 2 cm/h, it was observed that the longevity of the filter increases with increasing filter acceleration from 1 to 6.2 m/s^2 (Figure 6.4). At low perfusion rates, the centrifugal effect appears to be more important than the perfusion effect. Indeed filter rotation washes cells from filter surface and a 44% increase in filter longevity, from 9 to 13 days, was observed. At higher perfusion rate of 25 cm/h, the centrifugal effect was weaker and filter longevity was unchanged. In spite of a high filter acceleration of 6.2 m/s^2 large quantities of cells approached the filter membrane due to the high perfusion rate of 25 cm/h, and filter fouling occurred rapidly. Indeed, filter longevity was considerably reduced to 3 days and was independent of the filter acceleration used. However, longevity could be improved by keeping the perfusion rate at a high level of 25 cm/h and increasing the filter acceleration to 25 m/s^2 (Figure 6.4). Under

these conditions the centrifugal effect was high enough to counteract the pumping effect caused by the perfusion flux, thereby lowering cell–filter interactions and increasing filter longevity from 3 to 25 days.

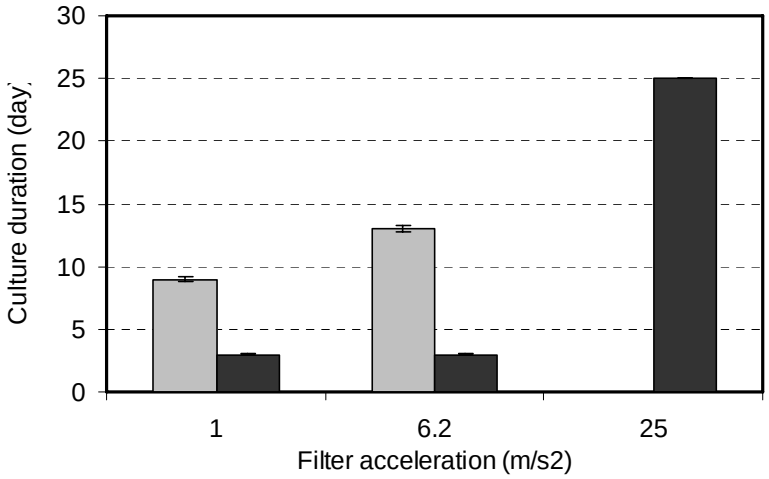

Figure 6.4: Duration of cultures with a spin–filter of mean pore size 8.5 μm as a function of filter acceleration during cell perfusion simulations at ■ 2 cm/h and ■ 25 cm/h.

The centrifugal effect appears to play an important role in reducing filter fouling and must be adapted as a function of perfusion rate employed. Thus in order to achieve long–term spin–filter cultures at high perfusion rates, the rate of rotation of the filter has to be as high as possible. However, there is a limit to this value, which is determined by the induced shear rate, above which cell disruption becomes significant.

Fouling of filters is related to clogging of pores due to cell deposition on filter surface. Cells are continuously deposited by the perfusion flow in such a way that pores are blocked and clarified medium can no longer pass through. Cell debris, and biological material released by dead cells, such as DNA and/or proteins, increase the tendency of filters to fouling and are considered to be not directly responsible for this phenomenon. This was confirmed by maintaining the viability of cultures constant above 95% in order that only fouling by whole cells could be determined. Furthermore viable and dead cells have been removed from the filter surface and quantified (Figure 6.5).

At low filter accelerations (1 m/s^2), it was observed that the filter longevity decreased when increasing the perfusion rate from 2 to 25 cm/h (Figure 6.4). This represents a rapid rate of filter fouling and should induce an increase of total cell deposit, which is indeed the case (Figure 6.5).

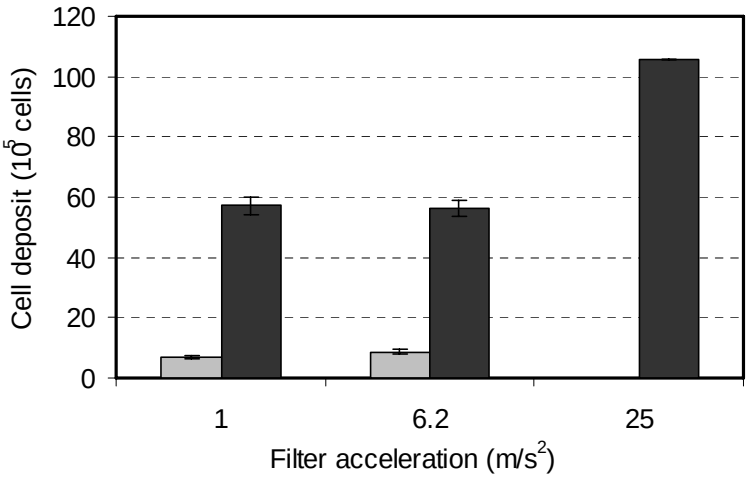

Figure 6.5: Quantification of cell deposit on the surface of a spin–filter with mean pore size of 8.5 μm as a function of filter acceleration during cell perfusion simulations at ■ 2 cm/h and ■ 25 cm/h.

Thus for a filter acceleration of 1 m/s^2, increasing the perfusion rate from 2 to 25 cm/h resulted in an increase in total cell deposit from $6.8 \cdot 10^5$ to $57.2 \cdot 10^5$ cells. At higher filter accelerations of 6.2 m/s^2, a similar phenomenon occurred, with cell deposits increasing from $8.7 \cdot 10^5$ to $56.3 \cdot 10^5$ cells. Considering that the total immersed filtration surface is equivalent to $2.36 \cdot 10^{-3}$ m^2 and that the projection surface of a spherical cell of 12 μm in diameter equals to $1.13 \cdot 10^{-10}$ m^2, the number of cells necessary to form a monolayer on the filter surface corresponds approximately to $2.09 \cdot 10^7$ cells. The open surface (pores) of the filter used represents a maximum of 5% of the total filter surface and thus the number of cells necessary to block the filter pores alone corresponds to approximately $1.04 \cdot 10^6$ cells. At low perfusion rates the cell deposits were below this critical value while at higher perfusion rates cell deposits were almost 6 times higher. This suggests that multi–layer cell deposits may form over a large part of the filter pores as well as over the metallic mesh.

Comparison of cell deposits on filters at a high perfusion rate of 25 cm/h indicates considerable similarities at both 1 m/s^2 and 6.2 m/s^2, which agrees with similar values for longevity of 3 days. As described earlier, filter centrifugation is not strong enough to counteract the perfusion rate and cells adhere to the filter surface, lowering filter longevity and thus culture duration. However, at a low perfusion rate of 2 cm/h, filter longevity varied as a function of filter acceleration increasing from 9 to 13 days, with cell deposition increasing from $6.8 \cdot 10^5$ to $8.7 \cdot 10^5$ cells, representing an increase of 28%, upon increasing the acceleration from 1 to 6.2 m/s^2. In spite of the fact that the filtration surface and pore

size were the same for both sets of experiment, it appears that filter fouling is not simply dependent on the available open filtration surface, otherwise the same level of cell deposit would be expected when complete filter fouling occurs. Thus clogging of filter pores appears to be dependent on the manner in which cells stick to the filter, that is governed by the forces acting on the filtration system. Increasing filter acceleration from 1 to 6.2 m/s^2, would be expected to eject cells more strongly from the filter surface and thereby reduce total cell deposit. However, in these experiments the cell deposit increased, that is probably due to the increase in culture duration. Similar results were observed by increasing filter acceleration to 25 m/s^2 for a 25 cm/h perfusion rate. In this case, filter longevity increased from 3 to 25 days and the final cell deposit increased from $56.3 \cdot 10^5$ to $105.4 \cdot 10^5$ cells. Thus the increase of culture time favoured cell attachment to the solid part of the filter mesh, without necessarily increasing cells deposition on the filter pores.

6.3.1.2 Filter fouling (pore size 14.5 μm)

Filters with pore sizes larger than the mean cell diameter would be expected to behave differently with respect to fouling. The larger available filtration surface would be expected to reduce the tendency to fouling and thus increase filter longevity. However, cells may pass through the filter, at a rate dependent on filter acceleration (see chapter 3). The presence of cells within the spin–filter may however influence filter clogging, due to centrifugal forces on the cells which have penetrated to within the filter, causing them to be expelled, and may as a result lead to filter fouling on the internal surface of the spin–filter. For these reasons cell perfusion simulations were performed with a spin–filter pore size of 14.5 μm at two different filter accelerations (6.2 and 25 m/s^2) and at low and high perfusion rates (2 and 25 cm/h).

At a high perfusion rate of 25 cm/h, the longevity of the filter with a mean pore size of 14.5 μm increased from 20 to 46 days when the filter acceleration was increased from 6.2 to 25 m/s^2 (Figure 6.6). As previously observed, the effect of acceleration appears to play an important role in reducing the tendency of the filters to clogging. Under these culture conditions, cell retention was 50% and 70% for filter accelerations of 6.2 m/s^2 and 25 m/s^2 respectively. The increase in longevity of the filter, in which cell retention corresponded to 70%, may be due to fewer cells passage through the filter as well as to a higher filter acceleration effect. However if we compare the filters with two different pore

sizes of 8.5 and 14.5 μm at the same filter acceleration, it can be seen that filter longevity is increased for the larger pore size filter (Figure 6.6). Cell passage through the larger pore size filter seems not to enhance filter clogging and the centrifugal effect appears to be the major factor controlling the tendency of filters to fouling. Increasing the filter pore size reduces filter clogging due to larger open surface, whereas cell passage has little influence on pore clogging on the internal filter surface, since the pores are continuously washed by the perfusion flow.

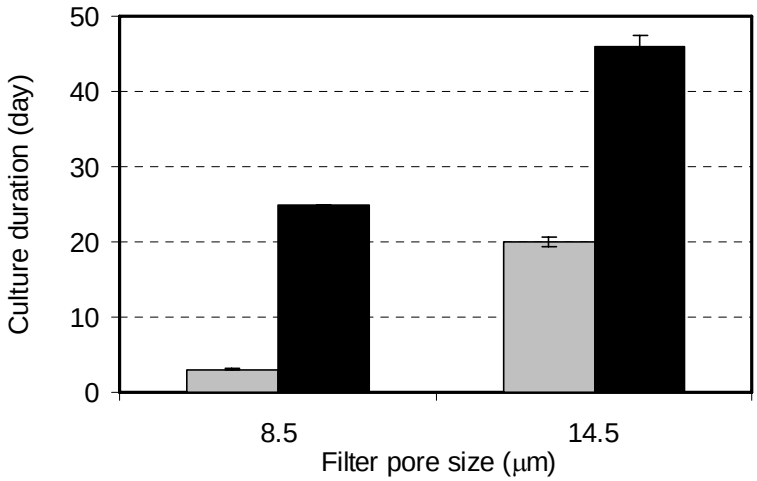

Figure 6.6: Duration of two spin–filter cultures with two different pore sizes, at 25 cm/h and at two different filter accelerations during cell perfusion simulations. ■ 6.2 m/s^2 and ■ 25 m/s^2.

Quantification of the filter deposits indicated that the amount of viable and dead cells increased from $27.9 \cdot 10^5$ to $98.1 \cdot 10^5$ cells when the filter acceleration was increased for a filter pore size of 14.5 μm, in a similar way to that observed for smaller pore size filters of 8.5 μm (Figure 6.7). An increase in filter acceleration delays filter clogging and cells appear to stick to the filter membrane differently. By comparing the two different filter pore sizes, it can be observed that there is a difference in cell deposits for the same filter acceleration. Thus, at 6.2 m/s^2 the deposit was composed of $56.3 \cdot 10^5$ and $27.9 \cdot 10^5$ cells for filters with pore size of 8.5 μm and 14.5 μm respectively. The metallic screens used in this study are made of stainless steel and have a positive surface charge density, whereas cell surface proteins are generally negatively charged. Cell adhesion should thus be facilitated on the solid filter membrane. However, this is counterbalanced by the reduced metallic surface available for cell adhesion for larger pore size filters (Figure 6.7). Additionally, the perfusion flow washes more efficiently the pores of filters with larger pore size and filter clogging is reduced. A similar phenomenon occurs at an acceleration of 25

m/s^2, where cell deposits for the 14.5 μm pore size filter is smaller than for the 8.5 μm pore size filter. However, the difference between the different pore size filters is less significant than previously, with the longer culture time being compensated by lesser available surface for cells to stick to.

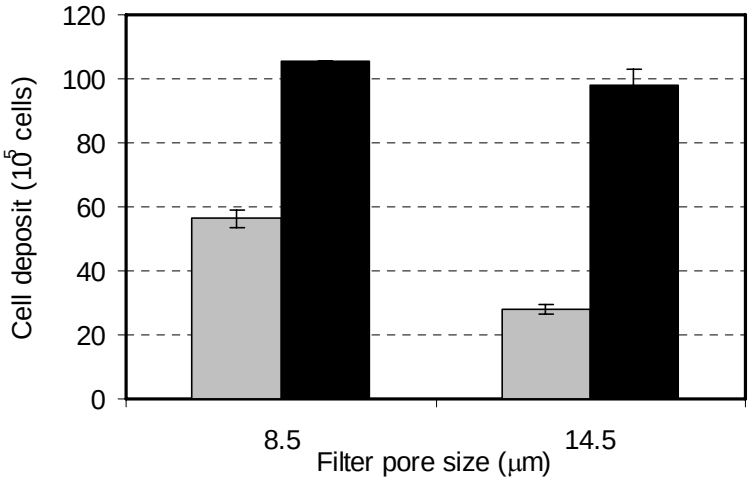

Figure 6.7: Quantification of cell deposit on spin–filters of different pore sizes at 25 cm/h and at two different filter accelerations during cell perfusion simulations. ■ 6.2 m/s^2 and ■ 25 m/s^2.

The importance of filter acceleration in pore clogging has been highlighted in the present study. During cell cultures, the use of high perfusion rates necessitates employing high filter accelerations and it has been shown that the use of larger pore size filters yields higher filter longevity. Viable and dead cells are deposited on the filter surface in different ways due to the different forces acting. Cell deposition on the filter surface does not necessarily affect filter performance in a negative way since, in spite of larger levels of cell deposit, higher filter longevity was observed and thus higher cell perfusion duration.

In the present study, cell growth on the filter surface was deliberately reduced by lowering the experimental temperature. Only cell–sieve interactions governed by filter acceleration and perfusion rate were considered since these were identified as the principle parameter affecting clogging of filter pores.

6.3.2 Method for reduction of filter fouling

The main limitation to the application of spin–filter systems for cell separation in perfusion cultures is the susceptibility to filter clogging. Shear generation at the liquid–filter

surface, through pulsation flow, vortex generation, back–washing or vibration techniques is therefore necessary to reduce this phenomenon (Gundogdu et al., 2003; Kobayashi et al., 2003; Lee and Lueptow, 2001; Najarian and Bellhouse, 1996). Pulsation flow and vortex generation techniques induce high shear rates, which may be harmful for mammalian cells, whereas back–washing methods interrupt the continuous filtration process. Vibration of the filter is a new method that has been developed mainly to remove fouling of ultrafiltration and microfiltration membranes during water treatment or protein recovery. Vibration may be generated using mechanical energy, such as a torsion spring system (Postlethwaite et al., 2004) or a shaking system (Gundogdu et al., 2003) or through ultrasonic (US) methods (Chai et al., 1998; Kobayashi et al., 2003). A US transducer placed within the water–bath containing the fouled membrane prevented fouling and improved separation rates at optimal US frequencies. The US frequency employed was in the range from 28–100 kHz and was similar on both sides of membrane, however the US intensity was reduced significantly by the membrane holder (Kobayashi et al., 2003). Ultrasonic systems have also been used as cell separation devices during continuous cell cultures (Woodside et al., 1998; Zhang et al., 1998). Vibrating piezo–electric ceramic transducers in response to an applied frequency and alternating voltage signal generates a standing wave field inside a separation chamber. The cells are rapidly trapped in the pressure node planes, where the pressure amplitude is zero and then aggregate at local maxima of the acoustic energy (Doblhoff–Dier et al., 1994; Kilburn et al., 1989; Pui et al., 1995), while medium, free of cells, is withdrawn. The frequency used in most separators is between 1 and 3 MHz, below this range cell cavitation may be induced, which results in local medium heating and cell disruption (Shirgaonkar et al., 2004).

In the present study, instead of transmitting the US vibration to the filter through the fluid medium, which would imply high–energy transmission and might induce cell disruption, the filter was directly vibrated using an US ceramic piezo–actuator (PZT). This piezo–actuator converts electrical energy into mechanical motion and the energy transmitted to the filter via the piezo–actuator is much smaller than that transmitted via the fluid. An evaluation of the reduction in fouling of spin–filters was carried out during CHO cell perfusion culture.

6.3.2.1 Effect of frequency scanning and transducer voltage on filter displacement/vibration

The ceramic piezo actuator was placed on the section part of the spin–filter support. When an electric voltage was applied to the piezo actuator, the ferroelectric ceramic dipoles increase their alignment proportional to the voltage and results in an expansion of the piezo along the axis of the spin–filter (radial mode). Applying an AC sinusoidal voltage induces rapid expansion and contraction of the piezo that carries along filter support and induces filter vibration in the vertical direction (in the axis direction). The maximum breakdown voltage of the piezo actuator corresponds to 220 V peak–to–peak (V_{pp}) and in order to measure the maximal filter support displacement, the frequency was scanned, at different voltages.

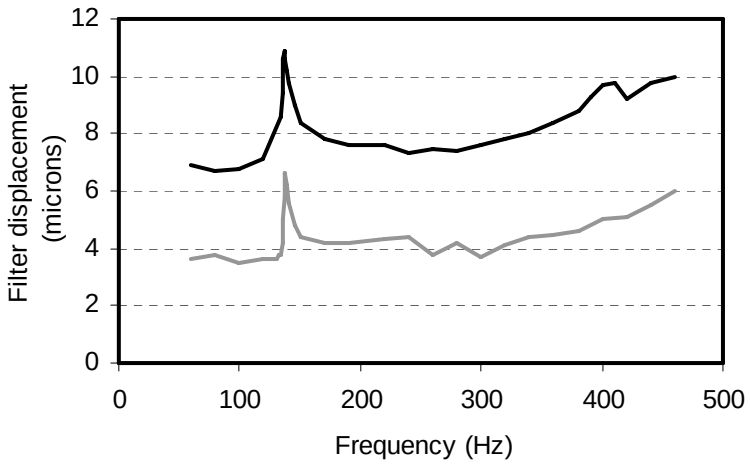

Figure 6.8: Filter displacement as a function of frequency applied to the filter support at –– 60 V and **––** 100 V.

Support displacement (the vibration amplitude) was measured directly in the actual cell perfusion set–up with a laser displacement meter (LC–2430, Keyence, Urdorf, Switzerland) placed under the support, in the axis alignment. The larger the mass that the piezo has to move, the larger the voltage applied has to be. For this reason, a purpose–built filter support was made from a light material such as Teflon, instead of stainless steel. The frequency was scanned from 50 to 450 Hz and support displacement was measured at 60 and 100 V (Figure 6.8). At a fixed voltage of 60 V, it is observed that there is an optimal and maximal support/filter displacement at 137 Hz, that corresponds to the resonance frequency. The displacement corresponds to 6.5 μm, but this increases linearly

with increasing voltage. At 100 V, the maximal displacement corresponds to 10.5 μm. Above a frequency of 350 Hz, the support/filter displacement also increases, however the signal (reading the Keyence displacement signal with help of an oscilloscope) no longer corresponded to a clean sinus wave and interferences appeared, which could damage the piezo actuator.

Once the piezo working conditions had been established, it was necessary to test the viability of cells in the presence of the ultrasound–vibrated filter. At 100 V and during 6 h of piezo operation, cell viability remained stable over 95% over the whole range of frequencies tested from 120 to 150 Hz. The filter vibrations were found to induce very low shear at the filter surface, and cells were not damaged therefore this technique was shown to be suitable for application with animal cell cultures.

6.3.2.2 Ultrasound–vibrated spin–filter cell culture

A vibrating filter was used in an attempt to reduce filter clogging and thus increase the culture duration by reducing the attachment of cells to the filter surface and by discarding cells from the filter pores.

Firstly, a cell perfusion culture was performed with a stationary spin–filter having a pore size of 8.5 μm that is much smaller than the mean cell diameter. These conditions having a small wet filtration surface and small filter pore size represent a worst–case scenario with respect to filter fouling. The culture was inoculated with a cell density of $2 \cdot 10^5$ cell/ml and a maximal viable cell density of $4.7 \cdot 10^6$ cell/ml was reached after 6.9 days of culture, at which time the filter was completely clogged and the cell concentration decreased due to cell wash–out by the perfusion flow (Figure 6.9). When the spin–filter is functioning correctly, clarified medium is withdrawn from within the spin–filter, however, when the pores of the filter become blocked, the flow through the filter is quasi–zero and the reactor working volume increases until it is removed by an over–flow device. Under these conditions the cell retention falls to zero, and the cell concentration in the reactor decreases.

In order to highlight the reduction of filter fouling when using a vibrated spin–filter, a second cell culture was performed with the spin–filter in the same conditions, i.e. similar filter pore size of 8.5 μm and immerged filter surface and filter at rest. The optimal piezo conditions found previously, of 100 V and 137 Hz were used and the piezo actuator was

operated continuously during the whole period of the culture. The culture was inoculated at $3 \cdot 10^5$ cell/ml, a value slightly higher than previously but sufficiently high in order to reduce the lag phase. This resulted in higher viable cell densities at an earlier stage of the culture. Since filter fouling has been shown to be dependent on cell density and perfusion rate, after 112 h of culture a small quantity of culture broth was replaced by fresh medium in order to adjust the cell density to that of the previous culture and to permit comparison of the filter duration of both cultures (Figure 6.9). The maximum viable cell density reached corresponds to $1.2 \cdot 10^7$ cell/ml, a value almost three–fold higher than that obtained in the absence of filter vibration. The culture lasted 14.7 days, when using the vibrated spin–filter, before the filter become clogged, corresponding to an increase of 113% in culture duration. Thus mechanical vibration of the filter, induced by a piezo actuator placed within the filter, was clearly shown to reduce filter fouling.

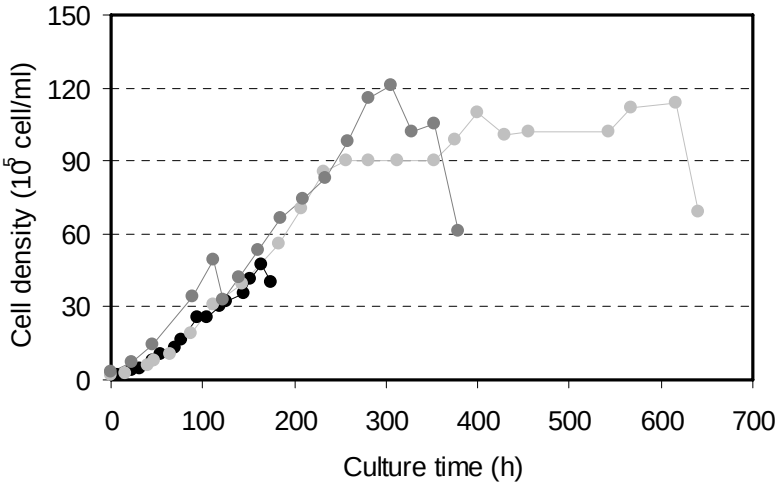

Figure 6.9: Evolution of CHO cell density as a function of culture time for perfusion cell cultures operating with a spin–filter having a mean pore size diameter of 8.5 μm. ● stationary filter without PZT, ● stationary filter with PZT and ● filter rotating at 150 rpm without PZT.

The two previous cultures were performed using spin–filters at rest. In order to compare the effect of filter vibration and filter rotation on the fouling of spin–filters, a culture was undertaken under identical conditions, using a spin–filter with the same filter pore size (8.5 μm) and immerged filter surface, rotating at 150 rpm. The cell density achieved was $1.1 \cdot 10^7$ cell/ml and the culture lasted 25.7 days, corresponding to a similar cell density but an increase of 75% in culture time, compared to the stationary vibrated spin–filter culture (Figure 6.9).

From these results, the effect of filter rotation is clearly more important than the effect created by filter vibration. However, at the end of the culture, the filter containing the piezo was removed and analysed and it was observed that PZT failure had occurred. Indeed, degradation of PZT insulation led to dielectric breakdown due to culture medium penetration between the piezo actuator and the disc support. The adhesive used to attach the piezo to the latter was probably not spread out in a homogeneous way and created zones of different distortion that permitted the piezo to detach from the disc. This may well have arrested filter vibration before the end of the culture. Additionally, the piezo actuator was operated continuously at a high voltage of 100 V. The lifetime of the piezo is dependent on the applied voltage and thus an optimization of the working time of the piezo has to be undertaken. Since filter fouling is a slow process, the filter could be vibrated in a discontinuous manner in order to extend the lifetime of the PZT actuator. A further limit to the lifetime of the piezo–actuator is the working frequency. It was found that maximal filter displacement occurred at the resonant frequency, which was the operational frequency used during the cell culture. However, piezo actuators are not designed to be driven at their resonant frequency (with full stroke and load), as the resulting high dynamic forces can endanger the structural integrity of the ceramic material. If the PZT actuator is operated at a frequency different from the resonant one, filter displacement would be lower, however, the piezo lifetime would be much longer. In order to increase filter vibration at a working frequency other than the resonant frequency, the voltage could be increased, since it was demonstrated that filter displacement is proportional to the operating voltage. If the maximal operating voltage is applied, the filter vibration could be increased further by increasing piezo thickness or changing piezo actuator for a higher–load model.

Although in the present study piezo actuator was not operated at optimal working conditions, an important reduction in fouling of the filter was clearly demonstrated when the stationary filter was vibrated. Rotation of the filter was found to play the major role in preventing fouling although vibration would be expected to further improve filter performance. The importance of vibration of the filter has been demonstrated but further development of the piezo actuators and their made of attachment to the filters is required in order to enable stable, long–term application in cell culture perfusion systems.

6.4 Conclusions

Spin–filter fouling was found to be a slow–term process that is governed by the hydrodynamic forces around the filter. The centrifugal filter rotation as well as perfusion rate were found to play a major role in clogging of the spin–filter pores. There is a sharply defined limit for the perfusion flow at any filter acceleration, which has to be adapted depending on the working perfusion rate. At low acceleration rates (1 m/s^2), the longevity of filters with a pore size of 8.5 μm was observed to decrease when the perfusion rate was increased from 2 to 25 cm/h, whereas increasing the filter acceleration to 25 m/s^2 resulted in longevity increasing from 3 to 25 days at 25 cm/h. Filters with a larger pore size (14.5 μm) showed a reduced tendency to fouling. Indeed at a filter acceleration of 25 m/s^2 and a perfusion rate of 25 cm/h, filter longevity was improved to 46 days. This represents an increase of 84% by comparison to the filter having a smaller pore size of 8.5 μm.

High viable and dead cells deposits collected from fouled filters were found not to be correlated with low filter longevity. Indeed at low filter accelerations, below 6.2 m/s^2, an increase of perfusion rate resulted in increased deposition of cells on the filter surface and filter longevity decreased. On the other hand, at high filter accelerations (25 m/s^2), the increase in cell deposition did not result in a decrease of filter longevity, for filters with pore sizes of 8.5 μm or 14.5 μm. Filters with larger pore sizes have a smaller solid surface available for cells to adhere compared with filters having smaller pore sizes and as expected, cell deposition on the latter was found to be larger. The reduction of open surface was found to increase the tendency of filters to clogging and was demonstrated by a decrease in filter longevity and culture duration.

In order to reduce the tendency of filters to fouling, a method has been developed using ultrasonic technology. This consists in continuous vibration of the filter, during the cell perfusion culture, using a piezo actuator, which converts electric energy into mechanical motion. An increase of 113% in culture time was demonstrated when a stationary spin–filter was vibrated. Filter rotation at 150 rpm increased culture time by 75% compared to a stationary vibrated filter, however piezo working conditions and set–up were sub–optimal. Using a rotating and vibrating spin–filter would be expected to significantly reduce clogging of filter pores and enhance culture longevity.

References

Avgerinos, G.C., Drapeau, D., Socolow, J.S., Mao, J.–I., Hsiao, K., Broeze, R.J., 1990. Spin filter perfusion system for high density cell culture: production of recombinant urinary type plasminogen activator in CHO cells. Bio–Technol. 8:54–58.

Büntemeyer, H., Bohme, C., Lehmann, J., 1994. Evaluation of membranes for use in online cell–separation during mammalian–cell perfusion processes. Cytotechnology 15(1–3):243–251.

Chai, X., Kobayashi, T., Fujii, N., 1998. Ultrasound effect on cross–flow filtration of polyacrylonitrile ultrafiltration membranes. J. Membrane Sci. 148:129–135.

Deo, Y.M., Mahadevan, M.D., Fuchs R., 1996. Practical considerations in operation and scale–up of spin–filter based bioreactors for monoclonal antibody production. Biotechnol. Progr. 12:57–64.

Doblhoff–Dier, O., Gaida, T., Katinger, H., Burger, W., Gröschl, M., Benes, E., 1994. A novel ultrasonic resonance field device for the retention of animal cells. Biotechnol. Progr. 10:428–432.

Ducommun, P., Ruffieux, P.–A., Furter, M.–P., Marison, I., von Stockar, U., 2000. A new method for on–line measurement of the volumetric oxygen uptake rate in membrane aerated animal cell cultures. J. Biotechnol. 78:139–147.

Esclade, L.R.J., Carrel, S., Péringer, P., 1991. Influence of the screen material on the fouling of the spin filters. Biotechnol. Bioeng. 38:159–168.

Favre, E., 1993. Constant Flow–Rate Filtration of Hybridoma Cells Suspensions. J. Chem. Technol. Biot. 58(2):107–112.

Favre, E., Thaler, T., 1992. An engineering analysis of a rotating sieves for hybridoma cell retention in stirred tank bioreactors. Cytotechnology 9:11–19.

Fenge, C., Fraune, E., Freitag, R., Scheper, T., Schügerl, K., 1991. On–line monitoring of monoclonal antibody formation in high density perfusion culture using FIA. Cytotechnology 6:55–63.

Ganesh, G., Kumar, T.K.S., Pandian, S.T.K., Yu, C., 2000. Rapid staining of proteins on polyacrilamide gels and nitrocellulose membranes using a mixture of fluorescent dyes. J. Biochem. Bioph. Meth. 46:31–38.

Gundogdu, O., Koenders, M.A., Wakeman, R.J., Wu, P., 2003. Permeation through a bed on a vibrating medium: theory and experimental results. Chem. Eng. Sci. 58:1703–1713.

Iding, K., Lütkemeyer, D., Fraune, E., Gerlach, K., Lehmann, J., 2000. Influence of alterations in culture condition and changes in perfusion parameters on the retention performance of a 20 μm spinfilter during a perfusion cultivation of a recombinant CHO cell line in pilot scale. Cytotechnology 34:141–150.

Jan, D.C.–H., Emery, A.N., Al–Rubeai, M., 1992. Optimization of spin–filter performance in the intensive culture of suspended cells. In: Spier RE, Griffiths JB, MacDonald C, editors. Animal cell technology: developments, processes and products. Oxford: Butterworth–Heinemann. p 448–451.

Kilburn, D.G., Clarke, D.J., Coakley, W.T., Bardsley, D.W., 1989. Enhanced sedimentation of mammalian cells following acoustic aggregation. Biotechnol. Bioeng. 34:559–562.

Kobayashi, T., Kobayashi, T., Hosaka, Y., Fujii, N., 2003. Utrasound–enhanced membrane–cleaning processes applied water treatments: influence of sonic frequency on filtration treatments. Ultrasonics 41:185–190.

Lee, S., Lueptow, R.M., 2001. Rotating reverse osmosis: a dynamic model for flux and rejection. J. Membrane Sci. 192:129–143.

Maiorella, B., Dorin, G., Carion, A., Harano, D., 1991. Cross–flow microfiltration of animal cells. Biotechnol. Bioeng. 37(2):121–126.

Mercille, S., Johnson, M., Lemieux, R., Massie, B., 1994. Filtration–based perfusion of hybridoma cultures in protein–free medium: Reduction of membrane fouling by medium supplementation with DNase I. Biotechnol. Bioeng. 43:833–846.

Najarian, S., Bellhouse, B.J., 1996. Effect of liquid pulsation on protein fractionation using ultrafiltration processes. J. Membrane Sci. 114:245–253.

Postlethwaite, J., Lamping, S.R., Leach, G.C., Hurwitz, M.F., Lye, G.J., 2004. Flux and transmission characteristics of a vibrating microfiltration system operated at high biomass loading. J. Membrane Sci. 228:89–101.

Pui, P.W.S., Trampler, F., Sonderhoff, S.A., Gröschl, M., Kilburn, D.G., Piret, J.M., 1995. Batch and semicontinuous aggregation and sedimentation of hybridoma cells by acoustic resonance fields. Biotechnol. Progr. 11:146–152.

Shirgaonkar, I.Z., Lanthier, S., Kamen, A., 2004. Acoustic cell filter: a proven cell retention technology for perfusion of animal cell cultures. Biotechnol. Adv. 22:433–444.

Siegel, U., Fenge, C., Fraune, E., 1991. Spin filter for continuous perfusion of suspension cells. In: Murakami H, Shirahata S, Tachibana H, editors. Animal Cell Technology: Basic and Applied Aspects. Fukuoka, Japan: Kluwer Academic Publishers. p 434–436.

Woodside, S.M., Bowen, B.D., Piret, J.M., 1998. Mammalian cell retention devices for stirred perfusion bioreactors. Cytotechnology 28:163–175.

Yabannavar, V.M., Singh, V., Connelly, N.V., 1992. Mammalian cell retention in a spinfilter perfusion bioreactor. Biotechnol. Bioeng. 40:925–933.

Zhang ,J., Collins, A., Chen, M., Knyazev, I., Gentz, R., 1998. High–density perfusion culture of insect cells with a BioSep Ultrasonic Filter. Biotechnol. Bioeng. 59(3):351–359.

7

General conclusions and perspectives

The growing demand for bio–engineered proteins in mammalian cells has stimulated the development of new suspended cell culture techniques. The achievement of high cell densities and high volumetric productivities can be obtained using fed–batch or perfusion cultures. Perfusion culture may be preferred when the product is subject to degradation and when dynamic culture conditions change continuously and may affect product quality. Because of possible cell damage through pumping and high residence time of cells outside the reactor, external cell separation devices are normally avoided. Internal spin–filter appear to be the most suitable devices for continuous cell separation at large–scale operation. The main disadvantage of such devices is the reduced operational time, due to filter fouling. Increasing the filter pore size could reduce this phenomenon, however filters with pore size larger than the average cell diameter induce cell leakage. The lack of understanding of the mechanism of cell retention and spin–filter fouling makes difficult the scale–up and use over long–term operation of such devices. The aim of this thesis was to fill this lack and thus identify the main parameters that affect particle retention, understand the retention mechanism of spin–filters in order to achieve high cell density and long–term cultures, at small scale, as well as at large scale operation.

The first part of the work (chapter 3) was focused on the understanding of the retention mechanism of spin–filters, which pore size is greater than the mean cell/particle diameter. The use of baffles within the spin–filter was revealed to be crucial. It permitted good medium homogeneity and reduced cell accumulation within the spin–filter, which would otherwise lead to cell leakage and filter fouling from inside the spin–filter. The main parameters influencing particle retention were identified to be filter rotation velocity and filter pore size, while perfusion flow and particle concentration influenced particle retention to a lesser extent. Filter retention followed saturation dynamics with an initial direct correlation with respect to filter rotation rate. A plateau was reached above a filter tangential velocity of 0.45 m/s and 0.87 m/s for filters with pore size of 13 and 14.5 μm respectively and particle diameter of 13 μm. This result would signify that in order to get maximal retention, the filter has to be rotated as fast as shear forces involved are not harmful to the cells. However, for economic reasons, the minimal filter rotation at which retention is maximal should be applied. In order to reduce filter fouling, external draft tubes around spin–filters are normally used in the industry, however in the present study their use was found to influence the particle retention of spin–filters with large pore sizes. This influence was negative because of increased cell leakage due to the formation of Taylor vortices in the gap between the filter and the draft tube. Since the internal spin–filter is placed inside a bioreactor, the walls of the vessel could be considered to act as a draft tube. Thus the different particle retention rates between the configurations of spin–filters with and without external draft tube could be explained by different Taylor vortex regimes, the instabilities of which trap particles differently in retention zones. Measurements of the motion of particles at different vortex flow regimes using laser particle tracking would allow observing these phenomena and possibly explaining why the retention profiles are different and why they follow a saturation dynamics with an initial direct correlation with respect to filter rotation. Although the use of external baffles decreases spin–filter cell retention, concerning filter fouling, further studies should be carried out on the use of baffles around spin–filters with small pore sizes that allow 100% particle retention and verify if the operation time of the filter is similar to unbaffled spin–filters with large pore sizes.

The particle–flow system in spin–filters presents a very complex mathematical formulation that was found to be difficult to solve in order to estimate particle lateral migration near the filter surface. No suitable general expression that describes the particle trajectories in rotating Couette flow systems has been developed to date. In chapter 4, the

particle migration in the direction perpendicular (lateral) to the filter surface and governed by the forces acting on such a particle was simulated in order to attempt an explanation on particle retention mechanism, related to mass transport through the filter, and characterize the conditions in which spin–filter has to be operated in order to reach maximum retention. The particle migration near the rotating filter was identified as being dependent on the competition between forces that direct the particle towards the filter surface (Stokes and perfusion forces) and forces that direct it away from the filter surface (centrifugal sedimentation and lift forces). The lift force, invoked in cross–flow systems was adapted to spin–filter systems and was revealed to be important in particle lateral migration phenomenon in such systems. The established model predicts that the particle is rejected from the filter surface when the terminal particle velocity is positive and it is moved toward the filter screen when the velocity is negative. When the lift force is considered, the predicted particle lateral velocity was found to become positive at filter rotations above which maximal particle retention was observed experimentally. Based on this model, the filter angular speed at which the filter has to rotate could be predicted as a function of filter radius, when considering a terminal velocity close to zero that means that no particles would approach the filter surface and thus maximal retention rate would be expected. When the perfusion flow was decreased, the predicted filter angular rotation speed at which the terminal particle velocity is close to zero decreased. Experimentally, the same phenomenon was observed when measuring the angular rotation, above which the retention is maximal, at different perfusion rates. Similar retention rates were observed experimentally with filters, witch radius varied from 2.14 to 4.16 cm when conserving the acceleration of the filter and was demonstrated also during simulations. Although the theoretical model and experiments correlate at certain operational conditions and geometries of the spin–filter, its applicability is limited. Indeed, it was shown that perfusion flow has a smaller influence on the prediction of particle migration than experimentally observed. The validity of the model at large scale is questionable. Indeed, at filter radii greater than 0.075 m, the slip velocity of the particle relative to the fluid is very high and the condition of Reynolds number smaller than unity, required by the lift theory of the present study was found to not be valid. However the model, together with experimentation, demonstrated that filter acceleration is the parameter that has to be conserved during spin–filter operation, from small to large scale, in order to reach similar rates of particle/cell retention.

In chapter 4, it was shown that the retention mechanism of spin–filters is mainly dependent on the flow hydrodynamics in the vicinity of the external surface of the filter. Depending on the pore size of the filter, there is an optimal filter centrifugal rotation at which retention is maximal, at small as well as at large scale. For these reasons, an empirical model based on experiments has been developed in chapter 5 that predicts the effect of four parameters found to influence particle retention the most: the particle concentration, the filter acceleration, the filter porosity (ratio of filter pore size by the particle diameter) and the perfusion capacity (ratio of perfusion flow by the filtration surface), on particle retention. In animal cell culture the flow characteristics, such as the density or the viscosity vary slightly during the culture and were not considered to influence particle retention. A decrease of temperature during the cell culture, as is used during production phase of industrial process, should increase the medium viscosity and could change the particle retention profile found to be dependent on forces involved by flow inertia. However, in chapter 6, CHO cell retention at 28°C showed the similar retention rates as those obtained during cell perfusion at 37°C. The model revealed that filter porosity and filter acceleration are the most significant parameters in particle retention. At a fixed perfusion capacity of 13.5 cm/h and particle concentration of $5.5 \cdot 10^6$ particle/ml, particle retention increases from 0.2 to 0.9 when decreasing filter porosity from 1.4 to 1, at low filter acceleration of 5 m/s^2, whereas it increases from 0.6 to 1 at high filter acceleration of 35 m/s^2. For animal cell perfusion cultures using spin–filters, the model predicts the minimal filter acceleration that has to be used, using a certain filter pore size and fixed perfusion rate, in order to get maximum retention. The model was established during perfusion simulations of polymer beads with density very close to that of animal cells and was validated during two CHO animal cell cultures with two different spin–filter pore sizes. The use of spin–filters with large pore sizes would reduce filter fouling, however they induce more cell leakage and apparent cell growth is reduced. Additionally, it was observed that cell sampling or rapid changes of perfusion flow will more disturb flow patterns and decrease retention rate with spin–filters having large pore sizes than smaller ones. Thus a compromise has to be found between a high filter pore size that will induce more cell leakage and a lower one that will induce more rapid filter fouling. However filter porosity between 1.2 and 1.3 was revealed to be a good choice.

The last part of the work (chapter 6) focused on the study of spin–filter fouling mechanisms. Since filter fouling was revealed to be a long–term phenomenon, actual CHO cell perfusion simulations have been carried out until complete filter fouling. The

effect of filter pore size, filter acceleration and perfusion flow on spin–filter fouling has been studied. Filter acceleration as well as filter pore size was revealed to have an important effect concerning the reduction of filter fouling. At low perfusion rates, the increase of filter acceleration was found to enhance filter longevity for spin–filters, which pore size is smaller than the cell diameter. However at large perfusion flow, low filter accelerations do not contribute to filter fouling reduction, unless increased to high value, at which the centrifugal effect is high enough to counteract the pumping effect, caused by the perfusion flux. Although the increase of filter pore size increases cell passage through the filter surface, a reduced tendency to fouling of spin–filters was demonstrated for filters with pore size larger than the cell diameter. The cell passage has little influence on pore clogging on the internal filter surface, since the pores are continuously washed by the perfusion flow and the use of baffles inside the spin–filter creates turbulences at the internal surface preventing cells from sedimentation and accumulation within the spin–filter. The filter longevity could be increased by 84% when pore size was increased from 8.5 to 14.5 μm, during CHO cell perfusion cultures.

During this study, it appeared that filter fouling is not simply dependent on the available open filtration surface, but is dependent much more on the manner in which cells stick to the filter, that is governed by the forces acting on the filtration system and thus on operational parameters of the spin–filter and culture conditions. During cell cultures, the use of high perfusion rates necessitates employing high filter accelerations and it has been shown that the use of larger pore size filters yields higher filter longevity. In spite of a good optimization of the spin–filter parameters, filter fouling occurs. The only way to increase filter longevity is to keep a high cell viability and prevent cells adhering to the surface. One method was tested in the present study that consisted in vibrating the filter surface using a piezoactuator, which converts electric energy into mechanical motion. During a CHO cell culture, an increase of 113% in culture duration was demonstrated when using a stationary and vibrated spin–filter, compared with a stationary one, due to the reduction of filter fouling. But the effect of filter rotation was demonstrated to be more important than the effect created by the vibration of the filter. However, piezoactuator failure occurred before the end of the culture due to piezo working conditions and set–up being sub–optimal and further development of the piezoactuators, such as optimisation of the working time (discontinuous manner and on/off working periods) and working frequency, together with the method of piezo attachment to the filters is required. The

continuous or discontinuous filter vibration of a rotating spin–filter should have thus a high potential to reduce filter fouling and should be further studied.

In conclusion, the study of spin–filter systems during animal cell perfusion culture highlighted the complexity of the mechanism involved in cell retention. Although the importance of lift forces in such systems has been demonstrated, it is not sufficient to predict completely such mechanism. However, it revealed, together with experimentation, that the conservation of filter acceleration gives rise to similar retention rates, at small– and large–scales. Since it was found that filter retention followed a saturation dynamics with an initial direct correlation with respect to filter rotation rate, and filter fouling is reduced by high filter rotation rates and large pore sizes, it is necessary to use filters, which pore sizes are larger than the cell diameter and at high filter rotation rates. The cell retention model developed in this study for small scale as well as for large–scale processes permits to choose the optimal acceleration at which the filter has to be operated in order to achieve the highest retention rates at a certain filter pore size and for any animal cell. The filter porosity (ratio of filter pore size to cell diameter) should take values between 1.2 and 1.3, in order to avoid too much cell leakage and reduce filter fouling. The use of baffles inside the spin–filter is necessary in order to keep cell concentration homogeneous inside the filter and thus avoid cell sedimentation/ accumulation inside the filter and filter pore clogging on the internal filter surface. The use of piezoactuators was demonstrated to be a powerful technique for on–line reduction of filter fouling.

Florentina Vallez-Chetreanu

Born in Bucharest, 11th of March 1976
Nationality: Swiss/Romanian

Education

PhD thesis in Animal Cell Culture Bioprocess Engineering since 2001
Laboratory of Chemical and Biochemical Engineering, Ecole Polytechnique Fédérale de Lausanne (EPFL)
Thesis on "Characterization of the mechanism of action of spin-filters for animal cell perfusion cultures", financed by Serono Pharma SA, Fenil-sur-Corsier, Switzerland.
Directors: Dr I. Marison and Prof. U. von Stockar.

Master degree in Chemical Engineering, EPFL 1995 – 2000
Master title: Quantitative analysis of the carbon catabolite repression of two mutant strains of the yeast *S.cerevisiae*.
Laboratory of Chemical and Biochemical Engineering, EPFL. Director: Prof. U. von Stockar.

Professional experience

Project leader (PhD)
Laboratory of Chemical and Biochemical Engineering, EPFL since 2001

Management of suspended CHO cells in batch and perfusion cultures
Implementation of statistical design of experiments for cell culture scale-up processing
Training and supervision of a diploma student and trainees

Scientific assistant
Laboratory of Chemical and Biochemical Engineering, EPFL 2001 – 2005

Coaching of students for the course "Advanced biochemical engineering"
Responsible for the organization of the practical work of 3rd year students

Scientific collaborator
Laboratory of Chemical and Biochemical Engineering, EPFL (3 months) 2000

Production of a recombinant protein in collaboration with a pharmaceutical industry
Development of the upstream process at 15–L pilot scale
→ Protein is now in the production phase

Intern
Pittsburgh University, Pittsburgh, USA (3 months) 2000

Evaluation and development of an enzymatic buffer for chemical warfare agents degradation

2006 F. Vallez-Chetreanu, R. Phan-Tan-Luu, U. von Stockar, I. Marison. The use of response surface methodology to model particle retention by spin-filters. Submitted to Biotech Bioeng.

2006 F. Vallez-Chetreanu, U. von Stockar, I. Marison. Study of spin-filter particle retention for animal cell perfusion cultures. Submitted to J Biotech.

2005 F. Vallez-Chetreanu, U. von Stockar, I. Marison. Spin-filter as a separation device during animal cell perfusion cultures. Submitted to Biotech Bioeng.

2003 F. Vallez-Chetreanu, D. Voisard, A. Kadouri, U. von Stockar, I. Marison . Spin-filter scale-up feasibility on the basis of a small-scale particle retention model, 11th European Congress on Biotechnology, Basel, Switzerland.

2002 C. Herwig, F. Chetreanu, P. Niederberger, I. Marison, U. von Stockar. Quantitative analysis of the impact of *HXK2* and *REG1* deletion in *Saccharomyces cerevisiae* on invertase expression and respiration. Enzyme Microb Tech (2002), 31: 505-515.